

Università degli Studi di Genova -
Scuola Politecnica
Dipartimento di Ingegneria Meccanica, Energetica, Gestionale e
dei Trasporti (DIME)
Sez. TEC (Termoenergetica e Condizionamento ambientale)



Ph.D. Thesis in Technical Physics
XXXV Cycle

**MONITORING AND TRANSIENT MODELLING OF
SOLAR ASSISTED HEAT PUMP WITH HYBRID
PANELS: LIMITS AND POTENTIALS APPLIED TO
AN EXISTING PLANT**

Supervisors:

Prof. L.A. Tagliafico

Prof. A. Marchitto

PhD candidate:

Alessandro Cavalletti

Ringraziamenti

Questa è l'ultima parte che ho scritto della tesi, la più importante e in quanto tale non poteva che essere fatta alla fine. Più volte nel corso della tesi sono stato tentato di scriverla, ma mi sono annotato tutto senza scrivere nulla perché doveva essere fatta con la giusta calma e gratitudine, prendendo un momento per ringraziare tutti quelli che mi hanno accompagnato in questo percorso.

Prima di tutto grazie ai miei Tutor, Prof. Luca Tagliafico e Prof.sa Annalisa Marchitto che mi hanno aiutato e guidato in questi anni di cammino sotto ogni aspetto, aiutandomi a crescere e a portare avanti il mio progetto di ricerca. Vi devo davvero molto e spero di portare con me almeno un pizzico della vostra pazienza, preparazione e passione che trasmettete ai vostri allievi. Un grazie sentito anche a tutti quanti fanno parte del DIME-TEC, professori, ricercatori, dottorandi e assegnisti.

Come sempre grazie alla mia mamma Patrizia e a mio papà Paolo che sono mio costante appoggio e sprone a dare sempre il meglio. Siete stati e siete il mio riferimento in questi anni caotici ed è grazie a voi ed al vostro esempio se sono arrivato fin qui. Grazie alla mia inossidabile nonna Edda e alla sua grinta, spero di averne presa un po' anche io. Grazie a tutto il resto della mia famiglia, vicina e lontana.

Grazie a coloro che solo fisicamente oggi non sono qui, ma che sento ogni giorno al mio fianco ed il cui ricordo continua a darmi conforto e guida: nonna Doda, nonno Dodo e nonno Mario.

Grazie a coloro che si sono aggiunti alla mia famiglia (per loro grande fortuna): Alberto, Rossella, Luca e Alice. Negli ultimi mesi vi ho invaso casa e avete condiviso una buona parte del mio stress accumulato per riuscire a finire la tesi, a partire dalla ricerca spasmodica di una scrivania dove appollaiarmi per passare tutta la giornata a scrivere la tesi. Grazie anche a Elena e Franco che mi sono sempre stati vicini come se fossi loro nipote.

Grazie al mio amico di sempre Filippo la cui vicinanza e amicizia vince qualsiasi distanza geografica.

Grazie a tutti gli amici con i quali ho condiviso ansie e gioie di questo percorso: Francesco, Stefano, Luca Nietante e Luca Peruzzi. Un grazie particolare a Luca Aly per avermi aiutato nell'improbabile e ingrata missione di impaginare tutte queste pagine.

Grazie a tutti i maestri, i prof e tutti coloro che mi hanno accompagnato nella grande avventura dell'apprendimento. Grazie in particolare alla Maestra Roberta, Prof Ravettino, Prof Veronese e Prof Solari.

Grazie a Koby, il cucciolone che ormai sento un po' anche come mio, che è stato acciambellato sui miei piedi per gran parte della tesi, tenendomi compagnia e aiutandomi a svagare nelle passeggiate quando ero troppo assorto nei miei pensieri.

Infine, grazie Chiara, ho tenuto il meglio alla fine, perché a te non vanno solo i miei più profondi ringraziamenti per essermi stata vicina tutti questi mesi difficili, per avermi aiutato, consigliato e sostenuto, per esserti presa cura di me. Ho iniziato questo viaggio di dottorato solo, triste e molto dubbioso su tutte le porte che avevo davanti. Ma per mia immensa fortuna, letteralmente dal primo giorno di questo percorso, mi sei stata vicino ridandomi forza e fiducia in me. È per questo che dedico a te e al nostro cucciolone Koby questo lavoro e tutto quello che di buono può esserci.

Acknowledgement

The Palacus pilot plant, installed at Sport Palace “Carminio Romanzi”, University of Genoa, has been developed with a co-funding of FSE Regione Liguria, Bando Azione 2.1 “Efficienza Energetica e Produzione di Energia da Fonti Rinnovabili – Enti Pubblici” – Posizione n.2, included in the PRIN 2015 MIUR grant 2015M8S2PA “Clean Heating and Cooling Technologies for energy efficient smart grid”. The control and monitoring systems have been completed with the co-funding of the University of Genoa in the context of the “Grandi Attrezzature” 2018, DR n. 3404, 19/07/2018 project and CARIGE 2018/0012 project.

Abstract

The Solar Assisted Heat Pumps represent one of the most interesting examples in the field of heating systems based on the interface of different generators. The present work provides a general overview about the topic of the solar assisted heat pumps, with specific attention to the current limits and potentials. Then, the pilot plant at Palacus is presented: a solar assisted heat pump is interfaced with hybrid panels and it represents the missing link between laboratory prototypes and full scale working plants. The most interesting part of the plant and its core is represented by the data acquisition system which allows an almost automatic control of the plant and a continuous collection of the over 50 measured working parameters of the facility. Indeed, this extended database will be used to validate a numerical transient model developed in TRNSYS environment. Thanks to this model, different optimisation analyses will be carried out, to increase the plant efficiency. In particular the following topics will be enquired: insulation of the connection pipes between the heat pump and the solar field and strategies to exploit the SAHP-PVT from both the thermal and photovoltaic point of view. In addition, the plant will be simulated at five different locations over Italy representing the main climatic zones, to carry out a preliminary simplified assessment tool to predict the SAHP performance according to the degree days of the installation site.

SUMMARY

| | |
|--|----|
| Nomenclature | 6 |
| List of Figures | 8 |
| List of tables..... | 12 |
| 1. Introduction..... | 13 |
| 2. Solar assisted heat pumps – a review | 17 |
| 2.1 Main components of the SAHPs – heat pump | 21 |
| 2.2 Main components of the SAHPs – solar panels | 25 |
| 2.3 The solar assisted heat pumps | 31 |
| 2.4 The solar assisted heat pumps – state of the art and current limits | 37 |
| 2.4.1 Coupling of solar panels and heat pumps | 37 |
| 2.4.2 Low ambient temperature | 37 |
| 2.4.3 Lack of models for design, management and optimization of SAHPs..... | 38 |
| 2.4.4 Mismatch between heat requirement and heat supply | 38 |
| 2.4.5 Low level of end users’ acceptance of SAHPs..... | 39 |
| 2.4.6 Coupling of SAHP with existing heating systems..... | 40 |
| 2.4.7 SAHP - scale effect?..... | 41 |
| 3. The solar assisted heat pump with hybrid panels pilot plant at the Palacus sport palace - Genoa | 43 |
| 3.1 The Solar Assisted Heat Pump with Hybrid panels (PVT) pilot plant: a description | 43 |
| 3.1.1 Generation subsystem..... | 45 |
| 3.1.2 Storage subsystem | 55 |
| 3.1.3 Distribution and emission subsystem | 58 |
| 3.1.4 Control subsystem | 59 |
| 3.1.5 An overview over the plant performance | 63 |
| 3.2 The sport palace Carmine Romanzi – energy characterization..... | 64 |
| 3.2.1 DHW need | 64 |
| 3.2.2 SH need..... | 70 |
| 3.3 Critical issues resulting from the plant monitoring and management..... | 74 |
| 3.3.1 Acceptance..... | 74 |
| 3.3.2 Hybrid panels durability and reliability | 76 |
| 3.3.3 Hydraulic decoupling of circuits | 76 |
| 3.3.4 Efficient management of a PV/PVT solar field..... | 78 |
| 4. Modelling of the SAHP with PVT panels pilot plant by means of TRNSYS | 80 |
| 4.1 Objectives of the modelling | 80 |
| 4.2 Description of the main components of the plant and their numerical validation | 81 |

| | |
|--|-----|
| 4.2.1 Model validation criteria and measured data processing..... | 81 |
| 4.2.2 TRNSYS environment..... | 82 |
| 4.2.3 Model assembly and validation | 83 |
| 5. Optimization simulations to the SAHP-PVT pilot plant at Palacus and possible interventions.. | 119 |
| 5.1 Influence of the thermal losses due to the pipes connecting the solar field to the boiler room | 119 |
| 5.2 Changes in the regulation criteria to best exploit the SAHP-PVT | 123 |
| 5.3 Strategies to maximize the self-consumption of the photovoltaic field | 126 |
| 5.4 Performances of the SAHP-PVT at different climatic zones | 131 |
| 6. Conclusions and future developments | 136 |
| Publications | 143 |
| References | 144 |
| Annex – complete plant layout | 157 |

Nomenclature

Abbreviations

| | |
|------|-------------------------------------|
| HP | Heat pump |
| PVT | Photovoltaic/thermal |
| SH | Space heating |
| DHW | Domestic hot water |
| GB | Gas burner |
| WST | Water storage tank |
| MES | Manager energy services |
| CS | Exchange contribution |
| COP | Coefficient of performance |
| SCOP | Seasonal coefficient of performance |
| EER | Energy efficiency ratio |
| SAHP | Solar assisted heat pump |
| VCC | Variable capacity compressor |
| EEV | Electronic expansion valve |
| ATU | Air treatment unit |
| DAS | Data acquisition and control system |
| PLC | Programmable logic controller |
| DD | Degrees days |
| PES | Primary energy saving |
| IT | Information technologies |
| IoT | Internet of Things |
| AAL | Ambient assisted living |
| TRL | Technological readiness level |
| AE | Acceptability engineering |
| IHTP | Inverse heat transfer problem |
| H | Height |
| D | Diameter |
| CFD | Computational fluid dynamics |

Subscripts

| | |
|---------|----------------|
| nom | nominal |
| el | electrical |
| th | thermal |
| p | panel |
| tot | total |
| sol | solar |
| consump | consumption |
| work | working period |
| eff | effective |

| Symbol | Quantity | SI Unit |
|--------|-----------------|---------|
| L | Mechanical work | J |
| Q | Heat pump heat | J |
| T | Temperature | K |

| | | |
|------|-------------------------------------|--------------------|
| S | Entropy | J/kg K |
| E | Energy | J |
| m' | Mass flow rate | kg/s |
| c | Specific heat | J/kg K |
| T | Temperature | K |
| A | Area | m ² |
| G | Irradiance | W/m ² |
| COP | Coefficient of performance | - |
| SCOP | Seasonal coefficient of performance | - |
| E | Energy | kWh |
| g | Gravity acceleration | m/s ² |
| U | Transmittance | W/m ² K |
| u | Characteristic inlet fluid velocity | m/s |
| V | Volume | m ³ |
| W | Input work | J |
| p | pressure | N/m ² |
| P | power | W |

| Greek symbols | Quantity | SI Unit |
|----------------------|---|-------------------|
| τ | Time | s |
| η | Dimensionless efficiency | [-] |
| ρ | Density | kg/m ³ |
| λ | Thermal conductivity | W/m K |
| β | Volumetric coefficient of thermal expansion | 1/K |

LIST OF FIGURES

| | |
|---|----|
| <i>Figure 1. 1: crude oil prices per barrel historical chart (1)</i> | 13 |
| <i>Figure 1. 2: Estimated renewable share of total final energy consumption (4)</i> | 14 |
| <i>Figure 1. 3: Renewable share of total final energy consumption – reference year 2018 (4)</i> | 15 |
| <i>Figure 2. 1: distribution of SAHP producing companies by country- (16)</i> | 17 |
| <i>Figure 2. 2: new companies for SAHP production entering the market every year (16)</i> | 18 |
| <i>Figure 2. 3: prototype of solar assisted heat pump with hybrid panels at Cus Genova (21)</i> | 19 |
| <i>Figure 2. 4: solar assisted heat pump with bare solar thermal panels – Sestri Levante (GE) – (22)</i> | 19 |
| <i>Figure 2. 5: solar assisted heat pump pilot plant with hybrid panels at Palacus – Genoa</i> | 20 |
| <i>Figure 2. 6: Values of the Primary Energy Saving (PES) index according to the different 110 Italian municipalities (23)</i> | 21 |
| <i>Figure 2.7: working principle of a heat pump</i> | 22 |
| <i>Figure 2. 8: mechanical vapour compression heat pump scheme</i> | 23 |
| <i>Figure 2. 9: T-S diagram with a classic vapor compression inverse cycle</i> | 24 |
| <i>Figure 2. 10: covered and an unglazed thermal collector (respectively a and b), a PV and a PVT panel (respectively c and d) (37), (38), (39), (40)</i> | 26 |
| <i>Figure 2. 11: Hourly electrical demand during weekend, weekdays, seasons and years (41)</i> | 27 |
| <i>Figure 2. 12: hourly normalized hot water demand in a day for Italy (51)</i> | 27 |
| <i>Figure 2. 13: solar house built by MIT, in 1939, (52)</i> | 28 |
| <i>Figure 2. 14: solar thermal panels efficiency against the difference in temperature between the collector fluid and the ambient air temperature (16)</i> | 29 |
| <i>Figure 2. 15: output peak current intensity (I) against the peak voltage (V) of the PV module with different operating temperatures (57)</i> | 30 |
| <i>Figure 2. 16: energy balance for a PVT panel (16). The heat flows are expressed by means of capital q since they are not referred to the panel area</i> | 30 |
| <i>Figure 2. 17: example of the graphic method for SAHP categorization (16)</i> | 32 |
| <i>Figure 2. 18: plant of a parallel asset SAHP layout and its graphical representation (16)</i> | 33 |
| <i>Figure 2. 19: plant of a regenerative/parallel/series asset solar assisted/geothermal HP layout and its graphical representation (16)</i> | 34 |
| <i>Figure 2. 20: Schematic representation of a direct expansion SAHP.</i> | 34 |
| <i>Figure 2. 21: Schematic representation of an indirect expansion SAHP.</i> | 35 |
| <i>Figure 2. 22: preliminary steady state analysis about the serial/parallel asset convenience, based on the increase in the COP of the chosen HP and the collector yield in parallel/serial configuration (70)</i> | 36 |
| <i>Figure 2. 23: trend over the past two decades of the new surfaces built for both residential (red) and non-residential (green) applications (122)</i> | 40 |
| <i>Figure 3. 1: overview of the pilot plant – focus on the sport palace, the PVT field, the HP and the boiling room</i> | 44 |
| <i>Figure 3. 2: simplified scheme of the solar assisted heat pump pilot plant</i> | 44 |
| <i>Figure 3. 3: gas burners used to integrate DHW/SH needs in the heating system of the Palacus sport palace. a) burner for only DHW out of the heating season – 35 kW peak thermal power; b) burner for DHW and SH during the heating season – 320 kW peak thermal power</i> | 45 |

| | |
|--|-----------|
| <i>Figure 3. 4: Solar field, orientation from the satellite view (on the left – source Google Maps) and view of the site (on the right)</i> | <i>45</i> |
| <i>Figure 3. 5: 3D view (source Google Earth) of the field and of the shadings due to the surrounding hills/buildings.....</i> | <i>46</i> |
| <i>Figure 3. 6: panel stratigraphy.....</i> | <i>46</i> |
| <i>Figure 3. 7: PV and thermal modules of the hybrid panel – extract from the technical specifications</i> | <i>47</i> |
| <i>Figure 3. 8: hydraulic scheme of the connection between two rows of panels. The same pattern occurs for the remaining rows</i> | <i>48</i> |
| <i>Figure 3. 9: one of the two 10 kW inverters installed near the solar field</i> | <i>48</i> |
| <i>Figure 3. 10: hydraulic/electric connection between the solar hybrid field and the heating system</i> | <i>49</i> |
| <i>Figure 3. 11: heat pump installed near the Palacus sport palace</i> | <i>49</i> |
| <i>Figure 3. 12: three-dimensional plot of the COP depending on the outlet temperatures on the evaporator and condenser sides.</i> | <i>50</i> |
| <i>Figure 3. 13: water storage tanks on the cold (on the left) and hot side (on the right) of the heat pump.....</i> | <i>51</i> |
| <i>Figure 3. 14: view and performance curve of a single reference pump present in the plant. The model is the same adopted for P2, P3, P4 and P5 recalled in the text.....</i> | <i>51</i> |
| <i>Figure 3. 15: simplified schematic representation of the interaction among the different generators. Colour code: blue line – cold water; red line – hot water.....</i> | <i>53</i> |
| <i>Figure 3. 16: pump P1, view and performance curve of a single pump</i> | <i>54</i> |
| <i>Figure 3. 17: domestic water storage tanks - DHW 1 on the left and DHW2 on the right</i> | <i>55</i> |
| <i>Figure 3. 18: constant flow rate pump P9 for recirculation system (maximum consumption 103 W)</i> | <i>56</i> |
| <i>Figure 3. 19: simplified schematic representation of the DHW subsystem. Colour code: blue line – cold water; red line – hot water.....</i> | <i>56</i> |
| <i>Figure 3. 20: twin pumps P7 (in the foreground of figure a) and P8 (in the background of figure a and in figure b). Recirculation pumps P9 c) and internal recirculation pump P10 d).....</i> | <i>57</i> |
| <i>Figure 3. 21: main elements composing the emission system: radiators (gyms, offices and lockers) and air heaters</i> | <i>58</i> |
| <i>Figure 3. 22: weather station at the solar field – Palacus</i> | <i>60</i> |
| <i>Figure 3. 23: boiler room overview – the yellow rectangles identify the main hardware of the DAS</i> | <i>61</i> |
| <i>Figure 3. 24: one of the control screens accessible even remotely, reporting the plant scheme and the main measured parameters</i> | <i>61</i> |
| <i>Figure 3. 25: example of analog a) and digital b) sensors within the plant.....</i> | <i>62</i> |
| <i>Figure 3. 26: 3D view of the sport palace Palacus with the main outline of the different indoor environments (source Google Earth)</i> | <i>65</i> |
| <i>Figure 3. 27: satellite view of the facility and the external courts</i> | <i>66</i> |
| <i>Figure 3. 28: DHW usage based on DHW storage tank temperature profiles. Typical day trends for a) summer and b) winter</i> | <i>67</i> |
| <i>Figure 3. 29: average hourly daily profiles for residential (Right axis plot, orange line) and non-residential applications (left axis plot, green – office building, red – restaurant, blue – hotel) (142)</i> | <i>69</i> |
| <i>Figure 3. 30: reference DHW hourly profile implemented in the numerical simulation.....</i> | <i>70</i> |
| <i>Figure 3. 31: particular of the roof of the sport palace.....</i> | <i>70</i> |
| <i>Figure 3. 32: most common opaque panels and windows of the sport palace</i> | <i>71</i> |

| | |
|--|-----|
| Figure 3. 33: monthly need for space heating for the sport palace Carmine Romanzi..... | 71 |
| Figure 3. 34: reference profile for daily SH need considered for the sport palace Carmine Romanzi. The vertical axis is unitless since it depends on different parameters (e.g., external temperature, solar radiation) | 72 |
| Figure 3. 35: supply (orange line) and return (blue line) temperatures of the radiators circuit | 73 |
| Figure 3. 36: thermal energy provided by the heat pump (q_{cond}) against a reference working year. Out of heating seasons no value is reported since the bypass is likely to be active most of times. ... | 75 |
| Figure 3. 37: detail of the functional scheme of the solar field up to the interface with the HP evaporator. Colour code: blue line – cold water; red line – hot water; dotted lines indicate the solar bypass. More information is available in the Annex and in Figure 3. 15 | 77 |
| | |
| Figure 4. 1: scheme of the validation model for the PVT panels..... | 84 |
| Figure 4. 2: monthly photovoltaic production (measured in blue and simulated in orange). Reference year 2019 (134)..... | 85 |
| Figure 4. 3: reference day adopted to validate the hybrid panels during a sunny day (29/08/2019) – colour code: orange – solar radiation [W/m^2]; blue – external air temperature [$^{\circ}C$] | 86 |
| Figure 4. 4: reference day adopted to validate the hybrid panels during a cloudy day (04/11/2019) – colour code: orange – solar radiation [W/m^2]; blue – external air temperature [$^{\circ}C$] | 86 |
| Figure 4. 5: comparison between simulated (blue dotted line) and measured (orange line) panel temperature under the same weather conditions for cloudy (a) and sunny (b) days..... | 87 |
| Figure 4. 6: example of the volume segments composing the tank when stratification occurs (186) | 88 |
| Figure 4. 7: numerical and measured trends for water in DHW1 and DHW2 tanks during night when the plant is off..... | 89 |
| Figure 4. 8: schematic representation of the elements and regulation systems implemented inside the HP component (186) | 90 |
| Figure 4. 9: simplified TRNSYS model of the HP | 91 |
| Figure 4. 10: HP heating modes (1 – bypass active; 2 – HP on using the liquid source). Colour code: orange: outlet temperature within the tank; grey horizontal line: set point value to switch between the bypass and the HP working; blue: heating mode | 92 |
| Figure 4. 11: schematic representation of the differential controller working HP component (186) | 93 |
| Figure 4. 12: TRNSYS model to validate the variable speed pump and the associated controllers.. | 94 |
| Figure 4. 13: forcing function for the temperature at the outlet of the panel (T_H – orange line), the bottom of the 500 l solar storage interfaced with the HP (T_L – grey line) and the difference in temperature between solar field outlet and inlet water (ΔT_{pan} – grey line)..... | 95 |
| Figure 4. 14: variation of the control signal (grey line, right axis plot) depending on the difference between the upper (outlet panel temperature) and lower (temperature at the bottom of the solar tank) temperatures (yellow line) and the difference temperature between outlet and inlet water of the solar field (blue line)..... | 96 |
| Figure 4. 15: layout of the SAHP plant model used in the validation a) and simplified schematic representation b). Colour code: blue line – cold water; red line – hot water; green, dotted line – weather connections; pink dotted line – logical/control connection | 97 |
| Figure 4. 16: Validation of T2 (a), T3 (b), T4 (c), T5 (d) and T10 (e), as previously illustrated in Figure 4. 15..... | 101 |
| Figure 4. 17: solar tank, qualitative position of the inlet/outlet circuits and of sensor T10 | 102 |

| | |
|---|-----|
| <i>Figure 4. 18: layout of the SH subsystem numerical model a) and simplified schematic representation b). Colour code: blue line – cold water; red line – hot water; green, dotted line – weather connections; pink dotted line – logical/control connection</i> | 103 |
| <i>Figure 4. 19: detail of Figure 4. 18, outlet collector of the SH subsystem</i> | 104 |
| <i>Figure 4. 20: linear criterion for automatic evaluation of the T_{18} set point value as a function of the external ambient temperature (T_{amb_ext})</i> | 104 |
| <i>Figure 4. 21: hourly temperature for external air for a reference year obtained averaging the hourly values recorded over different years for the location of Genoa</i> | 105 |
| <i>Figure 4. 22: schematic representation of the heat exchanger component (186)</i> | 105 |
| <i>Figure 4. 23: simulated difference between supply (T_{18}) and return (T_{15}) water temperature of the radiator circuit according to the external air temperature (T_{amb_ext})</i> | 106 |
| <i>Figure 4. 24: Supply temperature for the radiator circuit on January 31st, 2019</i> | 107 |
| <i>Figure 4. 25: Supply temperature for the radiator circuit on March 15th, 2019</i> | 108 |
| <i>Figure 4. 26: Supply temperature for the radiator circuit on March 15th, 2019</i> | 108 |
| <i>Figure 4. 27: layout of the DHW subsystem numerical model a) and simplified schematic representation b). Colour code: blue line – cold water; red line – hot water; green, dotted line – weather connections; pink dotted line – logical/control connection</i> | 110 |
| <i>Figure 4. 28: detail of the DHW circuit (yellow rectangle in Figure 4. 26)</i> | 110 |
| <i>Figure 4. 29: detail of the technical hot water to produce DHW (green rectangle in Figure 4. 26)</i> | 111 |
| <i>Figure 4. 30: comparison between DHW layout and assumption of the DHW boilers. Colour code: blue line – cold water; red line – hot water</i> | 112 |
| <i>Figure 4. 31: simulated (blue line) and measured (orange line) trends for T_{16} – temperature of the hot technical water entering the DHW tank</i> | 113 |
| <i>Figure 4. 32: simulated (blue line) and measured (orange line) trends for T_{14} a) and T_{19} b)</i> | 114 |
| <i>Figure 4. 33: complete overview of the plant layout modelled in TRNSYS environment. Please refer to the subsystems illustrated before for a better insight into the plant as a whole. Colour code: dotted pink line – control/logical connection; red line – hot water pipes; blue line – cold water pipes; dotted green line – weather connection</i> | 115 |
| <i>Figure 4. 34: Monthly primary energy need, simulated (blue) and design (orange) values</i> | 117 |
| <i>Figure 4. 35: Monthly thermal energy delivered by the SAHP-PVT (including the solar bypass), simulated (blue) and design (orange) values</i> | 117 |
| <i>Figure 4. 36: Monthly thermal energy delivered by the integration gas burners (both SH and DHW), simulated (blue) and design (orange) values</i> | 118 |
| | |
| <i>Figure 5. 1: comparison of the monthly thermal energy delivered by the SAHP in the case of insulated connection pipes (blue, negligible thermal losses) and not insulated (orange)</i> | 121 |
| <i>Figure 5. 2: comparison of the monthly PV production with insulated and not insulated pipes</i> | 122 |
| <i>Figure 5. 3: percentual electric consumption during different time slots as outlined in Figure 5. 4 (left axis plot) and monthly peak absorbed power (yellow – right axis plot)</i> | 129 |
| <i>Figure 5. 4: definition of the three different time slots F1, F2 and F3</i> | 129 |
| <i>Figure 5. 5: plot of the thermal energy produced by the solar bypass at different climatic zones</i> | 133 |
| <i>Figure 5. 6: plot of the thermal energy produced by the SAHP at different climatic zones</i> | 133 |
| <i>Figure 5. 7: simulated SCOP of the SAHP-PVT at different locations, regression line and correspondent equation</i> | 134 |
| <i>Figure 5. 8: climatic zones over the Italian territory (200)</i> | 135 |

List of tables

| | |
|--|-----|
| <i>Table 2. 1: main experimental studies on SAHP, with HP sizes, average COP and references</i> | 42 |
| <i>Table 3. 1: PVT module technical information</i> | 47 |
| <i>Table 3. 2: COP according to the outlet condenser and evaporator temperatures [°C]</i> | 50 |
| <i>Table 3. 3: summary table of the main pumps within the pilot plant – SH subsystem, including information about their positioning, power and reference to figures</i> | 55 |
| <i>Table 3. 4: summary table of the main pumps within the pilot plant – DHW subsystem, including information about their positioning, power and reference to figures</i> | 58 |
| <i>Table 3. 5 Main annual operating data of the Palacus Sport Palace</i> | 63 |
| <i>Table 4. 1: Main characteristics and global thermal loss coefficient for the tanks of the pilot plant.</i> | 88 |
| <i>Table 4. 2: simulated and measured average daily COP during the initial testing of the facility (from 2014, April, 18th to May, 1st)</i> | 98 |
| <i>Table 4. 3: comparison between simulated (Sim) and design (Des) monthly performances</i> | 116 |
| <i>Table 5. 1: adopted criteria and chosen elements for efficiency simulation.</i> | 119 |
| <i>Table 5. 2: comparison of monthly performances with/without the connection pipes between the solar field and the boiler room</i> | 120 |
| <i>Table 5. 3: monthly electric production of the hybrid field with/without pipes insulation</i> | 122 |
| <i>Table 5. 4: primary energy need, energy provided by the SAHP-PVT and the percentual coverage in the case of insulated and not insulated pipes</i> | 124 |
| <i>Table 5. 5: comparison of the solar bypass with the SAHP from April up to October</i> | 125 |
| <i>Table 5. 6: estimation of the achievable savings – case of SAHP + burner on</i> | 125 |
| <i>Table 5. 7: estimation of the achievable savings – case of bypass + burner on</i> | 126 |
| <i>Table 5. 8: main results of the performance of the PVT coupled to the SAHP</i> | 127 |
| <i>Table 5. 9: total electrical need of the Palacus sport palace, information taken from the energy bills</i> | 128 |
| <i>Table 5. 10: estimation of monthly electric self-consumption basing on the information within the energy bills and the PV production</i> | 130 |
| <i>Table 5. 11: cities adopted to simulate the performance of the SAHP-PVT, with the correspondent Degree Days (DD) and climatic zones</i> | 131 |
| <i>Table 5. 12: duration of the heating season according to the climatic zone</i> | 132 |
| <i>Table 5. 13: monthly thermal energy produced by the SAHP-PVT (including the solar bypass) at the five cities</i> | 132 |
| <i>Table 5. 14: percentual extension of the climatic zones over Italy</i> | 135 |

1. INTRODUCTION

“We have been hostages of our way of thinking for a long time. We seem to act only because of fear. The topic of sustainability comes from fear as well, fear of destroying our planet and this unleashes the best energies we have. But in the name of fear. We seem to have lost that human capability to conquer the future because we want, because we are daydreamers, to have a better opportunity. We are no longer used to burning the bridges behind us. And this slows us down tremendously, because a part of our mind is still thinking how to save the past, while inventing the future.”

Alessandro Baricco

The current political situation, the crisis makes the topics of energy independence and decarbonisation even more actual, as the oil crisis in the 70s enhanced the very first steps in energy efficiency strategies. *Figure 1. 1* shows the historical chart for crude oil prices (1).



Figure 1. 1: crude oil prices per barrel historical chart (1)

When the war among Israel, Egypt and Syria broke out, in 1973, the prices for crude oil experienced a steep increase from less than 40 \$ up to 140 \$. Then the maximum peak reached occurred in 2008 (180 \$ per barrel) because of the tensions due to the nuclear policy carried out by Iran. Luckily, the peak in the price was concerned with a very brief period (differently from the crisis in 1973) and the trend oscillated between 60 \$ (2015) and 100 \$ reaching the historical lowest value (20 \$) during the coronavirus pandemics in 2020.

The Russian invasion of Ukraine has determined a new steep increase in the oil prices, occurred within just a couple of weeks, reaching values which are comparable to the ones in 1973 (100 \$, still increasing with no apparent sign of arrest). The political and economic situation are recreating very

similar conditions to the ones in 1973 in which the energy efficiency topic was taken in the centre stage on national policies.

The European countries are burning the bridges of fossil (Russian imported) fuels behind them, not for energy but for political reasons and this represents our greatest chance to definitively step into an energy system fully based on renewable and more green energy sources.

Actually, the immediate response of many European countries (e.g., Italy and Germany) is the reactivation of many coal-fired power stations which had just been dismissed to stop excessive pollution (2), (3). This is the clearest proof that all the efforts made in the past fifty years (from 1973) have not led to a concrete change in the energy generation process. Indeed, the current crisis has clearly highlighted that fossil fuels still lie in the core of our economy while the renewable sources are still left aside neither they are trusted to grant our energy demand.

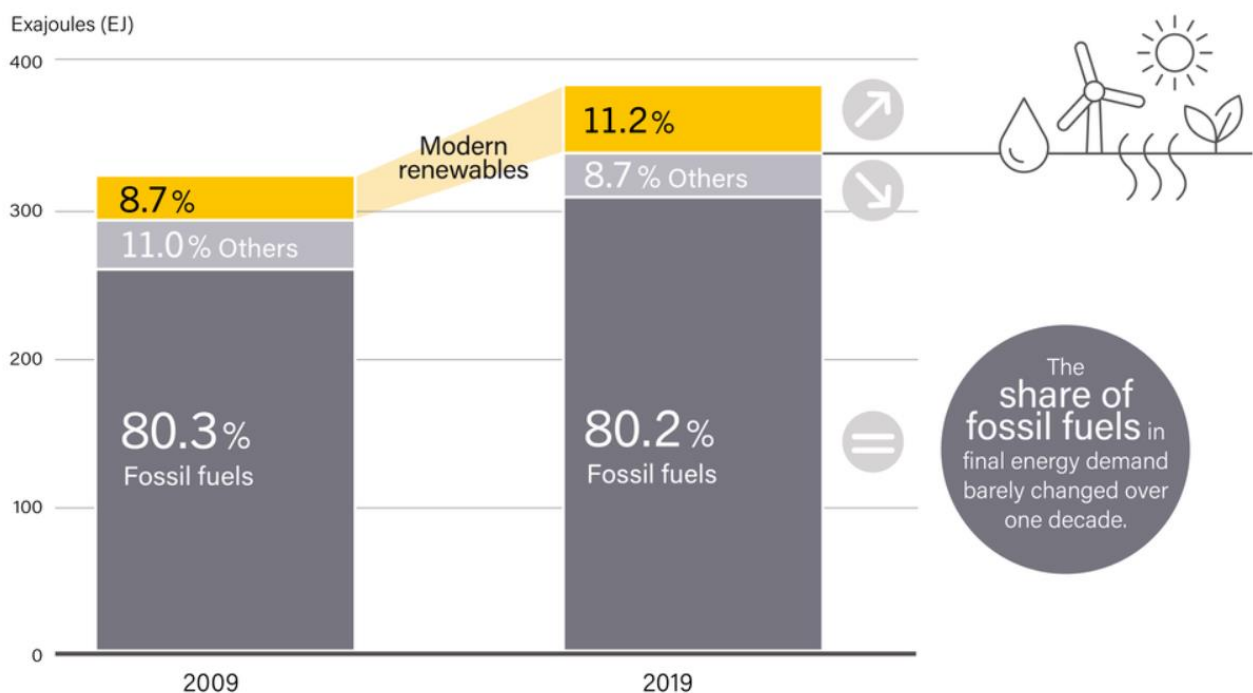


Figure 1. 2: Estimated renewable share of total final energy consumption (4)

Figure 1. 2 reports that the share of fossil fuels in the final energy demand has remained almost unchanged over the past decade. The total values reported above can be then distinguished into the three main energy consuming fields: climate control, transport and power (Figure 1. 3). For each, the percentage granted by means of renewable sources is very low. The maximum (27.1%) is reached for power plants, while the minimum (3.4%) corresponds to the sector of transport. As far as heating and cooling are concerned, the renewable energies take part for only 10.2%.

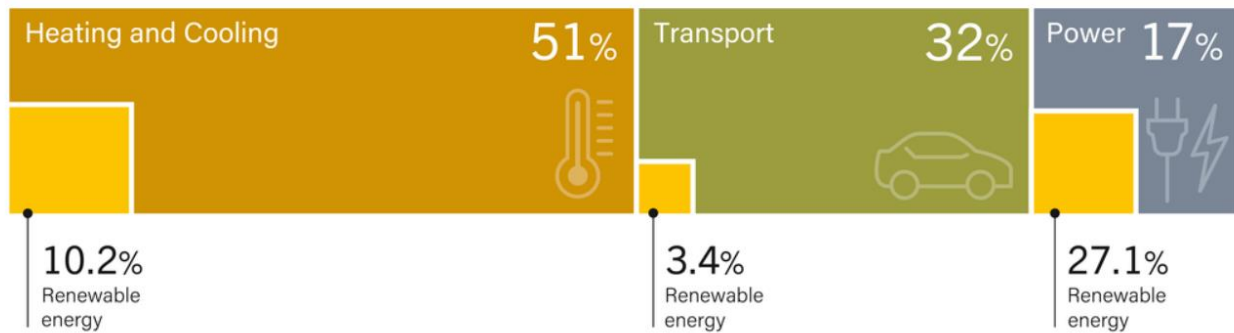


Figure 1. 3: Renewable share of total final energy consumption – reference year 2018 (4)

Once again, the watchword is sustainability: we don't have to abandon the goals reached in the past years in terms of comfort and green energy production, because the main energy fossil vectors are lacking. The challenge is tough, but the overturning of the trends above has become mandatory. The concepts of sustainability and innovation must become part of our way of thinking to shift from localised, polluting and monopolised fossil energy sources to others such as hydrogen, solar, wind, hydroelectric which still have a great unexpressed potential and a wider availability over the different countries.

The present work is focused on solar assisted heat pumps, which belong to the group of plants based on more renewable sources.

The solar thermal panels can be now considered both mature and technically reliable, thanks to their diffusion over the past couple of decades. However, they were mainly sold and employed as an integration to a conventional hot water or space heating system. Also due to the current events, the development of hybrid systems is the main target soon to grant a plant completely based on renewables, capable to cover the entire energy demand (space heating and domestic hot water) of buildings exploiting from time to time the available energy sources.

One very promising possibility is the combination of solar systems and heat pumps giving light to the so called solar assisted heat pumps. This technology has experienced a former diffusion in the stage of pilot plants which was not followed by a tangible market diffusion and a widespread application. The main obstacle was concerned with the need of a too advanced level of automatization to grant a continuous control on the plant to prevent any block.

Anyway, such plants still have an unexploited potential highlighted both by theoretical studies and by policies carried out by institutions. For instance, the International Energy Agency has provided a specific Task (Task 44) of the Solar Heating and Cooling (SHC) Programme, to work on methods towards most effective use of solar heat pump systems for residential use (5).

Their complexity influences their diffusion on the market and the lack of a common design approach leads to experimental facilities with very different layouts and working conditions since the installations are "hand-tailored". The components (e.g., solar panels, heat pumps) adopted in the plant might be either taken from the market or specifically built and a large variety of them is available (e.g., direct/indirect expansion heat pumps, hybrid/thermal solar panels). Some heat pumps might use different sources (i.e., air and solar) either in series, or parallel or both. As a consequence, the performances of the different theoretical/experimental solar assisted heat pumps are usually hardly comparable. Many works available in literature do not clearly define the boundary conditions applied

to the solar assisted heat pump, making it difficult to compare different systems in equivalent conditions. Anyway, a common feature of all plants is the transient regime working condition which in turn requires advanced numerical simulations since steady state analysis can lead to misleading results, even for preliminary analyses.

Chapter 2 provides a review about the solar assisted heat pumps from their introduction in the 80s up to nowadays, with a highlight on the gap between theoretical and experimental models. The formers clearly state the high efficiency and performance of such technology while the latters still reach results that not always meet the expected results.

Chapter 3 focuses on the case study of the hybrid solar assisted heat pump that provides space heating and domestic hot water to the Palacus sport palace. Some of its singular features consist in its size (e.g., heat pump peak thermal power of 48 kW) and in the coupling of the pilot plant to a real facility where the needs are not simulated in laboratory, but they are real and user dependent. Such installation is provided with an extended data monitoring and acquisition system (e.g., about 50 control points) which is intended to replace human management since an almost continuous control of the plant is required to choose the working conditions which always grant the best performance. The plant has been active since 2013 and the University working group has had the chance to join the plant management team, collecting relevant information about the plant working and its critical issues, mainly associated to the plant durability and its performance as components are subjected to aging and ruptures. In the present chapter the layout of the plant will be presented, united with the characterisation of energy demand for both space heating and domestic hot water production. Then the critical features shall be presented outlining the aspects that can be improved. Indeed, almost all works carried out deal with solar assisted heat pumps performance neglecting the influence of durability on the efficiencies.

Chapter 4 faces the modelling of the plant by means of transient numerical simulation in TRNSYS environment and it illustrates the validation of the different components of the facility reported in the previous chapter basing on the data collected by the monitoring and control system during the plant working. Then, some configurations for optimisation are presented as conclusive part of the chapter. The plant model allows a higher level of reliability since the validation is based on the information collected during the real working of the facility. The numerical model can be used to simulate different scenarios to understand which new configuration could lead to a more effective retrofit of the plant. In fact, the costs for plant revamping are high and preliminary previsions on the achievable performances also with respect to the cost-benefit analysis are mandatory. In addition, the numerical model of the plant represents the missing link in the future management of similar complex plants. The monitoring system collects real time the plant working parameters which are in turn sent to the model. Then, the model automatically updates, if necessary, the parameters data set basing on the simulations carried out.

Chapter 5 deals with the integrations applied to the pilot plant, basing on the results of the simulations carried out and presented in chapter 4. Some have already been implemented, while others are still in the design stage. The changes apply to the plant scheme, control and building integration.

Chapter 6 resumes the main results and conclusions, including the future developments as well.

2. Solar assisted heat pumps – a review

The former studies date back to 70s-80s (6), (7), (8), (9), (10) and they all aim to couple different kinds of solar panels to heat pumps, mutually increasing the benefits and efficiencies of the two systems. The original outline of the SAHP concept dates back to the 50's with Jordan, Sporn et al, (11), (12).

One of the earliest papers (13) describes a plant based on 70 m² of single glazed, flat black coated liquid circulating copper flat plate solar collectors coupled to an air-to-air split system heat pump. It was expected to provide about 70% of the annual space heating requirements and 55% of the annual domestic water heating requirements for the home. The system was conceived to work in parallel, with the possibility to use a direct solar heating option, by means of low temperature emission system.

The first relevant diffusion occurred after the oil crisis in 1979, but the SAHP have never reached a technological readiness level comparable to other heating systems, confining their application to pilot plants or academic research facilities. Indeed, today's standards completely neglect the case in which solar panels were coupled to a heat pump as a thermal source with a consequent lack of test and methods to assess the SAHP systems. Even the market reflects the absence of significant SAHP plants diffusion. During the first decade of 2000s, different authors carried out a statistical analysis about the systems on the market, identifying on average about 10 of them on the European market (14). Such estimation was increased up to 20 in (15) while (16) carried out a more organic enquiry in 2011-2012, identifying 128 combined solar thermal heat pumps provided by 72 companies from 11 countries.

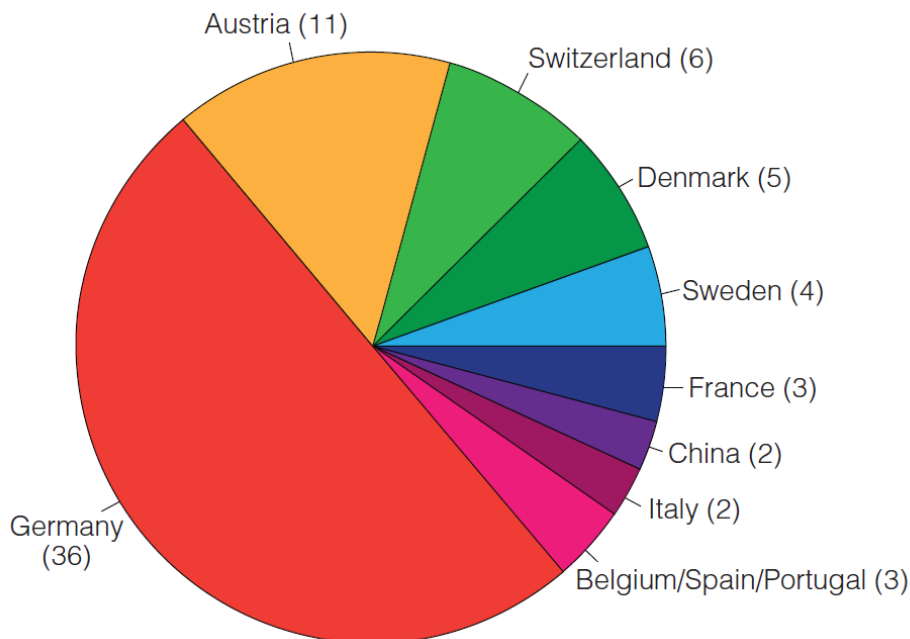


Figure 2. 1: distribution of SAHP producing companies by country- (16)

Figure 2. 1 gives very important information about the spatial distribution of SAHP technologies: among Europe, the countries with milder climate have almost no companies (Italy, France, Spain, Portugal) as well as the ones in the northern part (Sweden and Denmark) while almost 75% of companies are located in middle Europe (i.e., Germany, Austria and Switzerland). In addition, even emerging countries (China) were not really interested in the SAHP at the period of the research. In conclusion, such spatial distribution highlights one of the first actual limits of SAHPs described later

more in detail: the diffusion of solar assisted heat pump in southern countries with mild climate is low due to the lack of economic advantages with respect to the simpler and cheaper air to air heat pumps. Moving from the geographical spread to the distribution over time of SAHP companies (*Figure 2. 2*), just few new ones have entered the market in the past year. In addition, a direct link between the number of new companies and the oil prices can be noticed comparing *Figure 2. 2* with *Figure 1. 1*.

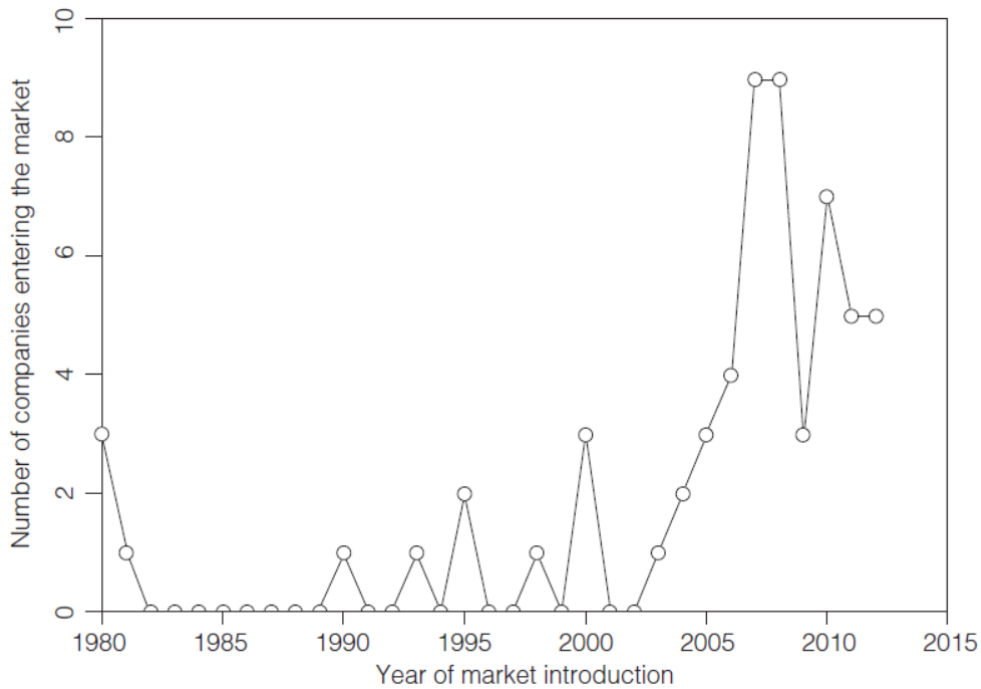


Figure 2. 2: new companies for SAHP production entering the market every year (16)

On the other hand, northern countries tend to adopt stable, low-temperature sources which are more suitable to colder climates (e.g., ground sources). For instance, about 590.000 ground source heat pumps are estimated to have been installed in Sweden in the past three decades. Nowadays about 5-10 new plants per year are installed on average (17). As far as countries with emerging economies are concerned, there is still no real interest in the SAHP diffusion due to the economic and policy asset of the country. However it is important to remember that a relevant contribution on the research topic is coming from countries with emerging economies such as China, (18), (19), (20).

Going more in detail, in northern Italy only about 1000 small SAHP plants have been installed during the past years. In our region (Liguria) there are only three operative facilities active: a direct expansion prototype with hybrid panels tested at Cus Genova (*Figure 2. 3*), the SAHP with PVT panels pilot plant at Palacus – Genoa (*Figure 2. 5*) and a SAHP heating system for a swimming pool located in Sestri Levante (GE) (*Figure 2. 4*).



Figure 2. 3: prototype of solar assisted heat pump with hybrid panels at Cus Genova (21)



Figure 2. 4: solar assisted heat pump with bare solar thermal panels – Sestri Levante (GE) – (22)



Figure 2. 5: solar assisted heat pump pilot plant with hybrid panels at Palacus – Genoa

Despite of the statistical analysis, the deep and cyclic interest arising about solar assisted heat pumps is concerned with the potential, linked to the configuration of low temperature sources with heat pumps. Such coupling extends the operating range even to conditions where the single components could not operate, for instance a day with low air temperature that would block or significantly reduce the efficiency of an air-to-air heat pump. For instance, *Figure 2. 6* illustrates the advantages in terms of Primary Energy Saving (PES) for solar assisted heat pumps simulated at the different 110 Italian municipalities (23).

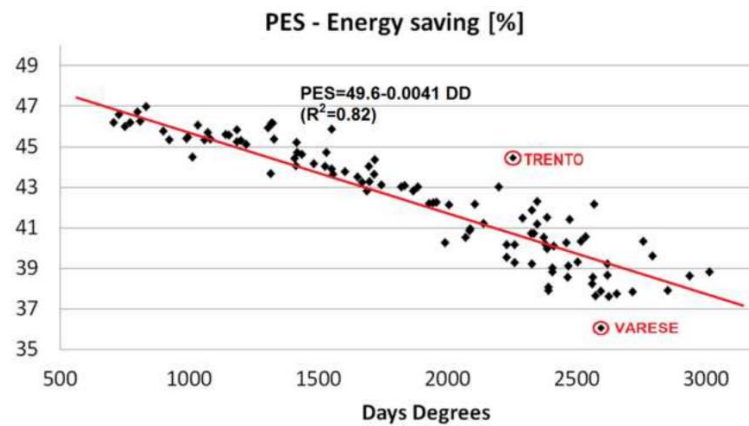


Figure 2. 6: Values of the Primary Energy Saving (PES) index according to the different 110 Italian municipalities (23)

In addition, the exploitation of multiple sources provides the plant with a further degree of resilience with different possible working conditions to use according to the climatic conditions. This improvement brings plant complications as well, in particular in the field of solar assisted heat pumps where many pilot plants are periodically built and then they are abandoned due to the lack of automatization and to the number of issues encountered managing the plants.

The present chapter is meant to provide an insight on the different, main components of solar assisted heat pumps, focusing both on the promising aspects which have been feeding the academic/industrial interest in such technology and on the actual limits which have slow down the widespread of SAHPs over the countries. A recall to a common graphic representation approach for SAHP is proposed, basing on the contents of IEA task 44 / HPP Annex 38 (16). Indeed, the great variety of components, element disposition (e.g., serial/parallel configuration of the low temperature sources) and applications (e.g., SH or DHW) lead to different plants which can be hardly comparable if not classified by means of a common approach.

2.1 Main components of the SAHPs – heat pump

The Heat Pump (HP) technology has an enormous potential for energy saving, since it allows to deliver heat at higher temperatures for more useful applications (e.g., Space Heating – SH). The principle has been well known since more than a century (24), but the interest in their application and development has raised only when the fossil costs have started to increase.

Basically, a heat pump is a heat engine operating in reverse according to the schematic representation reported in Figure 2.7:

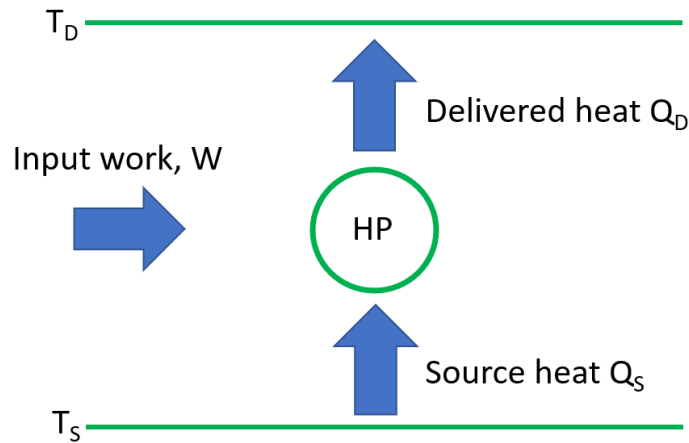


Figure 2.7: working principle of a heat pump

From the First Law of Thermodynamics, the amount of delivered heat Q_D at the higher temperature T_D is related to both the amount of extracted heat Q_S at the low temperature T_S and the work input W by means of Eq. 2. 1:

$$Q_D = Q_S + W \quad \text{Eq. 2. 1}$$

The Coefficient Of Performance (COP) is then defined as expressed in Eq. 2. 2 as a ratio between the useful effect (the delivered heat in the present case) and the input work to obtain it:

$$\text{COP}_{\text{HP}} = Q_D / W \quad \text{Eq. 2. 2}$$

Since a heat engine operating between a higher temperature T_D and a lower temperature T_S has a theoretical maximum thermodynamic efficiency (Carnot efficiency) as reported in Eq. 2. 3

$$\eta_C = (T_D - T_S) / T_D \quad \text{Eq. 2. 3}$$

Then the Carnot COP of an inverse heat engine such as the heat pump can be formulated by means of Eq. 2. 4

$$\text{COP}_C = T_D / (T_D - T_S) \quad \text{Eq. 2. 4}$$

Such value represents the upper theoretical value obtainable in a HP system. Real, measured COPs are usually far below such limit.

All heat pumps provide both a cooling and heating effect at the same time. A heat pump designed to cool at the lower temperature T_S rather than to heat at the higher temperature T_D can be called refrigerator with the consequent reformulation of Eq. 2. 2:

$$\text{COP}_{\text{Refrig}} = \text{EER} = Q_S / W \quad \text{Eq. 2. 5}$$

The relation between $\text{COP}_{\text{Refrig}}$ and COP_{HP} (Eq. 2. 6) can be outlined by combining Eq. 2. 1, Eq. 2. 2 and Eq. 2. 5:

$$\text{COP}_{\text{HP}} = \text{COP}_{\text{Refrig}} + 1 \quad \text{Eq. 2. 6}$$

Going more in detail in the working of a heat pump, the conventional cycle of vapour compression (Figure 2. 8) consists of two heat exchangers, a compressor, an expansion valve and a working fluid.

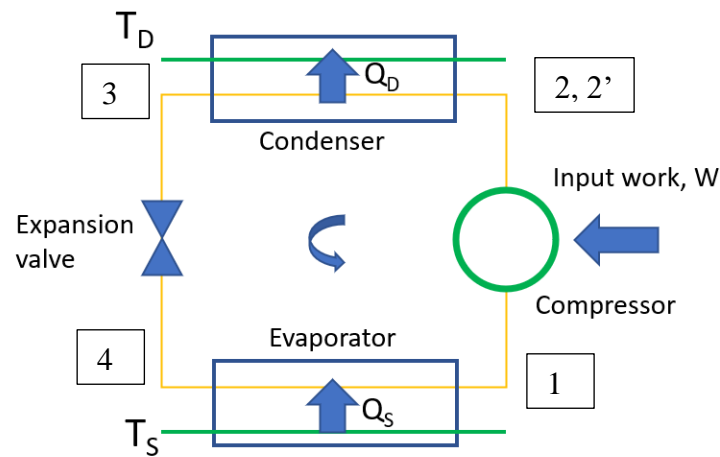


Figure 2. 8: mechanical vapour compression heat pump scheme

In the evaporator heat exchanger, the working fluid evaporates at the temperature T_{EV} by extracting heat Q_S from the low temperature source. It is then compressed and gives up its latent heat as it condenses at higher temperature T_{CO} in the condenser heat exchanger. The condensed liquid is then expanded through an expansion valve and is returned to the evaporator to complete the cycle.

The difference between the condensing and evaporating temperatures ($T_{CO} - T_{EV}$) is the gross or maximum possible temperature lift. The net temperature lift ($T_D - T_S$) is less than the gross temperature lift by the sum of the temperature difference driving forces in the evaporator and condenser heat exchangers. The Compression Ratio (CR) is the ratio of the corresponding pressures in the condenser and evaporator p_{co}/p_{ev} . All these parameters allow to determine the feasible working range of a heat pump, given the working fluid.

In practice the real heat pump cycle is in Figure 2. 9 (25). The numbers adopted correspond to the ones in Figure 2. 8 and the following main steps can be identified:

- 1-2: the vapour is compressed. Point 2' shows the result in case of an ideal (isentropic) compressor. The real case shall deviate due to two main issues: firstly, compression occurs in a definite amount of time giving rise to irreversibility with the heating of the fluid. Secondly, the volumetric efficiency is lower than 1 and this means that part of the vapour is compressed more times and it therefore absorbs energy at each cycle. The consequent excess of entropy and hence enthalpy depends on the compressor design and on the thermodynamic properties of the adopted fluid.
- 2-3: the first part is concerned with superheat removal and since usually the heat transfer coefficient for de-superheating is lower than the one for condensation itself, a relevant part of the condenser might be involved in this process. The pressure drop associated to the de-superheating, determines a lower temperature associated to the real condensing stage with a lower COP for the cycle. Once the saturation limit curve is entered, condensation occurs and if the condenser still presents available excess surface area, the fluid can be subcooled. The subcooling would increase the delivered heat Q_S , since the outlet temperature of the condensed fluid is below the one associated to the limit curve. Usually, sub-coolings of up to 20 K can be reached by means of additional (and expensive) exchangers which can be reasonable especially for industrial

applications. As far as domestic case studies are concerned, the subcooling can increase the difference in temperature of about 5 K without any relevant improvement in the COP of the HP and it just grants that only fluid in liquid state enters the expansion valve.

- 3-4: expansion takes place in the valve almost at constant enthalpy
- 4-1: a small pressure drop is needed to let the wet vapour flow inside the evaporator as evaporation occurs and eventually the fluid is overheated if excess surface is available yet. Anyway, the stage is approximated to take place at constant pressure as both evaporation and superheating occur throughout the evaporator.

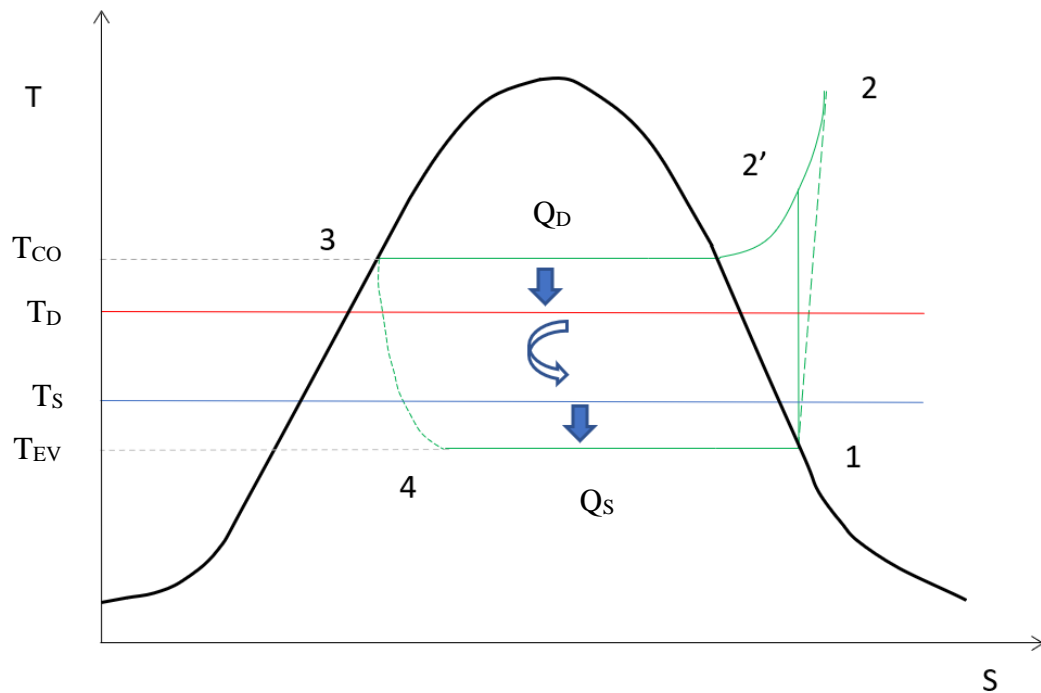


Figure 2. 9: T-S diagram with a classic vapor compression inverse cycle

Concerning the irreversibility within the real cycle which negatively affect its performance, the one associated to the expansion valve could be overcome by means of a reversible adiabatic engine providing part of the work of compression. In addition, the compression of saturated vapours results in their superheating with consequent added irreversibility due to the need to de-superheat the vapour. Such issue could be overcome by isentropic compression up to temperature T_{CO} and then compressing isothermally at this temperature up to the corresponding saturation pressure. Such improvements would increase the efficiency of the cycle, but they are too expensive to contemplate for the small obtainable increase in the COP.

As far as the COP of heat pumps is concerned, Eq. 2. 4 clearly shows that, given a fixed value of T_D , the performance of the cycle shall improve as the difference in temperature between hot and cold source ($T_D - T_S$) decreases. Indeed, T_D mainly depends on the application of the heat pump (e.g., SH) while T_S is more concerned with the (external) source with which the HP is interfaced. One of the most spread and simple solutions consists in interfacing the HP with the external air. This configuration, for instance in heating, is profitable only when the temperature of the external air shows very small fluctuations and it remains relatively high. This is typical of mild/hot climates, as occurs for most of Italian territory. Anyway, in the Countries of Northern Europe, the air temperature easily falls below 0 °C and its fluctuations over the day cannot allow the profitable use of HP

interfaced with the external air since the machine is exposed to blocks due to the freezing of the evaporator and the COP significantly reduces.

Therefore, more stable sources need to be identified. This is the case for instance HP interfaced with ground heat exchangers which usually have to reach depths of about 50 m – 100 m, according to the installation place, to reach a thermally stable layer. Except for specific geothermal areas characterized by high enthalpy, the cost for the plant construction increases also according to the kind of soil.

Another solution is concerned with the interface with water (e.g., the sea, a river, a lake, or an underground aquifer). This solution is almost always neglected for several reasons: risks of pollution, plant complexity and therefore costs, risk of death or radical change of the underwater ecosystem (which can already occur with a 1-2 °C variation).

In conclusion, the last, available source that can be interfaced with a HP either in alternative or in series to the ground heat exchanger is the solar one. The installation costs are highly influenced by the adopted type of panel (e.g., low efficiency solar thermal, collectors, hybrid panels) but they are normally lower than the ones for geothermal configuration, although solar panels represent a less stable source than ground.

The present work deals with this last option, enquiring the interface between solar panels and heat pumps.

2.2 Main components of the SAHPs – solar panels

The solar panels allow the conversion of solar energy either in usable heat (solar thermal panels – T panels) or electricity (photovoltaic panels – PV panels) or both (hybrid panels – PVT panels). The solar panels can be considered a mature technology since the former studies started in the end of the XIX century. Indeed, the first patent for domestic hot water production by means of solar thermal panels dates back to 1891 while the first patents for photovoltaic panels started to appear during the middle of the past century.

As far as hybrid panels are concerned, the very first theoretical studies were carried out during the 70s after the oil crisis occurred in 1973. Soon after the first test facilities were realized (26), (27), (28), (29), (30), (31), (32), (33), (34) adopting PVT panels, both air and water cooled, to increase the efficiency for electricity production. Then, during the 90s, researchers started to develop “hybrid” panels where the PV panel was assembled with a thermal module. The double aim was to cool the PV panel and exploit the heat (35), (36).

Among these three main groups, a large number of models is available on the market, also thanks to the continuous marketing of new panels with higher efficiencies. Figure 2. 10 shows respectively some of the most common panels available, in particular a covered and an unglazed thermal collector (a and b), a PV and a PVT panel (c and d).



a



b



c



d

Figure 2. 10: covered and an unglazed thermal collector (respectively a and b), a PV and a PVT panel (respectively c and d) (37), (38), (39), (40)

The cost of the panels is directly proportional to both their efficiency and the technological level required to produce them, starting from the unglazed solar thermal panels which represent one of the cheapest choices, up to the PVT panels which are associated to higher costs.

The actual prices, especially in Italy, are still experiencing a steep increase due to the tax relieves and more in general to the energy efficiency policies which are coming into force. Anyway, a hybrid panel is expected to cost between 2 and 3 times more than a PV panel, while the thermal panels can be installed usually with an expense between 20% and 50% of the one required for a PV panel.

In any case, some issues are shared by all the available models of solar panels:

- Time shift between daily peak production and daily peak needs: the highest production of a solar panel (both in terms of useful heat and electricity) corresponds to the hours in which solar radiation is stronger, usually at midday. On the other hand, the needs for a residential building not always occur when most of the solar energy is available. More in detail, two main daily peaks in the average hourly electricity consumption for residential buildings can be identified as shown in Figure 2. 11 (41)

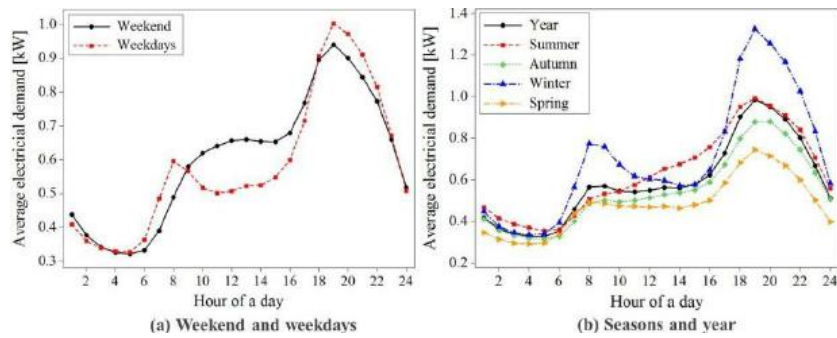


Figure 2. 11: Hourly electrical demand during weekend, weekdays, seasons and years (41)

The peaks tend to vary in terms of intensity and according to the different seasons, but they usually occur early in the morning (around 8 a.m.) and in the evening (at about 7 p.m.). This conclusion has been drawn in different countries (e.g., Australia – (41), Denmark – (42) Iran – (43), Italy – (44) and USA – (45) and it is associated to the periods in which people is more likely to be at home, independently from the day or the season.

The DHW consumption trend (Figure 2. 12) follows the same peaks as for the electrical need (Figure 2. 11) and it is quite uniform over different geographical areas (European Nordic Countries – (46), USA – (47), Canada – (48), Croatia – (49), Brazil – (50), showing the maximum need in the hours when usually inhabitants are likely to use DHW.

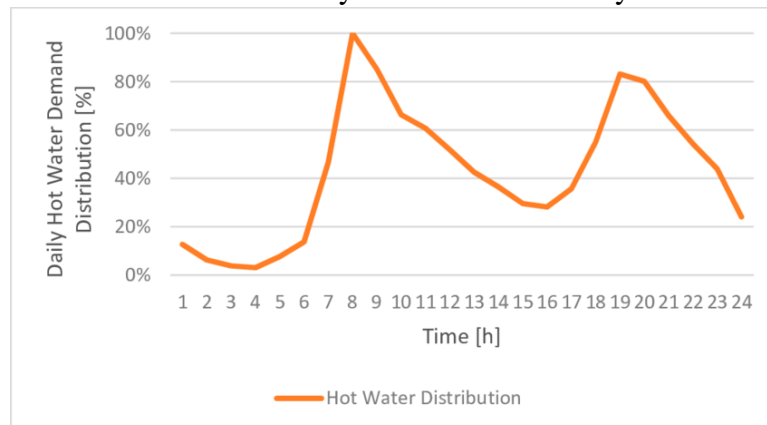


Figure 2. 12: hourly normalized hot water demand in a day for Italy (51)

Both peaks cannot be granted by direct usage of PV/PVT/thermal solar panels since the solar radiation available in those hours of the day is expected to be either low or absent. As a consequence, the systems based on solar panels need an additional element to provide thermal inertia. Solar thermal panels have always been coupled to storages since their very first applications (usually by means of water tanks) while photovoltaic systems need batteries to allow the energy storage and its usage later. Figure 2. 13 shows one of the former examples where the solar thermal panels were already connected to a thermal energy storage to gather the useful heat from the sun and exploit it when needed. Indeed, an intermittent (renewable) source needs to be coupled to an energy conversion system which can store the free available energy for a later use.



Figure 2. 13: solar house built by MIT, in 1939, (52)

This topic leads to the issue of self-consumption: the efficiency of a solar field directly depends on the amount of produced energy (either useful heat or electricity or both) that can be immediately used. Whenever a too relevant time shift occurs, the system requires energy storages negatively affecting the global efficiency, especially when PV/PVT panels are adopted. In fact, while thermal storages can even be effective over seasons for year-round heating, the current technology for batteries cannot reach such a wide time range. The national grid could replace batteries providing the inertia itself. Actually, this solution was tried up to 2019 by means of net metering and feed in tariff strategies, where people was allowed to exchange electricity with the national grid “compensating” the withdrawals with the electricity produced by the PV/PVT plant (53), (54). However, this possibility was fast abandoned due to the sudden and often unpredictable unbalance of the network between loads and withdrawals. Up to now the tax incentives in Italy (55), (56) provide an economic relief only for the initial installation cost. No refund is granted for the energy overproduction which is not self-consumed and it is immitted in the national grid. In other words, the current legislative framework aims to build almost stand-alone installations, maximising the onsite self-consumption.

The lower the panel temperature, the higher the efficiencies: besides of the useful effect (electricity or thermal energy), the working temperature of the panel has to be as low as possible to reduce losses and increase the efficiencies.

Figure 2. 14 shows the efficiency for unglazed and flat-plate thermal collectors depending on the difference in temperature between the collector fluid and the environment air.

Flat-plate collectors experience an improvement of at most 20% when the working temperature of the collector fluid is lower than the one of the surrounding air (negative part of the horizontal axis). On the other hand, the unglazed panels can even double the heat gain when working within a temperature range lower than the one of the ambient air.

The difference between the two technologies is associated to the level of insulation within the panels: the unglazed collectors usually present a very poor insulation, so the contribution of hotter ambient air can even become dominant with respect to the solar radiation. As the solar panels increase their temperature, the heat gain dramatically drops; only 20 K higher than the one of the ambient air leads to a negligible heat gain.

On the other hand, flat-plate collectors show a higher level of insulation and therefore the contribution of the heat exchange between ambient air and the panel becomes less relevant as the graph in the figure above tends to be more horizontal varying the difference in temperature between collector fluid and ambient air.

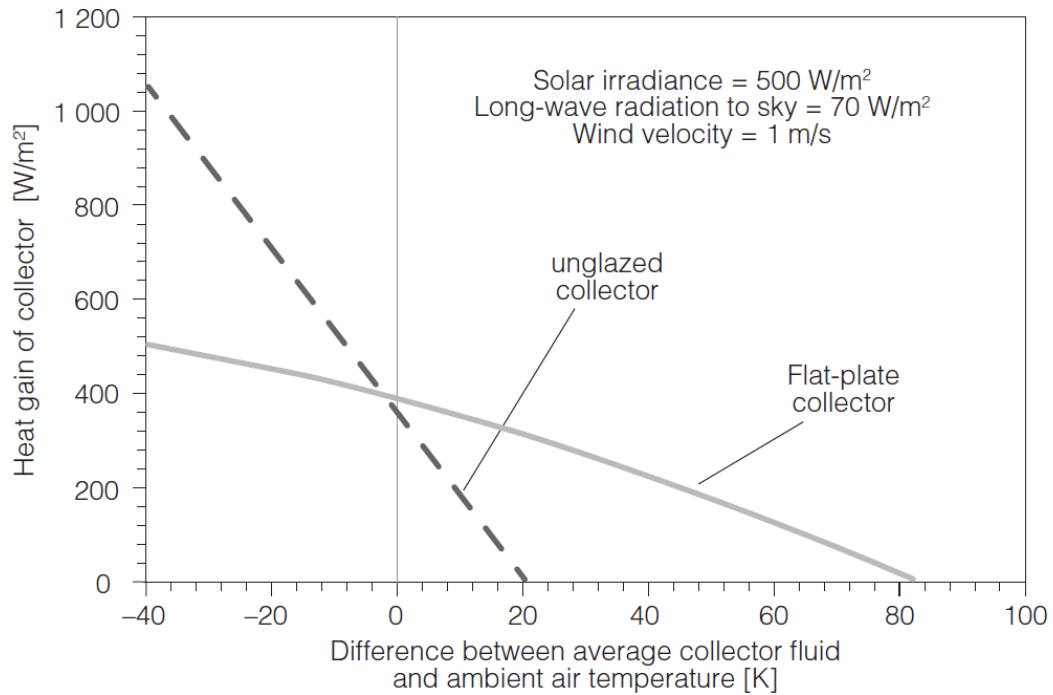


Figure 2. 14: solar thermal panels efficiency against the difference in temperature between the collector fluid and the ambient air temperature (16)

Unluckily, the working temperature of the fluid represents a design data, depending on the set point temperature that the plant is required to grant. For instance, solar thermal panels directly used to produce domestic hot water will always require a temperature of at least 50-60 °C causing the panels work at low efficiencies. On the contrary, a solar thermal panel interfaced with the evaporator of a heat pump would work at a lower range of temperatures, even reaching working temperatures below the one of the ambient air. Namely, the same panel can have far different efficiencies according to how it is employed and their operating range could be extended in case of optimal configurations (e.g., combination of solar collectors with a heat pump).

The dependence on the working temperature can be identified also in the case of PV solar panels, as shown in Figure 2. 15.

Basing on the power law, the electrical power provided by a solar panel is expressed as a product between the current (I) and the voltage (V), (Eq. 2. 7) and the cell can have a reduction of up to 30% of the provided power if its operating temperature increases of 60 K, if working at high voltages.

$$P = I V \quad \text{Eq. 2. 7}$$

Within this context, the PVT panels represent an interesting combination of thermal and photovoltaic panels. In principle, their thermal performance is expected to be lower than a standard thermal collector since the same amount of irradiation is partially converted also in electricity. In addition, the integration of thermal and photovoltaic panels requires compromises to fit the PV module with the thermal panel within one element. On the other side, the thermal side of the panel grants a low operating temperature which allows the PV cell to work at optimal temperatures with an increase in the efficiency.

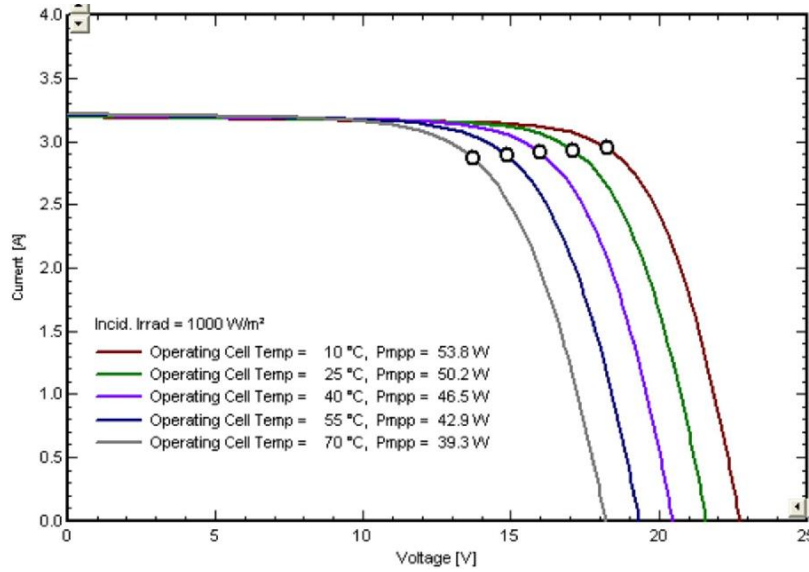


Figure 2. 15: output peak current intensity (I) against the peak voltage (V) of the PV module with different operating temperatures (57)

Eq. 2. 8 resumes the heat balance for a collector as schematized in Figure 2. 16:

$$\frac{\dot{Q}_{gain}}{A_{coll}} = \dot{q}_{gain} = \dot{q}_{rad} + \dot{q}_{amb,lat} + \dot{q}_{sens} + \dot{q}_k + \dot{q}_{rain} \quad \text{Eq. 2. 8}$$

Where

\dot{q}_{rad} is the exchange due to solar radiation, both short and long-wave length referred to the unit area

$\dot{q}_{amb,lat}$ and \dot{q}_{sens} represent the sensible and latent convective heat exchange with ambient air respectively

\dot{q}_k accounts for conduction. It is usually expected on the back of the panel

\dot{q}_{rain} is associated to the exchange with the rain

\dot{q}_{gain} is the useful effect obtained from the panel

In conclusion, one or more of these terms could be associated to both sides of the panel and they are all considered positive if incoming.

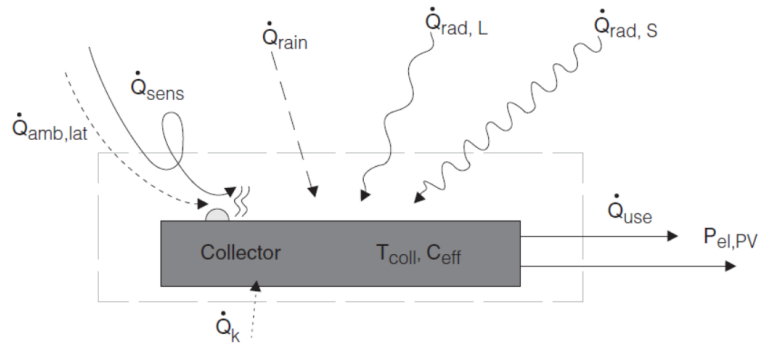


Figure 2. 16: energy balance for a PVT panel (16). The heat flows are expressed by means of capital q since they are not referred to the panel area

Eq. 2. 8 can be associated to Eq. 2. 9 which correlates the usable heat gain and the produced electric power to the internal energy exchange by means of the effective thermal capacitance of the collector.

$$\dot{q}_{use} = \dot{q}_{gain} - P_{el,PV} - \frac{\partial T_{coll}}{\partial \tau} c_{eff} \quad \text{Eq. 2. 9}$$

With

$P_{el,PV}$ electric power

$\frac{\partial T_{coll}}{\partial \tau} c_{eff}$ internal energy exchange expressed as the product between the collector effective thermal capacitance and the time derivative of the average collector temperature.

2.3 The solar assisted heat pumps

Basing on the advantages and limits of the heat pumps and solar panels illustrated in the previous paragraphs, their coupling represents an interesting compromise leading to benefits for both the main subsystems:

- Solar panel: the lower operating temperature allows a relevant benefit in the panel efficiency. Moreover, the panel still provides a relevant contribution even in days with low solar radiation since the low working temperature allows to take heat from the ambient air as well. In addition, in some plant configurations, the panel can also bypass the heat pump when the working temperature is near the required set point with an added energy saving.
- Heat pump: the solar panel represents a more stable source with which the evaporator can exchange heat with a relevant increase in the COP. Such configuration even extends the HP operating range to ambient air temperatures at which a normal air-to-air heat pump would either block or reach a very low COP. In case the solar panels were hybrid, part or most of electricity consumed by the heat pump would be covered without any withdrawal from the national grid, with a further improvement of the COP. Indeed, the coefficient of performance of a mechanically driven heat pump defined by Eq. 2. 2 is the ratio of the useful effect (heat output) to the work input to the compressor. This formulation does not account for the efficiency of usage or the method by which this work is produced. When comparing heat pump systems driven by different energy sources, the use of the Primary Energy Ratio (PER, Eq. 2. 10) (58) can be more appropriate:

$$\text{PER} = \text{Useful delivered heat} / \text{primary energy input} \quad \text{Eq. 2. 10}$$

The PER coefficient can be then related to the COP by means of Eq. 2. 11

$$\text{PER} = \eta \text{COP} \quad \text{Eq. 2. 11}$$

Where η is the efficiency with which the primary energy input is converted into work up to the shaft of the compressor. Assuming an electrically driven compressor with the electricity generated from a coal burning power plant, the efficiency may even reach values of 0.25. On the other hand, if the energy were entirely produced by a PV/PVT solar panel, the value would reach a theoretical limit of 1.00. Always on a theoretical side, the SAHP allows the elimination, or better a relevant reduction, of the primary fossil energy consumption, by replacing it with renewable energies.

Considering that the total self-consumption is not feasible nowadays the real value for η could reach up to 0.5-0.75 also depending on the characteristics of the energy storage (batteries) and on the distribution of time of the thermal needs (e.g., SH or DHW), since a little withdrawal from the grid is always present.

However, energy systems tend to be judged on their potential money savings rather than their potential energy savings and therefore the PER index should always be associated to its price. From this point of view, as the cost for the input energy PER increases, the economics of SAHPs will become more favourable, especially if the components of such systems are mass produced with lower initial installation costs. In conclusion, the number of operating hours per year plays a central role in the analysis as well since the more a facility is used, the shorter is the payback period.

Focusing back on the main topic, there are multiple configurations for solar assisted heat pumps, basing, for example, on the system function (i.e., SH, DHW, space cooling) and concept (the way different subsystems interact inside the plant) or heat and collector characteristics. In these terms, a single parameter such as the Seasonal COP or SCOP could be hardly comparable among different plants, due to location, sizing of the elements, application, refrigerant adopted and to the aspects illustrated above.

The present section is also meant to illustrate a common graphic approach to frame all the possible SAHPs to allow a comparison among the different solutions. The method (16), (59), is based on the energy flow charts which are commonly used in building energy engineering and it can be better understood focusing on *Figure 2. 17*. It tries to collect and resume the main descriptive criteria differently adopted by Authors: useful energy delivered, low temperature sources interfaced with the HP, quantity and function of energy storages and different interactions (14), (15), (59), (60). This plant depiction allows a common approach to classify especially from a qualitative perspective all the different plant configurations, before enquiring in detail the technical performance information.

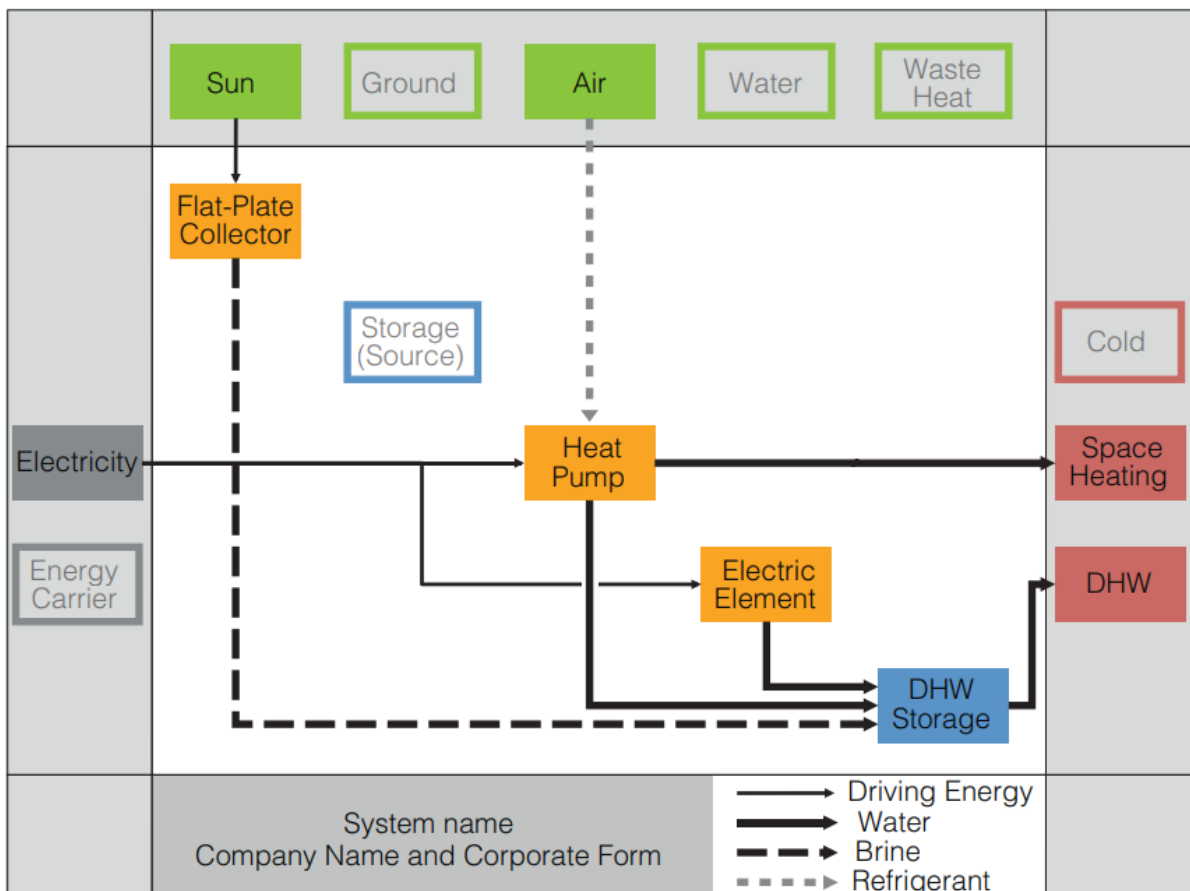


Figure 2. 17: example of the graphic method for SAHP categorization (16)

The plant lies in the centre of the graph while SAHP systems can be divided in most of cases into four key components: collector, heat pump, backup heater and storages (usually one on every side of the HP). The following colour code can be adopted:

- Objects code:
 - o blue: energy storing elements, for instance DHW tanks or batteries
 - o orange: energy transforming components, for instance solar panels or heat pumps
 - o green: energy sources (e.g., solar, geothermal, air but waste heat as well, if present)
 - o red: useful energy – i.e., DHW, SH or cooling
 - o dark grey: energy carrier of the system
- Background code:
 - o grey: region for boundary conditions
 - o white: area for the plant scheme.
- Line code: they grant the representation of energy flows among the different components and boundaries according to the medium which carries energy. Most of times, such graphical representation tends to depict energy flows in up-down and left-to-right direction.

Focusing on the different SAHPs assets, three main configurations are available which can be then combined to reach more efficient, yet complicated, plants:

- *Serial asset*: the low temperature elements (e.g., solar panels, geothermal boreholes) exclusively represent a source to which the heat pump is interfaced. No direct connection between the low temperature sources and the useful energy production (e.g., DHW or SH) is present. In this configuration, the collector working temperature may be lower than the one of the ambient air, in order to gain heat by means of both solar radiation and ambient air, with almost negligible thermal losses.
- *Parallel asset*: the low temperature sources can either work coupled to the HP or for direct production of useful energy independently from the HP, according to internal efficiency criteria (Figure 2. 18). In this asset the working temperature of the collector is expected to be higher than in the case of serial asset, affecting the panel efficiency as well (Figure 2. 14).

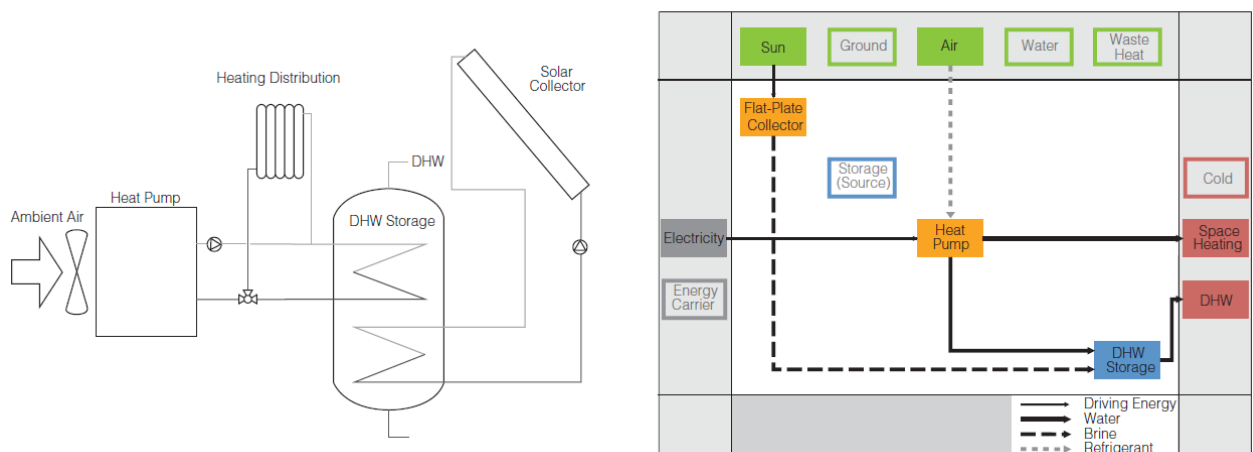


Figure 2. 18: plant of a parallel asset SAHP layout and its graphical representation (16)

- *Regenerative asset*: a low temperature, secondary source can be used to warm or heat again the primary source of the heat pump, as it can occur for solar thermal panels coupled to a geothermal heat pump (Figure 2. 19). This last arrangement can be seen as either a composition of sources in series or as a serial asset heat pump where the ground is used as highly inertial heat storage (61).

Very often the plants are designed by means of different combinations of these arrangements, since the serial asset allows only one operating mode, while every configuration can add a further degree of freedom to the plant, to reach always the best possible performance according to the boundary conditions.

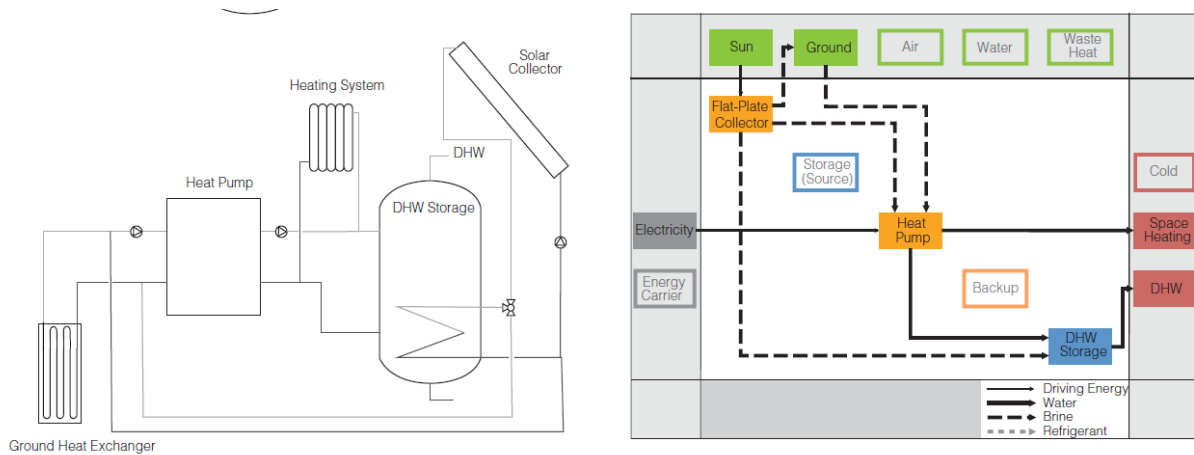


Figure 2. 19: plant of a regenerative/parallel/series asset solar assisted/geothermal HP layout and its graphical representation (16)

In addition to the assets above, the heat pump can either expand directly or indirectly. The direct expansion SAHP (Figure 2. 20) is the simplest configuration where the collector work as the evaporator of the HP as well. The panel is cooled down directly by the refrigerating fluid flowing inside which in turn evaporates. The exploitation of the phase change mechanism allows a very good stability of the collector working temperature while on the other hand freezing inside the collector might occur. In addition, as the collector size increases such configuration becomes less effective since the pressure drops inside the evaporator become more relevant and the distribution of the refrigerant inside the panels might no longer be uniform. Various studies are available in literature with theoretical/practical simulations leading to a COP between 4 and 6 (62), (63), (64), (65).

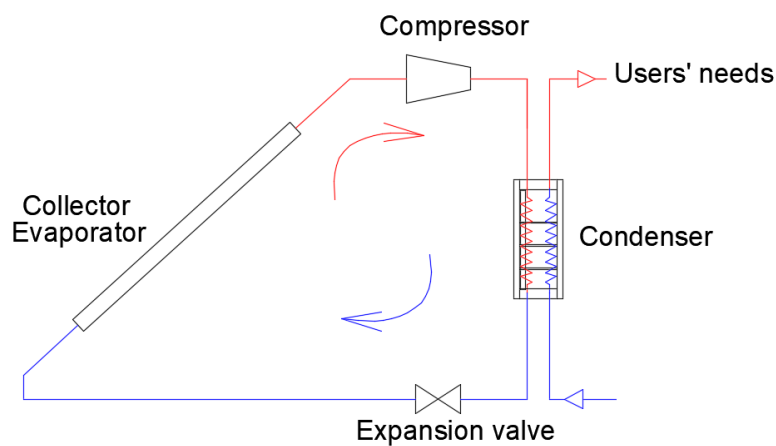


Figure 2. 20: Schematic representation of a direct expansion SAHP.

On the contrary, the indirect expansion SAHP (Figure 2. 21) has a more complex scheme with respect to the direct expansion one since in the basic configuration, an exchanger divides the heat pump circuit (with refrigerant flow inside) to the collector circuit (where a working fluid such as water is used). The exchanger works as the evaporator, benefitting from the thermal contribution of the collectors. Moreover, the hydraulic decoupling between the heat pump and the solar field allows more stability even with the increasing size of the collectors. On the other hand, the presence of more

components within the plant lead to lower efficiencies, making the use of indirect SAHPs advisable only in presence of middle/big solar fields. Concerning the COP, the experimental studies and the prototypes lead to COP between the range of 2.5-4. (66) (67), (68), (69).

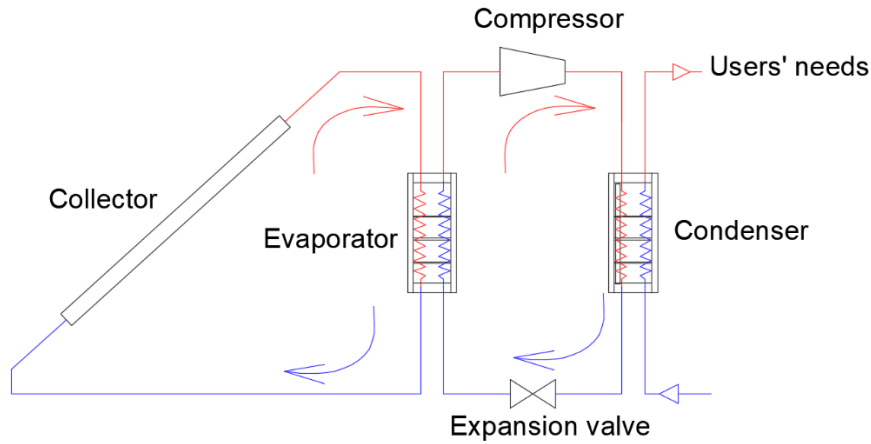


Figure 2. 21: Schematic representation of an indirect expansion SAHP.

More in general, the collectors can be interfaced both with the cold and the hot side of a heat pump. In the former case, the temperature of the cold source is increased with a consequent improvement of the HP COP. On the contrary, in the latter the panels can integrate or replace the heat provided by the HP. Clearly, if the HP is either absent or off, the solar irradiance is lost in case the collector temperature was lower than the required set point temperature to supply the energy needs of the facility (e.g., SH/DHW). In principle, the adoption of a higher COP and panel efficiency does not necessarily lead to better performances of the SAHPs. Haller, Frank et Al. (70), (71) formulated a theoretical principle to establish whether parallel or serial asset is most effective, according to the collector yield and the HP COP (Eq. 2. 12):

$$\frac{\Delta COP_{HP}}{(COP_{HP,par} - 1)} \cdot \frac{\Delta \eta_{coll}}{\eta_{coll,par}} > 1 \quad \text{Eq. 2. 12}$$

Where

$COP_{HP,par}$ is the COP associated to a HP working in parallel asset with another source, ambient air for instance

ΔCOP_{HP} is variation in COP using the solar source either in serial or parallel asset, $\Delta COP_{HP} = COP_{HP,ser} - COP_{HP,par}$

$\eta_{coll,par}$ is the collector yield in case the panels were used in parallel asset

$\Delta \eta_{coll}$ represents the difference between the panel efficiencies in serial and parallel assets,

$$\Delta \eta_{coll} = \eta_{coll,ser} - \eta_{coll,par}$$

Clearly, a difference in the efficiencies of the solar panels shall be expected since the working temperatures in the two configurations can be far different one from the other.

Eq. 2. 12 can be better understood by means of Figure 2. 22

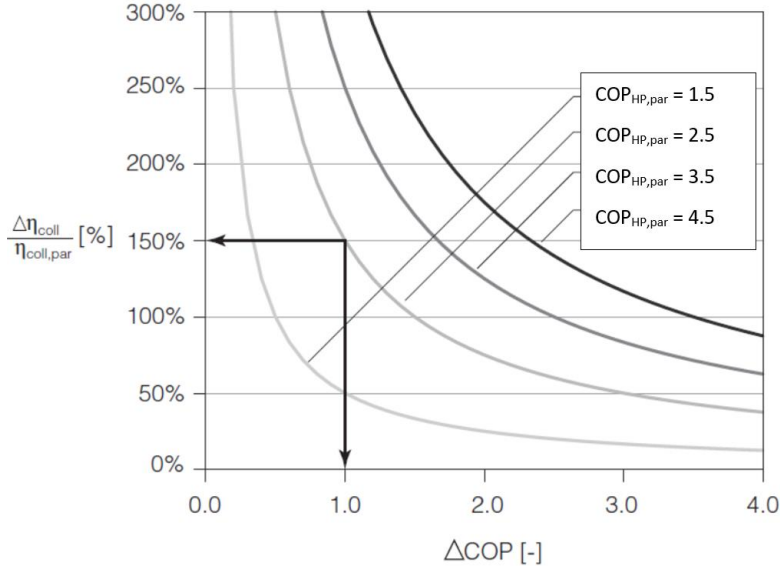


Figure 2. 22: preliminary steady state analysis about the serial/parallel asset convenience, based on the increase in the COP of the chosen HP and the collector yield in parallel/serial configuration (70)

Each line plotted in Figure 2. 22 is associated with a double source heat pump with an initial COP of 1.5, 2.5, 3.5 or 4.5. Each curve plotted splits the graph into two regions: the one over the line (upper right) where the panels should be put in serial asset and the one below where a parallel configuration is preferable. It can be easily noticed that the lower the initial COP in parallel asset, the largest the area where the serial asset should be preferred and vice versa. In addition, the parallel asset is mainly associated to configuration where small increases in the COP of the HP and/or in the collector efficiency are present. The steep increase of only one of the axes (either panel efficiency or heat pump COP) still leads to the parallel asset as the most likely preferable configuration.

For instance, the arrows in Figure 2. 22 show that a HP with an initial $COP_{HP,par}$ of 2.5 can benefit from serial asset only if at the same time the COP would increase of at least 1 and the ratio $\frac{\Delta\eta_{coll}}{\eta_{coll,par}}$ would be higher or equal to 150%. This would mean that the collector yield in parallel would be about 40% or lower than in the case of serial asset as shown by the passages in Eq. 2. 13.

$$\frac{\Delta\eta_{coll}}{\eta_{coll,par}} = \frac{\eta_{coll,ser} - \eta_{coll,par}}{\eta_{coll,par}} = \frac{\eta_{coll,ser}}{\eta_{coll,par}} - 1 = 1.5 \leftrightarrow \text{Eq. 2. 13}$$

$$\leftrightarrow \frac{\eta_{coll,par}}{\eta_{coll,ser}} = \frac{1}{1.5} = 0.4$$

In conclusion, it is important to remember that such results derive from a theoretical formulation which neglects the transient terms taking part to the energy balances (i.e., thermal capacities of storages) and therefore the limits above have to be considered accounting for a degree of uncertainty, given that the results still provide a preliminary, reliable piece of information about the most performant configuration for the SAHP.

As a consequence of Eq. 2. 13, the serial/parallel assets cannot be switched freely, but according to the ambient boundary conditions (mainly temperature and radiation), not to negatively affect the global performance of the SAHP. Therefore, under the assumptions of steady state regime, the collector yield has to be properly chosen according to the most likely working condition expected. Indeed, an eventual switch to the other configuration could not lead to the same benefits, due to the likely reduction of the efficiency shown in Eq. 2. 13. For instance, the serial asset shall be more

advisable in contexts where low and brief solar radiation is available, since the parallel working is less likely to occur.

The current studies (6), (70), (72), (73), (74), have widely highlighted the presence of a limit value for irradiance to establish whether parallel (larger values) or serial (smaller value) assets result more efficient. Such limit is a function of the efficiency curves of the elements composing the SAHP, mainly panels and heat pumps, and the required set point temperature, as formulated in some criteria for the switch between the two configurations (75).

2.4 The solar assisted heat pumps – state of the art and current limits

The previous chapters showed a lack in the diffusion of the solar assisted heat pumps both at small and at large scales. In this section a brief focus on the main limits and open challenges of this technology is proposed.

2.4.1 Coupling of solar panels and heat pumps

- *Issue:* considering a SAHP, the type and size of each component has to be properly designed to grant the achievement of high efficiencies. Indeed, if the HP stayed operative for long periods within a typical day with large electrical consumptions there would be a lack of energy efficiency with a relevant carbon footprint as well (76). In addition, the coupling of panels to the HP should account for the variability of solar radiation over the day, with respect to the periods in which the HP is operative.
- *Possible solutions:* the control strategy plays a fundamental role to grant plant efficiency especially when considering SAHPs. The enhancement of the SAHP has been studied by means of different strategies: correct sizing of the panels, the HP evaporator and more in general of the volumes inside the plant (77), (78), (79), (80), cascade heat pumps to grant high temperature set points, adoption of control strategies to manage the components of the HP (e.g., compressor and expansion valve) (81), (64), (82) and adoption of dual or multi source SAHPs (83), (84). In addition, phase change materials could provide more stability to the solar panels, with benefits also on the risk of frosting or stagnation, extending their operability period, decreasing at the same time the working period of the HP (85), (86), (87), (88).

2.4.2 Low ambient temperature

- *Issue:* in case of cold locations with low ambient temperature, the evaporator works at lower temperatures as well with respect to milder climates. This leads to a decrease in the performances coupled to a great number of functional problems, such as reduced volumetric efficiency, elevated compressor discharge temperature, reduction in the refrigerant flowrate in the HP circuit and higher compression ratio (89), (90), (91). The panels have a global worse performance due to the higher thermal losses determined by the larger difference in temperature between the panels and ambient air. In addition, many SAHP pilot plants were formerly realized using low efficiency panels, such as the unglazed flat collectors. Indeed, the lower operating temperature of a solar panel coupled to a HP would result in lower thermal losses independently from the level of insulation, since the temperature difference between panels and ambient air is very small. Therefore, the adoption of low efficiency panels would cut the initial costs for the plant, providing it with more simple and solid panels without any appreciable variation in the

efficiency, given that the climate of the location is not too harsh. Anyhow, in case of low ambient temperature, the eventual adoption of unglazed panels or similar ones would additionally worsen their performance, even with the risk of frosting.

On the HP side, the risk of frosting of the evaporator might occur as well with the reduction of its COP, since usually heat pumps use an electrical booster to de-frost their evaporator with a dramatic loss in its efficiency (about 40% - (92)). Moreover, the frosting of the panels might lead to blocks of the HP and damage the panels themselves, creating a great discomfort for the users and additional maintenance costs.

- *Possible solutions:* many solutions are under study, mainly focused on the HP, paying less attention to the panels. For instance, multi-stage or hybrid compressions within the HP cycle, cascade, trans critical cycles, auxiliary boilers, CO₂ cycles are analysed (93), (94), (95), (96), (97), (98), (99), (100). In addition, the compressor represents a common element to many causes of the COP reduction. Therefore, variable speed compressors were studied as well, showing how the replacement of a constant speed compressor improves the HP performance at low evaporator temperatures, but with a higher initial cost, negatively affecting the cost-effectiveness of the improvement.

2.4.3 Lack of models for design, management and optimization of SAHPs

- *Issue:* the simulation of the processes occurring inside and the interaction among each component of the SAHP lies in the core of design, performance prediction and optimization strategies (101), (102). Two approaches can be identified.

The former is concerned with each component and it is meant to correctly size each element and define its geometry. The aim is to understand the heat transfer mechanisms occurring within by means of CFD numerical codes (103). Such models couldn't allow the numerical representation of a SAHP as a whole due to its complexity and to the computational power required to run such an articulate model.

The latter accounts for the interaction of the different components inside the system. In this less detailed approach, each component can be conceived as a "black box" where results are obtained from initial information using numerical models and different formulations. No attention is paid to the real phenomena occurring inside the components, since the goal of the modelling is the global working of the system, losing the specific insights on the single elements. Within this context, numerical codes such as TRNSYS are used thanks to their reasonable accuracy derived from the simulation under transient regime (104).

- *Possible solutions:* the two approaches are dichotomous and a numerical model approaching both sides is not available yet. In addition, the numerical model should be coupled to the SAHP plant during all its useful life, always updated with the parameters measured from the real plant, to provide a tool to identify the optimal set point values and working configurations according to the different boundary conditions and end users' needs.

2.4.4 Mismatch between heat requirement and heat supply

- *Issue:* as illustrated in the previous sections, the SAHPs can reach high efficiencies when the solar radiation is available and therefore the HP can work with higher temperatures at the evaporator. Actually, the demand tends to be more elevated during periods of the day in which solar radiation is not available or it is negligible (Figure 2. 12). Therefore, a SAHP coupled to no

boilers would be expected to work in periods with low efficiencies with the risk of frosting at the evaporator. Such mismatch becomes even more emphasized during summer where the solar radiation reaches its peaks and it is very likely to be almost all unexploited (105), (106).

- Possible solutions: the main issue of mismatch can be overcome introducing inertial elements whose characteristics depend on the size of the time shift. For instance, the coupling of geothermal sources is a widely adopted solution to improve the inertia of the plant on a seasonal basis (107), (108). Another strategy is concerned with seasonal heat storages (e.g., the aquifer thermal energy storage (ATES), the borehole thermal energy storage (BTES), the tank thermal energy storage (TTES) and the pit thermal energy storage (PTES), (109), while the daily shift can be easily coped with by means of properly sized water storages. Clearly, the seasonal storages require a relatively high initial cost and, therefore, the best fitting solution has to be chosen basing both on the technological and economic sides with reference to the specific plant.

2.4.5 Low level of end users' acceptance of SAHPs

- Issue: as better described in the following chapter about the SAHP pilot plant, each project has minimum standards and quality levels to be reached during all its useful life. Furthermore, a project has to satisfy the expectations of different groups, such as developers, financiers, customers and users. Their sentiments are subjective and they can be in contrast one with the other as well (110). Moreover, the prediction of whether a project (e.g., technology, plant) will become successful or not is a very tough task, besides of its theoretical expectations, since it depends on the level of adoption and acceptance. The term acceptance covers many issues, starting from the economical cost-effectiveness up to efficiency and the user-friendly interface to ease its use (111), (112), (113), (114).

For instance, the innovative technologies such as SAHPs are often uneconomic and require either a skilled technical maintenance staff or an advanced self-control system and this leads to a general state of hesitation for investments in this field. Indeed, a project does not have to be only efficient to be successful, but it has to meet the investors' expectations. Recent statistics show for example how in Italy about one third of projects is globally rated as unsatisfactory or inadequate and they tend to be abandoned after their realisation (115).

- Possible solutions: the correct and exhaustive evaluation of acceptance has to become part of both plant design and plant management since it might cause a facility to be either successful or not. Up to now, the traditional heating plants (e.g., gas burners) haven't emphasised this need, due to their simplicity and their working with simple regulation (e.g., on/off) under almost steady regime. However, the relevance of acceptance is expected to grow as complex technologies and plants (e.g., the SAHP-PVT) take place on the market. No unique or common approach have been presented or widely adopted, so far. A numerical approach to connect quantitative values to qualitative feelings is lacking since most of studies are carried out by means of enquiries. This approach often neglects that the answers collected might not really and fully represent people's opinion. Moreover, the temporal validity range of these surveys is often limited or not appropriately considered. A numerical approach to estimate acceptance basing on quantitative, measurable values (e.g., flow rates, working hours of the different components, temperatures) is under study (116). This method requires a Data Acquisition System (DAS), to collect almost real time the measurement of the different key parameters of the plant.

2.4.6 Coupling of SAHP with existing heating systems

- **Issue:** from the point of view of energy efficiency, a SAHP becomes effective when operative at the optimal working temperatures. Usually one of the most effective coupling is represented by SAHP and convector heaters or radiant floor systems, which require an inlet temperature between about 30-45 °C (117), (118), (119). The same problem happens when DHW applications are considered. Such emission systems are usually easy to install in new or totally refurbished buildings where a proper design has taken place. On the other hand, in existing or inhabited buildings such interventions could not be achievable. Indeed, the standard heating system for Italian buildings is represented by a gas burner coupled to high temperature radiators (about 70-80 °C), with not-insulated distribution pipes. While the change of the generator could take place, the insulation of the pipes and the change of the emission system would lead to the following issues:

- the building should not be inhabited
- the cost could experience a relevant rise, since the intervention might affect decorations and finishes
- the new distribution line might interfere with private/common parts of the building with consequent economic and legal problems
- the intervention may not be allowed due to the constraints to which the building might be subject. The Italian National Institute of Statistics (ISTAT) estimates that over half of the Italian territory is subjected to constraints (e.g., architectural or landscape) (120), (121).

In addition, the percentage of new buildings or important refurbishments in Italy dramatically fell during the past decades (*Figure 2. 23*), therefore the most likely case for SAHP application is concerned with the refurbishment of existing heating plants.

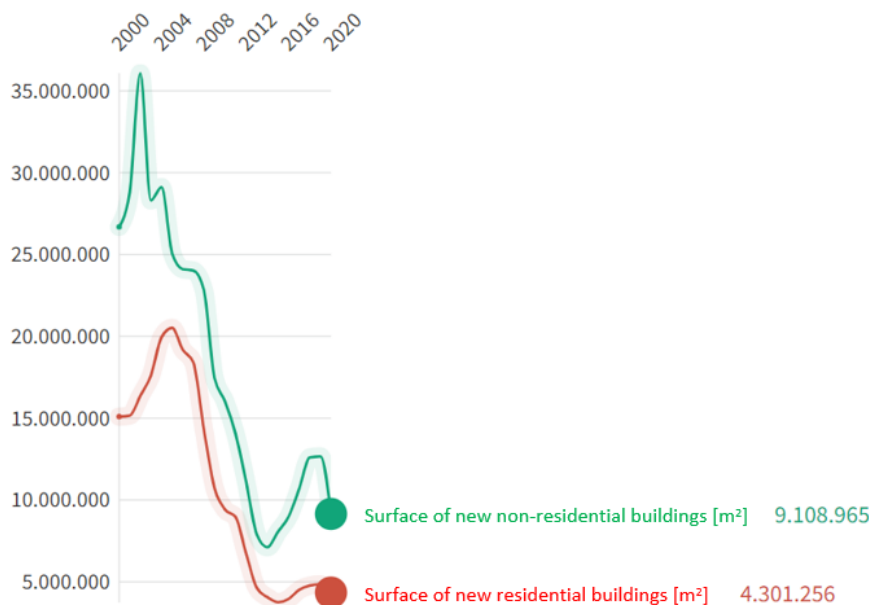


Figure 2. 23: trend over the past two decades of the new surfaces built for both residential (red) and non-residential (green) applications (122)

- **Possible solutions:** the issue can be coped with by means of two different strategies, depending on the specific case study:
 - adoption of compatible emission systems whenever possible – especially in new buildings

- installation of backup gas burners, to provide or integrate the need when the SAHP itself cannot grant it. The existing plants are likely to fall in this case, since the gas burner might be re-used for this function. This solution either preserves or introduces fossil fuel-based technologies which are expected to work seldom, only with very harsh climate or in presence of high needed power (e.g., during the start-up of the heating system). As better outlined later, the presence of a backup-system improves two critical aspects as well:
 - i) the SAHP work almost under transient conditions since they depend on highly variable parameters such as air temperature or solar radiation. The correct working of the system requires a proper monitoring and management system with a continuous control on the system parameters to grant always plant efficiency and avoid its blocks.
 - ii) people tend to show a low level of interest in new technologies, feeling confident with the oldest ones. Indeed, many users still prefer a less efficient gas burner instead of a heat pump. Therefore, the adoption of a “hybrid” system plays a central role also in the market, making the technology more attractive to the customers thanks to the presence of a burner which make the heating system look more “reliable” than a completely innovative one. Such issue, known with the name of acceptance will be recalled in the next chapter concerned with the specific case study of the SAHP with hybrid panels at Palacus.
- Some producers are testing heat pumps with higher working temperature, to grant a higher compatibility with the existing emission systems. This solution has a great potential, but each specific model needs to be properly enquired to assess its working and the absence of other negative aspects (e.g., toxic/flammable refrigerant fluid).

2.4.7 SAHP - scale effect?

- Issue: as previously described, the SAHP is a very promising technology with very high theoretical COP and very encouraging results from the experimental facilities. *Table 2. 1* resumes the main experimental studies carried out in the past fifteen years with some additional information. Anyway, the biggest heat pump has a peak thermal power of about 16 kW_T while the solar fields, when the information is available, reach an extension of 22 m². These limits can be considered suitable for direct expansion SAHPs since the increase in size would lead to operational problems (e.g., refrigerant distribution, temperature uniformity over the panels). On the other hand, the indirect SAHP should allow the overcome of the problem, but no extensive testing of big size SAHP is available. The enquiry on larger and more complex systems should be carried out on a sufficient number of test facilities, to assess the eventual occurrence of “scale effects” mainly concerned with operational problems linked to the increased size of the plant.

| Authors | Year | Size | Direct/ Indirect expansion | COP (average) | Ref |
|-----------------|------|---|-------------------------------|------------------|-------|
| Kuang et al | 2006 | 10 m ² solar field, HP size 6 kW _T | Direct | 3.0 | (123) |
| Bridgeman et al | 2008 | HP size 5.5 kW _T | Indirect | 2.9 | (68) |
| Nuntaphan et al | 2009 | 4 m ² solar field, HP size about 4 kW _T | Indirect | 3.8 | (124) |
| Bakirci et al | 2011 | 20 m ² solar field, HP size about 5.4 kW _T | Indirect | 3.6 | (69) |
| Rodriguez et al | 2012 | 5.6 m ² solar field, HP size about 2.5 kW _T | Direct | 2.3 | (125) |
| Wang et al | 2015 | HP size 3.0 kW _T | Indirect | 2.3 | (84) |
| Zhou et al | 2016 | 22 m ² solar field, HP size about 16 kW _T | Direct | 4.5 | (126) |
| Qu et al | 2016 | 8 m ² solar field, HP size about 5.4 kW _T | Direct | 3.8 | (127) |
| Xu et al | 2018 | HP size about 3.5 kW _T | Indirect | 3.0 | (128) |
| Besagni et al | 2019 | 8 m ² solar field, HP size about 6.8 kW _T | Direct | 3.1 | (129) |
| Long et al | 2019 | HP size about 4.3 kW _T | Indirect | 4.2 | (130) |
| Wang et al | 2022 | HP size about 11 kW _T | Indirect | 2.5 | (131) |
| Leonforte et al | 2022 | 18 m ² solar field, HP size about 11.5 kW _T | Direct | 2.9 | (132) |

Table 2. 1: main experimental studies on SAHP, with HP sizes, average COP and references

- *Possible solutions:* besides of the issue about the higher initial cost, the experience carried out on the case study presented in the following chapter shows that a relevant increase in the plant size may lead to operational problems. Indeed, the larger solar field and heat pump come with more sophisticated and complex subsystems, united with more possible working conditions. In addition, the SAHP technology works most of time under transient conditions and therefore the optimal set point of the working parameters is expected to change according to the external climate. In fact, an almost real time monitoring and regulation is made necessary both to avoid the block of the facility and to grant the optimal working condition and set point parameters. This aspect cannot be performed by means of manual control for two reasons:
 - the transient regime could require actions on the plant even more times in a day
 - the number of variables and control points to manage become too many to be manually controlled. In addition, a post-processing of the parameters could be required to establish the best working condition to enable making human control impossible.

3. The solar assisted heat pump with hybrid panels pilot plant at the Palacussport palace - Genoa

This section provides an overview on the case study analyzed in the present work. The sport palace “Carmine Romanzi”, with multiple activities and relevant consumption profiles in terms of SH and DHW needs, is coupled to a solar assisted heat pump with hybrid panels (SAHP-PVT). The application of an experimental facility to a real structure with real needs represents an almost unique case, constituting the missing link between a pilot plant with laboratory simulated needs and commercial, mass-produced systems applied to real buildings. In addition, the plant is equipped with a data monitoring and control system (DAS) which allows an almost real time acquisition of values (e.g., temperature, solar radiation) associated to the different working conditions of the plant (as better described below, about 50 measurement points and 15 control points have been installed in the plant). Firstly, a specific overview on the SAHP-PVT and its components is presented. Then a description of the sport palace is provided, paying attention to the energetic needs and the consumption profiles while the last part of this chapter is concerned with the main issues aroused from the plant management and monitoring.

Brief historical note: Carmine Romanzi, after whom the sport palace is named, was the Rector of the University of Genoa (1968-84) and a brilliant researcher in the field of microbiology. Moreover, he was one of the main contributors to the liberation of Genoa in 1945 from the Nazi occupation, thanks to his active role in the Italian Resistance that led to the unconditional surrender of the General Meinhold, chief of the occupation German’s army in the region.

3.1 The Solar Assisted Heat Pump with Hybrid panels (PVT) pilot plant: a description

The pilot plant was built in 2012-2013 as an integration of the existing system based on gas burners (133). The present section analyses the main subsystems of the plant, i.e., generation, storage, distribution, emission and control, explaining their working and providing the reader with technical information. *Figure 3. 1* focuses over the plant and its main components:

- the sport palace – representing the DHW and SH needs
- the PVT field – producing both hot water and electricity, interfaced with the heat pump
- boiling room – containing the distribution pipes, DHW storages, integration gas burner and the heat exchanger interfaced with the HP and the solar field.

Before of the detailed description, it must be remarked that each component has not been specifically built or designed. The SAHP-PVT under study is the result of the assembly of the most suitable commercial products available on the market. This aspect represents a first interesting challenge, since the adoption of commercial components instead of laboratory made ones simplifies an eventual mass production of similar systems. Indeed, the hand-made components may result optimal for a specific case study, but reveal unsuccessful in similar, yet different applications.

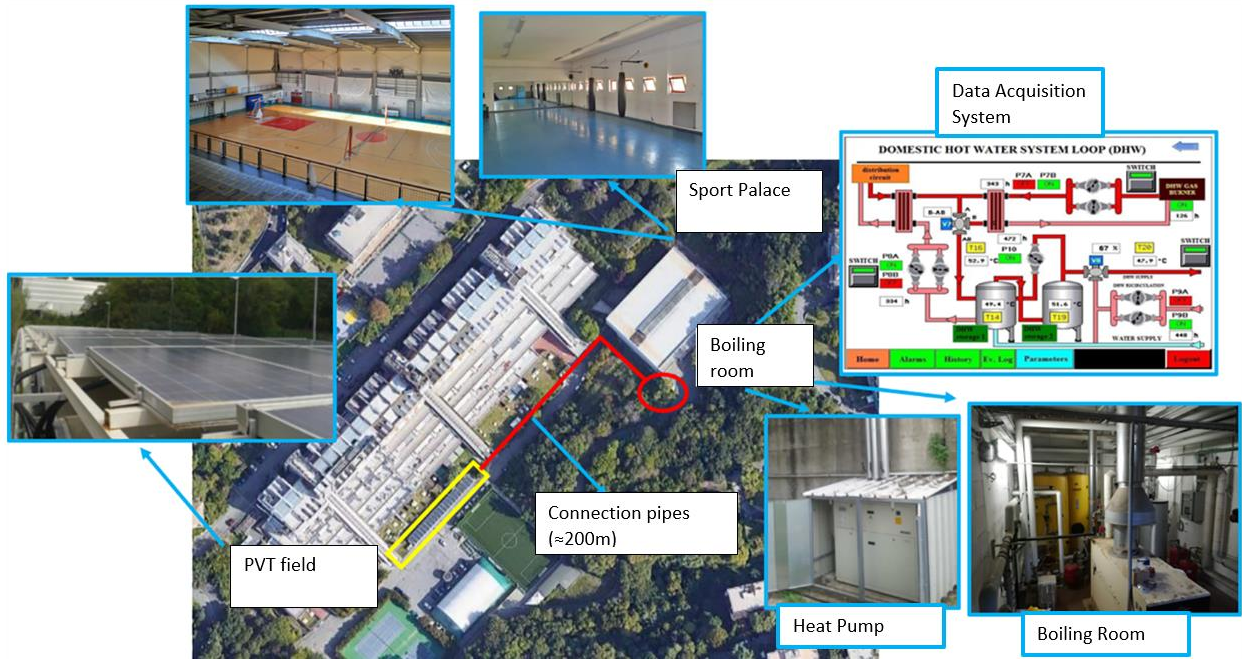


Figure 3. 1: overview of the pilot plant – focus on the sport palace, the PVT field, the HP and the boiling room

Figure 3. 2 provides the simplified plant scheme as well, with the identification of the four main subsystems and all the elements (i.e., generators, storages, control system etc) which will be required in detail in the following paragraphs.

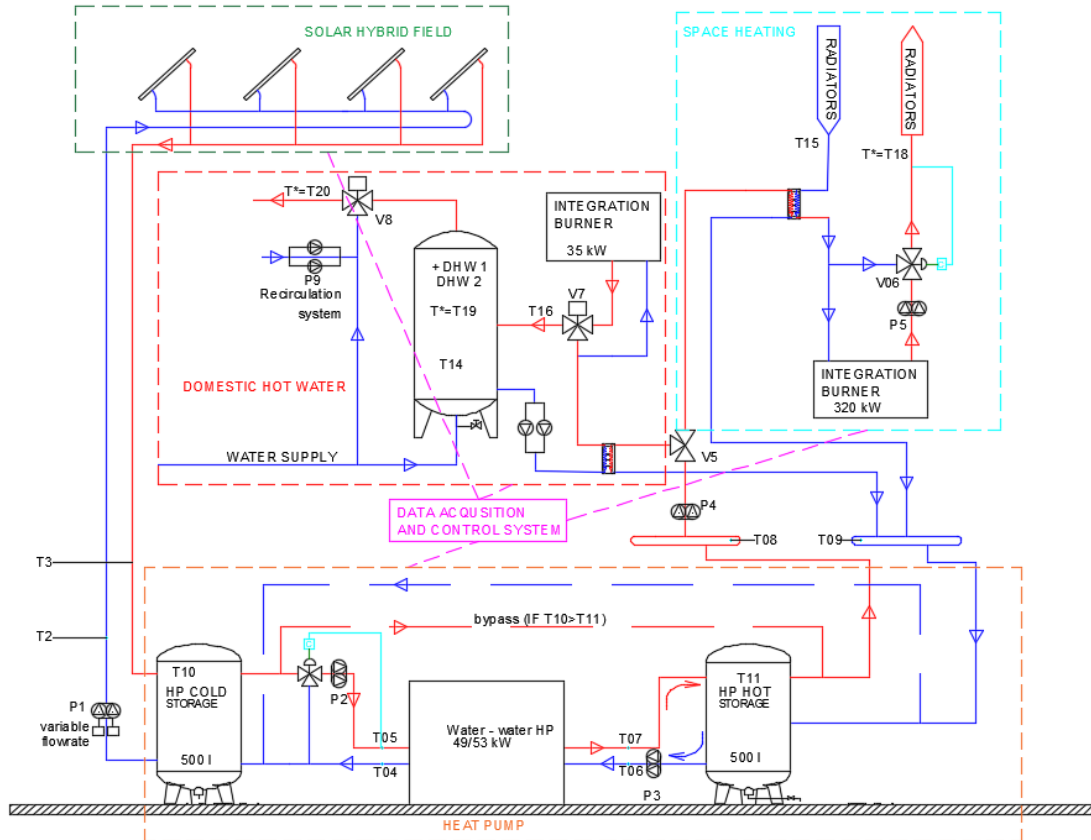


Figure 3. 2: simplified scheme of the solar assisted heat pump pilot plant

3.1.1 Generation subsystem

More generators can be identified:

- gas burners: the former of 35 kW is used for DHW during summer (*Figure 3. 3 a*) while the latter (320 kW) is active during the heating season to integrate both DHW and SH needs (*Figure 3. 3 b*). Their function has shifted from main generator of the plant to integrative generator based on non-renewable sources (gas), to grant the possibility of coupling to the existing emission subsystem (described later). The issue becomes of paramount importance, when revamping existing heating systems, as outlined in the previous sections.



a)



b)

Figure 3. 3: gas burners used to integrate DHW/SH needs in the heating system of the Palacus sport palace. a) burner for only DHW out of the heating season – 35 kW peak thermal power; b) burner for DHW and SH during the heating season – 320 kW peak thermal power

- Solar hybrid field: it is composed by 80 polycrystalline hybrid modules covering a gross surface area of 160 m² (net capturing area of 120 m²). The panels are at a 45 °degree azimuth orientation towards South/West with a tilt angle of about 6 ° (*Figure 3. 4*)



Figure 3. 4: Solar field, orientation from the satellite view (on the left – source Google Maps) and view of the site (on the right)

Concerning the shadings, no relevant obstruction is present (*Figure 3. 5*), making the location optimal for the solar field. Only the hill (on the left in *Figure 3. 5*) and the building of the Faculty of Maths and Physics (on the right in *Figure 3. 5*) cast a shadow over the field in the first and last hours of the day respectively.



Figure 3. 5: 3D view (source Google Earth) of the field and of the shadings due to the surrounding hills/buildings

The solar collectors are hybrid, namely they grant the conjoint production of both electricity and domestic hot water leading to a lower working temperature with higher efficiencies both on the thermal (*Figure 2. 14*) and on electric sides (*Figure 2. 15*).

Figure 3. 6, Figure 3. 7 and Table 3. 1 show the PV and the thermal module below united with the main technical information.

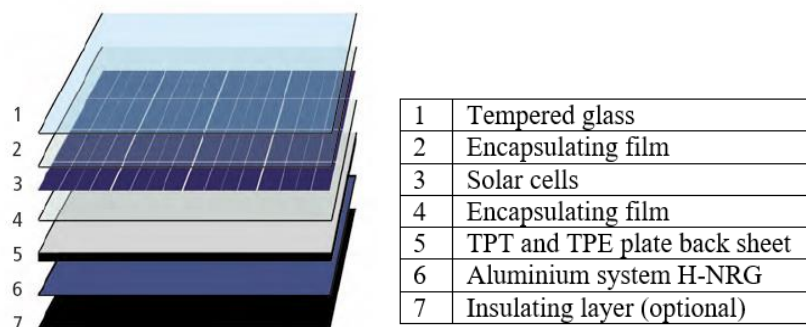


Figure 3. 6: panel stratigraphy

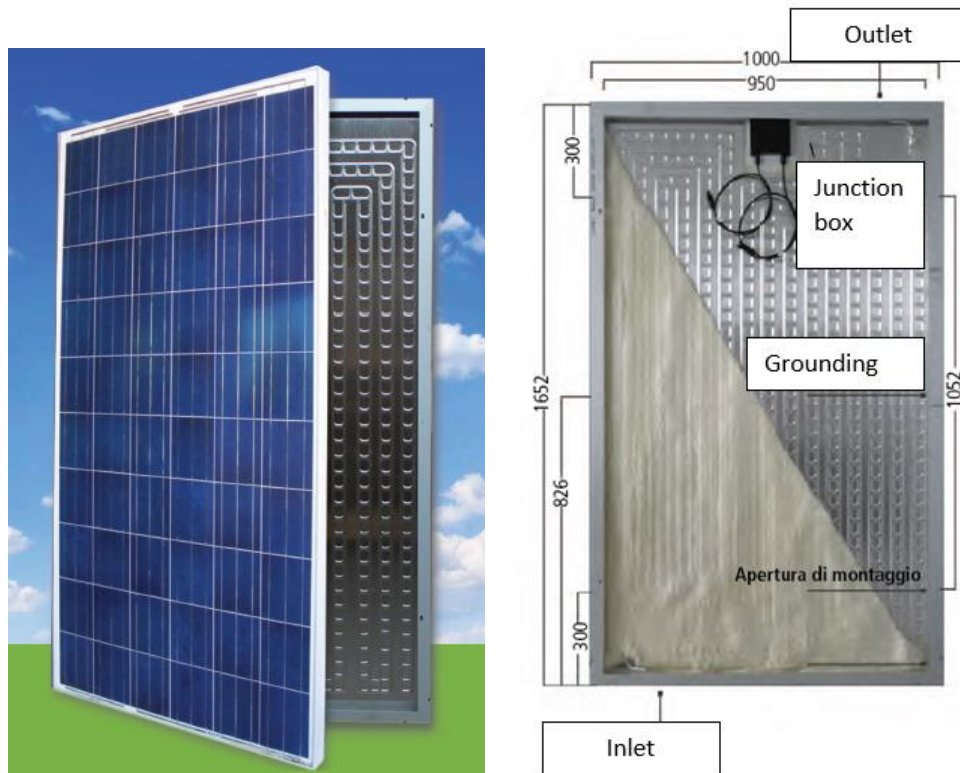


Figure 3. 7: PV and thermal modules of the hybrid panel – extract from the technical specifications

| | |
|---|-------|
| Gross surface [m ²] | 1.65 |
| Absorbing surface [m ²] | 1.46 |
| Fluid volume within the panel [l] | 0.8 |
| Panel weight without fluid [kg] | 34 |
| Peak power [W] | 230 |
| MPP (Maximum Power Point) voltage range [V] | 30 |
| MPP current [A] | 7.67 |
| Open circuit voltage [V] | 36.8 |
| Short circuit current [A] | 8.34 |
| Panel efficiency [%] | 13.9 |
| Power temperature coefficient [%/°C] | -0.45 |
| Current temperature coefficient [%/°C] | -0.36 |
| Voltage temperature coefficient [%/°C] | 0.05 |
| NOCT (Nominal Operating Cell Temperature) [°C] | 45 |
| Panel optical performance (η_0) | 0.513 |
| Linear thermal loss coefficient (a_1) [W/m ² K] | 7.68 |
| Quadratic thermal loss coefficient (a_2) [W/m ² K ²] | 0.014 |

Table 3. 1: PVT module technical information

As a consequence, the field is designed to produce under peak conditions 50 kW_T and of 20 kW_E. The panels are arranged in 20 rows, with 4 modules each, as better outlined in Figure 3. 8 where the hydraulic connection of two rows is reported.

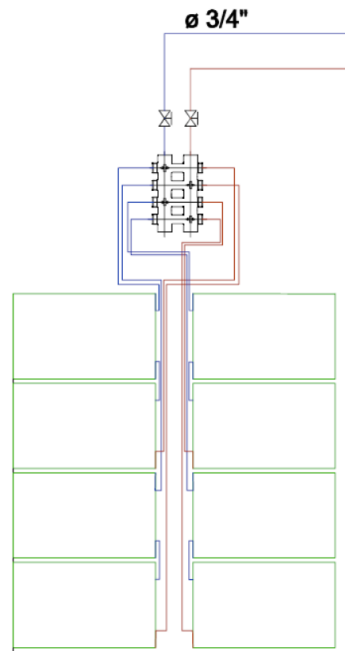


Figure 3. 8: hydraulic scheme of the connection between two rows of panels. The same pattern occurs for the remaining rows

On the PV side, the panels produce DC electricity and a connection with two inverters allow its transformation in AC (*Figure 3. 9*). Then the electricity is sent to a bidirectional meter (*Figure 3. 10*).



Figure 3. 9: one of the two 10 kW inverters installed near the solar field

The solar panels are then hydraulically and electrically connected to the heating plant located at the Palacus sport palace by means of about 200 m pipes/electric cables (*Figure 3. 10*).

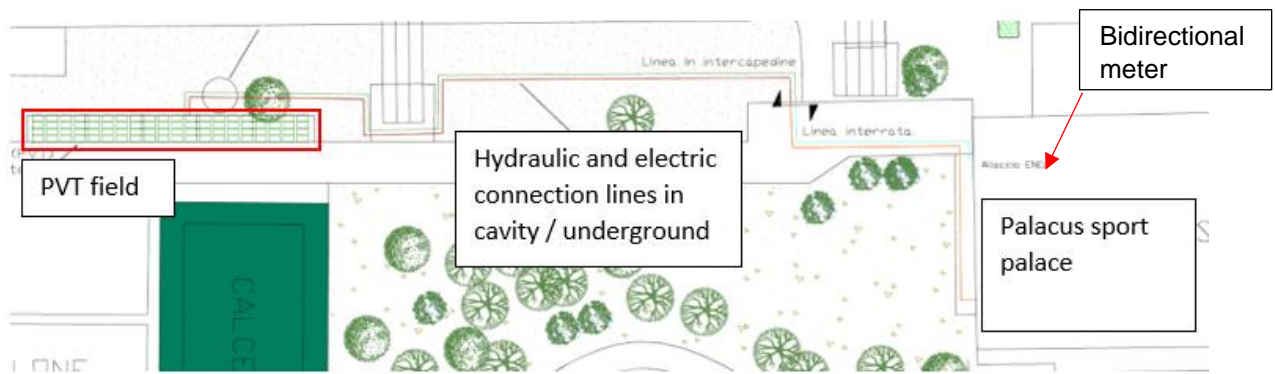


Figure 3. 10: hydraulic/electric connection between the solar hybrid field and the heating system

- Heat pump: it is installed near the sport palace and it can reach 48.2 kW_T with a consumption of 11.91 kW_E under peak conditions (model WRL_H 026/161 – Aermec, Figure 3. 1 and Figure 3. 11)



Figure 3. 11: heat pump installed near the Palacus sport palace

The heat pump exchanges on both sides with water, using R410A as refrigerant fluid and implementing hermetic scroll compressors (model WRL160-H – Aermec). Figure 3. 12 and Table 3. 2 show the COP depending on the outlet temperature at the evaporator ($T_{out,eva}$) and at the condenser ($T_{out,cond}$). Table 3. 2 also show the working ranges: between -8 °C and 18 °C on the evaporator side and between 25 °C and 60 °C on the condenser side.

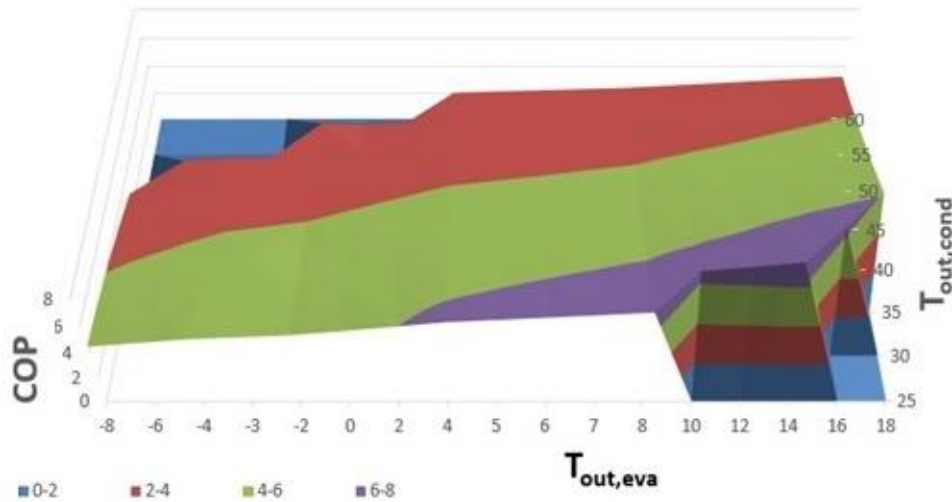


Figure 3. 12: three-dimensional plot of the COP depending on the outlet temperatures on the evaporator and condenser sides.

| COP | | $T_{out,cond}$ | | | | | | | |
|---------------|----|----------------|------|------|------|------|------|------|------|
| | | 25 | 30 | 35 | 40 | 45 | 50 | 55 | 60 |
| $T_{out,eva}$ | -8 | 4.46 | 4.26 | 3.9 | 3.41 | 2.82 | - | - | - |
| | -6 | 4.74 | 4.49 | 4.1 | 3.6 | 3.01 | 2.37 | - | - |
| | -4 | 5.03 | 4.72 | 4.30 | 3.78 | 3.19 | 2.55 | - | - |
| | -3 | 5.18 | 4.84 | 4.49 | 3.87 | 3.28 | 2.64 | - | - |
| | -2 | 5.33 | 4.97 | 4.50 | 3.96 | 3.36 | 2.73 | 2.39 | - |
| | 0 | 5.64 | 5.21 | 4.71 | 4.14 | 3.54 | 2.91 | 2.28 | - |
| | 2 | 5.97 | 5.47 | 4.92 | 4.32 | 3.71 | 3.08 | 2.46 | - |
| | 4 | 6.31 | 5.73 | 5.13 | 4.51 | 3.88 | 3.25 | 2.63 | 2.04 |
| | 5 | 6.48 | 5.87 | 5.24 | 4.60 | 3.96 | 3.33 | 2.72 | 2.13 |
| | 6 | 6.66 | 6.01 | 5.35 | 4.69 | 4.04 | 3.41 | 2.80 | 2.22 |
| | 7 | 6.84 | 6.15 | 5.46 | 4.79 | 4.13 | 3.49 | 2.89 | 2.31 |
| | 8 | 7.03 | 6.30 | 5.58 | 4.88 | 4.21 | 3.58 | 2.97 | 2.40 |
| | 10 | - | 6.60 | 5.82 | 5.08 | 4.39 | 3.74 | 3.14 | 2.57 |
| | 12 | - | 6.91 | 6.06 | 5.28 | 4.56 | 3.90 | 3.30 | 2.74 |
| | 14 | - | 7.23 | 6.32 | 5.49 | 4.74 | 4.07 | 3.46 | 2.91 |
| 16 | - | - | 6.58 | 5.70 | 4.92 | 4.23 | 3.62 | 3.08 | |
| 18 | - | - | - | 5.92 | 5.10 | 4.40 | 3.78 | 3.24 | |

Table 3. 2: COP according to the outlet condenser and evaporator temperatures [$^{\circ}\text{C}$]

Interaction among the different heat generators

The aforementioned generators interact one with the other to always grant the best possible efficiency, also depending both on the boundary/environmental conditions and the end-users' demand. In particular, the solar field is hydraulically connected with the heat pump on the evaporator side by means of a 500 l storage tank (Figure 3. 13 and Figure 3. 21). The same storage is present also on the condenser side for multiple purposes, such as stable heat transfer rate and temperature regulation.



Figure 3. 13: water storage tanks on the cold (on the left) and hot side (on the right) of the heat pump

Pumps P2 and P3 grant the circulation of water within the storages working at constant water flow rate (Figure 3. 14 and Figure 3. 21). Both pumps are twin, with alternating operativity periods, to prevent the block of the circuit in case of sudden arrest or rupture of one of the two.

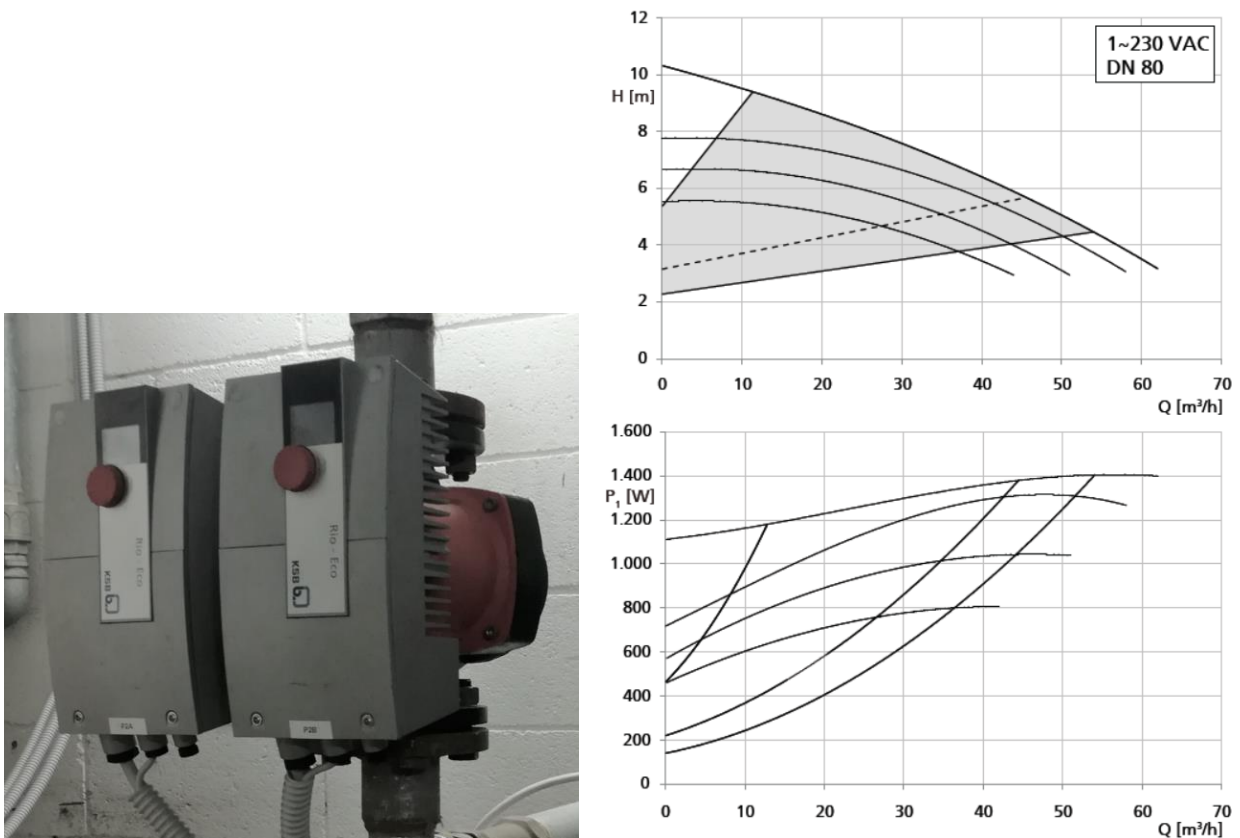


Figure 3. 14: view and performance curve of a single reference pump present in the plant. The model is the same adopted for P2, P3, P4 and P5 recalled in the text

The interface with the HP evaporator decreases the panel working temperature (e.g., 18-20 °C against 40-50 °C in case of DHW applications) and therefore even the contribution from the surrounding air becomes relevant, especially at mild Italian locations. The solar source increases its stability, thanks

to the smaller required set point value and the lower sensitivity of the panels to the solar radiation. The operativity time range of the panels extends even to the days when the contributions from the Sun are negligible.

The use of solar panels at a temperature close to the environmental one allows the adoption of poorly insulated panels/connection pipes since the difference in temperature between the fluid inside the pipes and ambient air is almost comparable. In fact, a very small heat flow is appreciated independently from the thermal resistance of either pipes or panels. This means that milder location will result more suitable to SAHP technology even in absence of insulation, while colder places will be likely to require a higher level of insulation.

In addition, the low working temperature carries two benefits:

- on the panel side, a relevant increase in both thermal and photovoltaic efficiencies
- on the heat pump side, the working temperatures at the evaporator are high enough to increase the COP of the HP, due to the lower work at the compressor thanks to the reduction of the jump in pressure required by the cycle between the evaporation and condensation points.

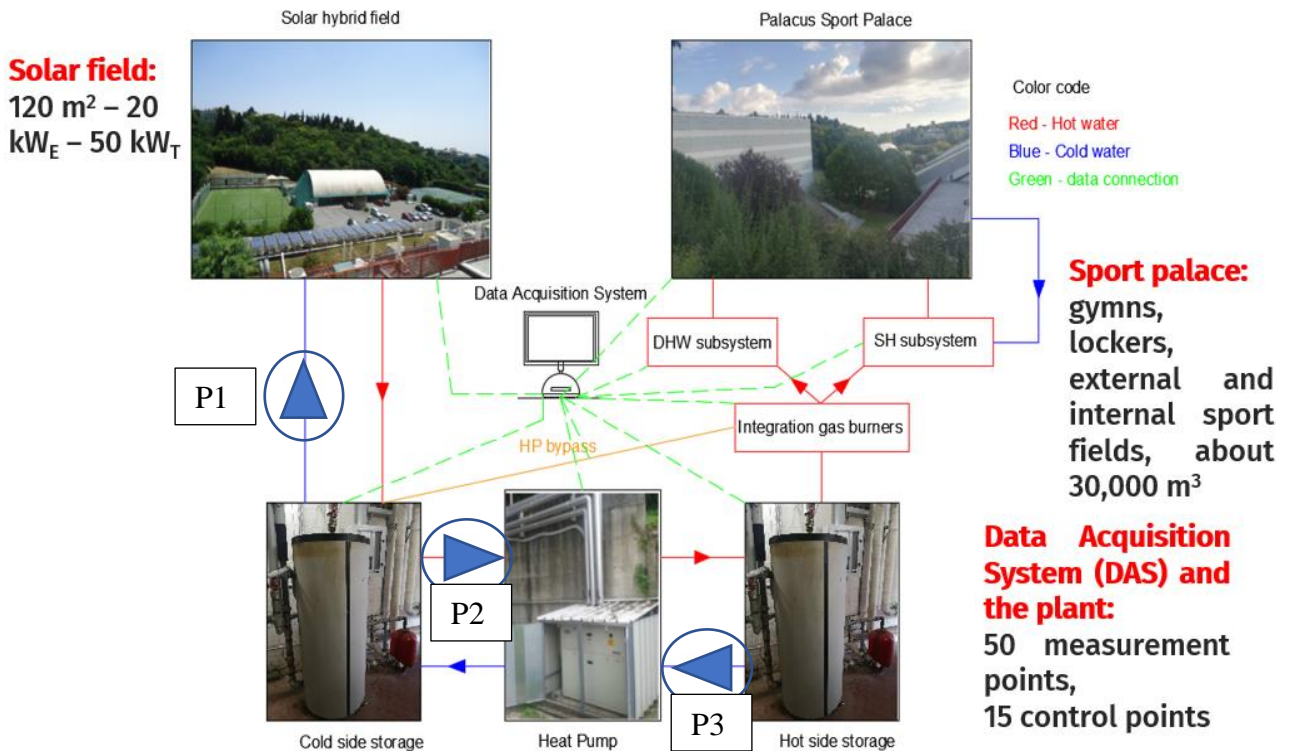
The gas burners are switched on, only when the SAHP cannot grant the needs itself (e.g., SH and DHW). The SAHP is designed to work either on DHW or SH by means of two heat exchangers. Valve V5 and pump P4 (*Figure 3. 15 b* for plant scheme and *Figure 3. 14* for pump technical information) allow the flow circulation and the switch between the two exchangers.

On the SH side, the existing air heaters in the sports hall and the radiators inside the lockers require a high set point temperature (60-70 °C) while the radiators work at about 50-60 °C. As far as radiators are concerned, the compatibility with the existing, high temperature heating system can be easily granted providing an additional heating of the water using the burners. The contribution is expected to be low, especially when high power is required (e.g., early in the morning when the facility has cooled down during night) while during the day, the HP is expected to be able to almost keep the set point temperature inside the sport palace. Concerning the air heaters, the higher working temperature hardly fits the working range of the HP, as better outlined in section “3.1.3 Distribution and emission subsystem”.

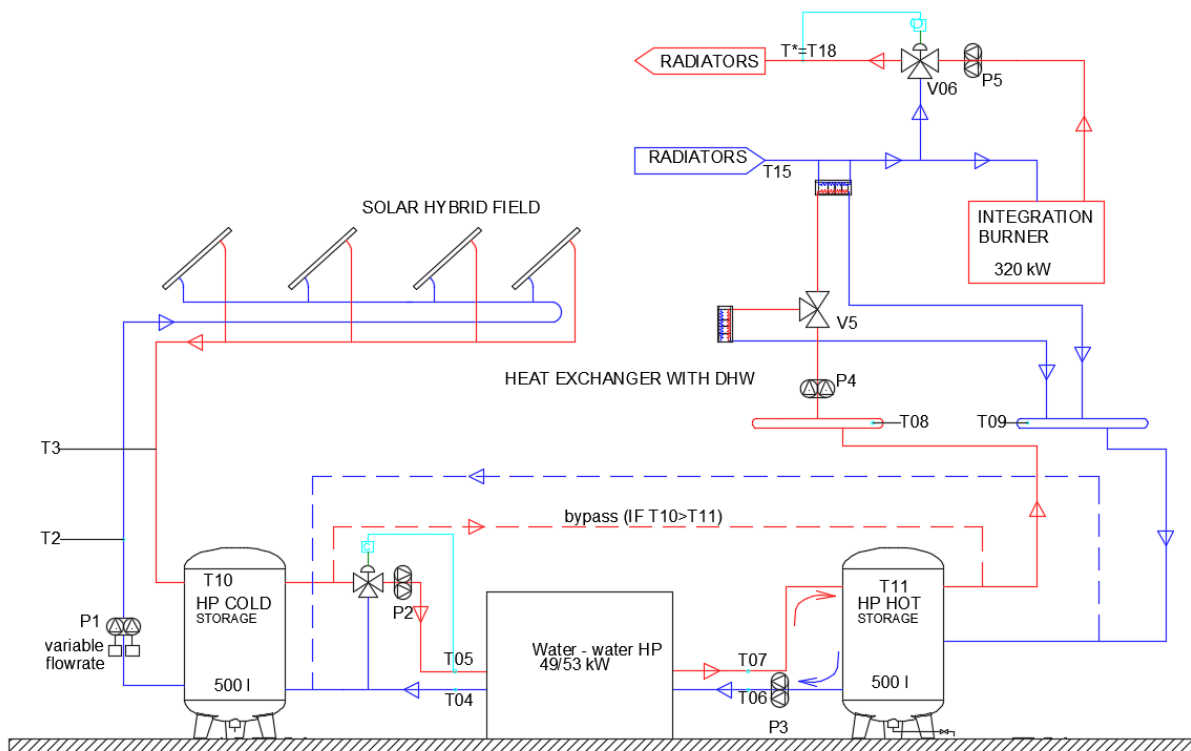
In conclusion, the coupling between HP and solar panels leads to other two improvements:

- the water heated within the panels can bypass the HP and it can be directly sent to the users when a limit temperature is overpassed (dotted red and blue lines in *Figure 3. 15 b*). This is more likely to occur in summer when the high temperatures and the strong solar radiation can heat the water far above the limit of 45 °C that enables the bypass. This configuration allows the plant to operate under different working conditions, it avoids the block of the HP due to the excessively high temperature of water inside the evaporator circuit and it exploits better the solar energy collected by the panels which would be wasted otherwise. Indeed, the HP requires on the evaporator side temperatures up to 20-25 °C. Higher values would lead to a block of the HP due to an excessively high pressure at the compressor, not compatible with the construction features of the installed HP. So, the working range between 25 °C and 45 °C would result critical since the water is too hot to be sent to the evaporator but it is too cold to activate the bypass. As a consequence, a mixing valve (*Figure 3. 15 b*) has been recently installed to grant the temperature at the maximum value of 25 °C. Independently from the working condition (i.e., in serial with the HP or with the bypass active), the twin pumps P1 (*Figure 3. 15* and *Figure 3. 16*) grant the water flow within the solar field. Only these pumps

are equipped with an inverter, allowing a variable flow rate which is chosen according to the difference in temperature between the outlet/inlet of the solar field. In addition, the switch on/off of the pumps depends on the temperature difference between the tank on the HP cold side and the outlet water coming from the solar panels.



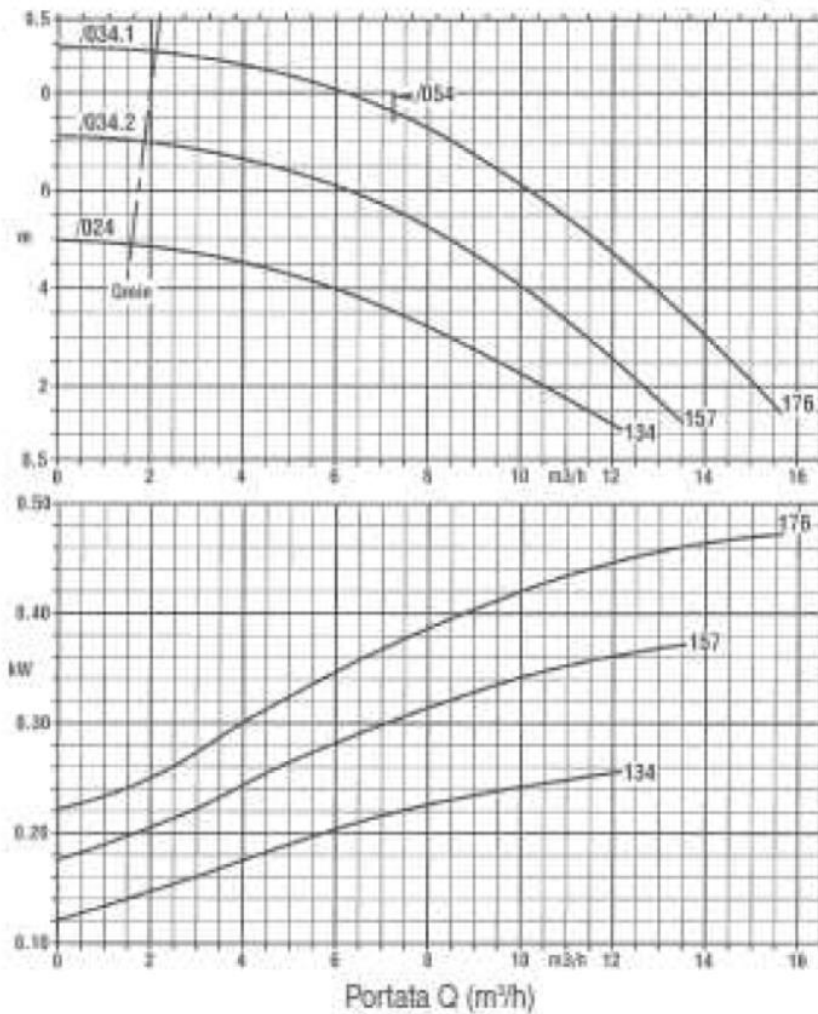
a



b

Figure 3. 15: simplified schematic representation of the interaction among the different generators. Colour code: blue line – cold water; red line – hot water

- The PV production is meant to totally (or almost totally) cover the HP energy consumption, united with the other energy intensive devices within the plant. At the moment, no PV storage is present since the original mechanism was based on the net metering and feed-in-premium strategies using the national grid as a virtual storage of unlimited capacity. This issue shall be better enquired in the following paragraph concerned with the critical issues resulting from the plant management.



Prevalence
H (m)

Power consumption
Pz (kW)

Figure 3. 16: pump P1, view and performance curve of a single pump

Table 3. 3 resumes the different codes assigned to the pumps, their application and the maximum consumed electrical power within the SH subsystem. In the end, the reference to the related picture is reported.

| Pump name | Application | Maximum consumed electrical power [W] | Figure |
|-----------|---|---------------------------------------|--------------|
| P1 | Between solar field and the 500-l storage interfaced with the HP evaporator | Variable | Figure 3. 16 |
| P2 | Between HP cold/solar storage and the HP | 1200 | Figure 3. 14 |
| P3 | Between HP condenser and HP hot storage | 1200 | Figure 3. 14 |
| P4 | Delivery pump to send hot water either to the DHW or SH | 1200 | Figure 3. 14 |
| P5/P6 | Delivery pump of the SH subsystem | 1200 | Figure 3. 14 |

Table 3. 3: summary table of the main pumps within the pilot plant – SH subsystem, including information about their positioning, power and reference to figures

3.1.2 Storage subsystem

On the SH side, no storage is present, except for the two 500 l tanks respectively interfaced with the hot and cold sides of the heat pump. The lack of a storage for SH, united to the required high temperatures (e.g., about 60-70 °C for air heaters and 50-60 °C for radiators) allows the HP work only as a pre-heat of the return water for the radiator circuit (Figure 3. 15 b).

On the DHW side, two tanks (named after DHW1 and DHW2 - Figure 3. 17) are present, with 1500 l capacity each. The choice of two tanks instead of one of double volume was imposed by the sizes of the boiling room which was not suitable for bigger tanks. Each storage has an external insulating layer with a related thermal loss coefficient of 2.6 W/m² K (134), (135).



Figure 3. 17: domestic water storage tanks - DHW 1 on the left and DHW2 on the right

DHW1 and DHW2 are put in serial asset: DHW1 is heated either by the integration gas burner or by the heat exchangers connected to the SAHP circuit (Figure 3. 19). DHW1 is also connected with the

cold water coming from the water supply. Then the top of DHW1 is connected with the bottom of DHW2. This configuration makes the two tanks work as if they were stacked one on the other. An internal recirculation system (dotted red line in *Figure 3. 19*, *Figure 3. 20 d*) is then established between the two tanks connecting the top of DHW2 with the high part of DHW1 to avoid excessive stratification. A recirculation system grants the supply of hot water also in long non usage period *Figure 3. 20 c*). From DHW2, the hot water is mixed by means of a three-way valve with the recirculation system by means of the twin pumps P9 (*Figure 3. 18*) and then sent to the users.

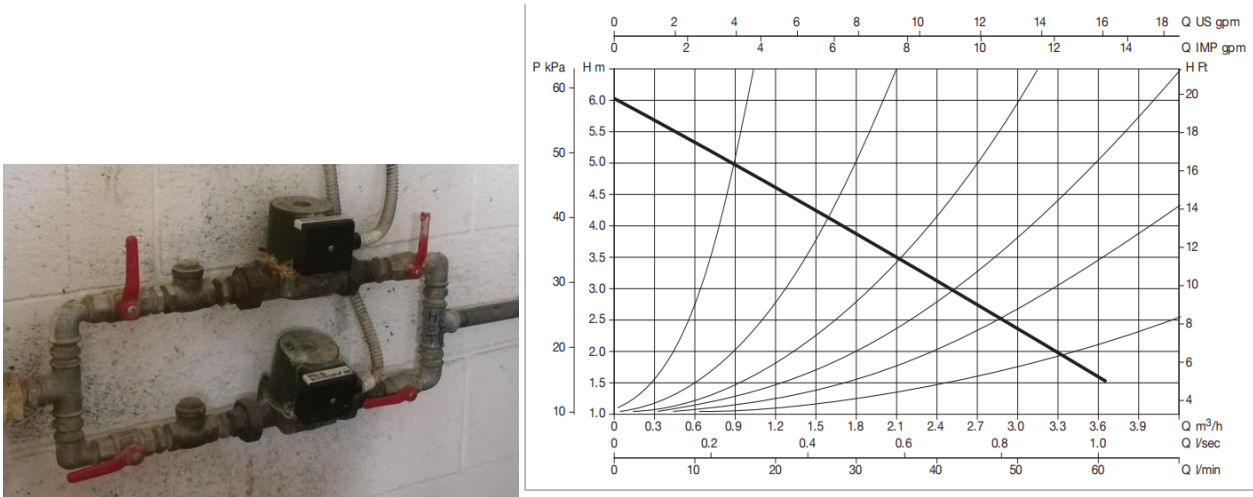


Figure 3. 18: constant flow rate pump P9 for recirculation system (maximum consumption 103 W)

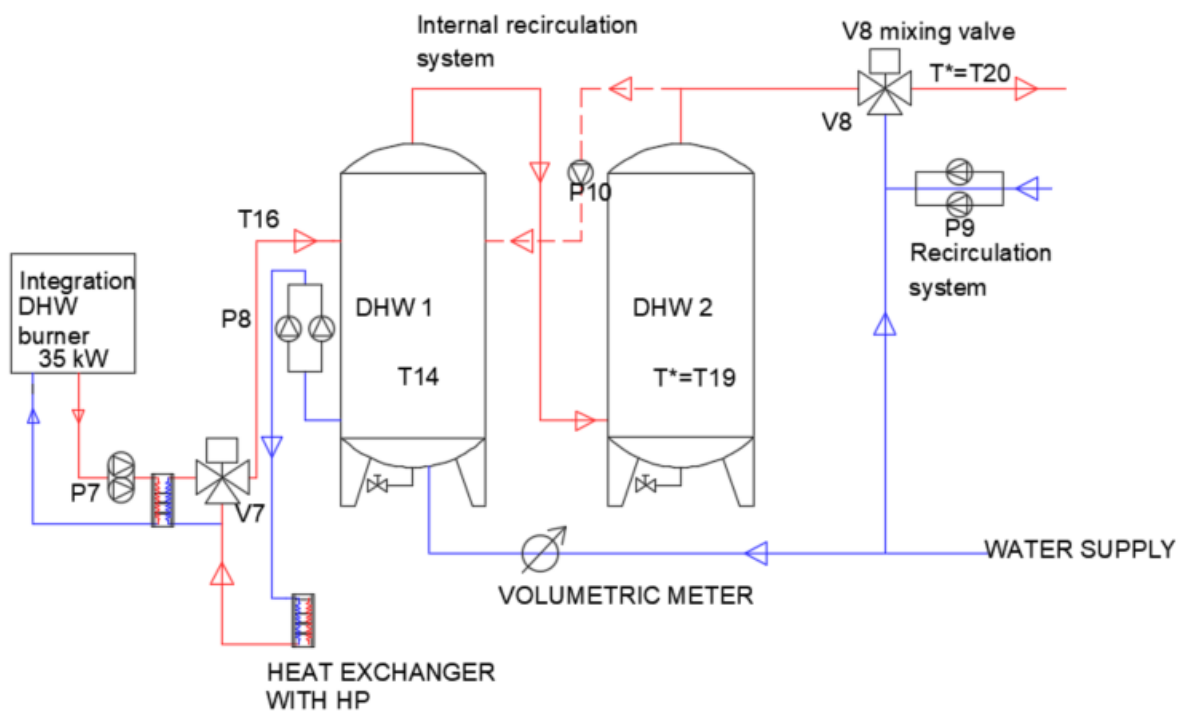


Figure 3. 19: simplified schematic representation of the DHW subsystem. Colour code: blue line – cold water; red line – hot water



a)



b)



c)



d)

Figure 3. 20: twin pumps P7 (in the foreground of figure a) and P8 (in the background of figure a and in figure b). Recirculation pumps P9 c) and internal recirculation pump P10 d).

Table 3. 4 resumes the different codes assigned to the pumps, their application and the maximum consumed electrical power within the SH subsystem. In the end the reference to the related picture is reported.

| Pump name | Application | Maximum consumed electrical power [W] | Figure |
|-----------|--|---------------------------------------|-------------|
| P7 | Circulates the hot water from the burner to the heat exchanger | 140 | Figure 3.20 |
| P8 | It grants the heating of the DHW by means of two exchangers connected to the HP and the burner | 225 | Figure 3.20 |
| P9 | Recirculation system | 135 | Figure 3.20 |
| P10 | Internal recirculation between the two DHW tanks | 140 | Figure 3.20 |

Table 3. 4: summary table of the main pumps within the pilot plant – DHW subsystem, including information about their positioning, power and reference to figures

3.1.3 Distribution and emission subsystem



Figure 3. 21: main elements composing the emission system: radiators (gyms, offices and lockers) and air heaters

The pipes connecting the emission system pass into the cavity walls to reach the different internal environments. The first part of pipes within the boilers room is insulated (about 2-3 cm thick) while the remaining part is poorly insulated since it is linked to the pre-existing heating system.

Concerning the emission system, two main types can be identified (Figure 3. 21): radiators with a working temperature of about 50-60 °C and air heaters with a working temperature of 70 °C. Given

that the temperature drop between outlet and inlet water of the air heater circuit could reach about 10 °C, the contribution of the SAHP is negligible since the working temperatures on the hot side are at about 50 °C. Indeed, the contribution of the SAHP in terms of space heating is concerned only with the radiator circuit, as shown in *Figure 3. 15 b*.

3.1.4 Control subsystem

It represents one of the most interesting and relevant components of the plant. This aspect is almost overlooked in traditional heating systems, since their simplicity allows a manual control even for larger sizes, especially in civil/residential applications. While on the industrial side a good management and control system is synonymous of efficiency, the awareness of this concept in non-industrial application has been taking place in these years, as more complex plants are installed, to meet the need for environmental-friendly plants. Through the monitoring process, information is collected and the achievement of the goals can be assessed.

The Data Acquisition System (DAS) installed at the Palacus sport palace enhances all the following aspects:

- it ensures communication among all the subsystems, increasing the reliability of the plant
- the almost real time management and control performed by the DAS allows the integration of the several components (e.g., solar field, heat pump, integration burner) according to both the end users' needs and the external climatic conditions.
- the DAS increases the plant productivity, exploiting the most efficient asset according to the boundary conditions
- alerts can be set either to immediately get notification in case of occurrence or to prevent critical situations to occur.
- in addition to the alerts, a report about the status parameters of the system can be obtained easing the trouble-shooting process.
- the DAS can be accessed and controlled both on-site and remotely. The latter allows in most of cases to reboot the system or make it operative again without any physical intervention. In some cases (e.g., rupture of a component), the DAS still plays a central role to perform a preliminary remote check-up of the plant to implement a quick and effective solution.
- the DAS allows the detection of gaps and issues to correctly address the resources to improve the system, reducing their waste.
- the collected information represents a reference for the decision-making process to identify mistakes, success, configurations that can be adapted and replicated for future projects.

In the specific case study, the plant is provided with:

- over 50 measurement points which allow the measurements of a large number of parameters: from the temperatures/flow rates inside the system (e.g., of the solar field, inside the storage tanks etc), the external climatic conditions (e.g., irradiance, wind speed, air temperature) up to the status parameters referred to the valves, pumps and other components (e.g., working hours for pumps). In addition, the system collects any warning to identify system failures or even prevent them.
- Over 15 control points represented by automatic mixing and three-way valves, on/off controls of the different components. Annex reports the complete functional scheme of the plant outlines the location of the measurement and control points as well.

The sensors are divided into two main groups:

- weather station + solar field: located near the solar field, it collects the main parameters associated to the solar panels and to the weather. It is connected to the internet by means of a specific multinet (programmable controller) and it collects information about panel temperature, solar radiation, air temperature, relative humidity, wind speed (*Figure 3. 22*).



Figure 3. 22: weather station at the solar field – Palacus

- Boiling room: it hosts the core of the DAS. The internet connection allows both the remote control and the communication with the solar field/ weather station. A Programmable Logic Controller (PLC) manages both the control and acquisition systems, with an interface accessible either on-site or remotely from the web application. The user interface consists of different panels containing the graphic representation of the different parts of the plant (as shown in *Figure 3. 15 b*) and *Figure 3. 19*) united with the measured parameters (e.g., temperature, status parameter of pumps), *Figure 3. 24*.

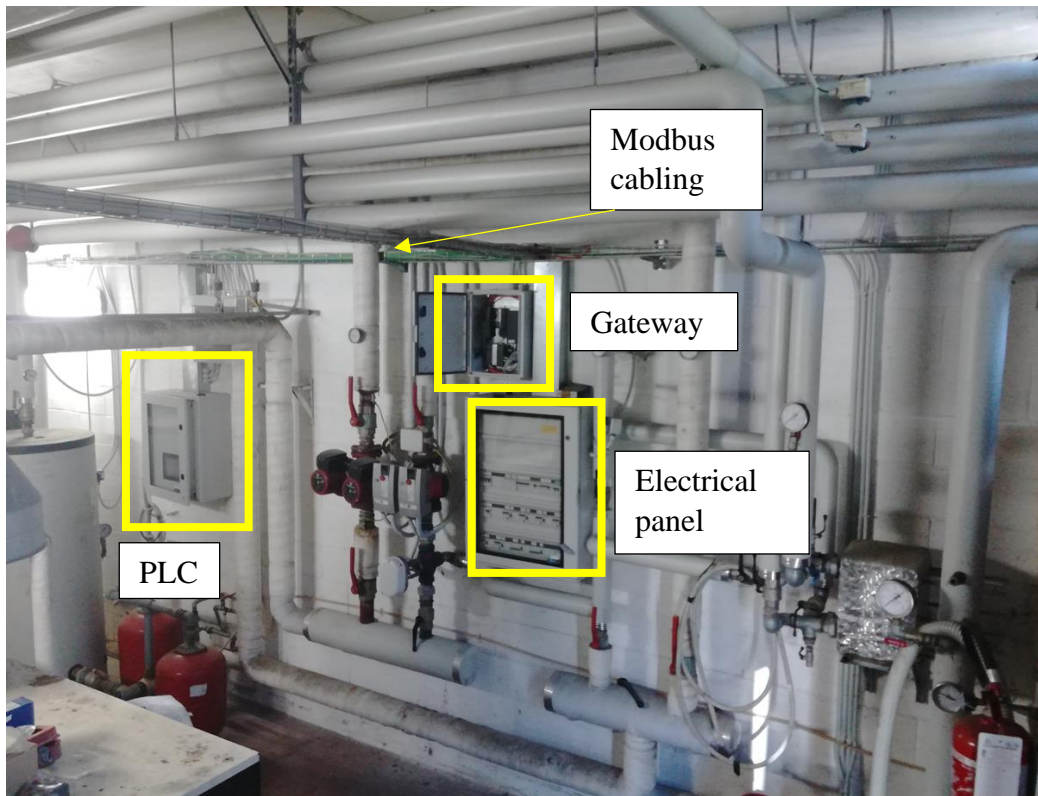


Figure 3. 23: boiler room overview – the yellow rectangles identify the main hardware of the DAS

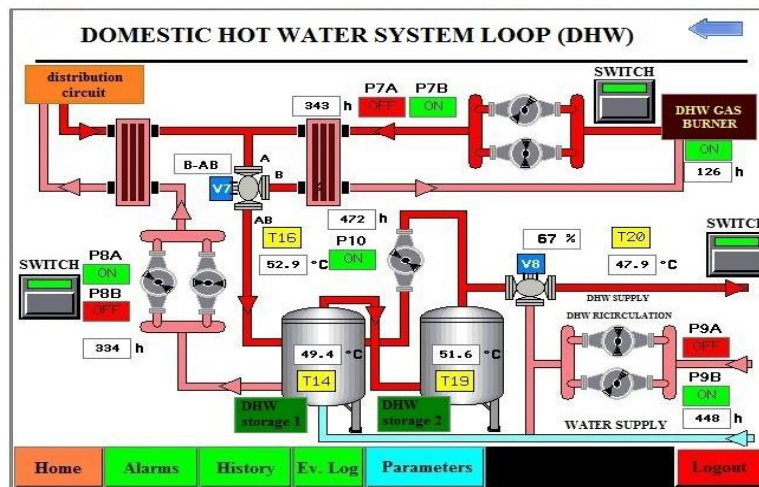


Figure 3. 24: one of the control screens accessible even remotely, reporting the plant scheme and the main measured parameters

In addition, some measurement points are analog while most of them are digital (Figure 3. 25)



a)



b)

Figure 3. 25: example of analog a) and digital b) sensors within the plant

One of the main roles of the DAS consists in the management of the different generators interacting one with the other (i.e., solar field, heat pump and integration gas burners). The following working pattern can be activated:

- usage of only gas burners. It represents the old system adopted before the plant revamping. It can be used under critical situations (e.g., rupture of the HP) to prevent the interruption of the SH and DHW services. From the point of view of efficiency, this configuration has to be the least adopted.
- direct usage of the solar field with the bypass of the HP. It is more likely to be used during summer when the water heated by means of the panels can be directly sent to the DHW subsystem. The bypass has the double role of both increasing efficiency when favourable conditions occur and avoiding the block of the HP due to excessively high temperatures on the evaporator side (e.g., 45 °C).
- usage of the solar field coupled to the HP. It represents the reference case, especially during the heating season, where the plant can reach its maximum efficiency.

In the last two cases, the integration gas burners can step in, every time the SAHP or the solar field cannot grant themselves the required thermal needs.

Coupled to the previous working conditions, the DAS manages about 70 automatic control and maintenance criteria. For instance, periodical high temperature cycles to prevent the growth of Legionella bacteria inside the DHW tanks or the constant control on key parameters to switch the active components of the plant off before critical conditions occur (e.g., control temperature of water inside the solar panels to avoid freezing or stagnation, activation/deactivation of the solar bypass with automatic setting of all the diverters). The following chapter concerned with numerical modelling will recall the different regulation criteria built inside the model to reproduce the working of the real plant.

On the data acquisition side, the DAS collects the measured parameters performing a preliminary processing: the information is stored every 2 minutes as the average of measured values. This operation allows the reduction of the memory size required without losing relevant transient phenomena. In addition, the collection of any eventual warning allows to divide the sets of measures

associated to the normal working conditions from the ones linked to system failure or inactivity for maintenance reasons. The measurements are accessible from the web as well, by means of a dedicated, protected access from the university network.

3.1.5 An overview over the plant performance

This last section resumes the performance of the plant, basing also on the calculations performed in the original design and the works and PhD thesis (136), (137).

| | Primary energy need (SH radiators + DHW) [kWh] | Energy provided by SAHP-PVT [kWh] | SAHP-PVT Elec consump [kWh] | Int burner - SH [kWh] | Int burner - DHW [kWh] | PV prod – [kWh] |
|----------|---|--|------------------------------------|------------------------------|-------------------------------|------------------------|
| J | 11.870 | 3.108 | 863 | 7.873 | 889 | 1.029 |
| F | 10.721 | 3.476 | 964 | 6.000 | 1.245 | 1.405 |
| M | 11.240 | 5.210 | 762 | 4.141 | 1.889 | 2.328 |
| A | 5.744 | 3.147 | 427 | 2.003 | 593 | 2.298 |
| M | 2.968 | 1.626 | 221 | 0 | 1.342 | 2.877 |
| J | 2.872 | 1.574 | 213 | 0 | 1.298 | 2.359 |
| J | 2.968 | 1.574 | 583 | 0 | 1.394 | 2.683 |
| A | 2.968 | 1.626 | 221 | 0 | 1.342 | 2.901 |
| S | 2.872 | 1.574 | 213 | 0 | 1.298 | 2.134 |
| O | 2.968 | 1.205 | 211 | 0 | 1.763 | 1.547 |
| N | 9.987 | 3.889 | 1.080 | 4.910 | 1.188 | 1.082 |
| D | 11.870 | 3.235 | 898 | 7.685 | 950 | 967 |
| T | 79.048 | 31.244 | 6.656 | 32.612 | 15.191 | 23.610 |

Table 3. 5 Main annual operating data of the Palacus Sport Palace.

The expected coverage of SH/DHW needs by means of the SAHP-PVT is of about 40%. This percentage is mainly due to the difficulties in the coupling of the SAHP-PVT to a high temperature emission system. Even on the DHW side, the high set point temperature, needed for sanitary reasons, requires the intervention of the gas burner, especially early in the morning and late in the afternoon-evening (according to the month under study).

On the performance side, the HP interfaced with the solar field reaches an average monthly COP of about 3.6. Such result is obtained as a ratio between the energy provided by the SAHP and the electricity consumed in the considered month.

Considering a yearly performance instead, the total thermal energy provided by means of the SAHP-PVT (either SAHP or solar bypass according to the season) is 31.244 kWh while the electrical consumption is of about 6656 kWh, leading to a yearly COP of about 4.7. This improvement is due to the energy delivered by means of the solar bypass during summer which relevantly increases the useful effect, with a very small, added electric consumption due to the circulating pumps.

In addition, the PV production can cover the monthly energy need of the SAHP, with an overproduction of about 60%. This issue occurs mainly in summer, since the sizing of the PV field is referred to the months with lowest solar radiation (i.e., January or December).

Out of the heating season, the need tends to become constant at about 3000 kWh/month associated only to the DHW needs. Anyway, very small fluctuations can be noticed in *Table 3. 5* mainly due to the different number of days within the months (30 and 31 respectively). The designers assumed negligible the thermal losses due to the difference in temperature between the boiler and the room. In addition, when the bypass is active, both the SAHP-PVT and the gas burner are expected to equally contribute to cover the primary energy need, because of the reduced thermal energy provided by the solar field.

Actually, the temperature reached by the solar panels, united with the reduction of the energy need (about one third with respect to months such as January or December) makes more convenient the direct usage of the hot water with the integration gas burner. Also on the functional side, the temperature of the solar panels can reach values of about 40-45 °C which are not compatible with the operative maximum temperature on the evaporator side (18 °C). Clearly, the convenience of the solar bypass is directly influenced by the location and its climate.

The plant designer obtained these results basing on almost steady state, simplified approaches. One of the strongest assumptions underlying the results is the neglect of relevant thermal losses along the connection pipes between the solar panels and the solar storage (about 200 m supply + 200 m return long pre-insulated pipes). As outlined in the previous chapters, the assumption can be considered acceptable during the heating season, when the temperature of the water flowing inside the pipes is comparable to the one of ambient air. On the other hand, the temperature becomes far higher than the ambient air during summer, causing not negligible thermal losses which have not been accounted in *Table 3. 5*.

Nevertheless, the results will be used in the next chapter as a further information to validate the global performance of the assembled numerical model once the same assumptions have been implemented (i.e., negligible thermal losses of the connection pipes of the solar field).

3.2 The sport palace Carmine Romanzi – energy characterization

3.2.1 DHW need

The facility mainly hosts a major sports hall with six lockers with three showers and three sinks each. The ground floor is occupied by the administrative offices and some weight rooms. The utility rooms (e.g., boiler room) rooms are on the back of the building (Figure 3. 26). An AHU (Air Handling Unit) room is present as well; actually, this part of the plant is under revamping and it will be connected to the SAHP-PVT to provide hot water to the heating battery.

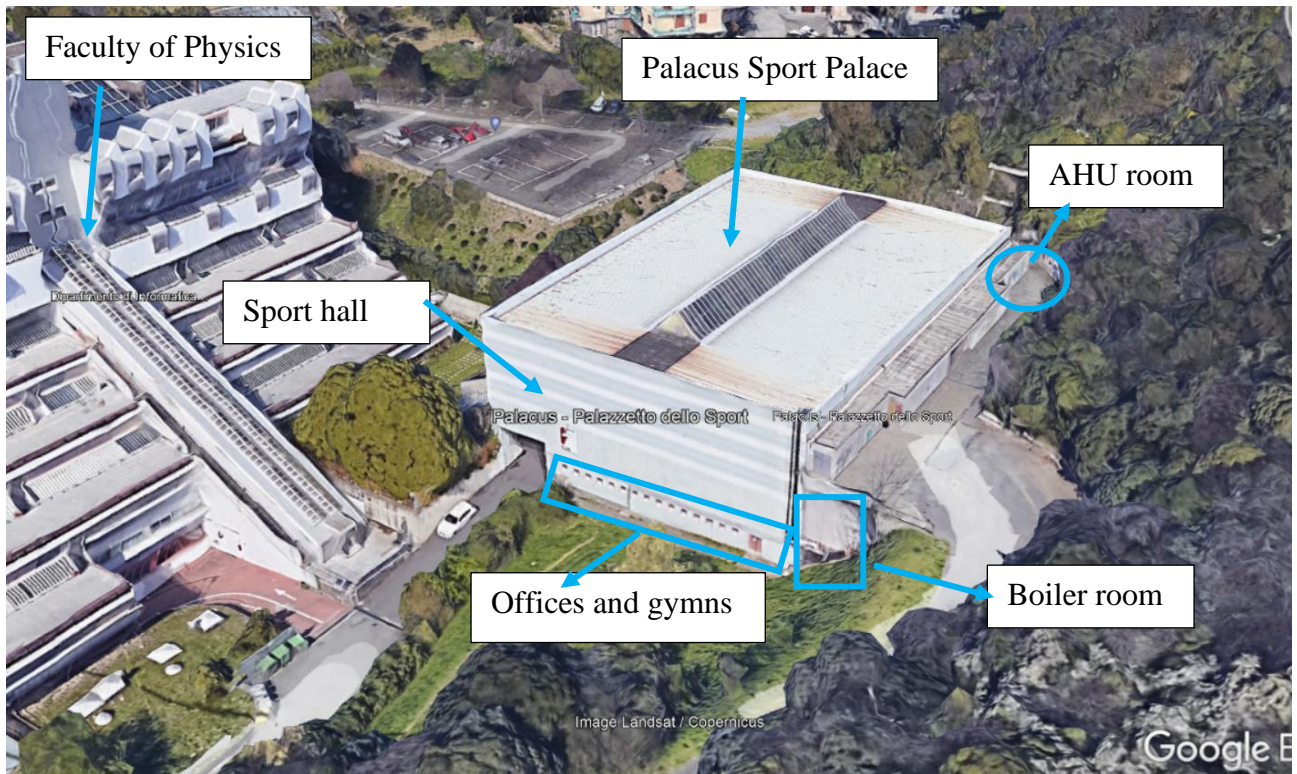


Figure 3. 26: 3D view of the sport palace Palacus with the main outline of the different indoor environments (source Google Earth)

The lockers of the facility are also available for the athletes attending to the external sport courts (six tennis courts and one soccer field - Figure 3. 27) which are used even at night especially during weekends and in the milder seasons (i.e., summer and part of spring/autumn).

The sport palace is a multi-use facility, reference point for both university sport events and the neighbourhood; indeed, many sport classes are held for children, sportsman and amateurs of all ages. Therefore, the users of the facility are expected to be heterogeneous in terms of age, gender and usage over the day. No relevant concentration in the typical daily DHW consumption profile is expected, due to the large amount of sport classes scheduled during the opening hours, along with the chance of autonomous individual or group sport activity. In addition, the complex is open seven days a week, operating from 8 a.m. to 10 p.m. while the courts rental extends up to midnight during summer.

In addition, no relevant variation in the total daily amount in DHW is expected between winter and summer. Without going into excessive detail, Figure 3. 28 shows the temperature trends of water inside the DHW tank of the plant at Palacus during a typical summer (Figure 3. 28-a) and winter (Figure 3. 28-b) day.

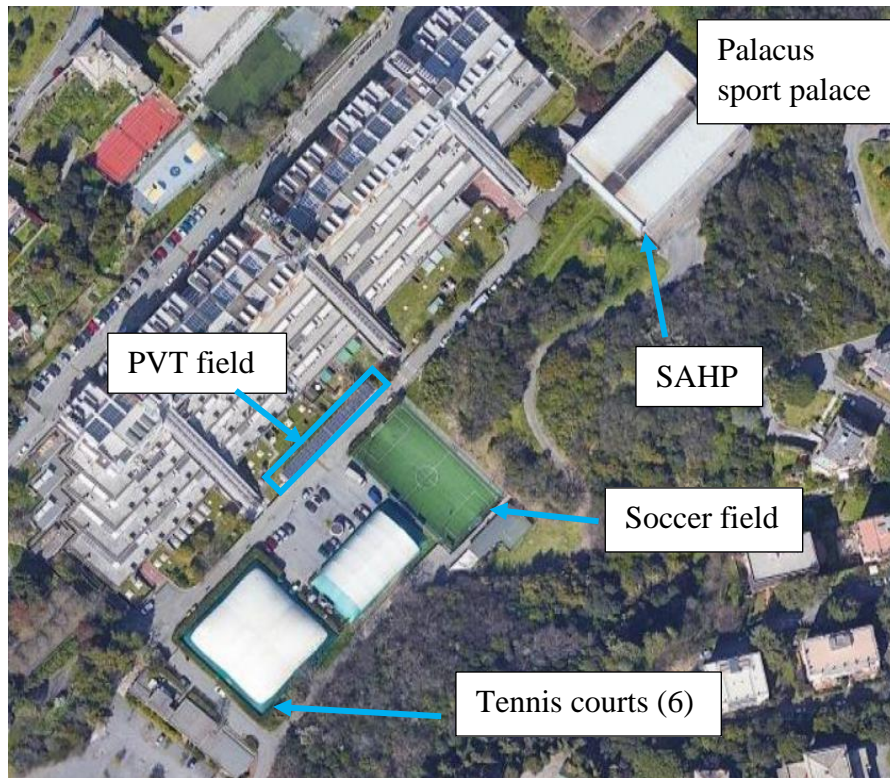


Figure 3. 27: satellite view of the facility and the external courts

Each decrease in temperature from the set point value is due to cold water flow rate at the bottom of the tank, caused by a withdrawal of hot water from the top (e.g., for showers). The comparison of the DHW trends during the different years, resumed by the two graphs (Figure 3. 28), allows the following conclusions:

- during summer about nine main withdrawals occur, with respect to about four/five occurring during winter. This trend is in accordance with the reduced usage of the external courts of the facility during winter, with a lower frequency of showers in the lockers.
- Each peak has the same intensity, since it determines very similar decreases in temperature.
- Besides the increase of DHW usage, the temperature in the DHW tank decreases of about 0.5 °C after each usage (the tank has a volume of about 3000 l) while during winter the decrease almost doubles. This result can be associated to the more likely colder showers during summer with a lower consumption of DHW.
- the difference between the two initial trends is highly influenced from the initial condition (the initial average storage temperature is about 52 °C and 49 °C respectively during summer and winter) with a longer time taken by the heating system to reach the set point (about a couple of hours for summer and about four hours for winter). This difference is also linked to the first relevant withdrawal which occurs in both cases at about 10 a.m. Actually, during summer, the set point has been almost reached and a decrease can be appreciated. On the other hand, in winter the heating system is still heating up and therefore the withdrawal can be outlined only by the change in the slope occurring from 10 a.m.
- the duration of each withdrawal remains almost unchanged during the year without any appreciable variation between summer and winter.
- Besides of the starting period (about from 8.00 a.m. up to 10.00 a.m.), part of the withdrawals occurs during the heating phase; this can be observed by the different inclination of the upward

sloping of the temperature curves shown in *Figure 3. 28*. For instance, during summer, the slope of the initial re-heating is steeper than the ones during the middle of the day, because of DHW usages during the heating phase of the DHW tanks.

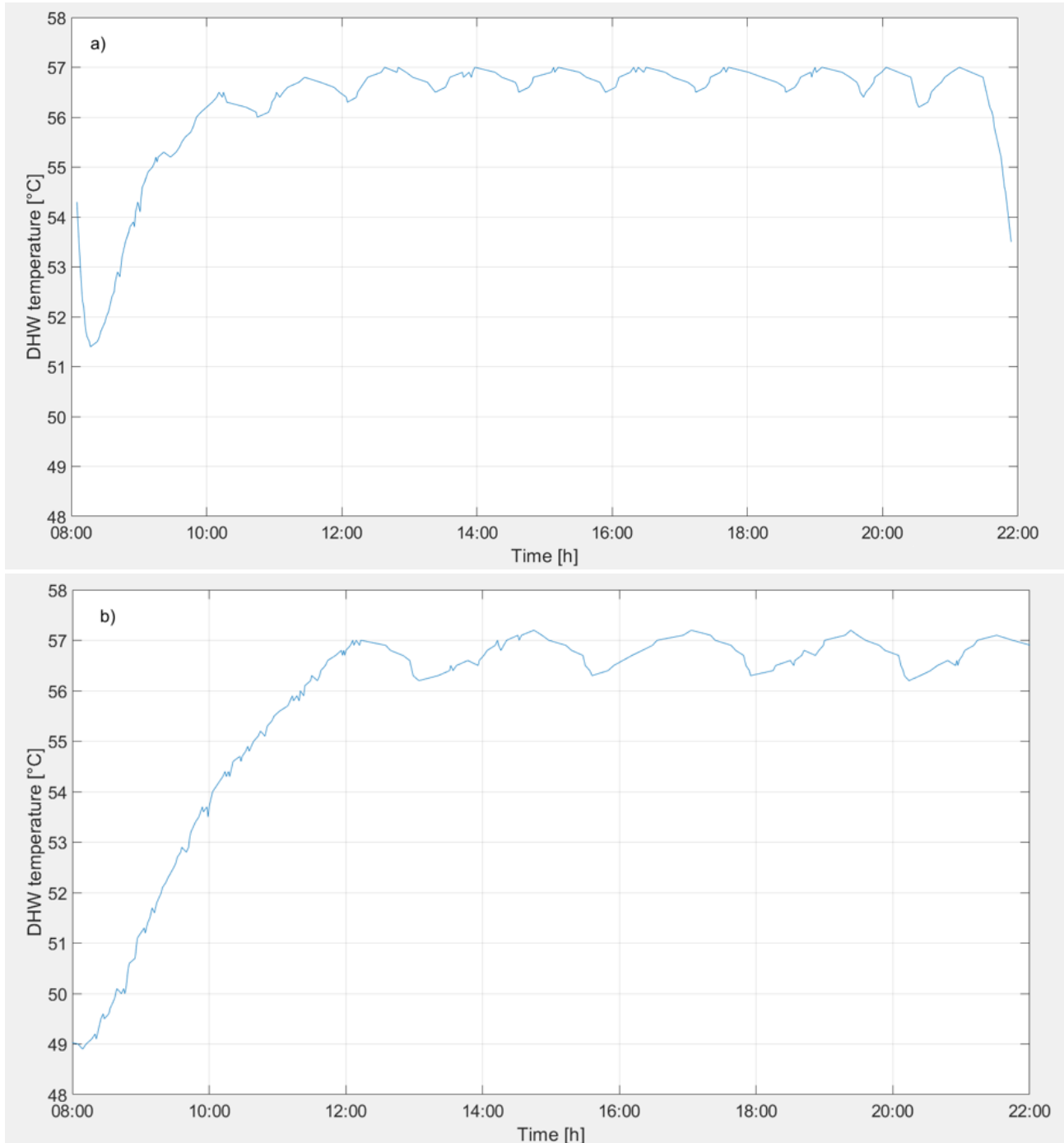


Figure 3. 28: DHW usage based on DHW storage tank temperature profiles. Typical day trends for a) summer and b) winter

As far as the total yearly energy need for DHW production is concerned, the original plant design (dating back to 2012) estimated about 30 MWh based on the measured data and recorded trends of the past years. This value is comparable to the one obtained with the approach contained in (138), (139). The primary energy need is given by the contribution of different terms: mainly the energy to heat the water added to the thermal losses (e.g., due to the distribution pipes, water storages, recirculation systems) minus any eventual free energy gain or recovery (Eq. 3. 1).

$$Q_{gn,W,out} = Q_W + Q_{I,W,er} + Q_{I,W,d} + Q_{I,W,s} - Q_{W,ghp,in} \quad \text{Eq. 3. 1}$$

With

$Q_{gn,W,out}$: primary generation energy need for DHW [kWh]

Q_W : useful energy need for domestic hot water production [kWh] - Eq. 3. 2

$Q_{I,W,er}$: thermal losses due to the supply subsystem [kWh], assumed equal to 0 as prescribed in (138)

$Q_{I,W,d}$: thermal losses due to the distribution subsystem [kWh] - Eq. 3. 4

$Q_{I,W,s}$: thermal losses due to the storage subsystem [kWh] - Eq. 3. 5

As better described below, the heating system under analysis has no recirculation system, a couple of water storage tanks with a total capacity of 3 m³ and the formulation of each term is briefly reported as follows:

Useful energy needs for DHW production - Q_W :

$$Q_W = \rho_W c_W \sum_i [V_{Wi} (T_{er,i} - T_0)] N \quad \text{Eq. 3. 2}$$

Where

ρ_W : water density [kg/m³]

c_W : water specific heat [kWh/kg K]

$T_{er,i}$: required set point brewing temperature [K], fixed at 40 °C

T_0 : the initial temperature of the inlet water from the supply, approximately equal to the soil temperature as the water supply pipes are underground [K]. The ground temperature (besides of the surface layer of the ground) corresponds to the local average seasonal air temperature. The average seasonal air temperature for Genoa is of 14.7 °C, (140).

N : the number of days for the period considered for the calculations

i -index: a counter for eventual different activities requiring hot water at different set point temperatures

V_{Wi} : the daily required volume of water. It can be estimated for non-residential application by means of Eq. 3. 3

$$V_W = a N_U \quad \text{Eq. 3. 3}$$

With

a : specific daily need, fixed at 50 l/day for sport palaces, gyms

N_U : dimensionless parameter determined according to the building under analysis; concerning sport palaces it equals the number of showers present in the facility

Thermal losses due to the distribution subsystem - $Q_{I,W,d}$:

$$Q_{I,W,d} = (Q_W + Q_{I,W,er}) f_{I,W,d} \quad \text{Eq. 3. 4}$$

Where

Q_W : useful energy need for domestic hot water production [kWh] - Eq. 3. 2

$Q_{I,W,er}$: thermal losses due to the supply subsystem [kWh], assumed equal to 0 as prescribed in (138)

$f_{I,W,d}$: loss factor of the distribution subsystem [-] which can be determined by means of tabular approach for existing plants

Thermal losses due to the storage subsystem - $Q_{I,W,S}$:

$$Q_{I,W,S} = \frac{S_s}{d_s} (T_{avg,W,S} - T_a) t \lambda_s \quad \text{Eq. 3. 5}$$

With

S_s : storage external dispersal surface [m^2] – determined according to the geometrical dimensions of the storages

d_s : insulating layer thickness [m] – 5 cm for the case study

λ_s : insulating layer conductivity [W/m K] – about 0.10 W/m² K

t duration of the period under analysis [h]

$T_{avg,W,S}$: average water temperature inside the storage, fixed at 60 °C in the approach in (138)

T_a : ambient temperature of the boiling room containing the storages [°C], equal on average to 16 °C for the case study.

Applying formulations from Eq. 3. 1 to Eq. 3. 5, the estimation of DHW primary need is about 29700 kWh, with very good accordance with the design assumption and the energy efficiency analyses performed in previous PhD works (136), (137).

In conclusion, the DHW need can be considered constant over the different months, with a preliminary estimation need of about 2700 kWh, obtained equally dividing the annual need over eleven months (the facility is typically closed during August). This value corresponds to about 70-80 m³ of DHW consumed, with a daily average of 1.5-2 m³.

With specific reference to the hourly DHW consumption profile, very few works in literature enquire the field of non-residential buildings, although some specific applications show very high DHW consumptions (e.g. restaurants or hospitals where the peaks in DHW consumption can be related to intensive cleaning and meal cooking). Clearly the larger number of variables than in the residential case makes any experimental survey even tougher. For instance, a daily water consumption between 440 and 4400 l/day has been found in (141) for DHW consumption in restaurants, with a strong dependence on the number of both customers and dishes served. (142) shows a very interesting and complete review of the researches available in literature, highlighting the lack of exhaustive and methodical analysis for DHW profiles for different buildings types, on different climates and geographical zones. These aspects cannot be neglected since the limited available works on the topic shows very relevant variations for different building types.

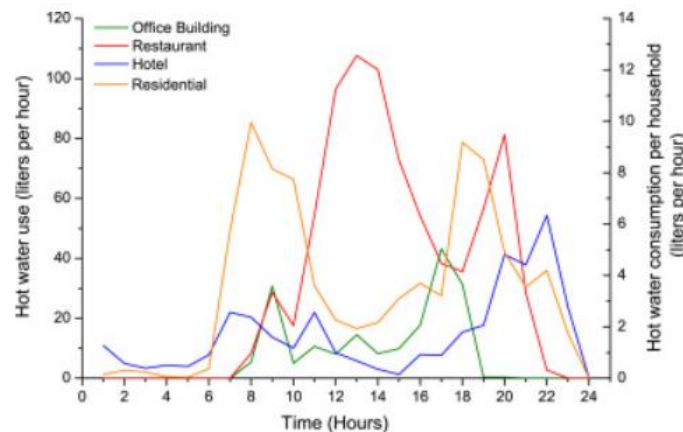


Figure 3. 29: average hourly daily profiles for residential (Right axis plot, orange line) and non-residential applications (left axis plot, green – office building, red – restaurant, blue – hotel) (142)

Concerning the specific case study, the following averaged hourly DHW profile has been implemented (*Figure 3. 30*), basing on the measured information. Its accuracy can be found in the following aspects:

- An average of five main peaks is registered on a typical, reference day. These peaks reproduce the massive usage of the lockers at the end of group trainings.
- The total daily consumption of water (area swept by the curve) is of about 1.5 m^3 . Such value is within the limits deduced above.
- The section about the validation of the numerical model (Section 4.2.3) will show the comparison between the measured trends for water temperature inside the DHW tanks and the simulated one, caused by the DHW profile plotted in *Figure 3. 30*, with very little variation.

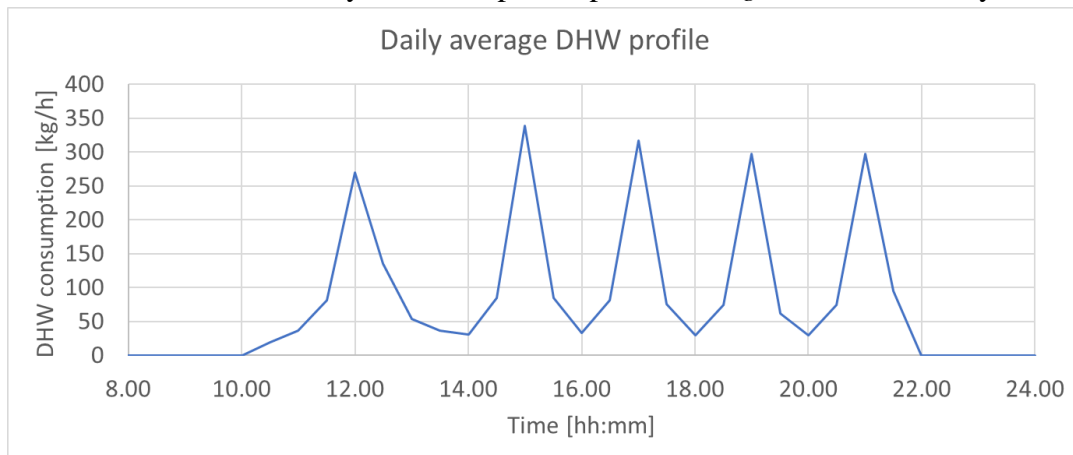


Figure 3. 30: reference DHW hourly profile implemented in the numerical simulation

3.2.2 SH need

The building dates back to the period the nearby Faculty of Physics was constructed (between 1974-1987). Therefore, the envelope of the structure is poor in terms of energy performance. The vertical structure is made of reinforced concrete pillars and beams as well as the bleachers for the public, with opaque closures towards the outside made of concrete bricks with an average transmittance between $1\text{-}1.2 \text{ W/m}^2 \text{ K}$, also considering the contribution of single glass-aluminium doors and windows (*Figure 3. 32*). The roof is made in exposed steel beams and a covering made in part of opaque panels with an average transmittance of $1.5 \text{ W/m}^2 \text{ K}$, with central shed glasses (*Figure 3. 31*).



Figure 3. 31: particular of the roof of the sport palace



Figure 3. 32: most common opaque panels and windows of the sport palace

The building has important external shadings mainly towards North, North-East and North-West while on the other directions it is well exposed to the solar radiation, with a relevant benefit in terms of energy needs for heating.

Basing on the design project dating back to 2012 and to the following efficiency analyses carried out in previous PhD projects (136), (137) estimated an energy need for the pre-heating of the radiator circuit by means of the SAHP of about 44 MWh related to a dispersal surface of more than 3000 m².

This yearly value can be then split into the different months of the heating season (Figure 3. 33) while the SH need is zero during summer and part of autumn/spring since the heating system is off.

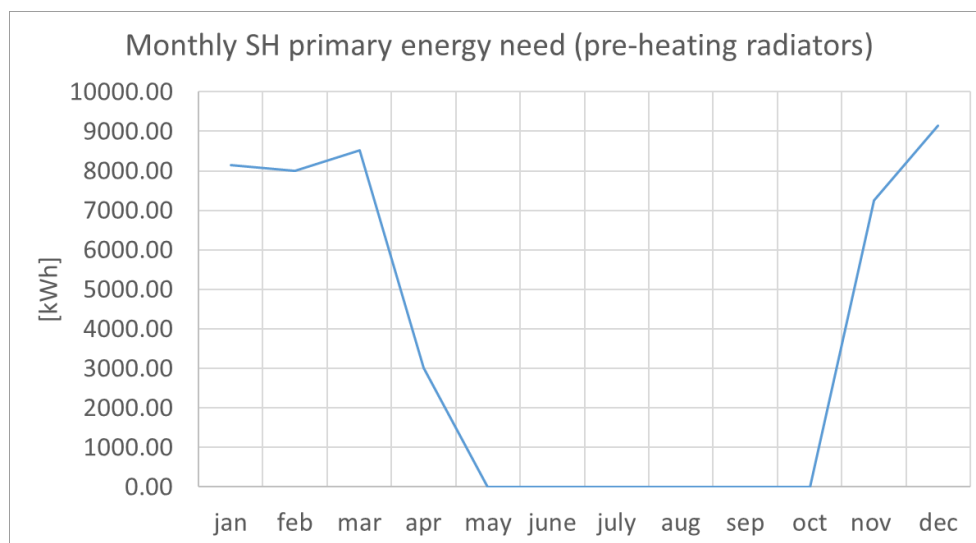


Figure 3. 33: monthly need for space heating for the sport palace Carmine Romanzi

With reference to the opening hours of the structure reported above, the heating system is operative only from about 7-8 a.m. up to 10 p.m. with very slight fluctuations over the year. The shape of the SH daily demand profile used in the current work is based on the one used in other researches about the sport palace (136), (137) and it is in accordance with similar topics dealt in previous studies (143), (144)- Figure 3. 34.

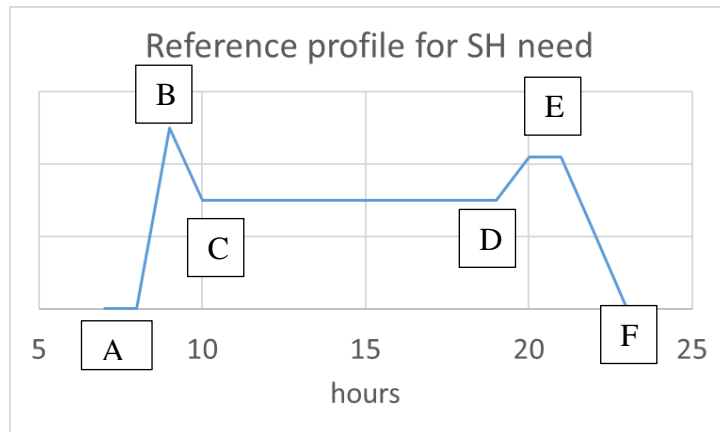


Figure 3. 34: reference profile for daily SH need considered for the sport palace Carmine Romanzi. The vertical axis is unitless since it depends on different parameters (e.g., external temperature, solar radiation)

With reference to Figure 3. 34, the following points can be identified:

- *Starting of the plant:* about half an hour before the opening (8.00-8.30 a.m.) the plant usually starts and one the highest daily peak is reached in terms of power, to reach the set point value in all the internal environments which have cooled down during night (Section A-B in Figure 3. 34). Clearly the slope of the line depends on the initial conditions (e.g, air temperature, solar radiation availability) and on the required set point, united with the characteristics of the envelope. For this reason, no value has been assigned to the vertical axis since it is expected to vary during the different months of the heating season. Then, a steep decrease in the need occurs when the set point is reached (Section B-C in Figure 3. 34), reaching an almost constant value.
- *Steady state regime:* the SH heating need can be approximated as constant during the central part of the day (Section C-D in Figure 3. 34) since the plant works to keep the set point temperature, with no significant effort with respect to the initial heating. The starting and ending points of this part depend both on the initial and boundary conditions. In particular, point D is likely to occur later in mildest days (e.g., in April) due to longer solar radiation for instance.
- *Second peak and switch off:* in the evening, a second peak is usually appreciated (Section D-E in Figure 3. 34), due to the fall in temperature during night. Anyhow, this peak is likely to be lower or equal to the first one early in the morning, since the environmental conditions are comparable, but the structure is already/almost at the set point temperature. In some cases, the peak (point E) can be followed by a horizontal section, depending on both the usage of the structure and the external climate. Then, the switch off of the plant occurs (Section E-F in Figure 3. 34) since the facility closes. In addition, Italian laws establish a maximum daily time for heating system operativity, according to the climate zone. The present case study is located in Genoa (climate zone D – between 1401 and 2100 Degree Days) and the plant can be operative up to 12 hours a day during the heating season (from November, 1st up to April, 15th).

Concerning the numerical modelling, the contribution of the SAHP is limited only the pre-heating the water returning from the radiator circuit which serves only the lockers (for additional information, please see section 3.1.3 and Annex). In turn, the lockers are placed inside the structure, either in touch

with heated (e.g., sports hall, offices) or unheated (e.g., crawlspace) environments, with no direct solar radiation. Consequently, two main observations can be drawn:

- the SH referred only to the radiator circuit shows very small variations over the heating season due to its location inside the structure. This aspect is supported from the recorded measurements of both the supply and return temperatures of the radiator circuit along the different months (respectively T18 and T15, *Figure 3. 15b*). In *Figure 3. 35* an almost constant difference in temperature of about 2-3 °C can be noticed during the different days. This trend remains almost unchanged all the heating season long. In addition, the difference between supply and return temperature seldomly approaches to zero values, meaning that the circuit is active very often during a typical day. On the other hand, the supply temperature varies between 50 °C and 60 °C according to the external ambient temperature. This control criterion will be better described in the following chapter about numerical modelling.

- the present study will simplify the modelling of the SH associated to radiators introducing a standard difference in temperature between outlet and inlet flow rates on the heat exchanger with the SAHP of either 2 °C or 3 °C, according to the external temperature all the heating season long. This assumption is supported by the following considerations:

- a) the difference of the temperature between supply and return water referred only to the radiators (within the lockers) can be considered weakly influenced by the external climate, thanks to the position of the environment inside the structure.
- b) the SAHP-PVT pilot plant is designed to preferably provide as much heat as possible to the DHW production. The SH subsystem is conceived as a secondary circuit with which heat exchange occurs only when the DHW is either within the set point values or in stand-by.
- c) *Figure 3. 35* reports the measured parameters of the water temperature inside the radiator circuit before and after the heat exchanger with the SAHP, showing that the difference in temperature is about 2-3 °C.

More details will be provided in the numerical modelling chapter (Section 4.2.3).

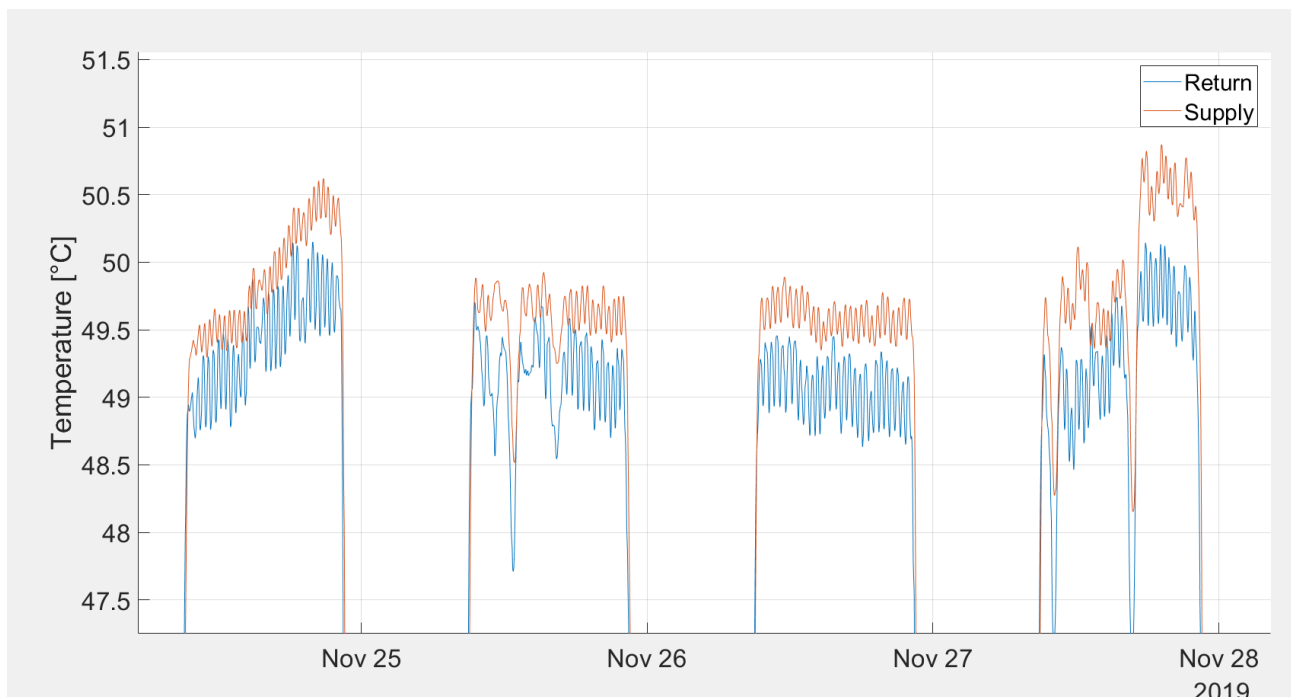


Figure 3. 35: supply (orange line) and return (blue line) temperatures of the radiators circuit

3.3 Critical issues resulting from the plant monitoring and management

This section provides the reader with the last element needed to have a complete view over the plant: the critical issues aroused during the plant monitoring and management. This aspect is of paramount importance, since it is the first step to increase the plant efficiency. Five main topic areas have been identified and they are briefly resumed as follows. These issues represent the starting point of the present study which aims at new interventions to increase the plant efficiency and solve or at least improve the problems described below.

3.3.1 Acceptance

When approaching a plant design, the common and recurrent target parameters to be met are concerned with the efficiency and the plant working (e.g., COP) with no attention at all to the reaction of the users to the new plant.

The term "efficiency" refers to the peak level of performance that uses the least number of inputs to achieve the highest amount of output. Efficiency requires reducing the number of unnecessary resources used to produce a given output, including personal time and energy. Efficiency is a measurable concept that can be determined using the ratio of useful output to total input. Increased efficiency minimizes the waste of resources such as physical materials, energy, and time while accomplishing the desired output (145).

According to the definition above, all traditional designs aim at the reduction of the denominator (i.e., the consumption, the employed resources), while the numerator (required output) is considered always present. Actually, a plant which is not used has a null efficiency, even if the least number of inputs were used. A complex and not accepted plant is very likely to reduce the input but also the output as well, since the final users tend to be more confident with well known, old technologies, even if they are less efficient.

Another neglected aspect of the definition is concerned with time. Even if it does not seem to play a direct role in efficiency (except for the time strictly needed to accomplish the task), people tend not to spend time to understand new technologies, besides of the attainable performances and savings.

All these concepts shortly exposed belong to the wider topic of acceptance, which has involved researchers from very different fields (e.g., social (146), (147), (148), psychological (149), (150), economic (110), (115), technical (116), (151), (152)) since a new element with very low acceptance could reveal unsuccessful for instance since people do not tend to invest in it. The concept of acceptance itself is very wide; it is conceived as "*a general agreement that something is satisfactory or right*" (153). The term "something" reported in the definition may apply the very different cases: from policies (e.g., about environment) up to new technologies.

The present section is concerned with the technological issues connected to acceptance, with specific attention to the case of the SAHP-PVT pilot plant at Palacus.

In fact, the original heating system of the facility was based on two gas burners. Then, the revamping coupled a solar assisted heat pump with hybrid panels to the existing plant. Actually, the change in the plant was quite radical:

- the old one worked almost independently from both the environmental conditions and the level of usage of the facility. The working of the burners always occurs under steady state regime and the control/maintenance activities are well known and established. The plant control can be performed without any advanced/automatic system, as it was based on few and

simple parameters (e.g., set point temperature for inlet water, set points of the external climatic weather sensors).

- the SAHP-PVT almost always works under transient regime, with its performance considerably dependent on the environment conditions and on the usage of the facility. The increased number of control parameters, united with the different possible working conditions requires a high level of self-control and automatization since a manual control could not manage the plant correctly. In case of blocks, the SAHP needs a manual re-start, after the causes of the block has been understood and removed if necessary. This operation requires added skills, mainly technical comprehension about the working of the main systems.

As a consequence of this change in the approach of the plant management, the technical staff preferred to switch from the SAHP-PVT to the burners many times during the heating season (especially in the former years), since they were afraid of possible blocks which would require an additional intervention. Another instance is concerned with failures or ruptures of the plant where the time took for the whole intervention increased. Indeed, the staff intervenes within the 24 h following the fault report and more time is needed to identify the component/components which need reparation/substitution. This operation would lead to a delay of about 2/3 days caused by a simple block in the HP.

This kind of plant inactivity which is either entirely or mainly linked to the issue of acceptance can be found in the measurements as well. Focusing on *Figure 3. 36*, the higher contribution of the heat pump in SH applications seems to be higher in the mildest months. This trend can be mainly attributed to the issue of acceptance, indirectly measured by means of an operative parameter. Clearly another, yet secondary, cause is represented by the efficiency comparison between SAHP and gas burners under critical conditions. In fact, under particular conditions (e.g., high power required for initial heating, united with cloudy day and low air temperature) the usage of the burners might result more efficient than the SAHP. On the other hand, the SAHP is very likely to be more convenient to keep the set point temperatures once the initial heating phase is concluded.

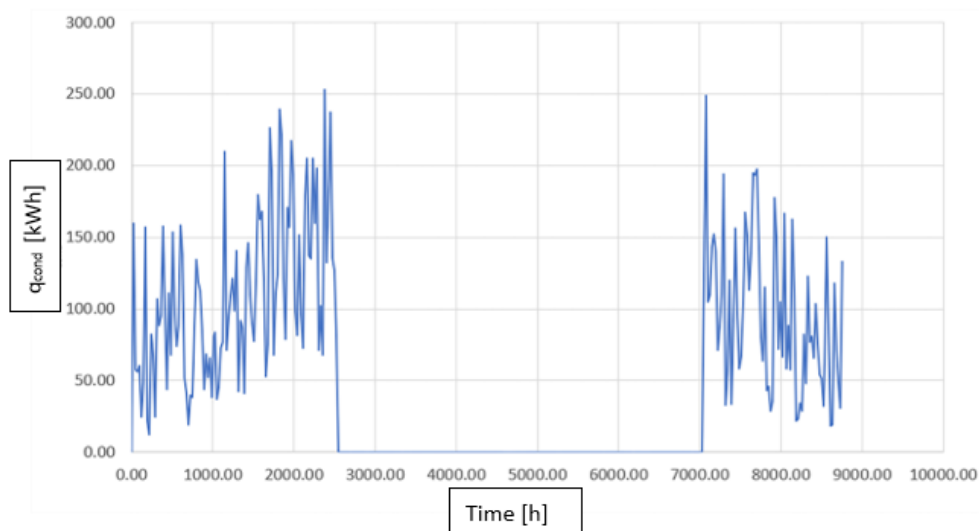


Figure 3. 36: thermal energy provided by the heat pump (q_{cond}) against a reference working year. Out of heating seasons no value is reported since the bypass is likely to be active most of times.

3.3.2 Hybrid panels durability and reliability

As illustrated previously, the hybrid panels installed at the facility present a polycrystalline layer below which a roll bond plate is welded allowing water to flow inside the panel (*Figure 3. 7*). Below the metal plate, the panel can be equipped with insulation. As far as the present case study is concerned, panels with no thermal insulation were adopted. Indeed, the panels have been designed mainly to work as cold source for the HP, therefore the expected average working temperature during all the heating season is likely to be very similar to the one of the air, with consequent negligible thermal losses, independently from the panel conductivity. On the economic side, this choice allows a reduction of the initial cost of the plant since low insulated panels can be adopted. In addition, the roll bond technology even cuts the costs of the panels, making the SAHP technology more affordable.

On the other hand, the chosen kind of panels can carry the following issues:

- the lack of insulation can dramatically reduce the panel performance when the bypass is active. Under these conditions, the temperature of the panels is high enough to bypass the HP and be directly sent either to the SH or the DHW subsystem. Consequently, the difference in temperature between water inside the panels and ambient air is no longer negligible and thermal losses are appreciated.
- the building technology of the thermal side of the hybrid panel allows an initial low cost but exposes the panel to the risk of debonding without the chance of any cost-effective reparation but the substitution of the panel. Concerning the specific experience gained on the pilot plant during about a decade, about 20% of the panels were subjected to leakages and the only effective intervention consisted in their hydraulic bypass until the substitution occurred. Apart from a small percentage linked to manufacturing defects, the leakages might have been affected by the issue of stagnation and the acid environment caused by excessive concentrations of glycol. This issue shall be better enquired in the following paragraph about the hydraulic decoupling of circuits.

On the side of SAHP performance, this intervention clearly reduced the heat delivered to the evaporator by means of the solar field, while the PV production did not experience relevant decrease in the production, since the hybrid panel could work also as only PV panel as well. Undoubtedly, the lack of water in the panel determined a higher working temperature with lower efficiencies, but the PV side of the hybrid panel was not completely compromised.

Annex D of UNI EN 15459 (154) provides the expected life span for different components implemented in buildings, including solar panels which are expected to be operative for about 20 years (Annex D estimates between 15 and 25 years). If just half of the expected life span has passed, the durability of the panels should be revised. On the reliability side, the possibility of disjoint working (e.g., only PV panel) allows a further resilience to the plant, even considering the reduced efficiencies.

3.3.3 Hydraulic decoupling of circuits

The hydraulic circuit of the solar panels is filled with a mixture of water and glycol, to prevent freezing of the fluid inside the panels and rust formation. Clearly, the presence of glycol can play a negative role in case of stagnation: when the fluid evaporates (especially during summer when high temperatures are reached and the solar field is very likely to be inactive) the concentration of glycol can determine corrosive phenomena. For this reason, a periodic check of the pH and glycol

concentration must be performed to avoid an excessive acid environment. Moreover, the presence of glycol can cause the formation of obstructions or limescale.

The importance of this issue increases with the size of the solar field: for the present case study, the total volume of water inside the solar circuit is estimated to be about 1000 l. This evaluation can be carried out considering 80 panels of 1 l capacity each, united with the water within the connection pipes (about 500 m of total length with a variable diameter between 2 and 3 cm) and the 500-l storage on the HP cold side as outlined in *Figure 3. 37*. Considering that a mixture of water with about 20% of glycol (as assumed in the original design) leads to freezing temperatures of about -5 °C, the volume of glycol can be approximated at 200 l.

Always basing on the plant layout, such mixture flows not only in the solar panels, but also in the storage on the HP cold side, up to the heat exchanger interfaced with the evaporator. On the operative side, this configuration exposes some critical parts of the plant, such as the heat exchanger on the HP evaporator, to the risks associated to the presence of glycol (e.g., limescale formation, obstruction). In addition, the part of the circuit with the tank (except for the HP) is within the boiling room (represented by means of the green lines in *Figure 3. 37*) and therefore no risk of freezing occurs.

The design choice was led by efficiency reasons, to avoid the addition of a heat exchanger with consequent losses in the fluid temperature.

In addition, the presence of a tank of relevant capacity (about half of the total estimated volume) and the considerable extension between the solar panels and the boiling room (about 200 m) might cause non-uniform distribution of the glycol along the circuit.

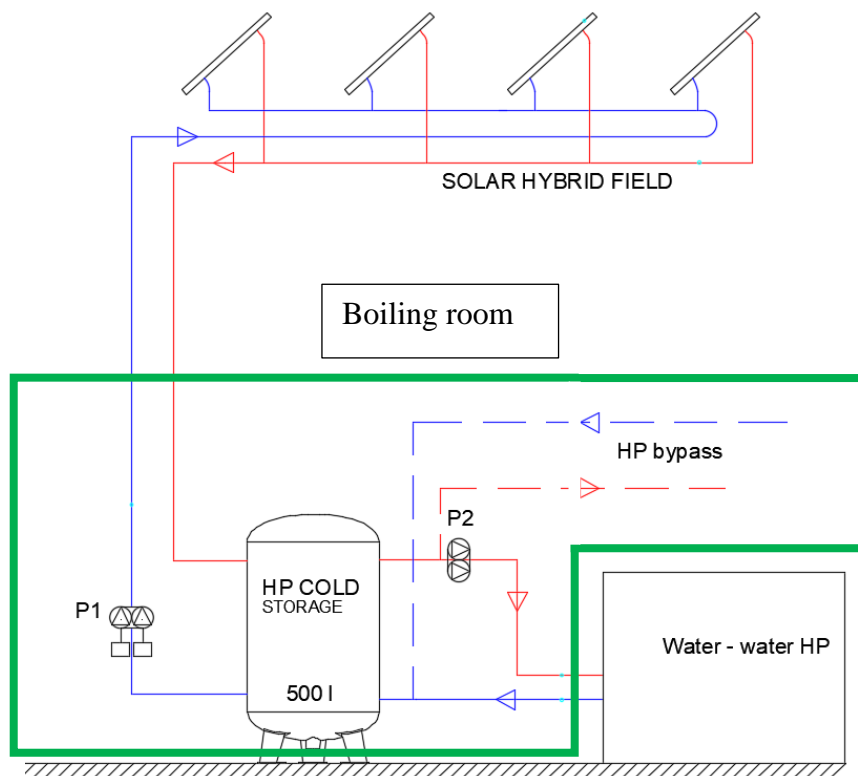


Figure 3. 37: detail of the functional scheme of the solar field up to the interface with the HP evaporator. Colour code: blue line – cold water; red line – hot water; dotted lines indicate the solar bypass. More information is available in the Annex and in Figure 3. 15

3.3.4 Efficient management of a PV/PVT solar field

The efficiency and economic convenience of PV/PVT solar fields depend on the number of electrical consumptions when solar irradiation is either low or unavailable.

The target and reference solution consists in a configuration where the produced electricity is directly consumed. As part of consumptions shift to periods where the PV production is either low or negligible, the economic convenience of photovoltaic fields tends to decrease, up to the limit case of a not cost-effective facility.

In other words, the temporal mismatch between electricity demand and production is the core element on which act to have a high-performance plant. Most of the researches and policies over the past two decades have focused on solving this problem. Up to now, only temporary and not resolute solutions have been proposed.

Two main strategies are taking place:

- Net metering: the excess PV production which is not self-consumed is sent to the national grid, acting as a virtual storage. Then, the user/producer can take the energy back when needed (e.g., during night or months with low solar radiation) with less expense than a standard withdrawal from the grid. Indeed, in the net metering only the additional charges are paid, while the electricity is not since it is as if it were produced from the solar field. Clearly, the maximum exchangeable quantity of electricity corresponds to the one immitted into the grid, on a yearly basis. At the end of every year, if the energy immitted is greater than the withdrawn one, a refund is given by the electrical grid operator (155)

With specific reference to the pilot plant presented, this strategy would completely solve the problem since the yearly PV production can entirely cover the HP needs, even with little over production (about 6% as outlined previously). Indeed, the plant benefited from this bonus.

Anyway, this strategy shows a weak point: it depends on the policies, which might dramatically change during the useful life span of the plant. Indeed, the Legislative Decree n.199 came into force on November 8th, 2021 states that the net metering criterion is going to be abolished within the end of 2022 (art.9, subparagraph 2) (156). This decree applies to both new and existing installations, with very negative consequences. Indeed, the incentive mechanism plays a central role in the affordability of PV/hybrid plants and it does influence the design criterion. Indeed, most of photovoltaic plants were designed to cover the winter needs by means of the summer over production. Therefore, a change in the incentive criterion causes an upheaval of the expected payback time.

- Installation of batteries: this strategy shows less dependence on future policies and it aims to maximise the self-consumption on-site trying to substitute the national grid as storage. Some main concerns can be illustrated:
 - a. inertia and capacity of the battery: while the national grid allowed a balance on a yearly basis, the battery is up to now able to work on a daily basis, to cover the night-time needs with the daily production.
 - b. LCA: batteries are granted to have a ten-year life span, but also they are composed of very polluting elements (e.g., heavy metals). In absence of incentives, this technology would hardly satisfy the cost benefit analysis.
 - c. power: to substitute completely the national grid, a PV storage system should be able to cover the peak power as well. The discharge power of the batteries is in most of cases suitable for domestic applications (about 5 kW), but not for installations with greater power. The SAHP - PVT pilot plant requires a peak electric power of 12 kW

just for the heat pump excluding every other energy consuming device. Consequently, the number of required batteries would even increase to grant both capacity and power.

With specific reference to the SAHP-PVT pilot plant under study, a relevant issue in the management of PV production has been identified (157), since about 60% of the total yearly production is not used by the SAHP-PVT. This problem occurs since the plant has been sized to cover the HP needs also in the months with minimum solar radiation. As a consequence, the PV production during the maximum solar radiation (e.g., June, July and August) becomes by far higher than the required one. On the other hand, the plant could have been designed to cover the need in the month with the highest solar radiation. In turn, this would have made the contribution of the PV field almost negligible during the heating season, always highlighting a relevant issue in the interface between HP/SAHP and PV fields.

4. Modelling of the SAHP with PVT panels pilot plant by means of TRNSYS

This chapter deals with the numerical modelling of the plant, to identify and preliminary evaluate the interventions and their influence on the global working of the plant.

The SAHP-PVT plants work under transient regime and they require a numerical code able to perform calculations removing the assumption of steady state regime, such as the TRNSYS environment.

After a former introduction about the main objectives of the modelling, the mathematical formulation of the main components of the SAHP-PVT is presented. Then the validation of the TRNSYS model, basing on the measured parameters by means of the DAS is performed.

4.1 Objectives of the modelling

The main target of the modelling approach consists in the ability to assess the plant performance, before its realisation, to check the respect of the energy efficiency requirements and evaluate its economic convenience.

The need for more refined, numerical simulations lies in the fact that calculations can be hardly performed by hand when the steady state regime assumption is removed. A more precise estimation of the plant performance is needed, according to the external environmental conditions and the required heat load. In addition, this issue acquires even more importance since the need is dictated by both operational planning and optimisation (144), (158), (159).

On one side, transient simulations can provide a better degree of approximation, reducing the uncertainties carried by a steady state approach. The numerical modelling allows to enquire even the aspects linked to pollution/reduction of fossil fuel usage, comfort of indoor environments and plant reliability (160). On the other side, a more precise approach requires additional information, to be able to analyse each component of the system under dynamic conditions. Anyway, an approach involving more parameters does not always lead to more precise results. In fact, the additional information has to be collected with an adequate precision, otherwise the model outputs could become even less reliable than the ones obtained under simplified, steady state assumption (143), (161), (162).

Actually, the topic of numerical modelling has to cope with many critical issues that can significantly reduce the reliability and the field of application:

- complexity of the system: differently from the steady state regime, analyses under transient regime need to be performed adopting a proper time step, over which the program performs all the calculations using as boundary conditions the results of the previous time step. The more complex the model, the higher the required computational capacity. In addition, one or more components may become unstable preventing the convergence of the solution (163). In the present study the model was assembled to prevent any numerical instability of the solution and to avoid any unjustified added complexity.

- lack of sufficient data for the validation stage: a great amount of information is required to properly validate each component of the plant, especially if different working conditions are available (164). In other words, the reliability of numerical transient models is directly affected by the extension of the data acquisition system on a prototype or on the plant itself, to carry out an exhaustive validation.

Going more in detail into the field of solar assisted heat pumps, the short diffusion of SAHPs has been accompanied by the lack of complete DAS, especially as the plant increases its size. The main

reason can be found in the initial cost: for instance, the DAS installed at the SAHP-PVT pilot plant under study represents about 20% of the total initial expense.

In addition, the involvement of different sources and technologies (e.g. storages, valves, solar panels, heat pump) introduces many working conditions which are not usually monitored by the on board minimal control systems. Concerning the specific SAHP-PVT under study, the almost real-time data acquisition performed by the DAS allows the overcome of this issue.

- choice of the numerical code: the studies carried out in literature can be divided into two main groups:

1) several Authors preferred to use self-compiled programs, with specific attention to the issue of interest to them (e.g. interface between plant and building, dynamic model of building, dynamic model of the plant) (165), (166). Some Researchers also opted for lumped approaches, (167), (168) which are not always suitable to model the plants under analysis. Programs tend to be specifically tailored for the plant under study, with the risk of losing general validity and applicability to other similar yet different case studies.

2) Other Authors prefer to develop their model starting from software environments where some elements are already available. This approach has been enhanced by programming environments such as MATLAB/Simulink where a more user-friendly interface is provided. (169), (170), (171). TRNSYS belongs to this group as well, providing a set of “built-in” elements ready to use. Anyway, the users are free either to write down their own codes for specific elements, not included in the initial library or to modify the existing components (172), (173).

Besides of the specific aims of the present work, the numerical modelling of a plant should become a concept strictly related to the facility itself for all its useful lifespan. The approach chain of data collection, model validation and efficiency analysis should not be relegated to specific studies. On the contrary, it should be performed almost continuously and in an automated manner for an almost real time update of the set point parameters to keep the plant efficient.

4.2 Description of the main components of the plant and their numerical validation

This chapter introduces the different components implemented to simulate the SAHP- PVT at Palacus, by means of the TRNSYS17 environment (174).

4.2.1 Model validation criteria and measured data processing

The model validation deserves a great importance, due to the transient regime, united with the different working criteria and interaction among the different components.

Indeed, the validation of each component singularly may not be always feasible, because the boundary conditions must reproduce the same measured conditions to which the reference information is associated.

On the other hand, only the validation of the entire model of the plant as a single element may lead to unsatisfactory results, due to the relevant number of parameters to set for each component and the large number of checks under different working conditions.

In conclusion, the validation of the model shall be carried out according to the following criteria:

- Validation of single components, whenever information about the component working on its own is available. The validation shall be concerned with both graphical comparison between

simulated and measured trend of chosen parameters over time and the comparison with average values.

- Validation of the smallest group of components when their working occurs simultaneously. Within this stage some elements singularly validated before shall be used again. In these two stages, the simulation time shall cover a time span of some days, a week at most.
- Validation of the global performance of the plant: this stage enquires the working of the plant from a wider point of view, focusing both on the trend of chosen parameters over time (e.g., temperatures, COP etc) and on the global production of the plant over a reference year.

The measurements employed to validate the model have been already post-processed to assign the data sets to either the different working conditions or any unexpected operation. Indeed, the DAS records both physical parameters (e.g., temperature) and logical ones (e.g., warning or flags to identify the activation/deactivation of specific working conditions), so that the measurements can be easily distinguished. No particular filtering process was adopted, not to lose the transient phenomena occurring. Any eventual and unwanted fluctuation of parameters over a very short time has been already smoothed by the DAS which averages the values over a time range of almost two minutes.

Concerning the models carried out, the simulation of transient systems with relevant mass flow rates poses a not negligible issue about the convergence analysis. In fact, the frequent switch on/off of the pumps (nominal flow rates between 5000 and 8000 kg/h) is very likely to cause a missed convergence of the non-linear equations involved, even accounting for hysteresis effects. Therefore, the optimal convergence values adopted in the simulations below are concerned with a very small time-step (variable between 1 minute for the validation of the SAHP up to 10 minutes for the simulation over a reference year) and a tolerance convergence of 0.35. As shown in the following sections, these values allow reliable, converged results without requiring an excessive computation time.

4.2.2 TRNSYS environment

This software allows the implementation of complex, dynamic systems, performing a transient analysis and solving sets of equations iteratively.

Some main characteristics can be identified:

- Components: they can be conceived as black boxes implementing a specific numerical model of a given element, instead of reproducing the physical phenomena occurring. For instance, many models (and therefore many components) about solar panels are available using different formulations. New, hand-made components can be introduced and the existing ones can be modified by means of the source code containing the set of equations and the models. Different groups can be identified:
 - o Plant components: they reproduce the working of a specific elements, such as a heat pump, connection pipes, heat exchangers
 - o Controllers: they can perform one or more user defined criteria to compute control variables which enable/disable the working of specific components (e.g., control variable to switch a water pump on/off)
 - o Physical phenomena/forcing function: they can reproduce/generate the boundary conditions, for instance concerning the weather or DHW withdrawal. The program allows the import of external files or the point-by-point definition of the forcing functions using any physical (e.g., water draw, temperature etc).
 - o Output: they can give the user numerical output of any variable inside the system both in a graphical and numerical way. The results can be saved and printed step by step or at a

chosen time range on external files according to user-defined paths. Computer/integrator components can perform additional result processing (e.g., daily integration of solar radiation) already within the program without requiring further post-processing.

Every component presents different main tabs:

- Parameter: it is referred to the time independent information (e.g., volume, specific heat).
 - Input: it is associated to the initial conditions (e.g., initial water temperature inside a pipe) that shall be replaced with the outputs of the previous time step by the program.
 - Output: the user chooses which output parameters available for the specific component shall be printed.
 - Derivative: it is usually concerned with initial inertia (where needed). For instance, this tab can be used to describe the water temperature at different nodes inside a water tank.
 - External files: the user inputs the path of the files to be eventually read by the component (if necessary) as input information, such as the HP performance.
- Connections: they allow the exchange of different information between the components of plant, such as control parameters, or between output and input quantities of different components (e.g., output water temperature of a solar panel and input water temperature of the connection pipe).
 - Solution: once the model has been assembled with components, connections and boundary conditions, the iterative solution can be run. Two different solvers are available: the successive substitution method, suggested for systems with a thermal capacity and Powels method, suitable for systems with many non-linear equations, like PV systems. The user can define both the start and end times of the simulation, united with the time step. This parameter can influence the convergence of the set of equations to be solved and the time taken to solve them, therefore it has to be properly chosen also according to the duration of the simulation (e.g., daily or yearly basis simulation) and the stability of the equations implemented in the model (convergence analysis of the model). All the models reported below adopt the successive substitution method.

4.2.3 Model assembly and validation

The three main components of the model shall be presented (i.e., hybrid solar panels, heat pump with bypass and storages) united with their validation. Then, the additional components such as hydraulic connections and control units shall be introduced, along with the global model of the SAHP-PVT, also testing the working of all the assembled components.

Solar panels

Brief description:

Concerning numerical modelling, performance models referred to standard test are used for different environments such as TRNSYS or others (e.g., MATLAB). Actually, the use of the collector (e.g., direct DHW production, interface with HP etc.) already reduces the possible, applicable models. In addition, the kind of solar panel may help to exclude further models: for instance, covered collectors usually present a negligible latent heat exchange while condensation has to be avoided to prevent internal damages.

As regards the hybrid panels interfaced to a HP, their working might occur also as ambient air exchangers (especially in mild climates) in absence of solar radiation. In this context, the expression of their efficiency as a ratio between the useful heat obtained and the incident solar radiation might not be representative and lead to unexpected results. Some models (and standards) suppose a linear correlation between inlet and outlet fluid temperature, when mass flow rates are small and no solar

radiation is available. More in general, specific attention should be paid to the working of solar panels models when non-standard working conditions are reached (e.g., very low mass flow rates, working temperature lower than the ambient one, no solar radiation available). In addition, when panels have the conjoint production of hot water and electricity (PVT panels) the solar radiation in common thermal collector models should account for the PV production.

The hybrid panels of the pilot plant have been modelled by means of TRNSYS type 50a-3 where a PV module is combined with a flat-plate collector. The model bases on the analysis and work of Florschuetz et al. (175), (176), (177), (178) for flat plate collectors operated at peak power. The model adopts the cells I-V curves to compute peak power or electricity production at given voltage. The parameters illustrated in *Table 3. 1* have been implemented (179). In addition, type 50a-3 requires just ambient temperature and incident radiation as boundary climatic conditions. *Figure 4. 1* illustrates the simple model implemented for the validation.

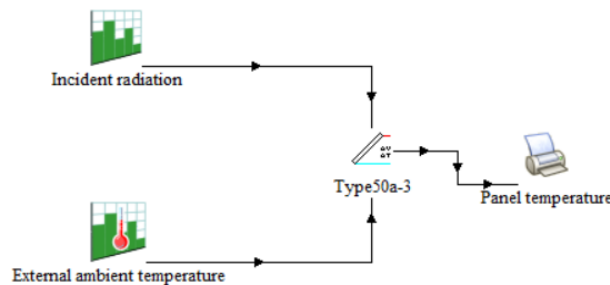


Figure 4. 1: scheme of the validation model for the PVT panels

Validation – Photovoltaic side:

The main information has been collected by means of the bidirectional meter which provides a cumulative monthly value about the PV production. The simulation has been carried considering the monthly and yearly average production of the PV panel and performing the analysis over a reference year (2019). The dependence of PV cell efficiency on the panel temperature cannot be neglected in hybrid applications and the adopted TRNSYS component expresses it by means of Eq. 4. 1

$$P_{PVT} = P_n [1 - \gamma(T_C - 25)] \quad \text{Eq. 4. 1}$$

Where

P_{PVT} is the effective power produced by the PVT panels

P_n represents the nominal (peak) power associated to the panel (technical information)

I is the solar radiation on the panel (measured and implemented in the validation model)

γ accounts the temperature coefficient losses (technical information)

T_C is the cell temperature (measured and implemented in the validation model)

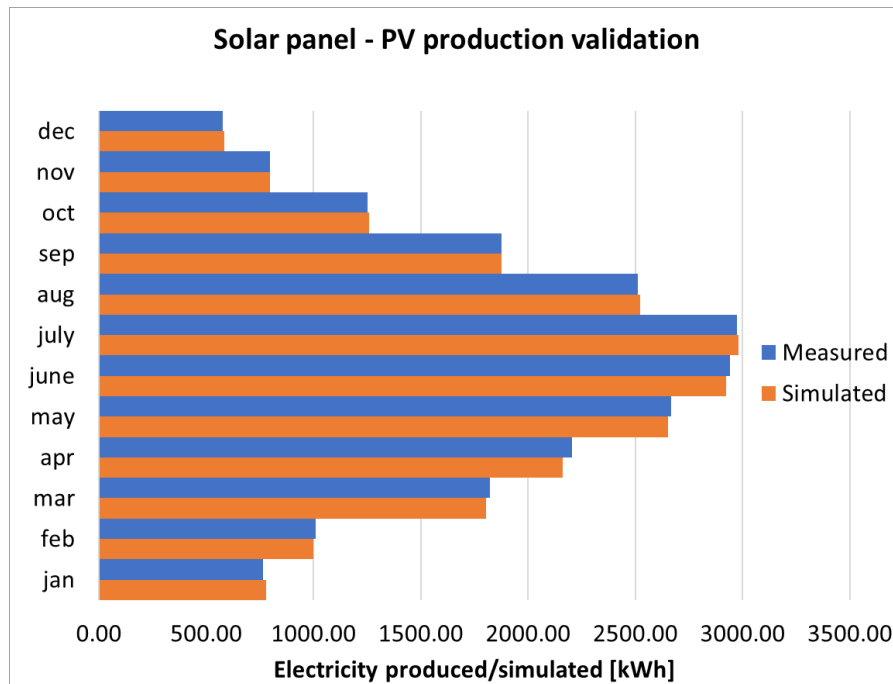


Figure 4. 2: monthly photovoltaic production (measured in blue and simulated in orange). Reference year 2019 (134)

Figure 4. 2 allows the comparison between the simulated and measured monthly PV production, for the year 2019. Since the maximum difference is not greater than 5%, the PV side can be considered validated. Unluckily, no more specific information (e.g., on hourly basis) is available, so the component cannot be furtherly tested.

Validation – Thermal side:

The panel temperature has been chosen as reference parameter. The measurements used to validate the model are concerned with two days in which the remaining part of the plant was not active for maintenance and so the same working conditions have been easily implemented in the validation model. The two chosen days are presentative of sunny (Figure 4. 3) and cloudy weather (Figure 4. 4), to enquire the response of the panel under different environmental conditions. The measured panel temperature during the cloudy and sunny days has been compared with the simulated one, obtained assigning the same weather conditions over the simulation time (24 hours).

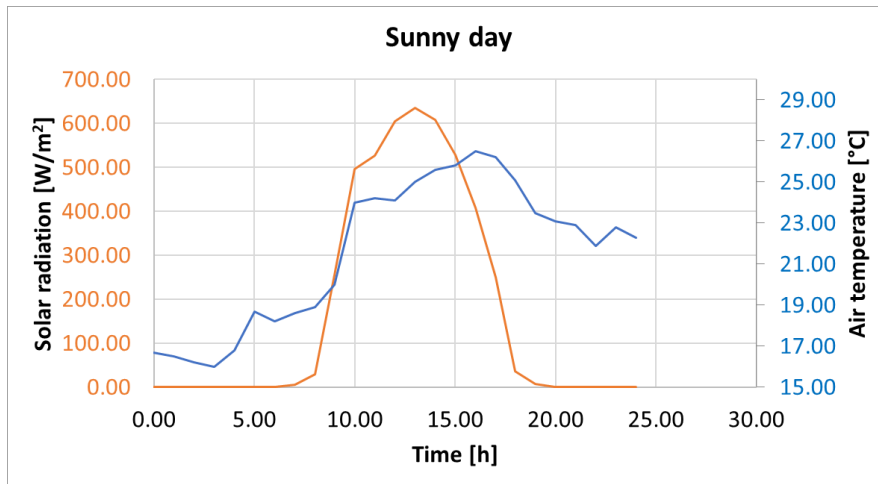


Figure 4. 3: reference day adopted to validate the hybrid panels during a sunny day (29/08/2019) – colour code: orange – solar radiation [W/m^2]; blue – external air temperature [$^{\circ}C$]

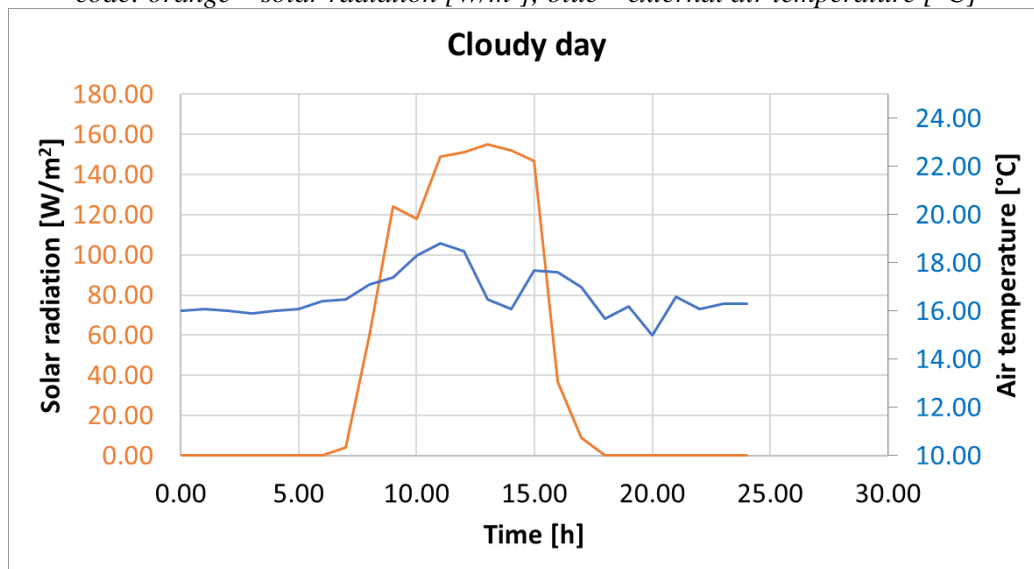
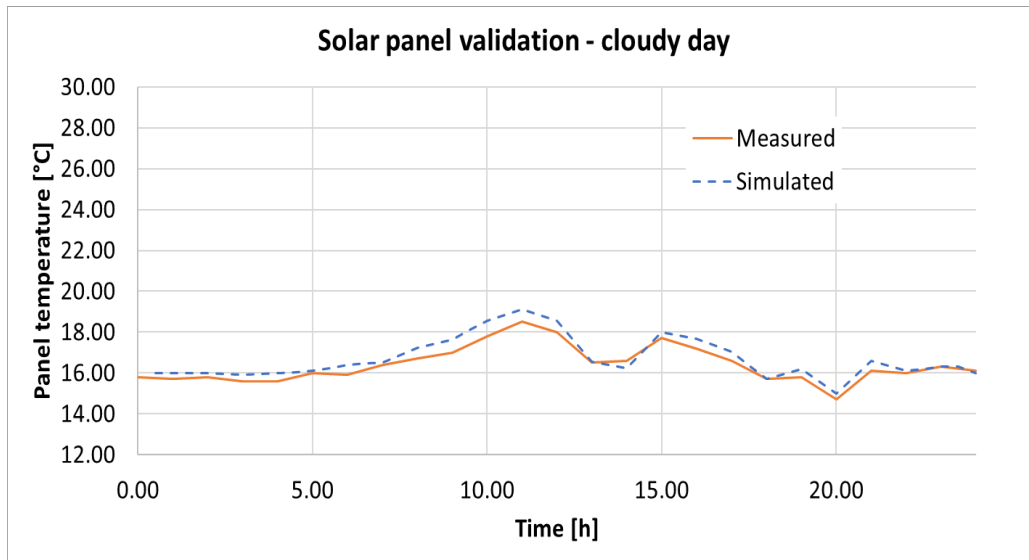
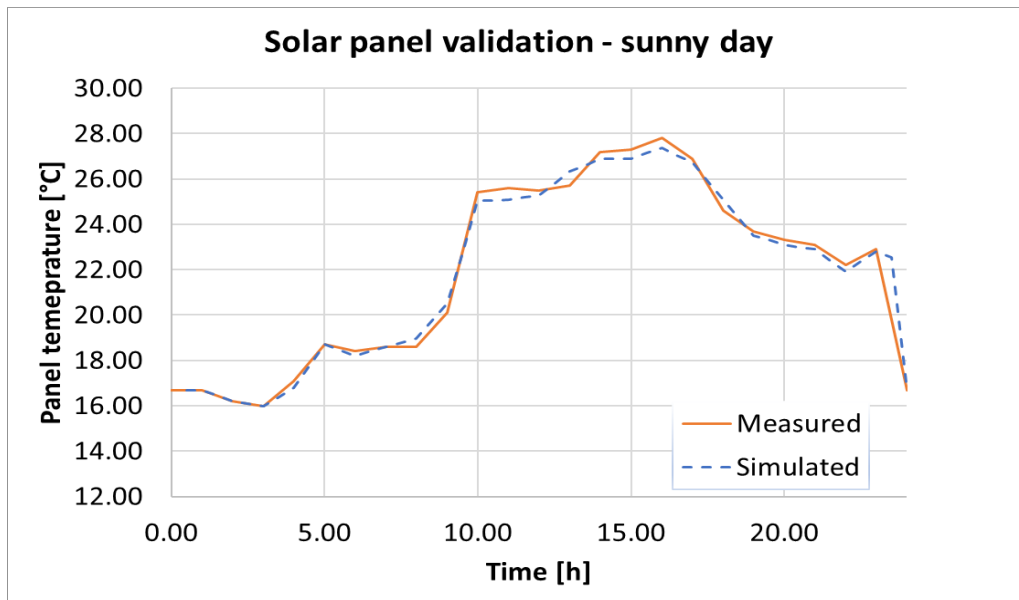


Figure 4. 4: reference day adopted to validate the hybrid panels during a cloudy day (04/11/2019) – colour code: orange – solar radiation [W/m^2]; blue – external air temperature [$^{\circ}C$]

Figure 4. 5 resumes the results obtained: in both cases, the two lines (orange – measured values and dotted blue – simulated values) differ of a maximum of $0.5^{\circ}C$ with an average difference of $0.3^{\circ}C$ and the results can be therefore considered acceptable.



a)



b)

Figure 4. 5: comparison between simulated (blue dotted line) and measured (orange line) panel temperature under the same weather conditions for cloudy (a) and sunny (b) days

Water storages

Brief description:

The modelling of water storages in TRNSYS environment leads to a wide group of different formulations, from the tanks considering stratifications, up to the ones with auxiliary heaters already implemented in the numerical code (180), (181), (182), (183), (184), (185). The topic has already been enquired in detail in a previous PhD thesis (136) with specific attention to the modelling of specific subsystems of the pilot plant at Palacus in TRNSYS environment. Therefore, the present section is meant as a brief recall about the main concepts, adopted in the following modelling.

Actually, the storages under study consist of two 500 l tanks, one interfaced with the hot side and the other with the cold one, and two 1500 l tanks used to store the DHW. The not negligible sizes require specific attention to stratification and therefore TRNSYS Type 4 has been chosen. Basing on previous studies (136), 6 nodes have been introduced inside the tanks: in fact, the tanks have a variable height

between 1.5 m and 2 m which implies the definition of six water volumes inside about 0.25-0.30 m thick. In this way stratification can be modelled as well, performing a mass and temperature balance among the volumes adjacent on to the other inside the tank (Figure 4. 6). In case the flow rates were too high, a mixing would gradually occur inside the tank, firstly involving the nodes near the bottom and then extending to the entire storage. The component allows the definition of internal auxiliary electrical heaters which have been removed for all the carried-out simulations.

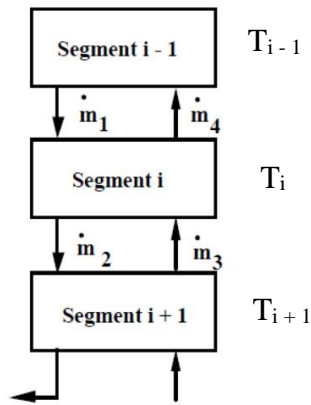


Figure 4. 6: example of the volume segments composing the tank when stratification occurs (186)

Validation

The physical properties of Type 4 about thermal inertia and thermal losses were computed basing on the geometrical dimensions and material characteristics measured onsite. As outlined in section 3.1.2 the storages are all made of steel, covered with an insulating coating; Table 4. 1 resumes the main information implemented

| Additional information - tanks | | |
|--------------------------------|---------------------------------------|--------------------------------------|
| Properties | λ (W/mK) | s (m) |
| Steel | 80 | 0.002 |
| Insulation | 0.028 | 0.04 |
| | $h_{int} = 100 \text{ W/m}^2\text{K}$ | $h_{est} = 25 \text{ W/m}^2\text{K}$ |

| Component | U (W/m ² K) | A (m ²) |
|---|------------------------|---------------------|
| Upper base | 0.68 | 0.93 |
| Lower base | 20.00 | 0.93 |
| Lateral surface | 0.68 | 7.35 |
| $A_{tot} = 9.21 \text{ m}^2, U_{glob} = 2.62 \text{ W/m}^2 \text{ K}$ | | |

Table 4. 1: Main characteristics and global thermal loss coefficient for the tanks of the pilot plant.

The validation of these parameter was possible thanks to the recording of the DHW tanks during night. Indeed, both the SAHP-PVT and the gas burners are off during this period and therefore the cooling of the boilers takes place. The trend over time (reference time about eight hours) should follow a decreasing exponential curve, but it is almost linear, because of the high thermal inertia of the boilers, compared to the small length of the cooling period. *Figure 4. 7* shows the validation between measured (dotted red line) and simulated (grey line) trends, with very good agreement, differences in temperature between simulated and measured ones lower than 0.2 °C. The same approach has been adopted to compute the thermal loss coefficient of the 500 l tanks and therefore validate their properties.

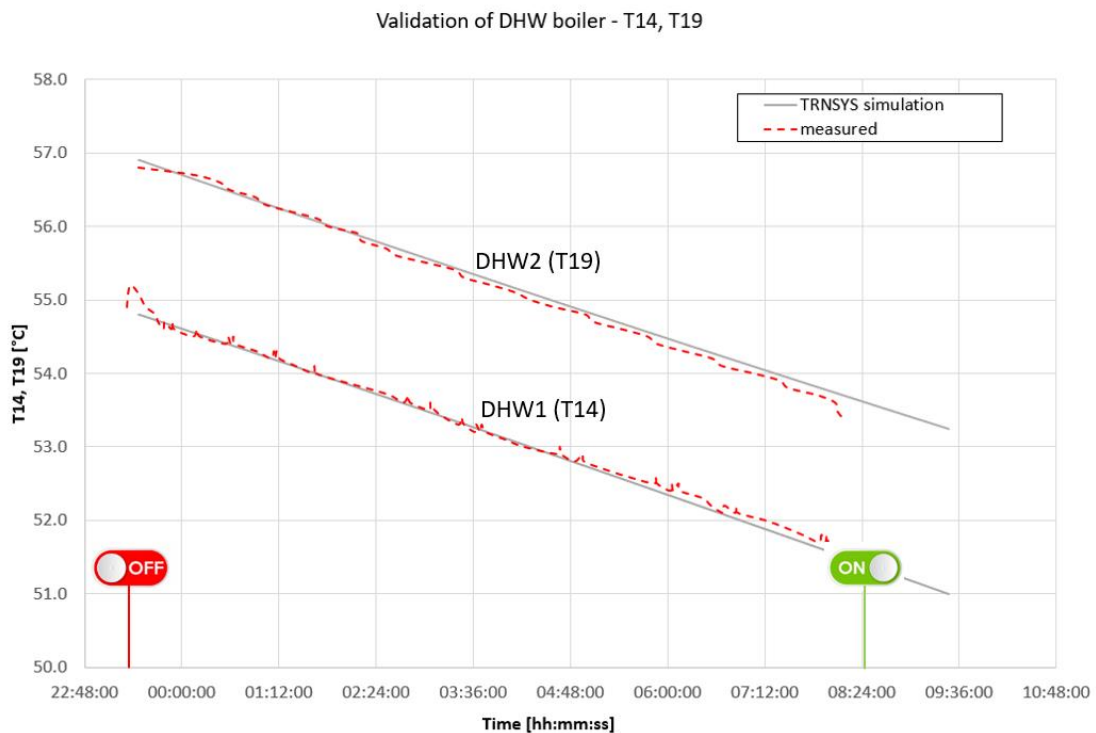


Figure 4. 7: numerical and measured trends for water in DHW1 and DHW2 tanks during night when the plant is off

Heat pump

Brief description:

EU Task 44 annex 38 previously discussed (T44A38) reports a comprehensive review about the components available to simulate heat pumps (187). Another interesting review work including chillers can be found in Jin and Spitler (188).

The models can be divided into two main groups: the former includes the standard HP where simplified calculations are available to estimate the performance of the machine. This is the case of “black box models” (189), (190) which are quite diffused every time extensive technical information about the HP working is available. In particular, the performance of the HP is input by means of COP/power consumption/delivered heat, referred to sampling points such as the hot source inlet temperature and the required output temperature. These components are often referred to as “quasi-steady-state” models since they can be implemented in transient simulations, without effectively reproducing the physical working of a transient phenomenon. In conclusion, these models can be

integrated with some dynamic effects (i.e., condenser/evaporator thermal inertia or even frosting/defrosting), (189).

On the other hand, more sophisticated and not common HPs require a tailored modelling reproducing the dynamics inside the system, varying the boundary conditions, even on long term periods, (188), (191), (192), (193), (194). This is the case of HP interfaced with geothermal sources where the interaction between the thermal needs and the ground heat source is of paramount importance to assess the global performance of the plant. Nevertheless, such detailed models are based on the simulation of the physical working of the HP and they are hardly employed in annual simulations, because of the excessive computation power required to reach the solution (e.g., solving the states and flows of the refrigerant fluid at each time step).

As regards the current simulation, the TRNSYS component chosen is Type 20. It belongs to the “black box” models, for two main reasons: firstly, the HP implemented in the pilot plant has exhaustive information about the measured performance maps and secondly the aim consists in assessing the global plant performance without detailed analyses of specific components.

In addition, a control input (Y_{hr}) is available for the HP: if it is 0, then no heating is required and the heat pump delivers no energy. If, on the other hand, Y_{hr} is 1, then an internal controller determines the heating mode:

- Direct liquid source heating: it occurs if the liquid source temperature is greater than T_{dh} , (heating mode = 1). The HP is switched off and the water directly flows to the tank on the condenser side.
- Heating using either the liquid (heating mode = 2) or ambient source (heating mode = 3): the source with the highest temperature is chosen. The model also automatically switches from the liquid to air source whenever the liquid source approaches the icing point. In conclusion, if both source temperatures fall below the user-specified minimums, then the HP is not allowed to operate in that (or both) mode(s) (heating mode = 4).

Furthermore, internal circulating pumps are already built in the model, with on/off functioning and automatic control when the HP is on.

Concerning the specific case study, the air source has been inhibited independently from the temperature, since it is not present in the pilot plant under study.

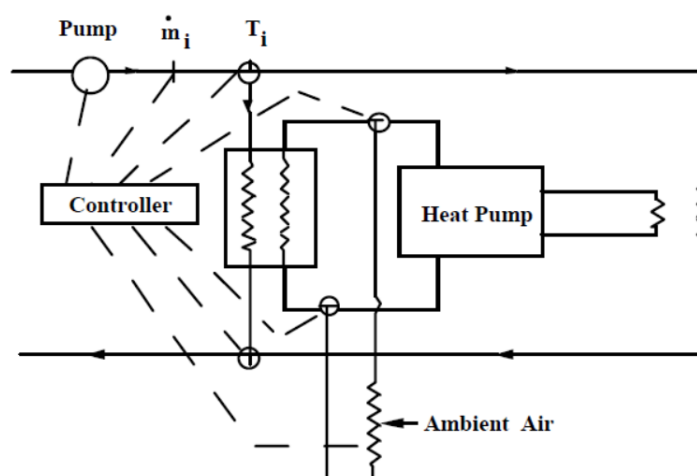


Figure 4. 8: schematic representation of the elements and regulation systems implemented inside the HP component (186)

Validation

The following simplified TRNSYS model has been built to validate the working of the HP (Figure 4. 9)

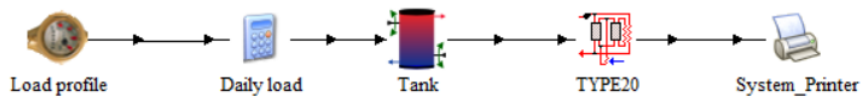


Figure 4. 9: simplified TRNSYS model of the HP

The following elements can be identified:

- Load profile/daily load: it represents the forcing function of the model, simulating a constant water flow rate of 100 kg/hr, at an initial constant temperature of 5 °C flowing inside the tank.
- Tank: the tank has a volume of 1 m³, leaving the same characteristics identified in the previous paragraph about tanks (*Table 4. 1*). The tank was given an initial temperature of 50 °C, assumed uniform at all nodes. In fact, the aim is to create a water flow on the cold side of the HP which firstly is higher than the set point temperature for the bypass and then it becomes lower to test the HP working with the liquid source.
- Heat pump: the component allows the import of “.txt” files containing the HP performances (i.e., the useful delivered heat flow, electricity consumption, power absorbed by the evaporator) according to different cold source temperatures. An interpolation then occurs for intermediate values. Actually, the program cannot extrapolate the results, therefore it is necessary to implement files with temperature ranges wide enough to exclude the need for extrapolations. For the current modelling, the information contained in the technical data and the one reported at *Table 3. 2* were implemented for the liquid source. The file about the air source has been defined as empty since it is not present in the pilot plant. The component requires few more information such as the minimum temperature for direct liquid heating – set at 45 °C and the minimum source temperature for liquid source (0 °C).
- System printer: it collects all the results shown below within a “.txt” file.

The simulation has been run for a week (168 hours) with an hour time step.

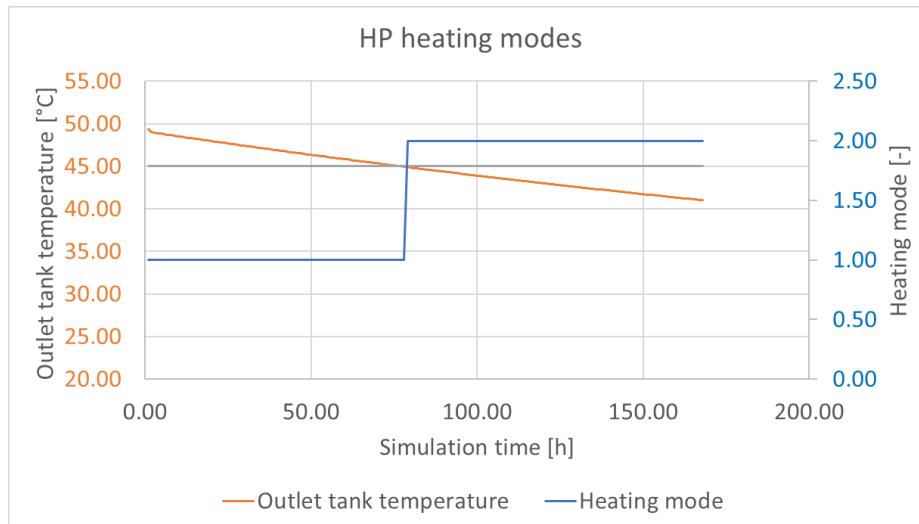


Figure 4. 10: HP heating modes (1 – bypass active; 2 – HP on using the liquid source). Colour code: orange: outlet temperature within the tank; grey horizontal line: set point value to switch between the bypass and the HP working; blue: heating mode

Figure 4. 10 shows that the HP starts with the bypass active since the outlet water from the tank is higher than the established set point (45 °C). Then, as the tank temperature lowers below 45 °C, the HP switches on, enabling the heating mode interfaced with the liquid source.

Two additional checks were performed in this model:

- Correct interpolation of the HP performance from the external input file varying the operating temperatures on the evaporator side
- Respect of the First Law of Thermodynamics: remembering Eq. 2. 1, the heat flow delivered by the condenser equals the sum of the electrical power consumed by the compressor and the heat flow absorbed at the evaporator for each time step.

Circulating pumps

Brief description:

Two types of pumps have been identified in the pilot plant:

- constant flow rate pumps: they are almost all the pumps in the plant, resumed in Table 3. 3 (except for the first line) and Table 3. 4. TRNSYS Type 3b has been chosen since it is a very simple model for water circulators where the only information required is about consumed power and mass flow rate. In addition, a control signal (either 1 – on or 0 – off) allows the activation/deactivation of the pump.
- variable flow rate pump: only pump P1 shown in the first line of Table 3. 3 has variable speed. Such component grants the water flow from the solar field up to the 500 l tank interfaced with the cold side of the HP. TRNSYS type 110 has been chosen, since it computes the mass flow rate using a variable control function whose value is between 0 and 1 applied to the maximum possible water flow rate (piece of information which has to be inserted). The DAS activates pump P1 only when the difference between outlet temperature of the solar field and the one in the solar storage interfaced with the HP cold side is at least 2 °C (see Annex for plant outline). On the other hand, when pump P1 is already active, the DAS switches it off when such difference lowers 1 °C. Furthermore, the speed of pump P1 is variable and depends on the temperature difference

between the outlet and inlet of the solar field. In particular, when the difference is higher than 5 °C, the pump operates full speed, while it varies linearly for values between 5 °C and 1 °C. More information about the position and working of pump P1 can be found in section 3.1.2.

Validation of the variable speed pump united with the control units

The automatic switch on/off and variable speed control according to different temperatures can be implemented by means of two control units available in TRNSYS:

- Type 2b: the tool is substantially an on-off differential controller by means of a function returning either 0 (off) or 1 (on). Such result in computed basing on the following key input information:
 - o Upper limit temperature, T_H [°C]
 - o Lower limit temperature, T_L [°C]
 - o Upper dead band dT_H [°C]
 - o Lower dead band dT_L [°C]

The working of the component can be described as follows: at a given time step, if the control signal of the previous iteration (or the initial value in case the very first time-step) is 0, then it becomes 1 only when $T_H - T_L$ overpasses the upper dead band (dT_H), without paying attention to the lower dead band. On the contrary, if the control signal of the previous iteration is 1 (on), such value becomes 0 only when $T_H - T_L$ becomes smaller than the lower dead band (dT_L). This means that if the control signal of the previous iteration is 1, it remains unchanged if $T_H - T_L$ is smaller than the upper dead band (dT_H), but still larger than the lower one (dT_L) and vice-versa. In other words, the upper dead band controls only the activation (control signal from 0 to 1) while the lower dead band just acts on the deactivation (control signal from 1 to 0). *Figure 4. 11* reports a graphical representation of the working.

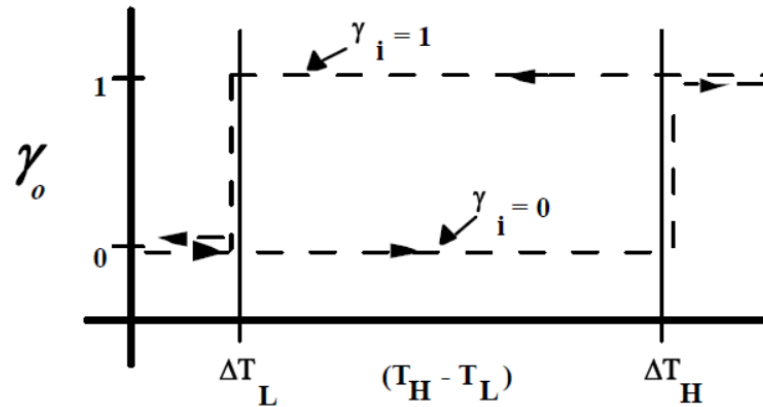


Figure 4. 11: schematic representation of the differential controller working HP component (186)

The controller is normally used with the input control signal connected to the output control signal, providing a hysteresis effect (*Figure 4. 12*, red circle). This instance of the Type2 controller is intended for use with the standard TRNSYS SOLVER 0 (Successive Substitution), and the result of the control function might oscillate between 0 and 1 within the same time-step when $T_H - T_L$ approaches either the upper or the lower dead band. To prevent this effect, the component requires as an input parameter, the maximum number of oscillations allowed during a fixed time-step before the control function stops oscillating. In absence of unstable convergences, usually 5 oscillations can be considered sufficient. The TRNSYS manual recommends choosing an odd number, to encourage the controller to stop at a different control value with respect to the previous time step.

The component Type 2b has a further safety high limit cut-out which forces the value of the control function to zero whenever the monitoring temperature (additional input parameter) exceeds the high limit temperature. This instance can be useful to avoid high (or boiling) temperatures inside the tank.

- Once the on-off controller has been implemented, the variable speed for pump P1 has been modelled by means of a computing routine which implements the following piecewise function (Eq. 4. 2):

$$control = \begin{cases} 1 & \Delta T_{pan} > 5^{\circ}C \\ \frac{\Delta T_{pan}}{5} & 0^{\circ}C < \Delta T_{pan} < 5^{\circ}C \\ 0 & \Delta T_{pan} < 0^{\circ}C \end{cases} \quad \text{Eq. 4. 2}$$

Where ΔT_{pan} is the difference between the outlet and inlet temperatures of the solar field.

During each time step, the two control signals are computed, multiplied and then assigned as border condition to the variable speed pump (Type 110).

The following simple TRNSYS model (*Figure 4. 12*) verifies the working of the pump and controllers

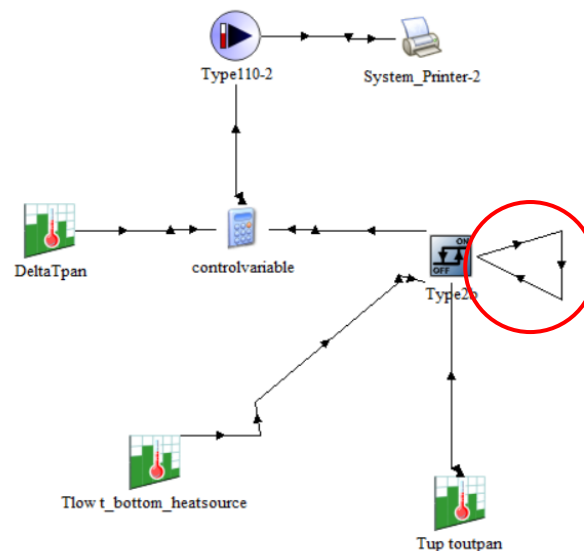


Figure 4. 12: TRNSYS model to validate the variable speed pump and the associated controllers

The two control units can be identified, united with the variable speed pump (Type 110). The red circle indicates the hysteresis effect provided by controller Type 2b formerly described.

In addition, three forcing functions concerned with temperature have been inserted (*Figure 4. 12*). They simulate respectively: the difference in temperature between outlet and inlet of the solar field, the lower temperature (T_L) in the case study associated to the temperature at the bottom of the 500 l solar storage and the upper temperature (T_H), representative of the outlet panel temperature for the pilot plant. *Figure 4. 13* shows the trends of the implemented temperatures. Please note that the values here adopted might leak of physical resemblance, since they are just meant to test the correct working of the model under different boundary conditions. The upper and lower dead-bands for Type 2b have been set to 3 °C and 1 °C respectively.

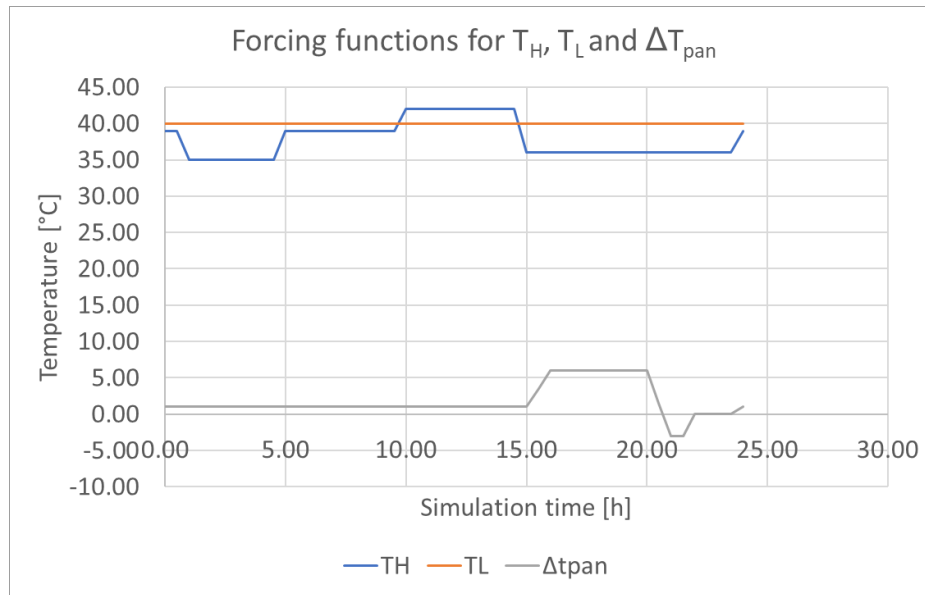


Figure 4. 13: forcing function for the temperature at the outlet of the panel (T_H – orange line), the bottom of the 500 l solar storage interfaced with the HP (T_L – grey line) and the difference in temperature between solar field outlet and inlet water (ΔT_{pan} – grey line)

The results are shown in Figure 4. 14:

- From hour 0 to 1: the difference $T_H - T_L$ is equal to 1, so the control signal remains at 0.
- From hour 1 to 5: the difference jumps to 5 °C and the control signal becomes 0.2. This number is the result of the multiplication between the Type 2b control signal (which is 1 since the temperature difference is 5 °C > upper deadband = 3 °C) and the coefficient computed by means of Eq. 4. 2, namely $1 \text{ °C}/5 \text{ °C} = 0.2$.
- From hour 5 to 10 the temperature difference drops to 1, but nothing occurs in the control signal since the lower dead band has not been under passed yet.
- From hour 10 to 15: the temperature difference becomes even negative, leaving the control signal at zero
- From hour 15 to 20: when the temperature difference over passes the higher dead band of 3 °C, the control signal increases up to 1, since the difference in temperature at the solar field (ΔT_{pan}) has become greater than 5 °C (at about hour 16), remaining unchanged up to hour 20).
- From hour 20 to 22: $T_H - T_L$ is still above 3 °C, but ΔT_{pan} becomes negative, therefore the control signal turns to zero.
- From hour 22 to 24: $T_H - T_L$ is still above 3 °C, but ΔT_{pan} is 0 °C, therefore the control signal remains null.

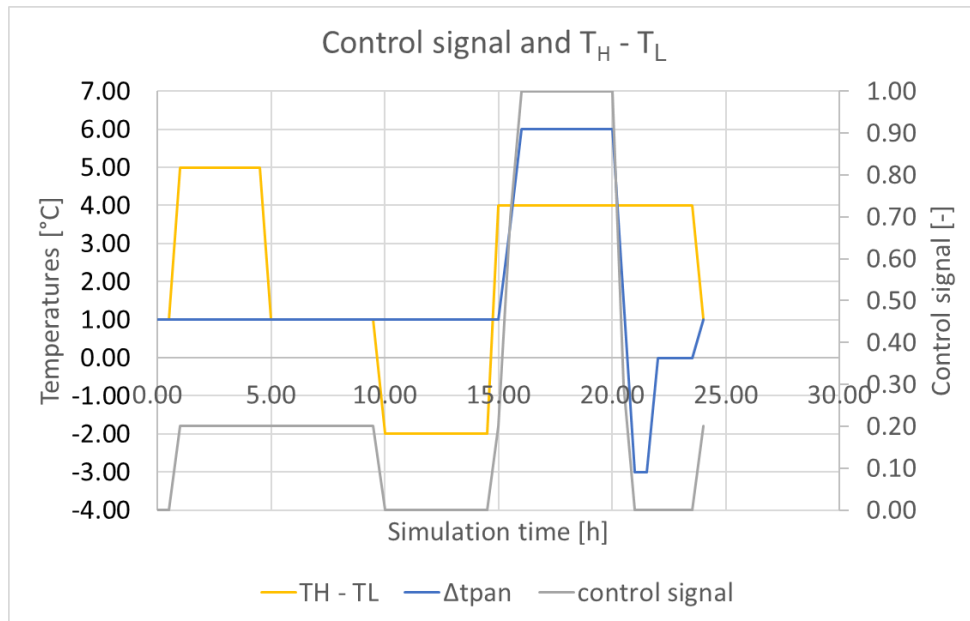


Figure 4. 14: variation of the control signal (grey line, right axis plot) depending on the difference between the upper (outlet panel temperature) and lower (temperature at the bottom of the solar tank) temperatures (yellow line) and the difference temperature between outlet and inlet water of the solar field (blue line)

Solar assisted heat pump:

Brief description:

The components singularly tested and described previously have been then assembled into a solar assisted heat pump. Such model can be still validated under simplified working conditions, referring to the measurements collected during the very first system testing carried out for a couple of weeks in April-May 2014, namely from April, 18th to May, 1st. During this testing, the SAHP was forced working, without considering the specific SH/DHW needs of the structure. In this way only the plant side can be validated, without still including the energy needs of the structure. The DAS collected the information about the external weather, united with the working temperatures at different points, reported in *Figure 4. 15*. A brief resume is proposed, referring to Chapter 3 and Annex for more complete information and plant outline:

- T2: inlet solar panel temperature
- T3: outlet solar panel temperature
- T10: temperature inside the water storage between the solar field and the cold side of the HP
- T4: temperature of the water entering the tank after being cooled by the evaporator
- T5: temperature of water before entering the heat exchanger with the HP evaporator

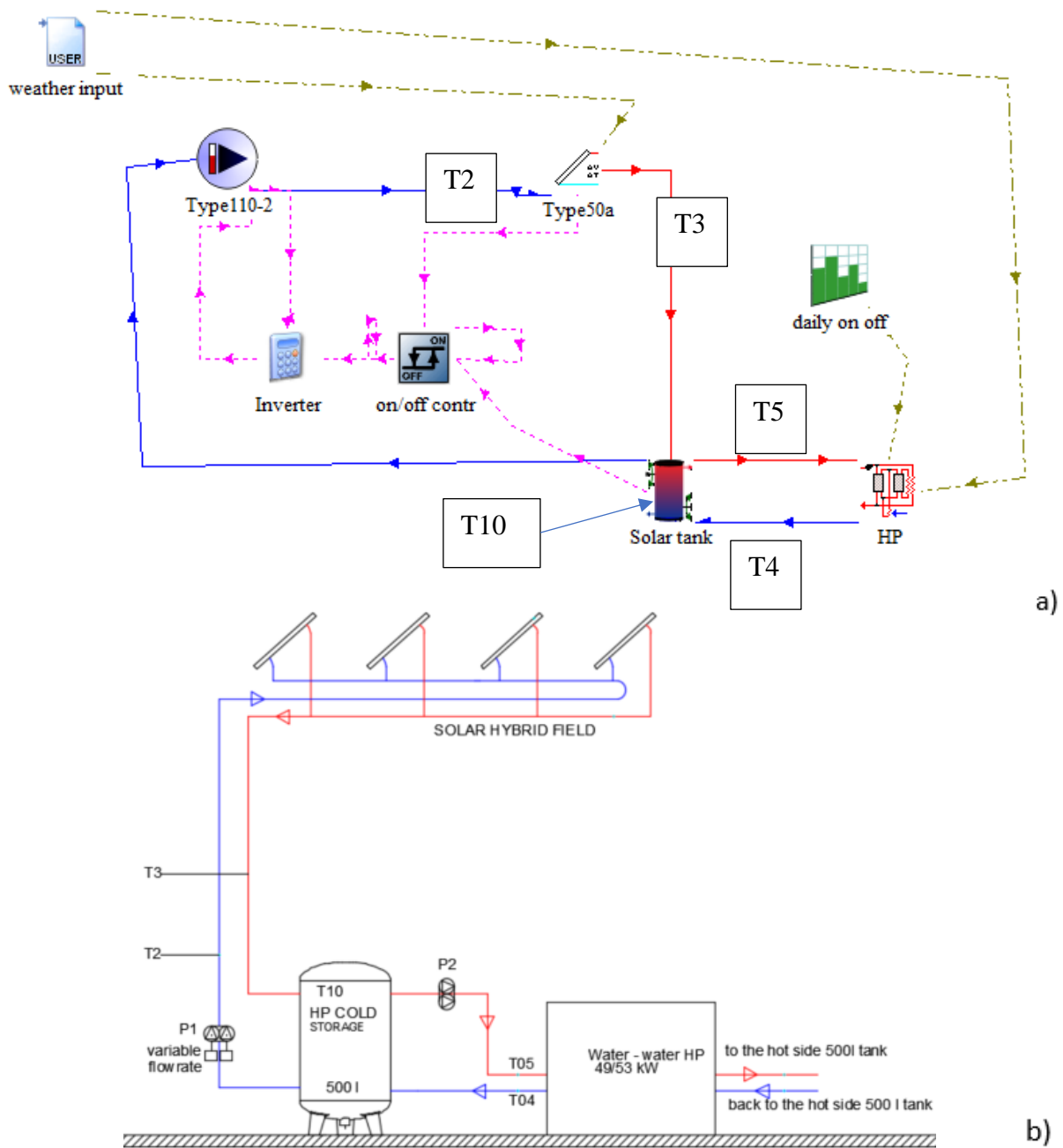


Figure 4. 15: layout of the SAHP plant model used in the validation a) and simplified schematic representation b). Colour code: blue line – cold water; red line – hot water; green, dotted line – weather connections; pink dotted line – logical/control connection

With respect to the complete plant layout, the mixing valve granting the set point temperature on the evaporator side lower than 25 °C (Figure 3. 15 b), has been neglected to reproduce the same working conditions of the measured information. Indeed, the implementation of the mixing valve dates back to a couple of years ago.

Besides of the components already described (e.g., heat pump, variable speed pump, solar panels etc), two further components can be identified:

- The weather input tool: it reads an input file with “.dat” extension containing for instance the information about weather (e.g., solar radiation, air temperature). This tool allows the simulation of the same climatic conditions occurred during the system testing days, to make the comparison of the measured and simulated parameters possible.
- Daily on/off tool: it belongs to the family of the forcing functions components. In the specific case, the component forces the on/off variable for the HP according to the predetermined schedules.

Validation of the SAHP:

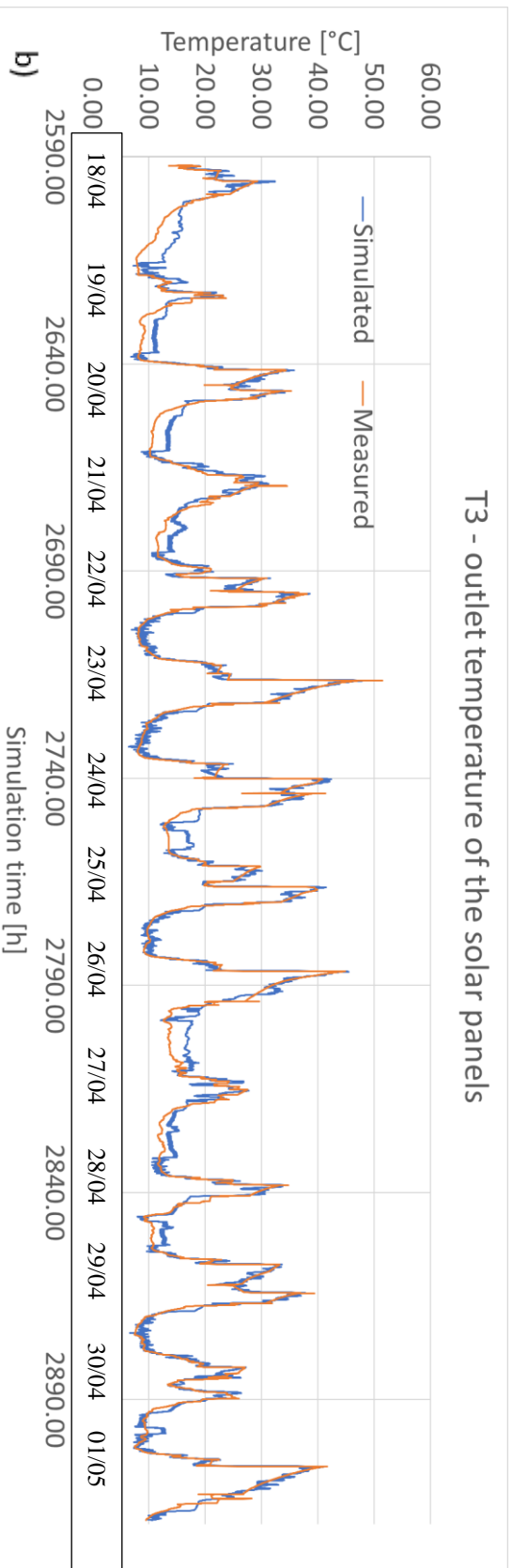
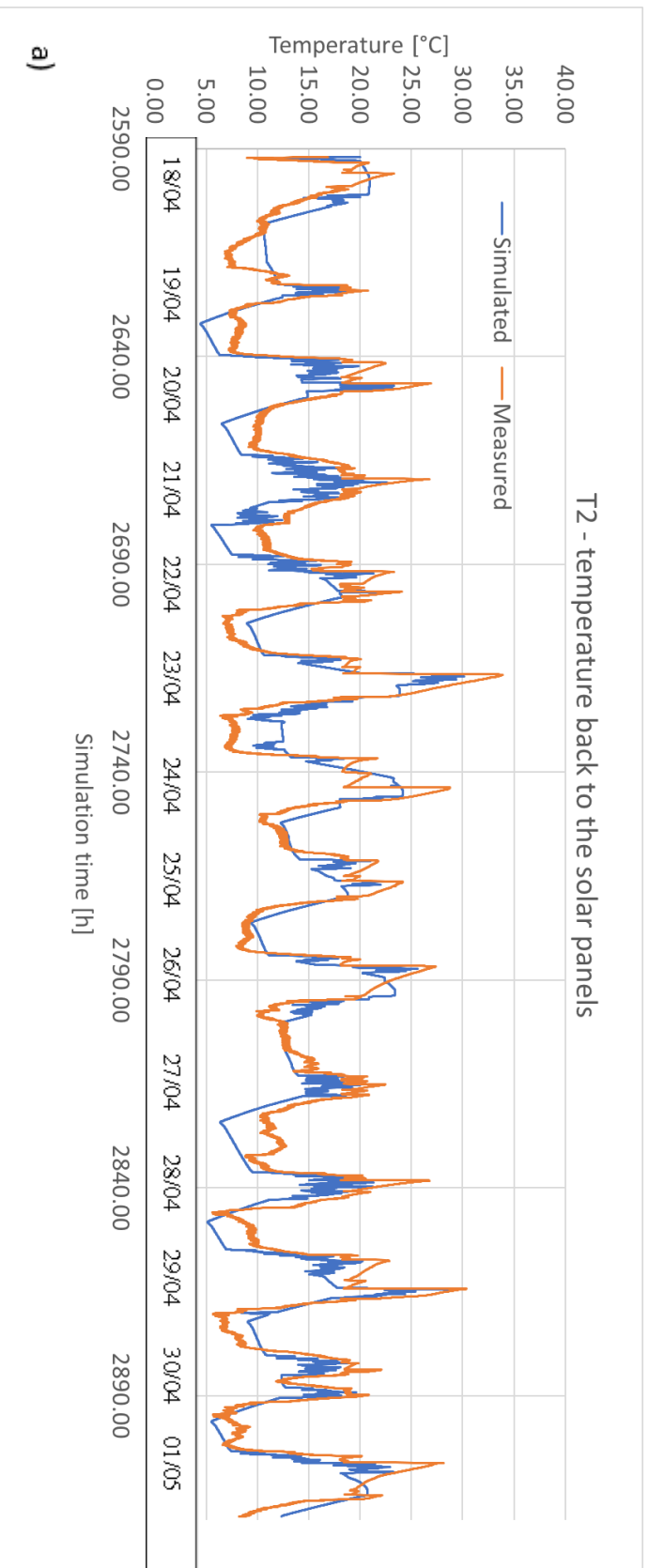
Actually, more attention is required to such stage, since the validation of plants working under transient regime is far more complicated than steady state ones. Indeed, the comparison of average reference values, for instance concerned with performance (e.g., COP) might result satisfactory even in the case of very different trends between simulated and measured working parameters. In other words, each time a transient phenomenon has to be validated, the only use of averaged parameters is likely to lead to inadequate validations. For this reason, a comparison with the trends of the temperatures identified above (T2, T3, T4, T5, T10 in *Figure 4. 15*) is added. The conceptual approach here illustrated follows the same criteria adopted in other similar works (160), (195), (196), (197), (198) et Al., where numerical validations of transient phenomena were carried out.

Table 4. 2 and *Figure 4. 16* resume the main results concerning the SAHP validation. In particular, the daily average performance of the SAHP is very well approximated, with variations which do not exceed 5-6%.

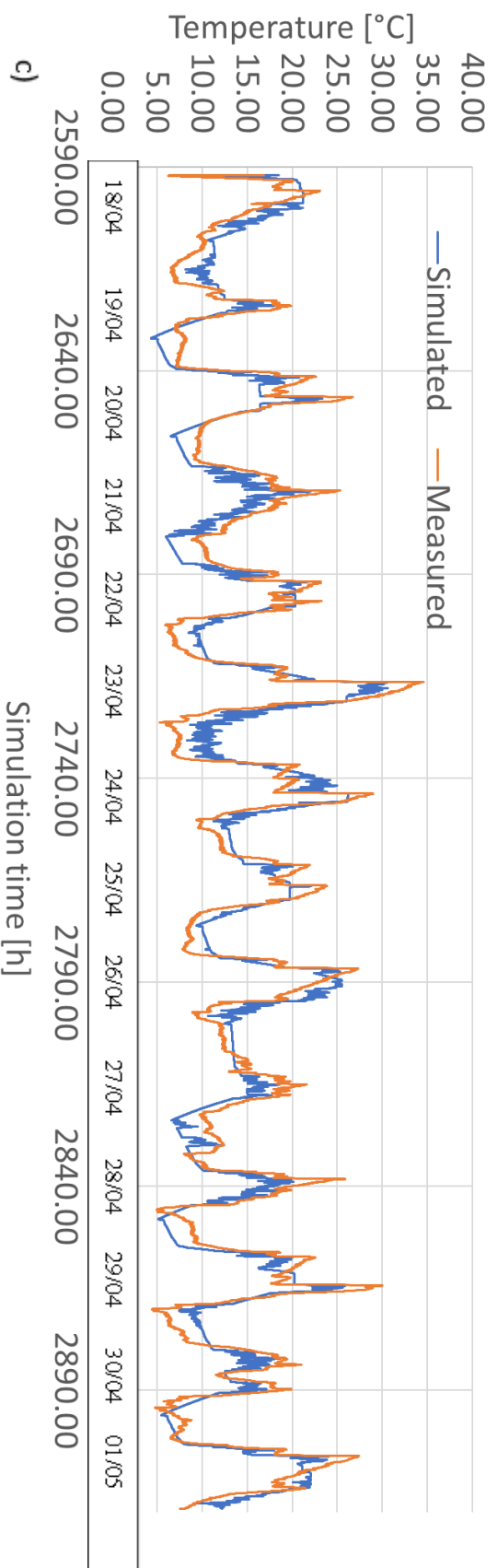
| Date | Average daily COP | | |
|------------|-------------------|----------|-------|
| | Simulated | Measured | Error |
| 18/04/2014 | 4.58 | 4.32 | 6% |
| 19/04/2014 | 4.09 | 4.12 | -1% |
| 20/04/2014 | 4.27 | 4.30 | -1% |
| 21/04/2014 | 4.16 | 4.39 | -5% |
| 22/04/2014 | 4.47 | 4.26 | 5% |
| 23/04/2014 | 4.65 | 4.44 | 5% |
| 24/04/2014 | 4.65 | 4.44 | 5% |
| 25/04/2014 | 4.49 | 4.32 | 4% |
| 26/04/2014 | 4.66 | 4.46 | 4% |
| 27/04/2014 | 4.25 | 4.40 | -3% |
| 28/04/2014 | 4.14 | 4.28 | -3% |
| 29/04/2014 | 4.47 | 4.28 | 5% |
| 30/04/2014 | 4.17 | 4.16 | 0% |
| 01/05/2014 | 4.63 | 4.38 | 6% |

Table 4. 2: simulated and measured average daily COP during the initial testing of the facility (from 2014, April, 18th to May, 1st)

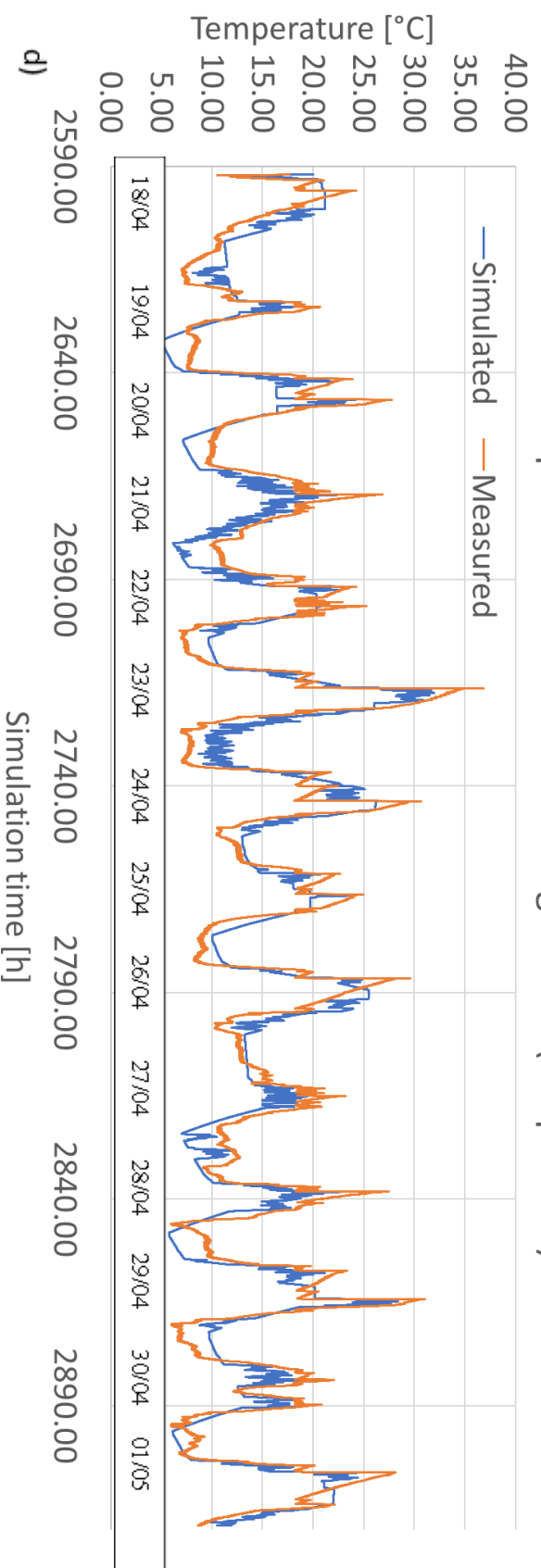
In addition, the trend of the temperatures formerly illustrated shows a good level of accuracy of the simulated results, against the simulated ones.



T4 - temperature back from the evaporator



T5 - temperature of water entering the HP (evaporator)



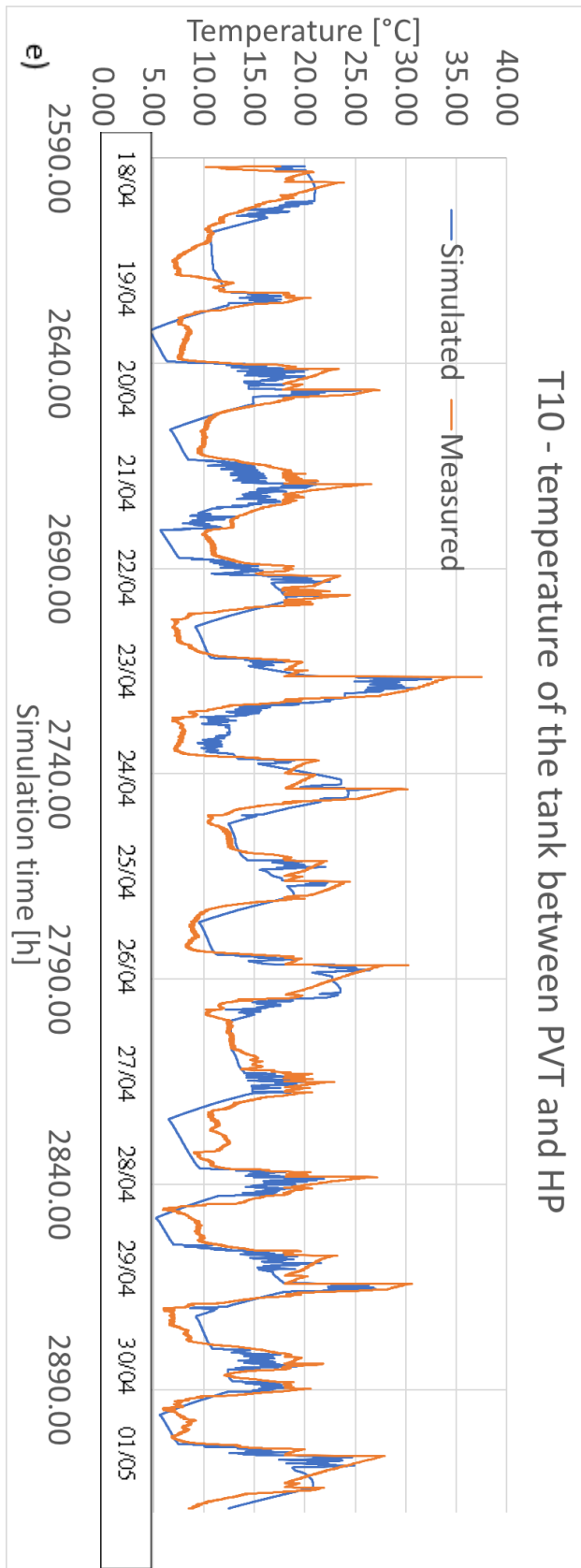


Figure 4. 16: Validation of T2 (a), T3 (b), T4 (c), T5 (d) and T10 (e), as previously illustrated in Figure 4. 15

Clearly, some variations can be noticed between the numerical and real data (Figure 4. 16) which in turn determine the fluctuations in the SAHP COP (Table 4. 2). Some main reasons can be found:

- *Missing weather data:* at the time of the SAHP initial test, the weather station was not fully operative, therefore information about air humidity and wind speed was missing.
- *Model simplification:* as illustrated in the previous chapters, the numerical model adopted for the validation bases on simplifying assumptions, such as the neglection of the thermal losses of the connection pipes between the solar field and the heat pump (about 200 m long). This topic shall be enquired in the following section, about the optimization simulations.
- *Position of sensor T10:* the temperature sensor of the solar tank (namely the water tank connecting the solar field to the cold side of the heat pump) is located at about $\frac{3}{4}$ of the total height, at the same level of the outlet water sent to the HP cold side. In addition, the water coming from the solar field enters the top of the tank, very next to the sensor (*Figure 4. 17*). As a consequence, such geometrical configuration and any eventual mixing can be hardly modelled by means of simplified components. In addition, when both the solar and HP cold side circuits are active, the sensor is more likely to measure the temperature of water directly flowing from the solar circuit to the HP instead of a temperature representative of the entire tank.

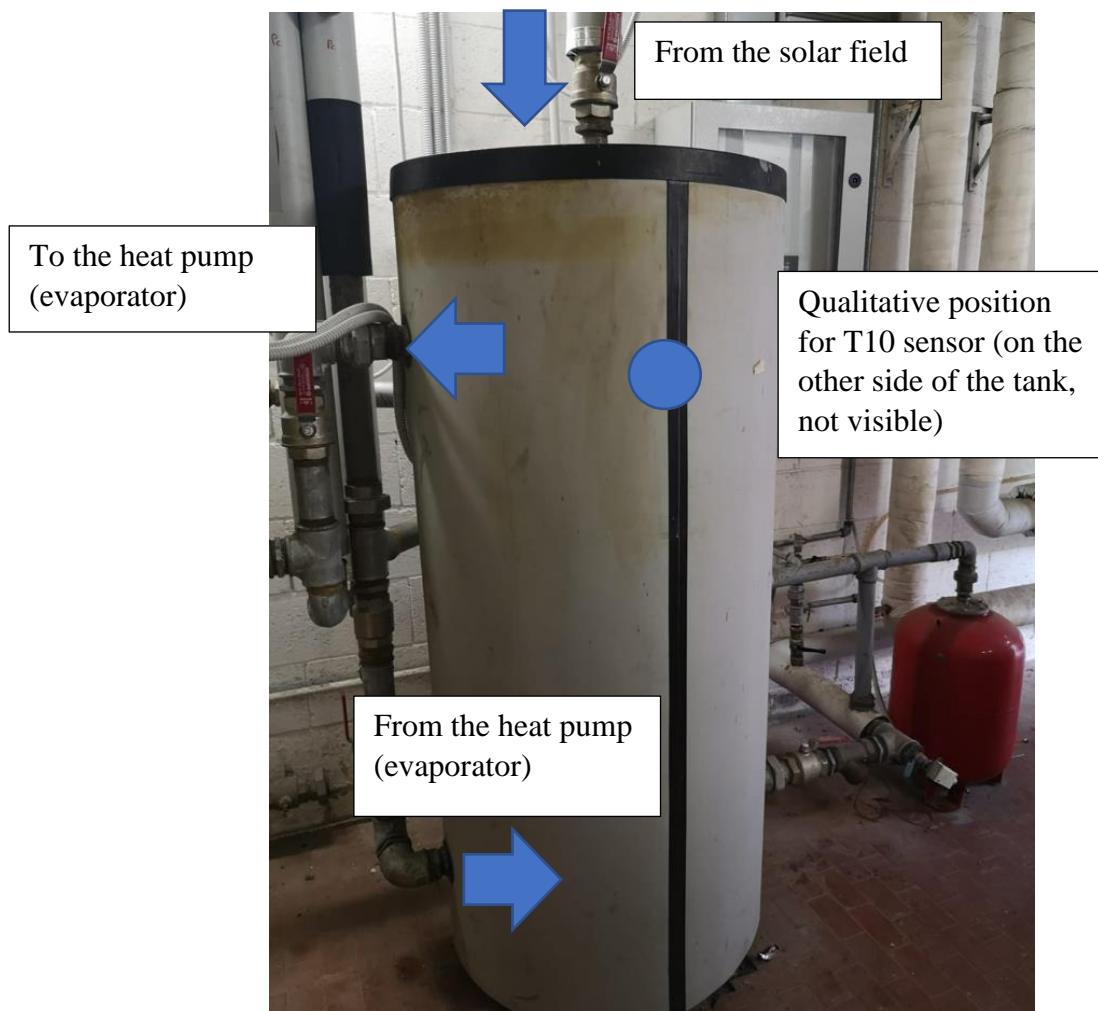


Figure 4. 17: solar tank, qualitative position of the inlet/outlet circuits and of sensor T10

T10 then influences the other temperatures as well, such as the temperature of the water entering the heat exchanger with the HP evaporator (T5) and in turn the working temperature of the HP cold side, leading to the variations in COP reported in *Table 4. 2*. Temperature T3 (outlet from the solar field) shows a better resemblance with the measured values since it is

less influenced by T10. Anyway, the trends are in good accordance with the measured temperatures and the fluctuations of the COPs are acceptable, so the model can be considered validated.

Space heating subsystem

Brief description:

Figure 4. 18 shows the part of the numerical model reproducing the SH subsystem.

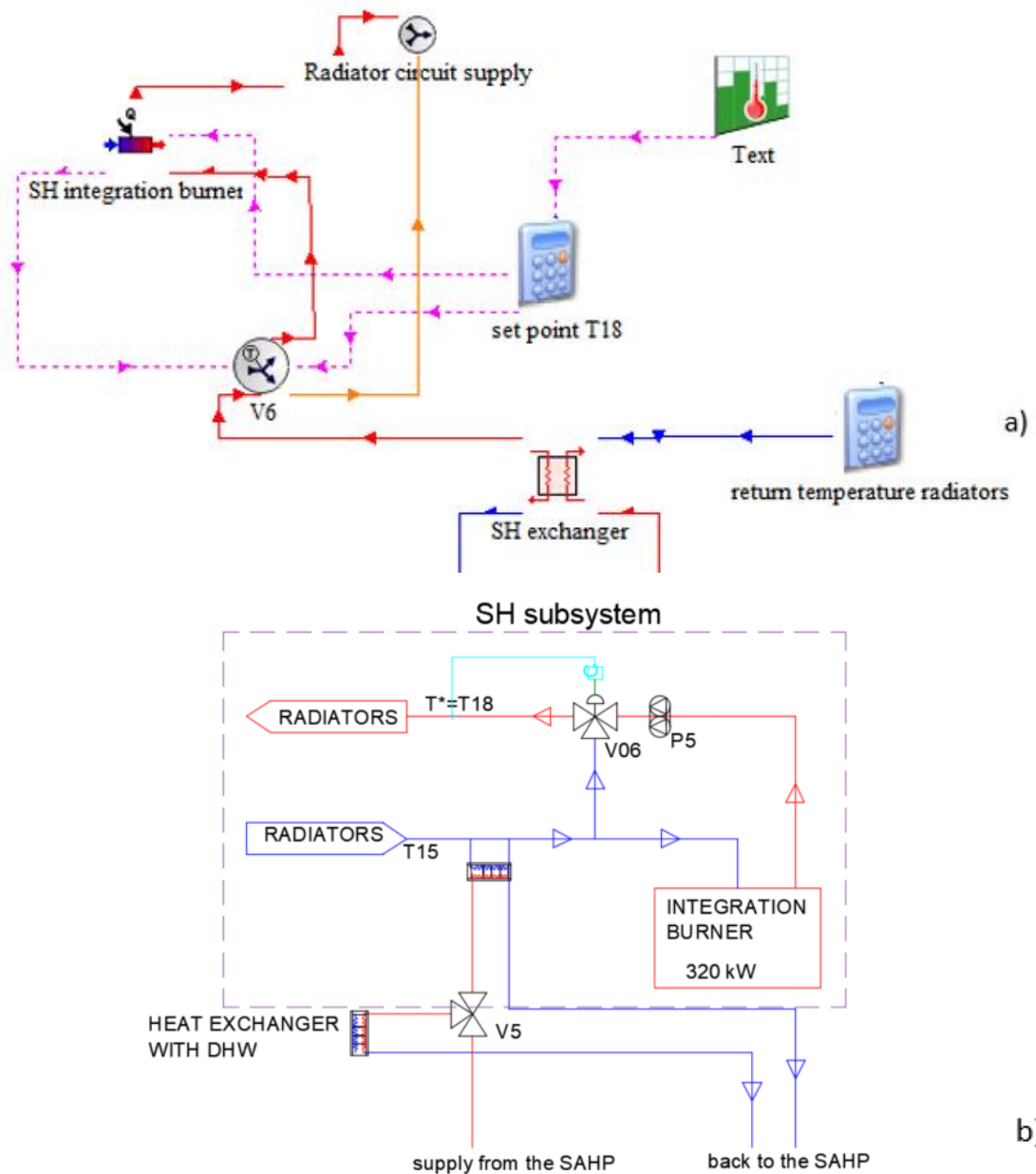


Figure 4. 18: layout of the SH subsystem numerical model a) and simplified schematic representation b). Colour code: blue line – cold water; red line – hot water; green, dotted line – weather connections; pink dotted line – logical/control connection

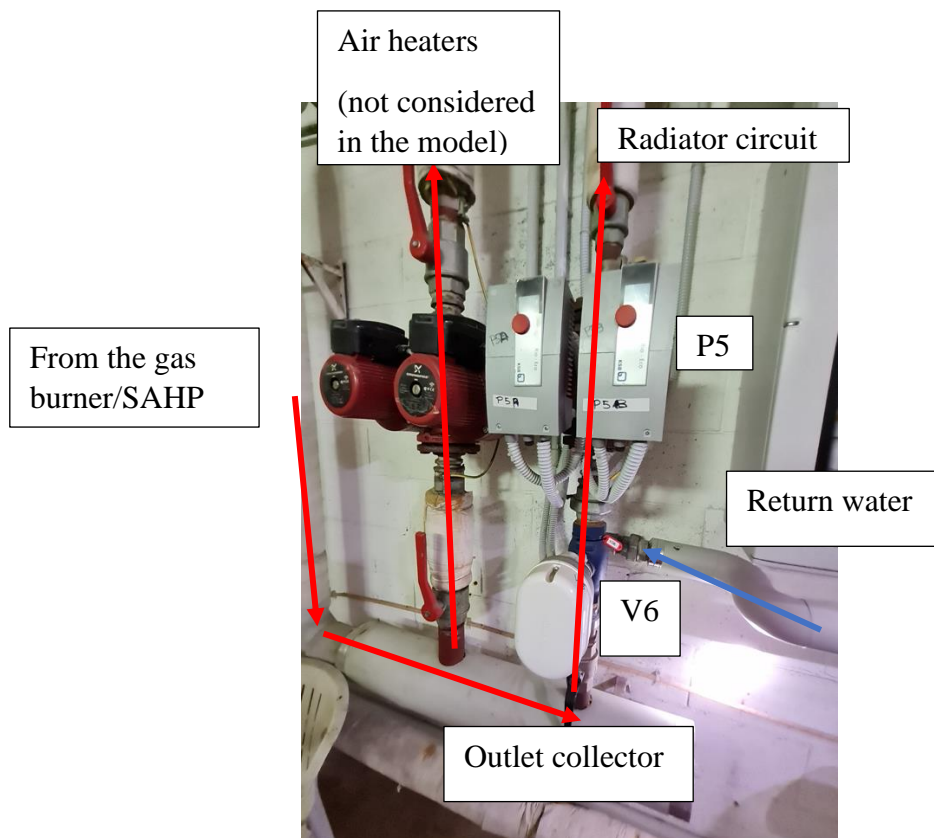


Figure 4. 19: detail of Figure 4. 18, outlet collector of the SH subsystem

In particular, the return water of the radiator circuit is pre-heated by means of a heat exchanger interfaced with the SAHP supply. Then, the mixing valve V6 grants the set point temperature T_{18} by sending part of the water towards the 320 kW integration gas burner (if necessary) and recirculating the remaining part. The value of T_{18} is not constant, but it is automatically updated by the DAS depending on the external temperature according to the following linear correlation (Figure 4. 20):

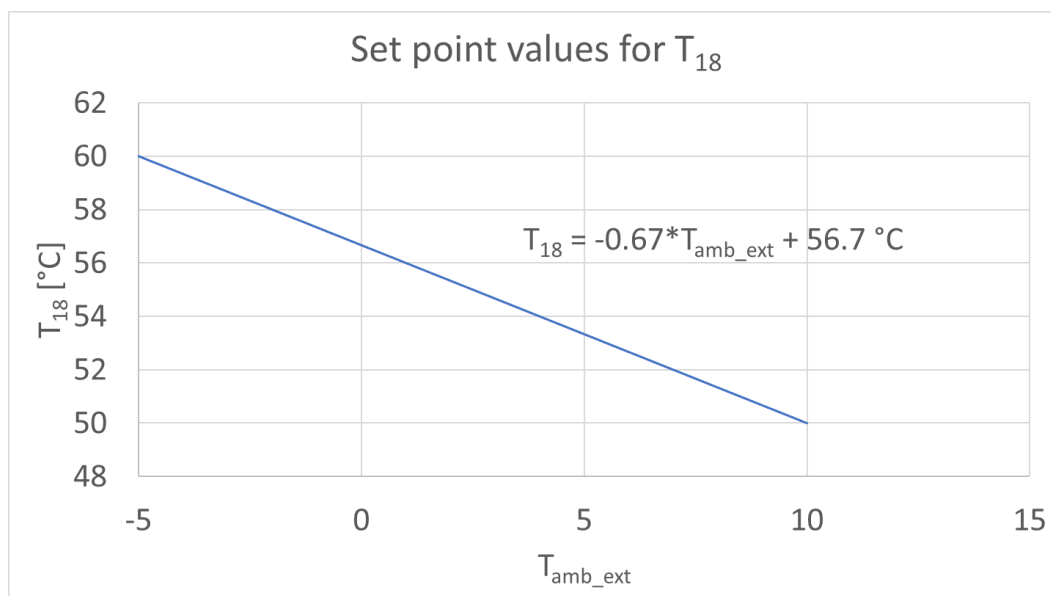


Figure 4. 20: linear criterion for automatic evaluation of the T_{18} set point value as a function of the external ambient temperature (T_{amb_ext})

Usually, the external temperature in Genoa is very likely to be higher or equal to 10 °C, during most of the heating season. Considering the yearly plot of the external temperature averaged over the recorded years by (Figure 4. 21), a temperature of 10 °C is likely to be overpassed in 90% of the times,

implying that the set point temperature for the radiators will be in most of cases closer to the lower limit of 50 °C than the upper one (60 °C).

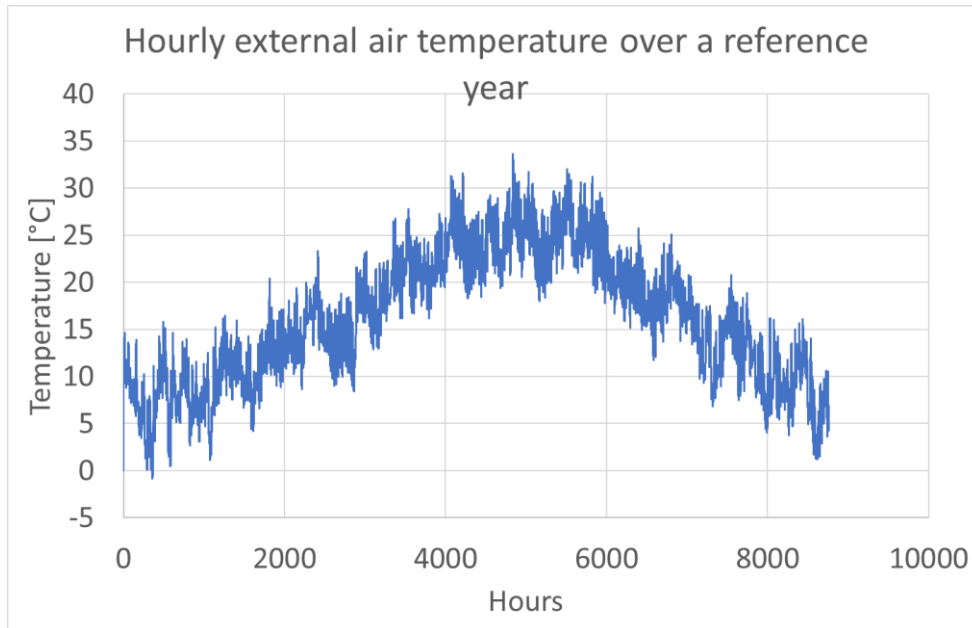


Figure 4. 21: hourly temperature for external air for a reference year obtained averaging the hourly values recorded over different years for the location of Genoa

Concerning the TRNSYS modelling, the following components have been implemented:

- heat exchanger (Type 5): such element reproduces the existing counter flow 50 kW exchanger which hydraulically separates the SH and SAHP circuits (Figure 4. 22). The model is based on the mathematical formulation proposed by Kays, London et al (199).

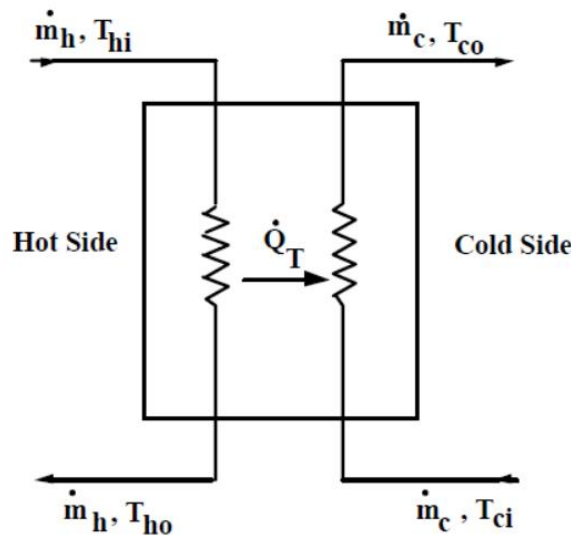


Figure 4. 22: schematic representation of the heat exchanger component (186)

The outlet temperatures and mass flow rates on both cold and hot sides are computed once the inlet mass flow rates and temperatures on both sides are known. The component also requires the overall heat transfer coefficient and the specific heats of the fluids flowing inside the element.

- auxiliary heater (Type 6): it provides additional heat whenever the inlet water is at a temperature lower than the set point value. Such component modulates the heat flow from zero up to the nominal (maximum) heat flow multiplied by the generator efficiency. If the set point temperatures required a heat flow higher than the maximum possible, the auxiliary heater would provide all possible heat, without being able to reach the set point. The component can compute the thermal losses associated to generation by inserting the overall loss coefficient and the temperature of the ambient where the generator is located.
- automatic mixing valve (Type 11): the working of the mixing valve is modelled in TRNSYS environment with two elements:
 - o a flow diverter with one inlet, proportionally split into two possible outlets (namely one sent towards the SH integration burner and the other directly connected to the mixing valve), depending on the required set point temperature (T_{18}) and on the inlet water temperature and flow rate (Type 11, mode 4 – tempering valve).
 - o A tee piece which just mixes two different inlet streams of the same fluid at different temperature (Type 11, mode 1 – tee piece).
- Calculator: it reproduces the regulation criterion described to choose the set point value of T_{18} (Figure 4. 20), depending on the measured external temperature (imported by means of Type 14, previously described).
- Calculator of the return temperature: it simulates the temperature and flow rate of the return water inside the radiator circuit. A variable difference between 2 and 3 °C is subtracted to the supply temperature to simulate the temperature of the return water of the radiator circuit, following the same principle illustrated for the set point value of T_{18} . Indeed, as illustrated in the section concerned with the SH needs (section 3.2.2), the radiators only heat the lockers which are associated to a thermal load not relevantly influenced by the different months of the heating season. Such assumption is supported by two aspects: firstly, the recorded trends of the supply and return water temperature of the radiator circuit show very little variations during the heating season. Secondly, the lockers are in touch either with heated (e.g., sports hall) or unheated environments (e.g., crawlspace), without being directly exposed to the solar radiation and the external environment.

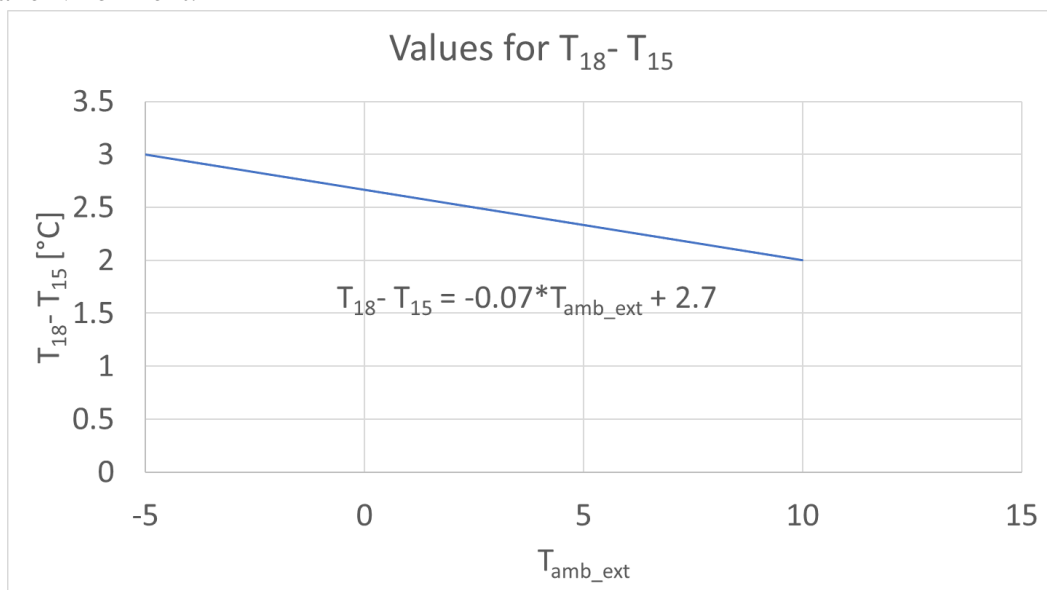


Figure 4. 23: simulated difference between supply (T_{18}) and return (T_{15}) water temperature of the radiator circuit according to the external air temperature (T_{amb_ext})

Validation of the SH subsystem:

The validation reported aims to check the correct response of the SH subsystem, referring to the measured available data. The TRNSYS model shown in *Figure 4. 18 a)* has been used, substituting the computation tool for the return temperature with the import tool, to apply the measured return temperature as boundary condition. The same approach has been followed to simulate the inlet/outlet temperatures and flow rates on the hot side of the heat exchanger with the SAHP.

On the other hand, the temperature of the supply water has been used to validate the SH subsystem. The same convergence parameters of the previous models have been adopted while a 5 minute time-step has been chosen.

The validation has been carried out for different days along the heating season, showing only the most significant ones in the present work:

- January 31st, 2019: it represents one of the coldest days, when the measured supply temperature T₁₈ almost reached 60 °C late in the afternoon. Two main issues make this trend uncommon among the recorded ones: firstly, the high supply temperature and secondly the steep increase, late in the afternoon, probably due to a rapid decrease of air temperature. Anyway, the simulated and measured temperatures are in good agreement, with maximum differences of about 1-1.3 °C (*Figure 4. 24*).

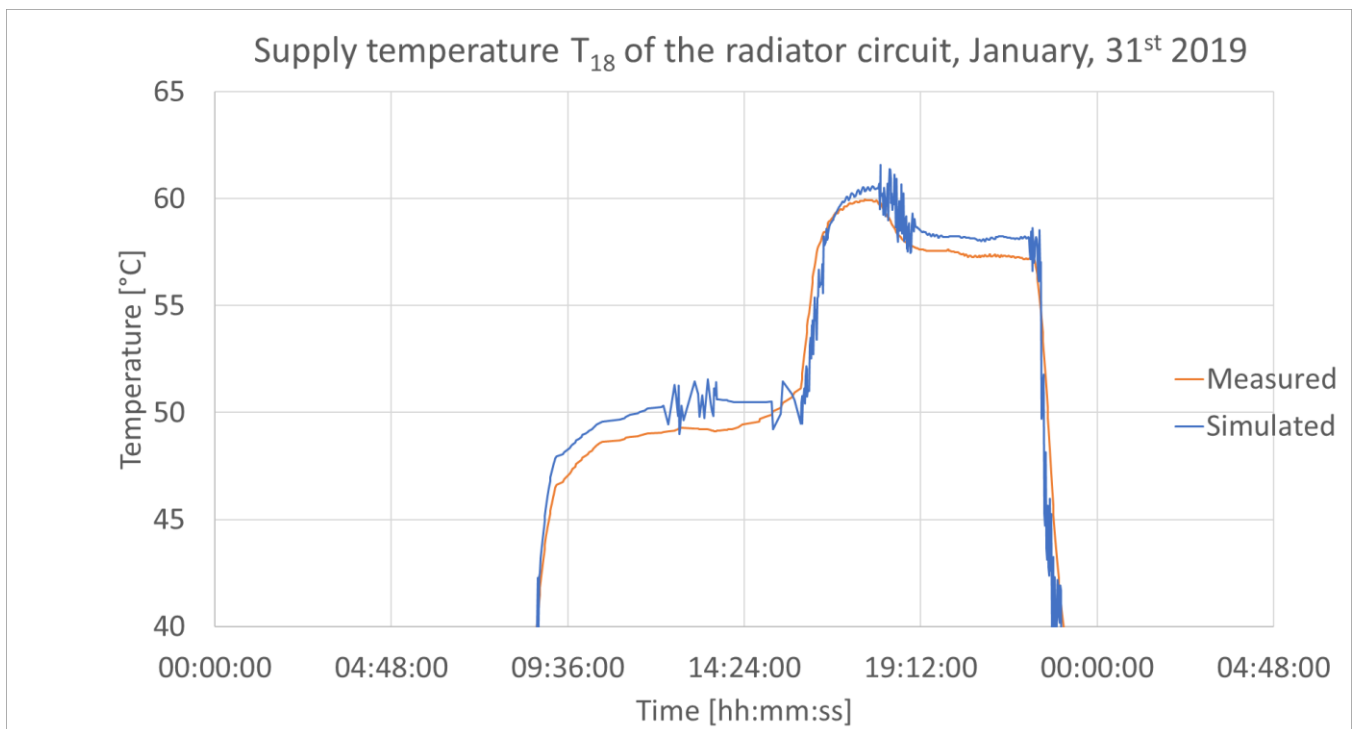


Figure 4. 24: Supply temperature for the radiator circuit on January 31st, 2019

- March 15th, 2019: it is associated to one of the most recurrent situations, where the supply temperature is at 50 °C. Good accuracy is shown, with differences between simulated and measured values lower than 1 °C (*Figure 4. 27*).

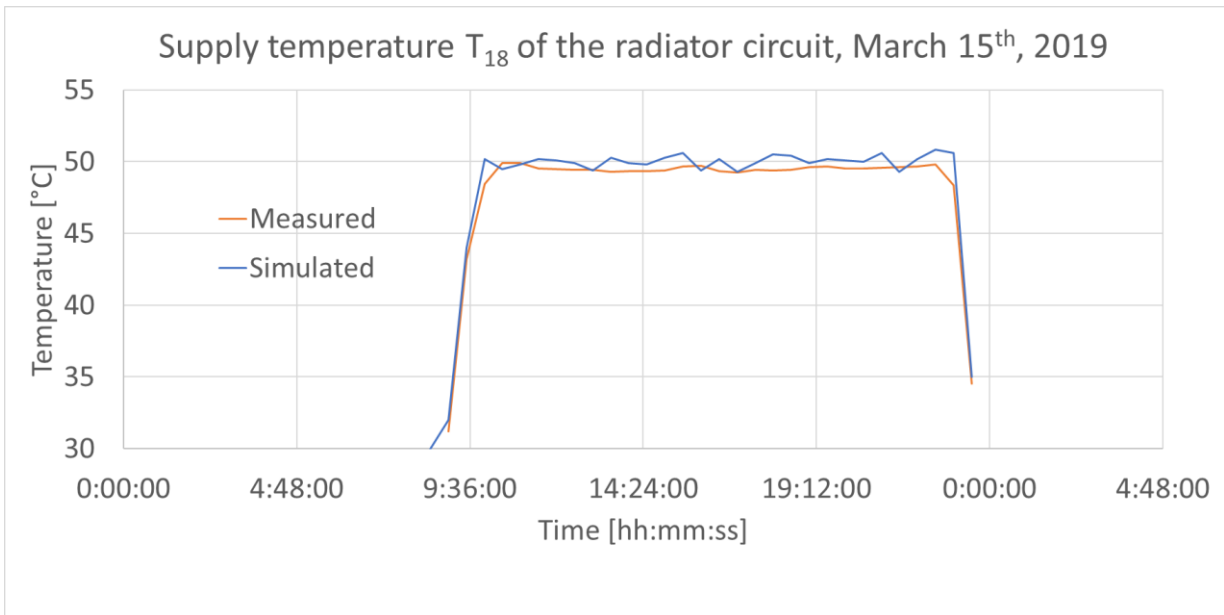


Figure 4. 25: Supply temperature for the radiator circuit on March 15th, 2019

- December 5th, 2019: the set point temperature is at about 52-53 °C and it is representative of a not frequent cold day in Genoa. Also in this case, no relevant oscillations in the measured trend are appreciated. The difference between measured and simulated values is lower than 1 °C, (Figure 4. 26).

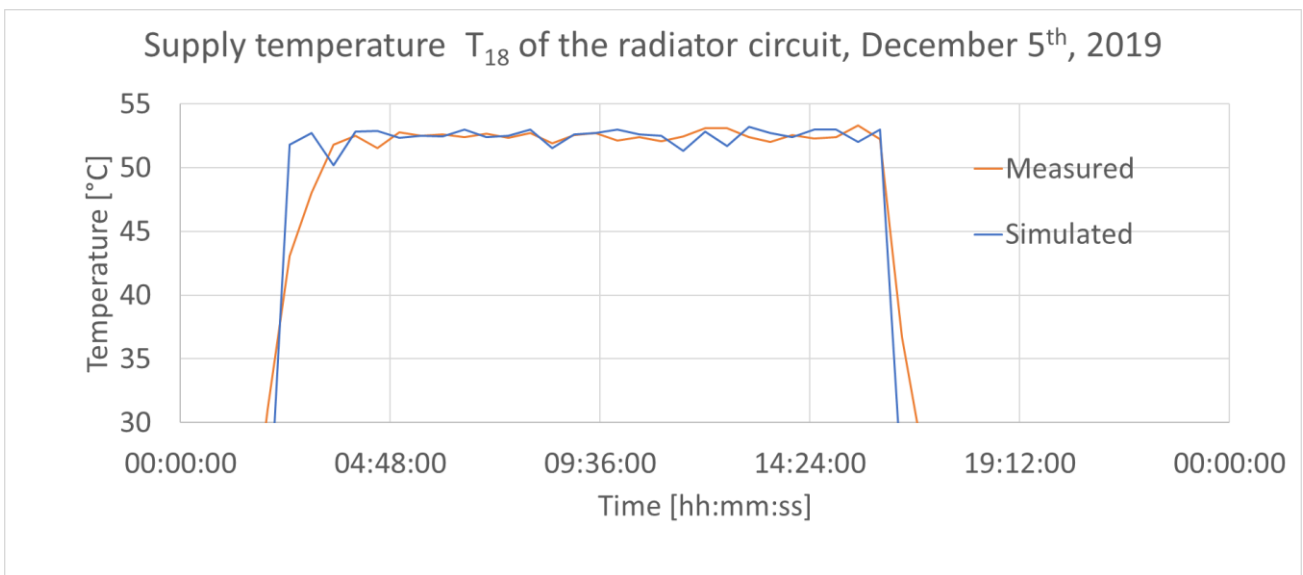


Figure 4. 26: Supply temperature for the radiator circuit on March 15th, 2019

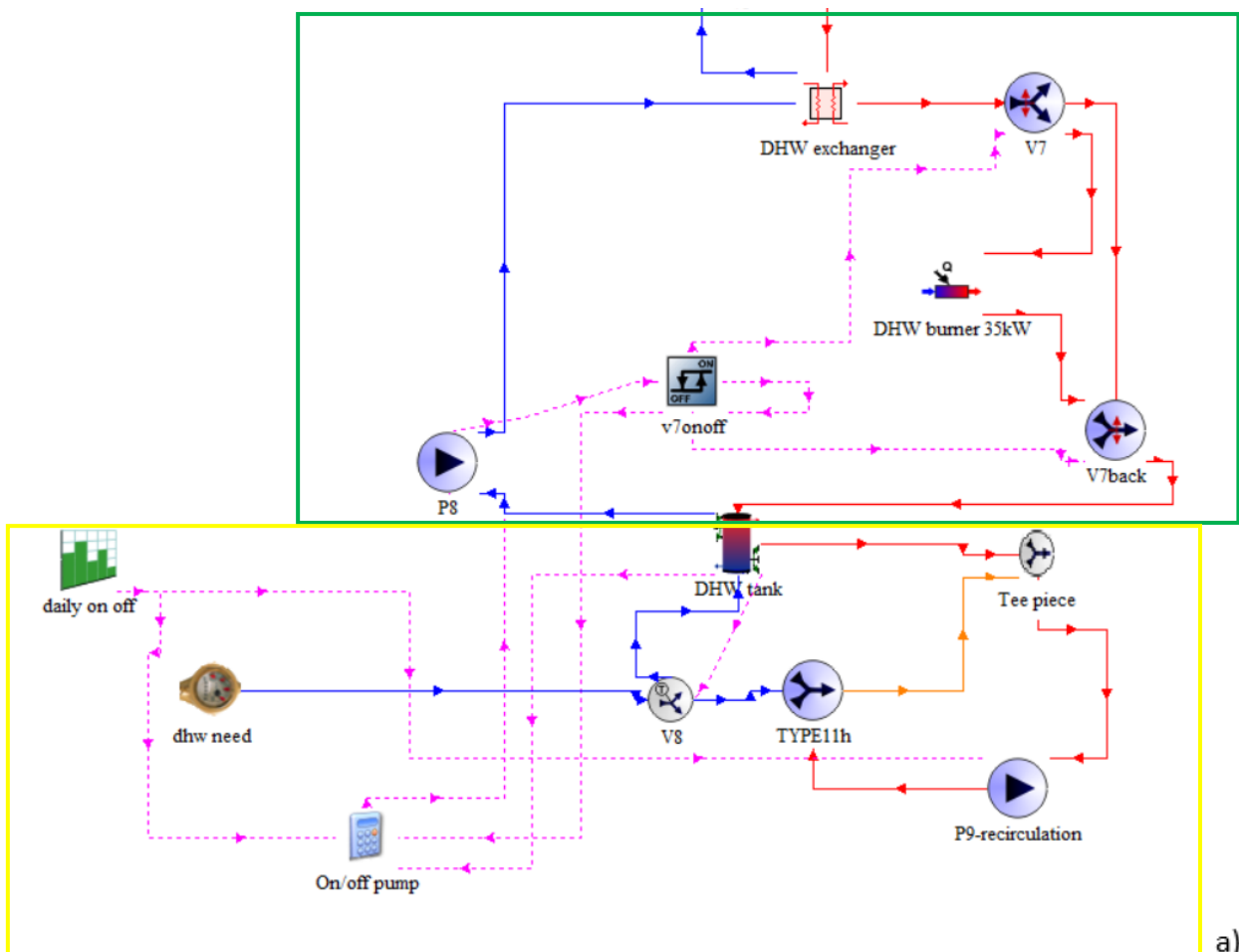
Domestic hot water subsystem

Brief description:

Figure 4. 27 shows the part of the numerical model reproducing the DHW subsystem and a layout to allow a comparison between real plant and simulated model. Figure 4. 27 a) can be furtherly split into two groups:

- Circuit of technical hot water used to maintain the set point values (green rectangle, upper part of *Figure 4. 27 a)* and *Figure 4. 29)*: starting from the heat exchanger interfaced with the SAHP circuit, the technical hot water is then heated by the integration gas burner, in case the temperature of the outlet water from the heat exchanger is lower than the set point value. Otherwise, the burner remains in stand-by condition. Finally, the hot water is used to heat up the DHW tanks. The activation of the pumps inside the system follows two specific regulation criteria managed by the DAS: the former switches the pumps on, when temperature T14 (sensor in the lower tank of the DHW tank) lowers a set point value (actually set at 52 °C, to fight the bacteria of Legionella). The latter manages the priority between SH and DHW subsystems establishing that the diverter valve V5 must send the hot water coming from the SAHP circuit to the DHW heat exchanger, instead of the SH one, if T14 lowers the DHW supply set temperature (48 °C). This last regulation creates a hierarchic working where the SAHP preferably provides heat to the DHW subsystem instead of the SH one.
- Circuit of DHW (yellow rectangle, lower part of *Figure 4. 27 a)* and *Figure 4. 28)*: the cold water supply is divided into two flows, according to the mixing valve V8 which maintains the DHW supply temperature at the fixed set point. So, part of the water flows inside the DHW tank from the bottom, while the rest of the cold water is mixed with the recirculation circuit (pump P9) and then sent to the mixing valve.

The adopted components have already been described for the SH and SAHP subsystems, so no further comment is necessary.



a)

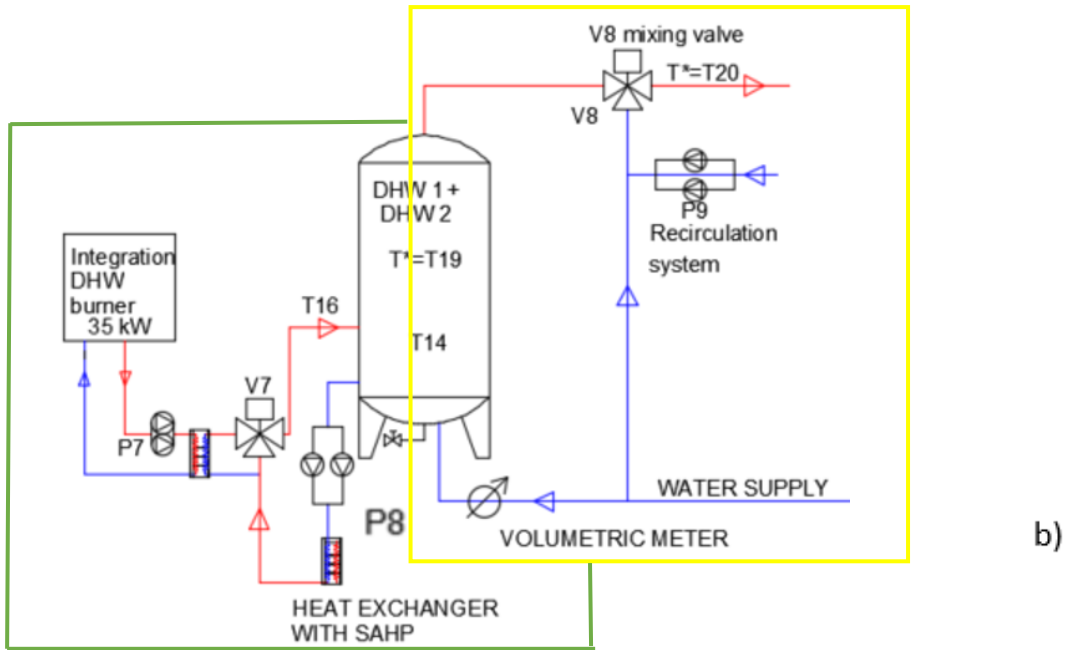


Figure 4. 27: layout of the DHW subsystem numerical model a) and simplified schematic representation b).
 Colour code: blue line – cold water; red line – hot water; green, dotted line – weather connections; pink dotted line – logical/control connection

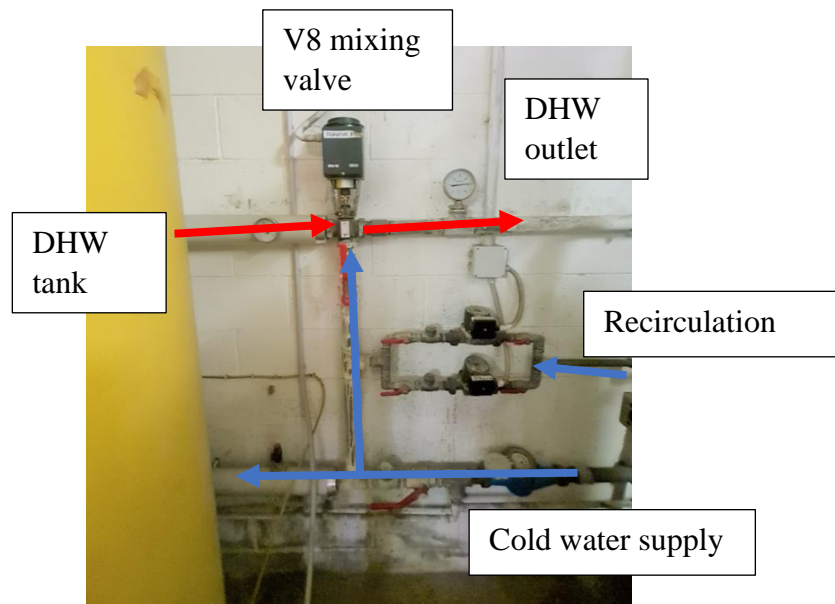


Figure 4. 28: detail of the DHW circuit (yellow rectangle in Figure 4. 27)

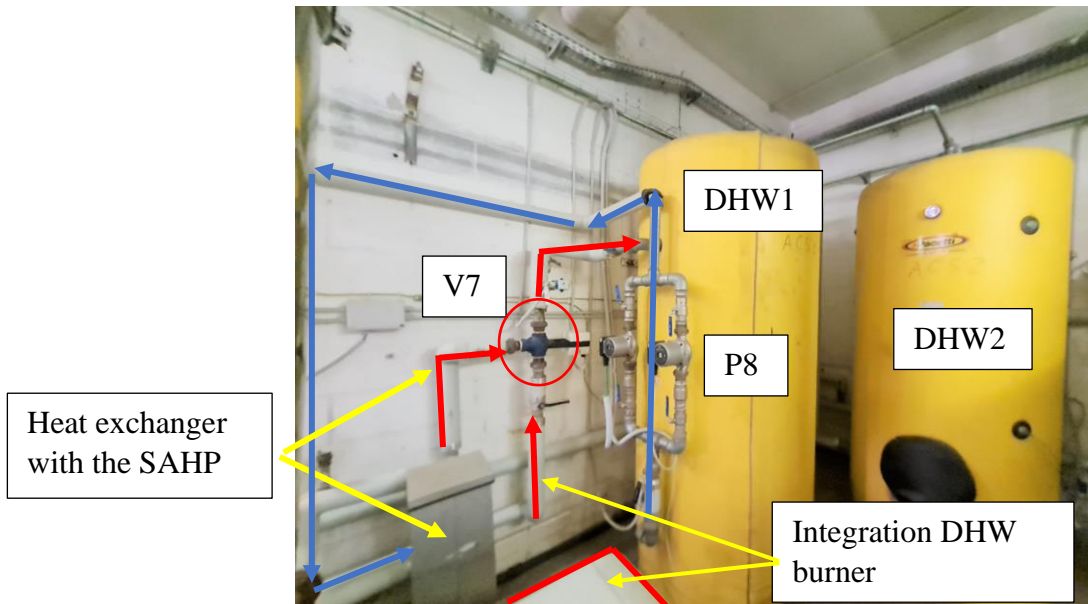


Figure 4. 29: detail of the technical hot water to produce DHW (green rectangle in Figure 4. 27)

Comparing the model to the real plant layout (reported as Annex or schematized in Figure 3. 19), two DHW tanks of 1500 l capacity each are installed inside the boiler room. This choice instead of a unique boiler was due to the sizes of the room which were not compatible with the dimensions of 3000 l boiler. Nevertheless, the pipes connect the top of the first DHW tank (named DHW1) to the bottom of the second one (named DHW2), making them work as if they were stacked one on the other (Figure 4. 30). In fact, DHW 1 has been conceived as colder tank (about 50-52 °C), where the cold water from the supply enters and it is heated by means of the SAHP/integration burner. DHW2 is a tank at a higher temperature (about 54-56 °C) from which the hot water is sent to the users by means of the mixing valve. In addition, a small internal recirculation pump (P10) connects the top of DHW2 with the upper part of DHW1 to avoid DHW1 reaching an internal temperature higher than DHW2. Indeed, the heating of DHW2 would take place only when a water draw occurs and the assumption of stacked tanks would not be valid from the thermal point of view without P10. Such topic was enquired in detail in a specific PhD work (136) on the same pilot plant to which we refer for additional information and simulations. Consequently, a unique tank of total volume has been implemented in the model.

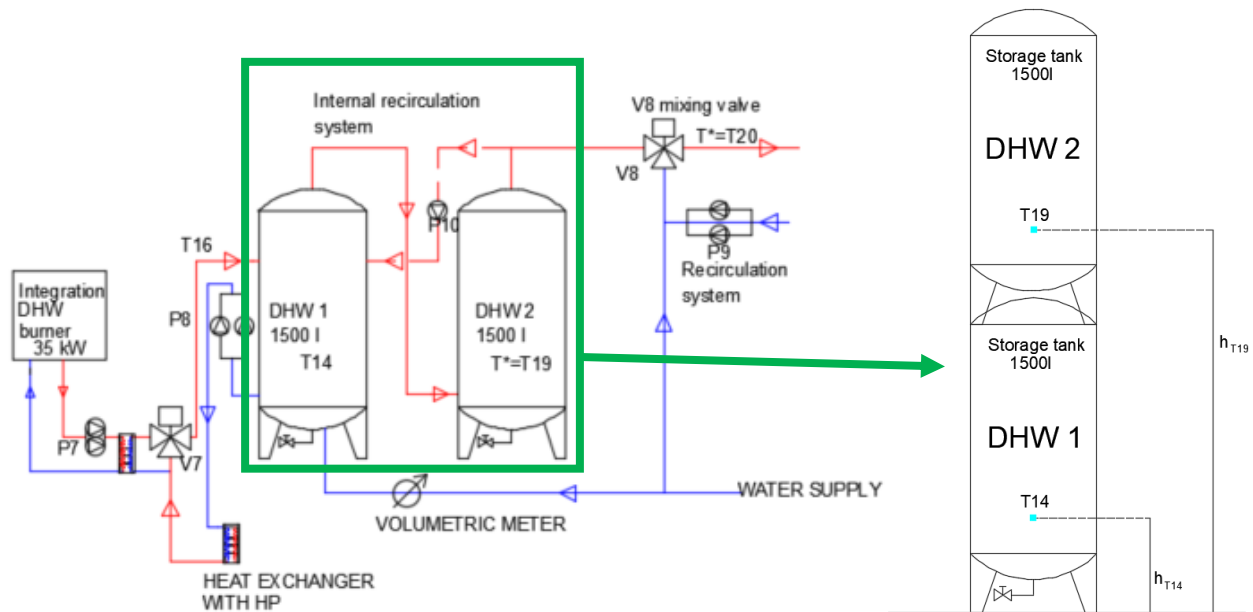


Figure 4. 30: comparison between DHW layout and assumption of the DHW boilers. Colour code: blue line – cold water; red line – hot water.

Validation of the DHW subsystem:

The validation has been carried out considering three main control variables:

- Temperature T16 representing the inlet flow of hot technical water heating the DHW tanks, to verify the correct working of the elements within the green rectangle in Figure 4. 27 a).
- Temperatures T14 and T19 inside the DHW tanks, to validate the water consumption profile described in section 3.2.2 and correctly simulate the heating of the DHW by means of the SAHP/integration burner. As shown in Figure 4. 30 the sensors are installed in the lower part of each tank. In order to make the results of the simulation comparable to the measured data, two specific nodes, at the same height of the existing ones were considered. Since the two existing DHW tanks were united into one with double volume (and double height), the height of the node reproducing T19 accounts also for the total height of the first boiler as reported in Figure 4. 30 on the right.

Besides of the forcing function reproducing the water supply, the numerical model presented in Figure 4. 27 a) has been validated reading the measured inlet/outlet temperatures and flow rates on the hot side of the heat exchanger with the SAHP. In this way, the SAHP circuit can be considered as a part of the boundary conditions and a specific focus can be paid to performances of the DHW subsystem. The validation has been run considering different, specific days and comparing the trends of the control variables identified before. Figure 4. 31 and Figure 4. 32 show for every control parameter the comparison between simulated and measured values. Checks on different days in other moments of the year were omitted, since T16 shows very little variation and T14/T19 cannot be validated with a high level of precision, because they do depend on the specific daily load occurred and the forcing function simulating the withdrawals in standardised. The aim of the comparison of temperatures T14 and T19 is to test the accuracy in reproducing the same shape of the curve which recurs in a very similar pattern all year long.

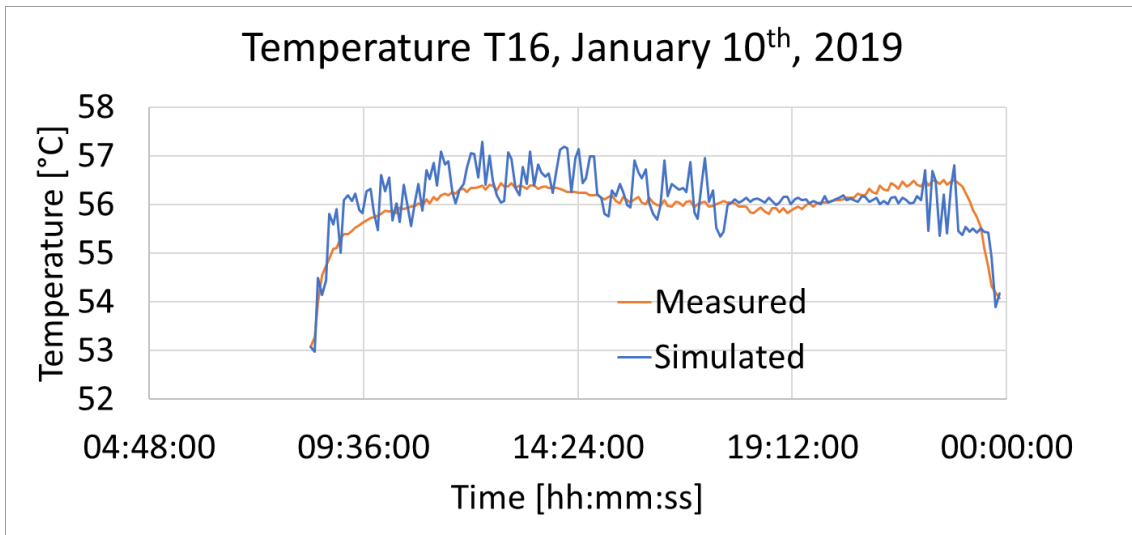
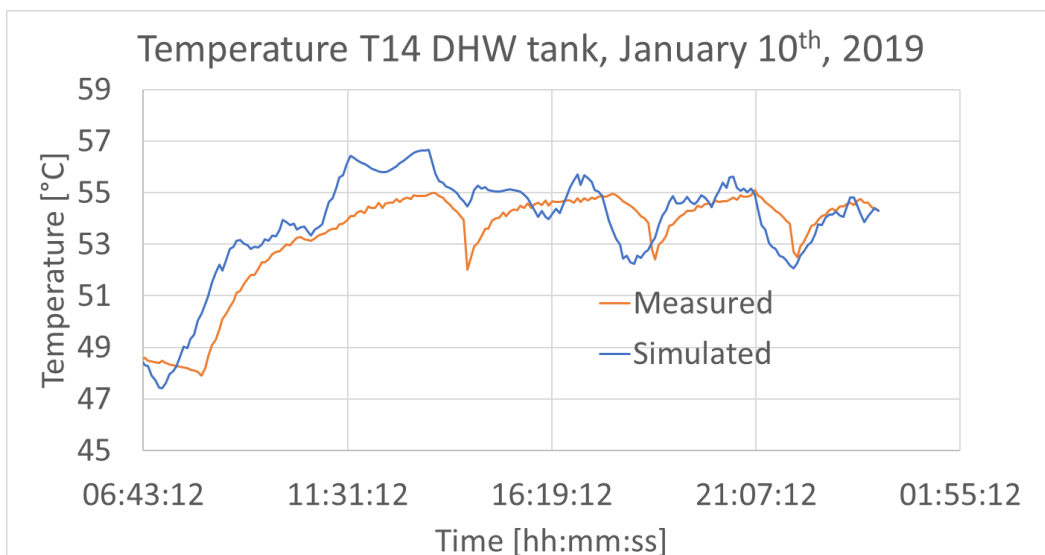


Figure 4. 31: simulated (blue line) and measured (orange line) trends for T16 – temperature of the hot technical water entering the DHW tank

The two curves plotted in *Figure 4. 31* show good agreement, in terms of both shape and values, with a maximum difference of 1.2 °C.

Also, the shapes of curves of the temperatures T14 and T19 inside the DHW tanks still reproduce a very similar shape to the measured ones (*Figure 4. 32 a*) and b)). Firstly, the oscillating trend represented by alternating withdrawal and heat up; secondly, the most marked fluctuation of simulated T14 since it is closer to the cold flow inlet from the water supply, as highlighted by the measurements. In addition, the oscillation between measurements and simulation reaches up to 2/2.5 °C of difference because of the adoption of a standard DHW consumption profile. The maximum error committed is of about 5% and therefore the standard hourly usage profile introduced in 3.2.1 can be considered validated for the specific case study.



a)

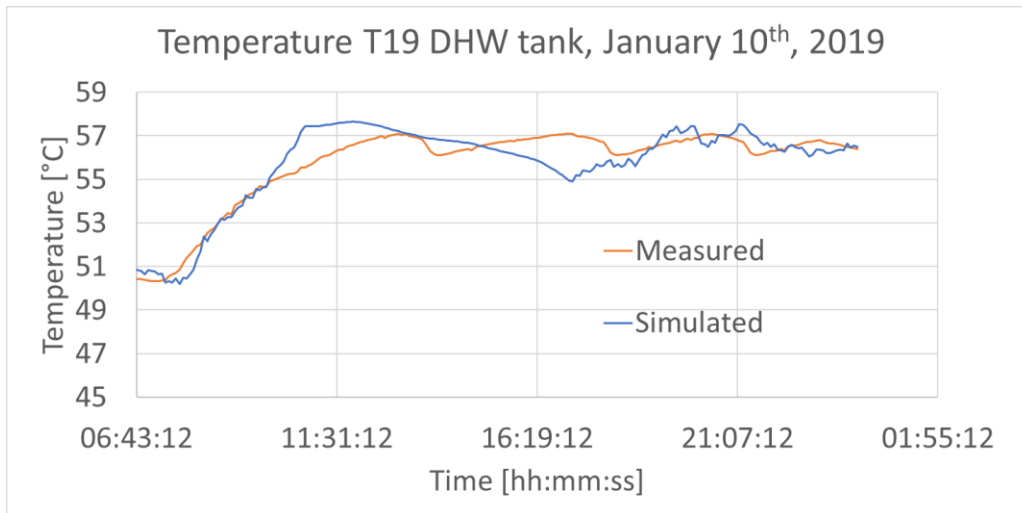


Figure 4. 32: simulated (blue line) and measured (orange line) trends for T14 a) and T19 b)

b)

Solar Assisted Heat Pump Integrated with Solar Panels – SAHP - PVT

This section presents the model layout, obtained by means of the union of the different subsystems validated before. The connection pipes between the solar field and the boiler room have been inserted by means of TRNSYS Type 31. This element simulates the behaviour of a fluid flowing inside a pipe, with specific attention to the thermal losses. As concerns the simulations reported in this section, the global thermal loss of the pipes will be set equal to zero, to reproduce the design assumption of negligible thermal losses. Then, in the next chapter such assumption shall be removed and the difference between the two case studies will be compared. The other pipes have been neglected, since their path is within either the boiler room or the heated volume.

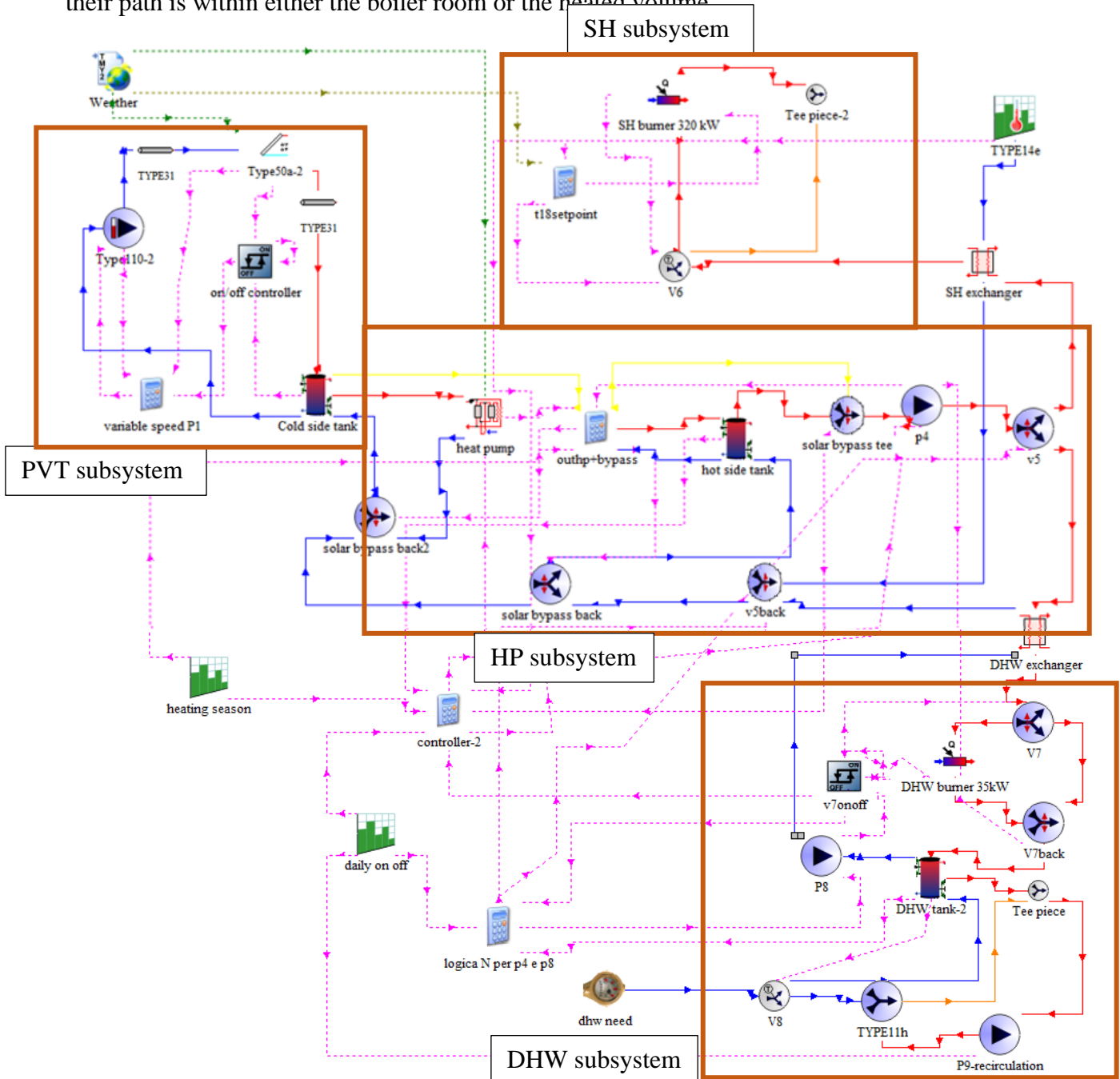


Figure 4. 33: complete overview of the plant layout modelled in TRNSYS environment. Please refer to the subsystems illustrated before for a better insight into the plant as a whole. Colour code: dotted pink line – control/logical connection; red line – hot water pipes; blue line – cold water pipes; dotted green line – weather connection

Table 4. 3 reports the comparison between the design values (already presented in Table 3. 5) and the results of the numerical validation carried out by means of the TRNSYS numerical model (Figure 4. 33):

| | Primary energy need (SH radiators + DHW) [kWh] | | SAHP-PVT [kWh] | | Electrical consumption SAHP-PVT [kWh] | | integration burner - SH [kWh] | | integration burner - DHW [kWh] | | PV production – [kWh] | |
|----------|--|-------|----------------|-------|---------------------------------------|------|-------------------------------|-------|--------------------------------|-------|-----------------------|-------|
| | Sim | Des | Sim | Des | Sim | Des | Sim | Des | Sim | Des | Sim | Des |
| J | 12118 | 11870 | 3202 | 3108 | 821 | 863 | 7414 | 7873 | 1502 | 889 | 1577 | 1029 |
| F | 10281 | 10721 | 3322 | 3476 | 856 | 964 | 5861 | 6000 | 1098 | 1245 | 1583 | 1405 |
| M | 10965 | 11240 | 5107 | 5210 | 1131 | 762 | 4735 | 4141 | 1123 | 1889 | 2580 | 2328 |
| A | 6178 | 5744 | 3229 | 3147 | 561 | 427 | 1456 | 2003 | 1493 | 593 | 2339 | 2298 |
| M | 3174 | 2968 | 1169 | 1626 | 132 | 221 | 0 | 0 | 2005 | 1342 | 2598 | 2877 |
| J | 2950 | 2872 | 1266 | 1574 | 137 | 213 | 0 | 0 | 1684 | 1298 | 2590 | 2359 |
| J | 2845 | 2968 | 1697 | 1574 | 168 | 583 | 0 | 0 | 1148 | 1394 | 2970 | 2683 |
| A | 3032 | 2968 | 1524 | 1626 | 157 | 221 | 0 | 0 | 1508 | 1342 | 2656 | 2901 |
| S | 3059 | 2872 | 1116 | 1574 | 124 | 213 | 0 | 0 | 1943 | 1298 | 2290 | 2134 |
| O | 3329 | 2968 | 540 | 1205 | 84.9 | 211 | 0 | 0 | 2789 | 1763 | 1589 | 1547 |
| N | 8827 | 9987 | 3418 | 3889 | 851 | 1080 | 4464 | 4910 | 946 | 1188 | 1442 | 1082 |
| D | 11359 | 11870 | 3141 | 3235 | 748 | 898 | 6870 | 7685 | 1348 | 950 | 1392 | 967 |
| Total | | | | | | | | | | | | |
| | 78118 | 79048 | 28731 | 31244 | 5771 | 6656 | 30800 | 32612 | 18587 | 15191 | 25606 | 23610 |

Table 4. 3: comparison between simulated (Sim) and design (Des) monthly performances

Some observations can be drawn:

- *Primary energy need*: the yearly performance differs for less than 1% with a very good agreement between design and numerical simulation as also shown in Figure 4. 34. The differences between the monthly values are mainly due to the different contributions of the SAHP-PVT and the integration gas burners as better outlined as follows. Concerning the months with only DHW need, the variation in the required primary energy is caused by two main aspects: the thermal losses of the 3000 l tank towards the environment (boiler room) and the different contribution of the integration gas burner which determines a higher required primary energy due to a lower generation efficiency (about 0.8/0.85).

- *SAHP-PVT*: the energy provided by the SAHP-PVT in the simulations is about 8% lower than the design value. In particular, the largest variations occur during the months out of the heating season (Figure 4. 35), when the bypass is on and the HP is not active. In fact, the values reported in the simulation columns when the bypass is active are computed basing only on the energy effectively delivered by the solar thermal field. Therefore, the distribution of the DHW need over the reference day does influence the actual productivity of the solar bypass. Such aspect could not be noticed in the design calculations since the normative approach does not account for any eventual time shift between solar availability and energy need. Considering the global yearly performance, the total energy delivered by the SAHP-PVT of 28.731 kWh against a total electrical consumption of 5771 kWh leads to a yearly COP of about 5. Given that the yearly COP basing on the design information was of about

4.7 (section 3.1.5), the transient simulation has led to a better approximation of the coefficient (7% increase).

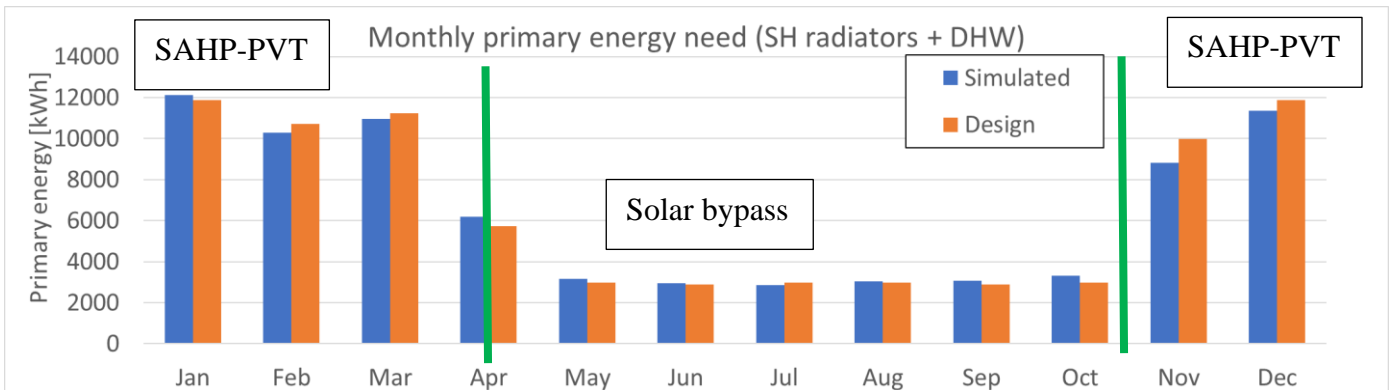


Figure 4. 34: Monthly primary energy need, simulated (blue) and design (orange) values

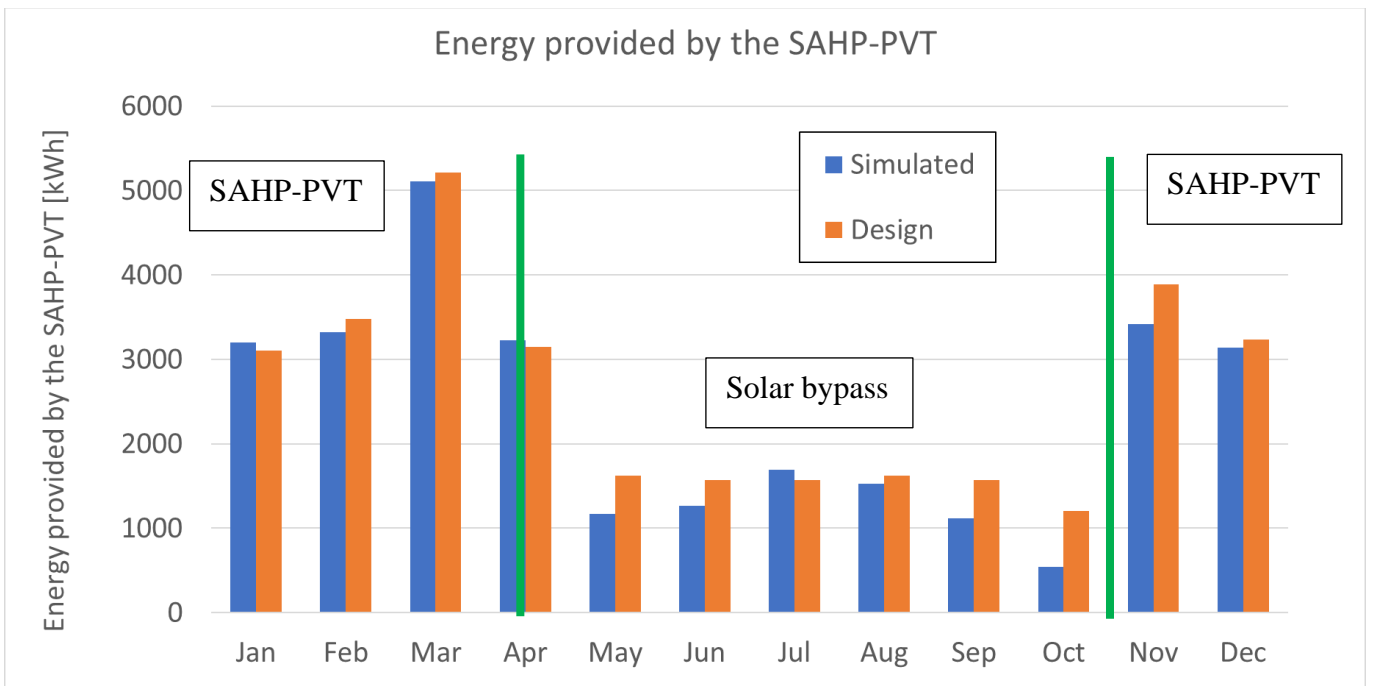


Figure 4. 35: Monthly thermal energy delivered by the SAHP-PVT (including the solar bypass), simulated (blue) and design (orange) values

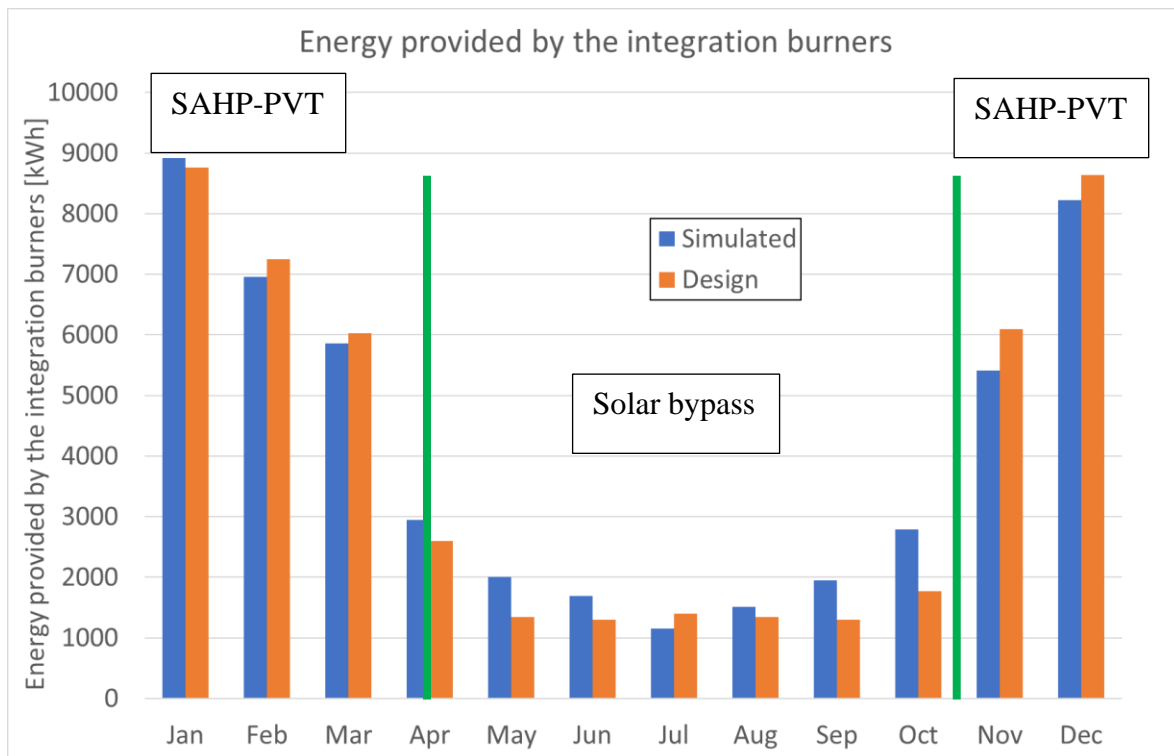


Figure 4. 36: Monthly thermal energy delivered by the integration gas burners (both SH and DHW), simulated (blue) and design (orange) values

- *Electrical consumption*: the difference of about 13% is associated to two main reasons: firstly, the design assumed a fixed COP during the heating season of 3.6 (simplification on the safe side) while the real performances of the installed HP have been implemented in the TRNSYS model (variable HP-COP during the heating season, between 3.6 and 3.9). Secondly, the electrical consumption out of the heating season is mainly due to the circulation pumps of the bypass. According to the carried-out simulations, their activation period (and consumption) is shorter because of the time shift between DHW need and solar availability. This issue has been already discussed in the previous point about the primary energy need.

- *Integration gas burners (DHW+SH)*: the simulated results are in good accordance with the design ones. Concerning the DHW, the increase (about 15%) is due to the major contribution required to the integration burner caused by the occurrence of relevant DHW withdrawals in the evening as well. The distinction between the DHW and SH gas burners also validates the working of valve V5, which preferably sends the hot water produced by means of the SAHP-PVT to the DHW and then to the SH subsystem.

- *PV production*: an increase of about 8% can be appreciated and it is linked to the variation of the input weather information. In fact, the previous validations were run considering the same, recorded weather conditions in order to make the simulated results comparable to the measured ones. The design values reported in Table 4. 3 have been obtained by means of standard, simplified weather information according to the installation site. On the other hand, the weather simulator in TRNSYS bases on the historical time series of irradiation, temperature, humidity, precipitation and wind, even extrapolating to get values of extreme. As a consequence, a slight variation from the design values is to be expected. For any further and more specific validation of the PV panels, please reference to Figure 4. 2 and the related paragraph.

5. Optimization simulations to the SAHP-PVT pilot plant at Palacus and possible interventions

The present chapter will deal with the optimisation simulations carried out by means of the validated model, evaluating the best interventions to increase the plant efficiency. The following table resumes both the investigated elements and the criteria which led to their choice for the optimisation analyses:

| Criteria | Chosen elements for efficiency simulations |
|---|---|
| Improve the plant efficiency, firstly acting on inadequate elements | Insulation of the connection pipes between the HP and the solar field |
| Increase the contribution of the renewable part of the plant, reducing the intervention of the gas burners as much as possible. | Changes in the regulation criteria to exploit the SAHP during Autumn and Spring |
| Maximise the on-site exploitation of the PVT field, independently from the current policies | Strategies to increase the self-consumption of the photovoltaic production |
| Estimate the SAHP potentials according to the installation site | Performances of the SAHP-PVT at different locations |

Table 5. 1: adopted criteria and chosen elements for efficiency simulation.

The first three points are more concerned with the specific plant outline, while the last one aims at a more general focus to help the diffusion of the technology over the territory.

In addition, the simulated interventions mainly involve different elements of the solar field (i.e., connection pipes and solar panels) since their revamping is under study, due to some leakages and general aging occurred in the past years.

The simulated interventions influence the optimisation process allowing a preliminary evaluation of the benefits, not only related to the substitution of the components, but also to different regulation criteria. For the first three proposed case studies, a brief cost-benefit analysis supports the technical results.

The carried-out results were performed both to study the plant efficiency from an academic point of view and to provide the technical committee in charge with the most effective actions for the plant revamping design.

5.1 Influence of the thermal losses due to the pipes connecting the solar field to the boiler room

The model in *Figure 4. 33* has been run over the reference year, adding the thermal losses of the connection pipes between the solar field and the HP/boiler room. The main results are resumed in *Table 5. 2*. For the following chapter, the case of highly insulated pipes shall be referred to “no pipes” or “insulated pipes”. In fact, the case limit of a very high level of insulation is an adiabatic element/ an element with negligible thermal losses. On the other hand, the term “pipes” or “not insulated pipes” will refer to the current plant layout where the connection pipes are not insulated.

| | Primary energy need (SH radiators + DHW) [kWh] | | SAHP-PVT [kWh] | | Electrical consumption SAHP-PVT [kWh] | | integration burner – SH [kWh] | | integration burner – DHW [kWh] | |
|----------|--|--------------|----------------|--------------|---------------------------------------|-------------|-------------------------------|--------------|--------------------------------|--------------|
| | No pipes | Pipes | No pipes | Pipes | No pipes | Pipes | No pipes | Pipes | No pipes | Pipes |
| J | 12118 | 11987 | 3202 | 3398 | 821 | 842 | 7414 | 7134 | 1502 | 1455 |
| F | 10281 | 10192 | 3322 | 3458 | 856 | 823 | 5861 | 5667 | 1098 | 1067 |
| M | 10965 | 11093 | 5107 | 4924 | 1131 | 1102 | 4735 | 4996 | 1123 | 1173 |
| A | 6178 | 6500 | 3229 | 2950 | 561 | 532 | 1456 | 1855 | 1493 | 1695 |
| M | 3174 | 3393 | 1169 | 657 | 132 | 137 | 0 | 0 | 2005 | 2736 |
| J | 2950 | 3086 | 1266 | 948 | 137 | 140 | 0 | 0 | 1684 | 2138 |
| J | 2845 | 3018 | 1697 | 1294 | 168 | 151 | 0 | 0 | 1148 | 1724 |
| A | 3032 | 3312 | 1524 | 871 | 157 | 154 | 0 | 0 | 1508 | 2441 |
| S | 3059 | 3181 | 1116 | 831 | 124 | 124 | 0 | 0 | 1943 | 2350 |
| O | 3329 | 3421 | 540 | 325 | 85 | 99 | 0 | 0 | 2789 | 3096 |
| N | 8828 | 8594 | 3418 | 3764 | 851 | 931 | 4464 | 3970 | 946 | 860 |
| D | 11359 | 11320 | 3141 | 3200 | 748 | 767 | 6870 | 6786 | 1348 | 1334 |
| Total | | | | | | | | | | |
| | 78118 | 79097 | 28731 | 26620 | 5771 | 5802 | 30800 | 30408 | 18587 | 22069 |

Table 5. 2: comparison of monthly performances with/without the connection pipes between the solar field and the boiler room

The contribution of the pipes plays both a negative and a positive role on the yearly plant performance:

- during the heating season, the energy delivered by the SAHP-PVT increases, since a little amount of thermal energy is collected by the pipes from the surrounding external environment (air+ground), which acting as an additional heat source. This in turn determines a higher temperature on the evaporator side with better performances (*Figure 5. 1*). Such improvement is more relevant in the coldest months when the water inside the circuit is more likely to be colder than the outside. Anyway, this improvement is not relevant, since the sum of the delivered thermal energy of the SAHP-PVT during only the heating season (January, February, March, part of April, November and December) increases of about 2% with respect to the case with insulated pipes.

- out of the heating season and especially during summer, the solar panels work with a high set point temperature (about 45 °C), since the bypass is active. This implies a higher difference in temperature between the water inside the pipes and the external, with not negligible thermal losses. Indeed, when the bypass is active, the monthly delivered thermal energy is about 60% of the one obtained assuming negligible thermal losses as shown in *Figure 5. 1*.

Energy provided by the SAHP-PVT

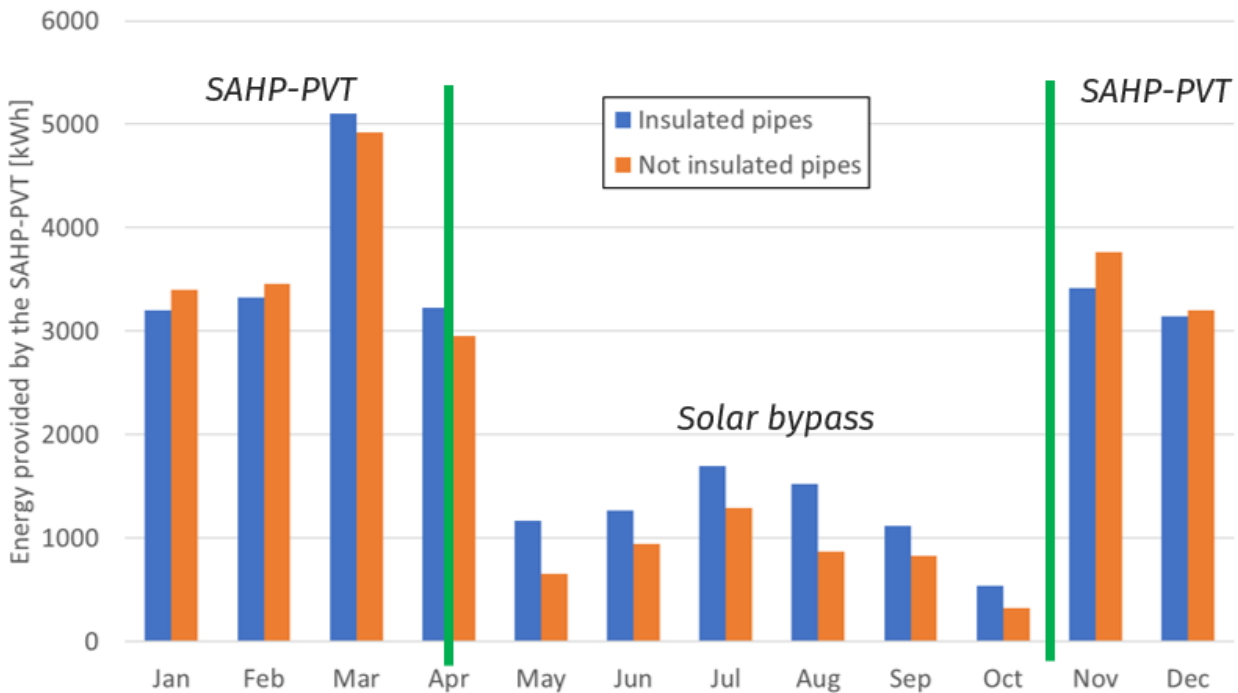


Figure 5. 1: comparison of the monthly thermal energy delivered by the SAHP in the case of insulated connection pipes (blue, negligible thermal losses) and not insulated (orange)

With respect to the yearly balance, the absence of insulation in the connection pipes causes a reduction of about 10% of the thermal energy produced by the SAHP-PVT (26.620 kWh against 28.731 kWh). Indeed, the total value of 28.731 kWh represents a limit case, obtained neglecting the connection pipes (i.e., considering the pipes as adiabatic). This variation determines an increase in the primary energy as well, since the integration gas burners have to provide about 2000 kWh of additional useful thermal energy, with a lower generation efficiency.

This means that the assumption of negligible thermal losses can be considered acceptable only during the heating season when the effect of insulation determines a variation of only 2% in the SAHP production.

On the other hand, every time the solar bypass is activated, the thermal losses become relevant, leading to an overestimation of the monthly produced thermal energy of about 60%.

On the photovoltaic side, the presence of insulation increases the working temperatures of the panels, with a decrease in the generation efficiency, as shown in Table 5. 3 and Figure 5. 2.

| PV production [kWh] | | |
|----------------------------|-----------------|---------------------|
| Month | insulated pipes | not insulated pipes |
| January | 1577 | 1626 |
| February | 1583 | 1611 |
| March | 2580 | 2567 |
| April | 2339 | 2581 |
| May | 2598 | 2718 |
| June | 2590 | 2691 |
| July | 2970 | 3071 |
| August | 2656 | 2755 |
| September | 2290 | 2383 |
| October | 1589 | 1678 |
| November | 1442 | 1549 |
| December | 1392 | 1431 |
| Total | 25606 | 26661 |

Table 5. 3: monthly electric production of the hybrid field with/without pipes insulation

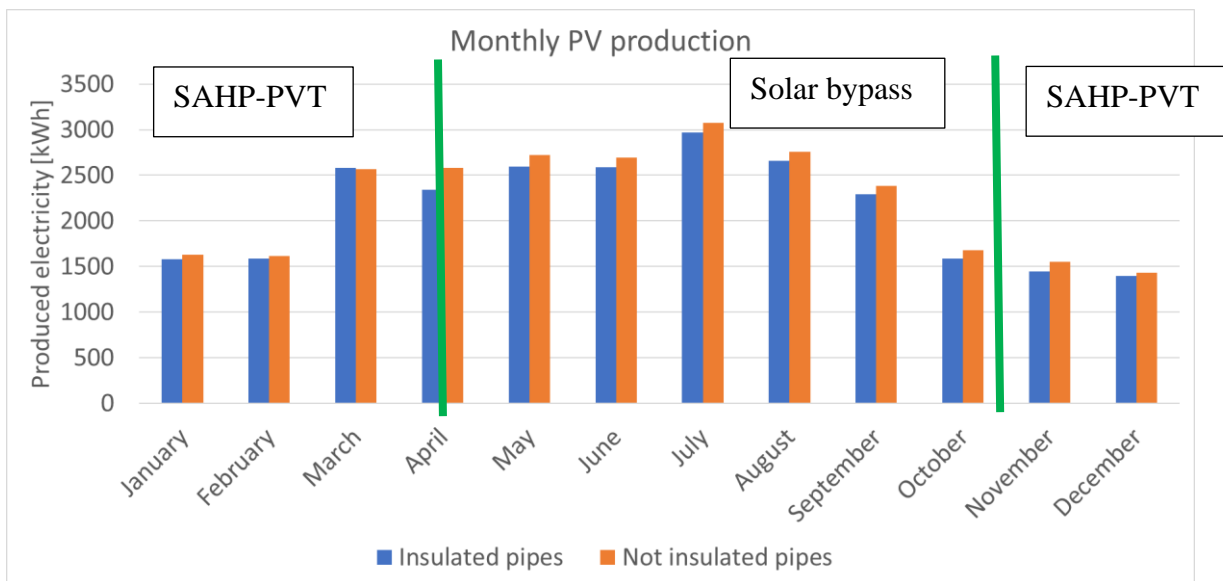


Figure 5. 2: comparison of the monthly PV production with insulated and not insulated pipes

The absence of insulation increases the annual production of about 1055 kWh (4%): the added thermal losses along the pipes contribute to maintain a lower working temperature at the panel with a benefit on the generation efficiency. This effect can be noticed all year long, especially during the ones out of the heating season, when the working temperature is likely to be higher.

From the economic point of view the following conclusions can be drawn

- Thermal side: the insulation of pipes can lead to an increase of about 2000 kWh_T/year by means of the SAHP-PVT. To estimate the correspondent saving, if the integration gas burner (efficiency

of about 0.8) had to provide the same energy, it would roughly require 2500 kWh, with a cost of 625 € (assumed unitary price of 0.25 €/kWh_T).

- PV side: the insulation increases the working temperature of the hybrid panels with a consequent reduction of their efficiency. The decrease is estimated in about 1055 kWh_E/year. Assuming a unitary price of 0.5 €/kWh_E, this would mean the loss of about 530 €, under the assumption of almost total self-consumption of the photovoltaic production.

So, the insulation of the connection pipes presents a cost-effectiveness which is variable according to the percentage of on-site consumption of the produced electricity.

Concerning the case study under analysis and the issue of the efficient management of a PV/PVT solar field (*please, see section 3.3.4 for an introduction on the topic and section 5.3 for a detailed analysis on the topic*), the actual plant layout and electrical consumption profile is not likely to truly benefit of the increased PV production, so the insulation of the connection pipes has been recommended to the Technical Committee in charge of the plant revamping as well.

In addition, the cost of the intervention should mainly depend only on the insulating materials, since the pipes run either in open air or in a crawlspace so no additional costs for excavations are to be expected. This intervention is still under design, so the next simulations will be referred to the actual state of the plant with not insulated pipes.

5.2 Changes in the regulation criteria to best exploit the SAHP-PVT

The results reported in *Figure 5. 1* allow a further study about the regulation criteria to best exploit the SAHP-PVT without any change into the plant layout.

Table 5. 4 reports the percentual coverage of the primary need by means of SAHP-PVT (including bypass) for the different months considering both insulated and not insulated pipes. Such results are referred to the current regulation criteria which force the switch off of the HP and the activation of the solar bypass as the heating season ends.

During the heating season, the SAHP covers about 30% of the total monthly need, while out of the heating season, the percentage varies from 30% up to 50% during the middle of summer.

Anyway, the contribution of the solar bypass is very low in October (about 10-15%). During April, the coverage (52%) seems comparable with the one of March (47%); actually, if the monthly value is split into the contributions of the SAHP (2695 kWh) and the bypass (534 kWh), it is clear that about 80% of the production during April is reached within the very first 15 days, when the HP is still on. Such estimation increases up to the 90% if the absence of pipes insulation is accounted. More in general, the monthly production associated to the solar bypass is about half of the thermal energy delivered by the solar assisted heat pump.

| | Primary energy need (SH radiators + DHW) [kWh] | | SAHP-PVT [kWh] | | % total need covered by means of SAHP/bypass | |
|---------------------|--|---------------------------|--------------------|---------------------------|---|------------------------|
| | Insulated pipes | Not insulated pipes | Insulated pipes | Not insulated pipes | Insulated pipes | Not insulated pipes |
| January | 12118 | 12028 | 3202 | 3398 | 26% | 28% |
| February | 10281 | 10192 | 3322 | 3458 | 32% | 34% |
| March | 10965 | 10320 | 5107 | 4924 | 47% | 48% |
| April, 1-15 | 6178 | 5700 | 2695 | 2719 | 52% | 52% |
| April, 15-30 | | | 534 | 231 | | |
| May | 3174 | 3140 | 1169 | 657 | 37% | 21% |
| June | 2950 | 2907 | 1266 | 948 | 43% | 33% |
| July | 2845 | 2991 | 1697 | 1294 | 60% | 43% |
| August | 3032 | 3140 | 1524 | 871 | 50% | 28% |
| September | 3059 | 2954 | 1116 | 831 | 36% | 28% |
| October | 3329 | 3118 | 540 | 325 | 16% | 10% |
| November | 8828 | 8895 | 3418 | 3764 | 39% | 42% |
| December | 11359 | 11082 | 3141 | 3200 | 28% | 29% |

Table 5. 4: primary energy need, energy provided by the SAHP-PVT and the percentual coverage in the case of insulated and not insulated pipes

As illustrated before, this issue is due to the occurrence of relevant DHW withdrawals when there is not enough solar radiation to produce DHW. In addition, the solar radiation available during the day in October or April is low if compared to months such as June or July.

As a consequence, the validated numerical model has been used to enquire the benefits deriving from the activation of the SAHP even out of the heating season.

Table 5. 5 highlights that the switch on of the HP is convenient only in October and April: indeed, during these months, the temperature within the tank between the solar field and the HP remains below 25 °C, granting the optimal working range of the HP without the activation of the solar bypass. During the other months, the simulated values fluctuate around the ones reached by means of the bypass from May to September, because of the high temperature in the solar circuit, which is very likely to enable the solar bypass, making the HP work occasionally. Besides of the missing increase in the produced thermal energy, the HP is subjected to almost continuous on/off during these months, which results unacceptable from an operational point of view. In fact, the chances of a block or failure in the machine become higher as the result of continuous stich on and off.

In conclusion, the activation of the HP even out of the heating season results highly recommendable only in October and April, representing the months in which the still low temperature and low solar radiance make the use of the solar bypass not convenient. For what concerns the other months out of the heating season, the solar bypass should be enabled as default, since the HP is very likely to be switched off due to the high temperatures within the boiler between the solar field and the HP.

| Months | Bypass on [kWh] | | SAHP on [kWh] | |
|---|-----------------|---------------------|-----------------|---------------------|
| | Insulated pipes | Not insulated pipes | Insulated pipes | Not insulated pipes |
| April, 15th-30th | 534 | 231 | 2389 | 1658 |
| May | 1169 | 657 | 1222 | 684 |
| June | 1266 | 948 | 1241 | 894 |
| July | 1697 | 1294 | 1714 | 1200 |
| August | 1524 | 871 | 1463 | 851 |
| September | 1116 | 831 | 1161 | 789 |
| October | 540 | 325 | 3199 | 2899 |
| Total | 7846 | 5157 | 12389 | 8975 |

Table 5. 5: comparison of the solar bypass with the SAHP from April up to October

The simulations have been run considering both insulated and not insulated pipes, as shown in Table 5. 5:

- with reference to the case with the solar bypass on, the insulation can increase up to 45% the delivered thermal energy (i.e., during August), since the operating temperature of about 40-50 °C increases the thermal losses

- when considering the case of SAHP on, the improvement associated to insulated pipes is of 35% for two reasons: during October and April, the HP is on, so the thermal losses are likely to be reduced because of the lower difference in temperature between the water inside the circuit and the external air. Secondly, the insulation determines a faster heating of the solar tank from May up to September, anticipating the activation of the solar bypass, even reducing the activation period of the HP.

Table 5. 6 concerns the cost estimation using the SAHP instead of the solar bypass. The first two columns show the additional thermal energy produced by means of the SAHP assuming insulated and not insulated pipes (taken from Table 5. 5). Then columns 3 and 4 report the electrical consumption of the SAHP while n. 5 and 6 the correspondent estimation assuming a unitary price of 0.5 €/kWh_E.

| Column | Additional thermal energy provided by the SAHP (values shown in Table 5. 5) [kWh] | | Electricity consumed [kWh] | | Cost [€] – assumed unitary price 0.5 €/kWh | |
|---|---|-----------------|----------------------------|---------------------|--|-----------------|
| | 1 | 2 | 3 | 4 | 5 | 6 |
| | Insulated pipes | Insulated pipes | Insulated pipes | Not insulated pipes | Insulated pipes | Insulated pipes |
| April, 15th-30th | 2389-534 = 1855 | 1658-231 = 1427 | 461 | 342 | 231 | 171 |
| October | 3199-40 = 2659 | 2899-325 = 2574 | 668 | 630 | 334 | 315 |
| Total | 4514 | 4001 | 5667 | 5106 | 565 | 486 |

Table 5. 6: estimation of the achievable savings – case of SAHP + burner on

On the other hand, *Table 5. 7* shows the cost estimation considering the solar bypass on. In this case, the gas burners have to cover the additional thermal energy which is no longer produced by the SAHP. The values in columns a and b are linked to the columns 1 and 2 assuming a gas burner generation efficiency of about 0.8. Columns c and d approximate the cost assuming a unitary price of 0.2 €/kWh_T.

| Column | Thermal energy no more provided by the SAHP (values shown in Table 5. 5 and 5.5) [kWh] | | Energy required to the gas burners [kWh] | | Cost [€] – assumed unitary price 0.2 €/kWh | |
|---|--|-----------------|--|---------------------|--|-----------------|
| | 1 | 2 | a | b | c | d |
| | Insulated pipes | Insulated pipes | Insulated pipes | Not insulated pipes | Insulated pipes | Insulated pipes |
| April, 15th-30th | 2389-534 = 1855 | 1658-231 = 1427 | 2310 | 1790 | 462 | 358 |
| October | 3199-40 = 2659 | 2899-325 = 2574 | 3357 | 3315 | 671 | 663 |
| Total | 4514 | 4001 | 5667 | 5105 | 1133 | 1021 |

Table 5. 7: estimation of the achievable savings – case of bypass + burner on

In conclusion, the comparison of *Table 5. 6* and *Table 5. 7* leads to a yearly saving of about 500 €, thanks to this modification in the plant regulation criteria, without any additional expense. So, the DAS has been already updated to keep the SAHP on even during April and October.

5.3 Strategies to maximize the self-consumption of the photovoltaic field

The numerical transient model validated on the real working of the pilot plant allows further considerations about the effective management of the PVT field. In fact, the comparison among the self-consumed electricity, the overproduction and the additional withdrawals from the national grid can be performed at each time step (*Table 5. 8*).

The results in *Table 5. 8* highlight that the total consumption of the SAHP (6030 kWh) cannot be covered by means of the PV field (26661 kWh) although both the annual and the monthly productions are higher than the related consumptions. In fact, part of the daily SAHP consumption profile occurs when the solar radiation is either low or unavailable, requiring an integration from the national grid (about 30% of the annual energy for the SAHP – 1864 kWh). The table also shows that the months with higher PV production are linked to very low consumptions: for instance, the solar bypass is active during summer and the only consumption of the solar circulating pumps is accounted, since the heat pump is off.

Actually, the current results neglect the electric need of the other devices within the boiler room (mainly the other circulating pumps) which roughly increase the total consumption (6030 kWh) of 25-30%. Anyway, there is still a relevant amount of produced electricity which is substantially lost, even accounting these additional consumptions. In fact, the electricity immitted into the national grid has no specific refund or incentive currently (*please, see paragraph 3.3.4 for further information*).

| Month | PV production [kWh] | Electric consumption – SAHP [kWh] | Self-consumption [kWh] | Additional withdrawal from the national grid [kWh] | Photovoltaic overproduction [kWh] |
|------------------|---------------------|-----------------------------------|------------------------|--|-----------------------------------|
| January | 1626 | 858 | 567 | 291 | 1059 |
| February | 1611 | 858 | 567 | 291 | 1059 |
| March | 2567 | 840 | 510 | 330 | 1101 |
| April | 2581 | 1125 | 670 | 455 | 1897 |
| May | 2718 | 558 | 558 | 0 | 2023 |
| June | 2691 | 151 | 151 | 0 | 2567 |
| July | 3071 | 152 | 152 | 0 | 2539 |
| August | 2755 | 176 | 176 | 0 | 2895 |
| September | 2383 | 169 | 169 | 0 | 2586 |
| October | 1678 | 146 | 146 | 0 | 2237 |
| November | 1549 | 123 | 123 | 0 | 1555 |
| December | 1431 | 950 | 488 | 462 | 1061 |
| Total | 26661 | 6030 | 4166 | 1864 | 22495 |

Table 5. 8: main results of the performance of the PVT coupled to the SAHP

Considering a unitary price of 0.5 €/kWh_E, the produced and not used energy (about 20.000 kWh/year) could mean an annual saving of 10 k€ or even more. So, according to the carried-out analyses, the PVT field does represent the less efficient subsystem of the pilot plant, where there is more room for improvement.

Basing on the writer's experience, the plant efficiency should not depend on incentives and policies to help the diffusion of the solar fields, due to their low reliability and continuous change. So, the only effective strategies concern the increase of the on-site consumption, either with batteries or including other energy consuming services or both. These main strategies are better enquired as follows:

- *Implementation of batteries to fully cover the energy need of the SAHP:* as limit case, this intervention would allow to cover the withdrawals from the grid of about 1864 kWh_E/year. Considering the carried-out numerical simulations (Table 5. 8), about 300-400 kWh_E are taken from the grid every month, with a daily average consumption of about 10-15 kWh_E. So, the implementation of batteries with a total capacity of about 20 kWh_E could be considered to reach the almost total coverage of the SAHP electric need by means of the PV field. On the economic side, the maximum saving of 1864 kWh_E means about 932 €/year (unitary price of 0.5 €/kWh_E). On the other hand, the current cost of the batteries available on the market is of about 1000 €/kWh_E. This means that the integration of batteries would require an initial installation cost of 20 k€. As a consequence, the simple payback time would result in about 20 years, showing the lack of convenience, since the useful lifespan of the batteries is up to now of just 10 years.
- *Extension of the energy-intensive devices connected to the bidirectional meter:* the sport palace is provided with many energy-intensive services, such as the lighting of the outdoor courts or the AHU under revamping which could benefit from the PV production. Actually, the DAS is not connected with the entire sport palace, so the only information about the total electrical need of the facility has been collected by means of the energy bills. In fact, both the DAS and the PVT

field were conceived in the original design to be exclusively connected to the SAHP which would have represented an independent element within the sport palace. *Table 5. 9* shows the monthly consumption of the facility divided into three time slots which are defined in *Figure 5. 4*.

| Month | Total electric consumption [kWh] | Electric consumption during F1 [kWh] | Electric consumption during F2 [kWh] | Electric consumption during F3 [kWh] | Monthly peak power [kW] |
|--------|----------------------------------|--------------------------------------|--------------------------------------|--------------------------------------|-------------------------|
| dec-17 | 10714 | 4214 | 3151 | 3349 | 38 |
| jan-18 | 14910 | 5744 | 3826 | 5340 | 37.6 |
| feb-18 | 13665 | 5294 | 4006 | 4365 | 36.8 |
| mar-18 | 14373 | 4667 | 4578 | 5128 | 34 |
| apr-18 | 14477 | 4016 | 3734 | 6727 | 32 |
| may-18 | 13252 | 3872 | 3725 | 5655 | 40 |
| jun-18 | 7814 | 2049 | 2301 | 3464 | 26.8 |
| jul-18 | 9805 | 2524 | 2662 | 4619 | 20.4 |
| aug-18 | 4143 | 923.6 | 1273.4 | 1946 | 19.6 |
| sep-18 | 4138 | 807 | 1539 | 1792 | 16.4 |
| oct-18 | 5327 | 1467 | 1911 | 1949 | 18.8 |
| nov-18 | 8292 | 3404 | 2489 | 2399 | 34 |
| dec-18 | 10939 | 4233 | 3062 | 3644 | 37.6 |
| jan-19 | 12322 | 5674 | 3778 | 2870 | 37.6 |
| feb-19 | 13451 | 6351 | 3726 | 3374 | 48.4 |
| mar-19 | 10963 | 4592 | 3409 | 2962 | 33.2 |
| apr-19 | 12021 | 4741 | 3222 | 4058 | 31.6 |
| may-19 | 16351 | 5483 | 4408 | 6460 | 40.4 |
| jun-19 | 16272 | 5287 | 4248 | 6737 | 29.6 |
| jul-19 | 16258 | 5730 | 4010 | 6518 | 30.4 |
| aug-19 | 2961 | 1037 | 839 | 1085 | 19.2 |
| sep-19 | 8081 | 2898 | 2277 | 2906 | 16.4 |
| oct-19 | 18143 | 6462 | 4833 | 6848 | 36 |
| nov-19 | 17638 | 5975 | 4724 | 6939 | 35.6 |
| dec-19 | 15266 | 5357 | 3891 | 6018 | 39.2 |
| jan-20 | 11177 | 5410 | 3255 | 2512 | 38 |
| feb-20 | 13887 | 5834 | 4680 | 3373 | 38.4 |
| mar-20 | 9179 | 3564 | 2790 | 2825 | 32.4 |
| apr-20 | 9665 | 3758 | 2715 | 3192 | 25.6 |

Table 5. 9: total electrical need of the Palacus sport palace, information taken from the energy bills

The considered period starts from December, 2018 up to April, 2020. Then no more recent information has been considered since it was influenced from the Covid restrictions and it would have led to a misleading characterisation of the electric need of the facility.

The same results have been plotted in *Figure 5. 3* for a clearer view of the electric need during the different months and the periods over the day (time slots F1, F2, F3).

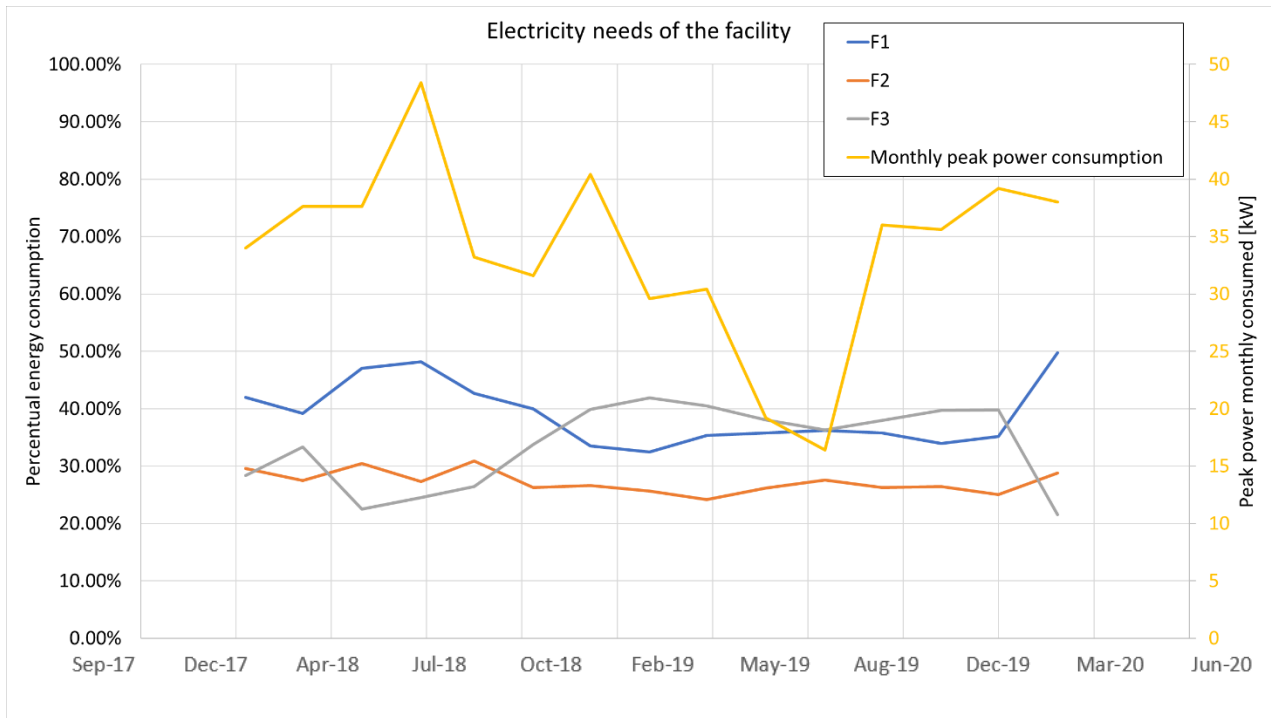


Figure 5. 3: percentual electric consumption during different time slots as outlined in Figure 5. 4 (left axis plot) and monthly peak absorbed power (yellow – right axis plot)

| Days/Time | 0 | 1 | 2 | 3 | 4 | 5 | 6 | 7 | 8 | 9 | 10 | 11 | 12 | 13 | 14 | 15 | 16 | 17 | 18 | 19 | 20 | 21 | 22 | 23 |
|------------------|----|----|----|----|----|----|----|----|----|----|----|----|----|----|----|----|----|----|----|----|----|----|----|----|
| Monday | F3 | F3 | F3 | F3 | F3 | F3 | F3 | F2 | F1 | F1 | F1 | F1 | F1 | F1 | F1 | F1 | F1 | F1 | F1 | F2 | F2 | F2 | F2 | F2 |
| Tuesday | F3 | F3 | F3 | F3 | F3 | F3 | F3 | F2 | F1 | F1 | F1 | F1 | F1 | F1 | F1 | F1 | F1 | F1 | F1 | F2 | F2 | F2 | F2 | F2 |
| Wednesday | F3 | F3 | F3 | F3 | F3 | F3 | F3 | F2 | F1 | F1 | F1 | F1 | F1 | F1 | F1 | F1 | F1 | F1 | F1 | F2 | F2 | F2 | F2 | F2 |
| Thursday | F3 | F3 | F3 | F3 | F3 | F3 | F3 | F2 | F1 | F1 | F1 | F1 | F1 | F1 | F1 | F1 | F1 | F1 | F1 | F2 | F2 | F2 | F2 | F2 |
| Friday | F3 | F3 | F3 | F3 | F3 | F3 | F3 | F2 | F1 | F1 | F1 | F1 | F1 | F1 | F1 | F1 | F1 | F1 | F1 | F2 | F2 | F2 | F2 | F2 |
| Saturday | F3 | F3 | F3 | F3 | F3 | F3 | F3 | F2 | F2 | F2 | F2 | F2 | F2 | F2 | F2 | F2 | F2 | F2 | F2 | F2 | F2 | F2 | F2 | F2 |
| Sunday | F3 | F3 | F3 | F3 | F3 | F3 | F3 | F3 | F3 | F3 | F3 | F3 | F3 | F3 | F3 | F3 | F3 | F3 | F3 | F3 | F3 | F3 | F3 | F3 |

Figure 5. 4: definition of the three different time slots F1, F2 and F3

Basing on the collected data reported above, the annual electric consumption of the facility is of about 120.000 kWh which are almost equally distributed over the three time slots (Figure 5. 4). It can be noticed that F1 identifies the part of the day with daylight, besides of holydays, Saturdays and Sundays which fall either in F2 or F3. So, during F1, the self-consumption of the produced electricity is very likely and the electricity need varies from a maximum of 40-50% up to a minimum of 35% of the total monthly need (Figure 5. 3). This means that roughly one third of the average yearly need (namely 36000 kWh) would be very likely to be covered by means of the PV solar field, without the implementation of any battery.

Table 5. 10 resumes the achievable results split into the different months obtained from the connection of the PVT field to all the energy intensive services of the sport palace. With reference to Table 5. 10, the following remarks can be outlined:

- The PV production has been taken from the previous shown results;
- the column concerning the monthly consumption during F1 is the average of the same months of the different years (e.g., January is the average of January 2018, January 2019 and January 2020 etc.).

- The additional withdrawals from the national grid have been computed assuming that only 65% of the monthly need during F1 is covered by means of the PV field, to account for the consumptions occurring when the solar radiation is either low or unavailable.
- The overproduction is just the difference between the PV production and the self-consumed energy.

| Month | PV production [kWh] | F1 consumption (average of each month in Table 5. 9) - [kWh] | Additional withdrawal from the grid [kWh] | Overproduction [kWh] |
|--------------|---------------------|--|---|----------------------|
| January | 1626 | 5609 | 3983 | 0 |
| February | 1611 | 5826 | 4215 | 0 |
| March | 2567 | 4274 | 1707 | 0 |
| April | 2581 | 4172 | 1591 | 0 |
| May | 2718 | 4678 | 1960 | 0 |
| June | 2691 | 3668 | 1284 | 307 |
| July | 3071 | 4127 | 1444 | 388 |
| August | 2755 | 980 | 343 | 2118 |
| September | 2383 | 1853 | 649 | 1179 |
| October | 1678 | 3965 | 2287 | 0 |
| November | 1549 | 4690 | 3142 | 0 |
| December | 1431 | 4601 | 3170 | 0 |
| Total | 26661 | 48443 | 25775 | 3992 |

Table 5. 10: estimation of monthly electric self-consumption basing on the information within the energy bills and the PV production

With this configuration, only 15% of the produced electricity is sent to the national grid, while the remaining part is directly self-consumed. It can be noticed that a relevant lack of usage of the PV field occurs only during August and September. This is due to the fall in the consumption since the facility is almost closed or partially open because of the holidays. Therefore, the estimated percentage of 15% of overproduction is not likely to be further reduced, in absence of any relevant change in the consumption profile of the sport palace.

In conclusion, the facility consumption profile is very likely to self-consume the PV production. Basing on the preliminary estimations carried out on the safe side, about 25000 kWh_E are self-consumed every year, leading to about 12.5 k€ of savings (assumed 0.5€/ kWh_E).

Furthermore, the initial cost of this intervention is expected to be very low since just a change in the electric meter is needed, to connect all the electric utilities under the bidirectional meter of the PV field.

Therefore, the installation of batteries is not preliminary considered cost-effective, for the following reasons:

- High initial installation cost
- The almost total PV production is already self-consumed when it is produced

- The delivered power of the batteries is not suitable with the maximum monthly required power (right axis plot in *Figure 5. 3*), which is always not lower than 15 kW and it is on average 30 kW, unless an extended number of batteries is installed (negatively affecting their cost-effectiveness).

The results of these efficiency analyses were provided to the Technical Committee in charge of the plant revamping to identify an optimal management criterion to best exploit the existing installed solar field. More in general, many PV/PVT plants are experiencing the same problems after the abolition of the net metering and therefore the same approach adopted for the specific case study can be applied to other similar plants.

5.4 Performances of the SAHP-PVT at different climatic zones

The results reported up to now were drawn from the specific pilot plant, although the adopted approach and the main conclusions can be applied to other case studies. In this section, a more general approach is adopted, since the validated numerical model of the SAHP-PVT has been simulated at five different cities over Italy which represent the five main climatic zones (*Table 5. 11*). The target is to provide a preliminary assessment tool of the SAHP-PVT performance, varying the Degree Days (DD) of the installation site.

| Climatic zone | Degree Days | City |
|---------------|-------------|-----------|
| A | 568 | Lampedusa |
| B | 899 | Crotone |
| C | 1185 | Bari |
| D | 1435 | Genova |
| E | 2404 | Milano |

Table 5. 11: cities adopted to simulate the performance of the SAHP-PVT, with the correspondent Degree Days (DD) and climatic zones

The simulations have been run under the following assumptions:

- 1) The external weather has been extracted choosing climatic stations with shadings similar to the pilot plant at Genoa, to make the results comparable.
- 2) The DHW need has been considered as almost independent from the installation site. This assumption is correct since it mainly depends on the usage of the facility (*please, see paragraph 3.2.1 for further information*). Actually, the location might influence the thermal losses linked to the water storage, but this aspect has been already considered correlating the temperature of the boiler room to the external one, which varies according to the location.
- 3) The SH need has been considered as almost independent from the installation site. This assumption can be considered acceptable as a first approximation, since the SAHP provides only a preheating of the return water inside the radiator circuit, as previously described

(please, see paragraph 3.2.2 and Annex with the plant layout for further information). In addition, the SAHP-PVT was designed to provide thermal energy with priority to the DHW subsystem with respect to the SH.

- 4) According to the current working criterion, the SAHP is active during the heating season, while the solar bypass is enabled for the remaining part of the year. The beginning and end of the heating season according to the climatic zone are shown in Table 5. 12.

| Climatic zone | Beginning-end of the heating season |
|---------------|--|
| A | December, 1 st – March, 15 th |
| B | December, 1 st – March, 31 st |
| C | November, 15 th – March, 31 st |
| D | November, 1 st – April, 15 th |
| E | October, 15 th – April, 15 th |

Table 5. 12: duration of the heating season according to the climatic zone

Table 5. 13 resumes the total thermal energy delivered for each month at the different locations.

| | A - Lampedusa | B - Crotone | C - Bari | D - Genova | E - Milano |
|--------------|---------------|--------------|--------------|--------------|--------------|
| Jan | 4668 | 4213 | 4004 | 3398 | 1863 |
| Feb | 4393 | 4014 | 3690 | 3458 | 2513 |
| Mar | 2641 | 5299 | 5099 | 4924 | 4137 |
| Apr | 802 | 654 | 560 | 2950 | 2429 |
| May | 1131 | 1062 | 974 | 657 | 508 |
| Jun | 1284 | 1144 | 1110 | 948 | 730 |
| Jul | 1815 | 1696 | 1631 | 1294 | 983 |
| Aug | 1945 | 1856 | 1546 | 871 | 764 |
| Sep | 1385 | 1289 | 1185 | 831 | 395 |
| Oct | 1192 | 999 | 897 | 325 | 2328 |
| Nov | 764 | 293 | 2471 | 3764 | 2368 |
| Dec | 4838 | 4476 | 4086 | 3200 | 1411 |
| Total | 26858 | 26995 | 27253 | 26620 | 20429 |

Table 5. 13: monthly thermal energy produced by the SAHP-PVT (including the solar bypass) at the five cities

The results have been plotted when only the solar bypass is active (Figure 5. 5) and during the heating season when the SAHP is on (Figure 5. 6).

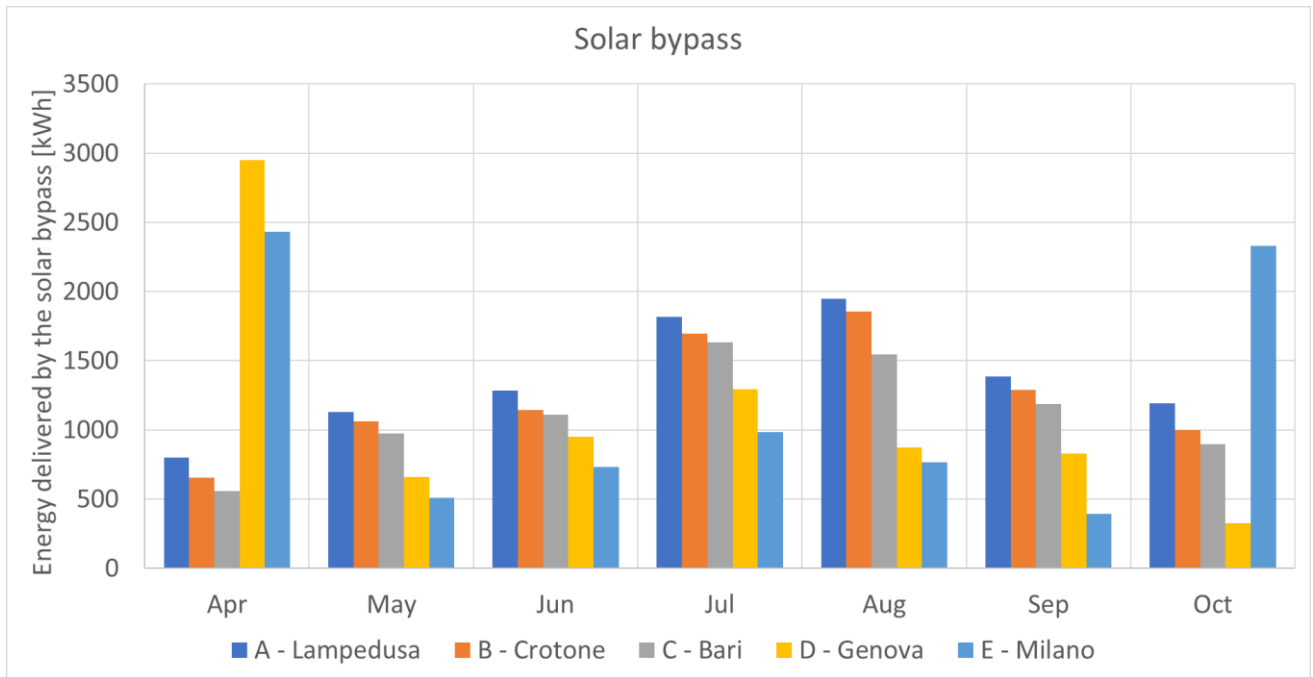


Figure 5. 5: plot of the thermal energy produced by the solar bypass at different climatic zones

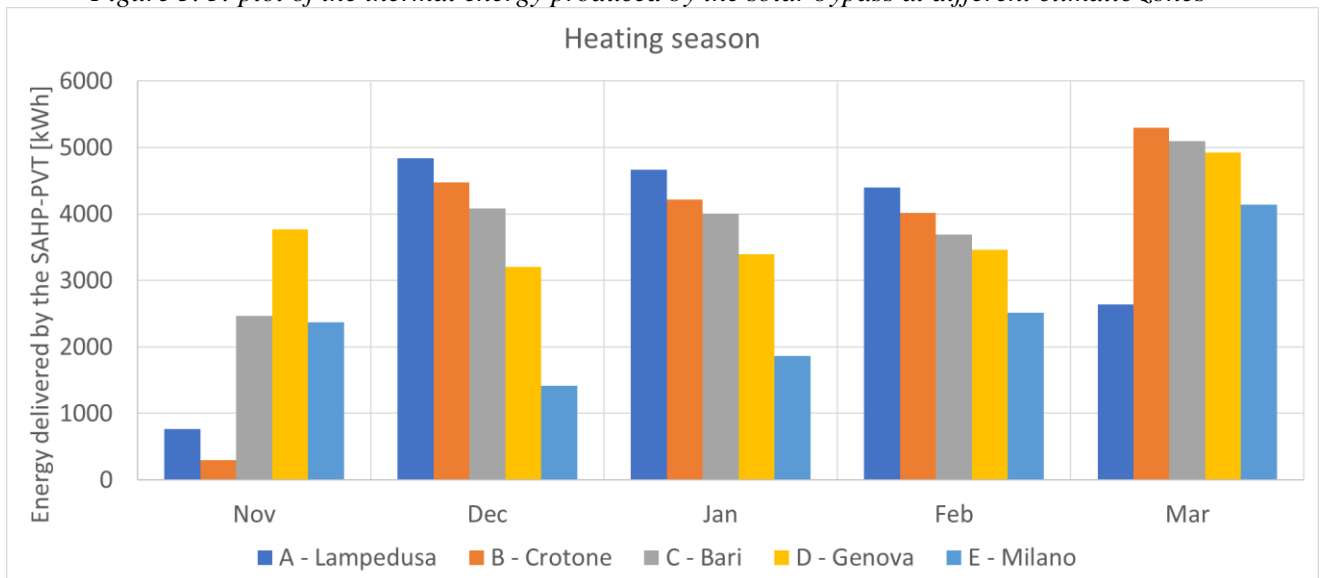


Figure 5. 6: plot of the thermal energy produced by the SAHP at different climatic zones

The following observations can be drawn from the comparison of Figure 5. 5 and Figure 5. 6:

- The months of November, March, April and October can be misleading, since apparent unexpected performances are recorded. Indeed, during these months some cities are already/still out of the heating season, with the solar bypass on, while others have the SAHP switched on.
- A global improvement of the SAHP-PVT performance can be noticed at locations with lower DD; in particular the delivered thermal energy almost doubles for both the solar bypass and the SAHP from the climatic zone E up to A or B.
- Independently from the climatic zone, the thermal energy produced by means of the bypass is about half of the one obtained with the SAHP. Unluckily, the activation of the SAHP even out of the heating season is less likely at mildest locations since the temperatures reached at the evaporator might be too high and cause either blocks of the HP or activations of the solar bypass

with intermittent switch on and off of the HP. This aspect has been already enquired for the climatic zone D in paragraph 5.2).

In conclusion, the Seasonal COP (SCOP) of the HP has been evaluated, using the following formulation:

$$SCOP = \frac{\sum_{i=1}^{365} (Q_{cond} + Q_{bypass})}{\sum_{i=1}^{365} L_{HP+circulators}} \quad \text{Eq. 5. 1}$$

Where:

Q_{cond} and Q_{bypass} represent the useful effect, namely the thermal energy delivered by the SAHP and the solar bypass respectively [kWh]

$L_{HP+circulators}$ accounts for the electric consumption of both the SAHP and the circulators inside the boiler room [kWh]

Figure 5. 7 reports the SCOPs obtained by the simulations of the SAHP-PVT at the five different cities, united with the regression line. It can be seen that the approximation is very good (less than 2%), allowing to preliminary assess the SAHP-PVT performance just knowing the degree days of the location, assumed that the solar field installation site is free from any relevant obstruction or shading.

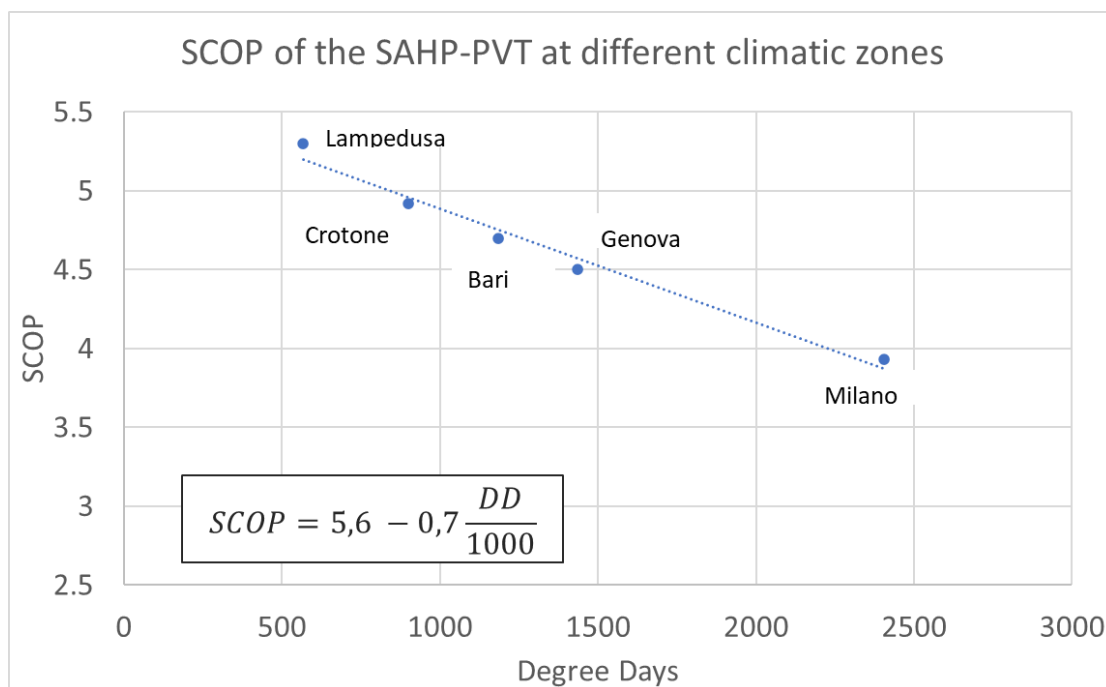


Figure 5. 7: simulated SCOP of the SAHP-PVT at different locations, regression line and correspondent equation

In addition, the equation of the regression line reported in Figure 5. 7 also allows the estimation of the maximum, theoretical SCOP for the considered plant layout. In fact, considering the limit case of the degree days tending to zero, the extrapolated value of the SCOP is of 5.6. This value can be only implemented by changing either the plant layout, or increasing the efficiency of one or more components or both.

In conclusion, the present study assessed the great potential of the SAHP-PVT technology, which is inversely proportional to the DD of the location. Considering both the achievable SCOP and the delivered thermal energy, such technology is highly advisable for cities falling into the climatic zones A, B, C and D, while the performance of the system needs to be specifically evaluated in zone E. Considering the distribution of the Italian territory (Figure 5. 8 and Table 5. 14), only the South and part of the central regions (especially on the West Coast) are highly compatible with the SAHP-PVT technology. On the contrary, the North, including all the Po Valley and the Apennines (about 43% of the Italian territory) require additional evaluations referred to the specific case study.

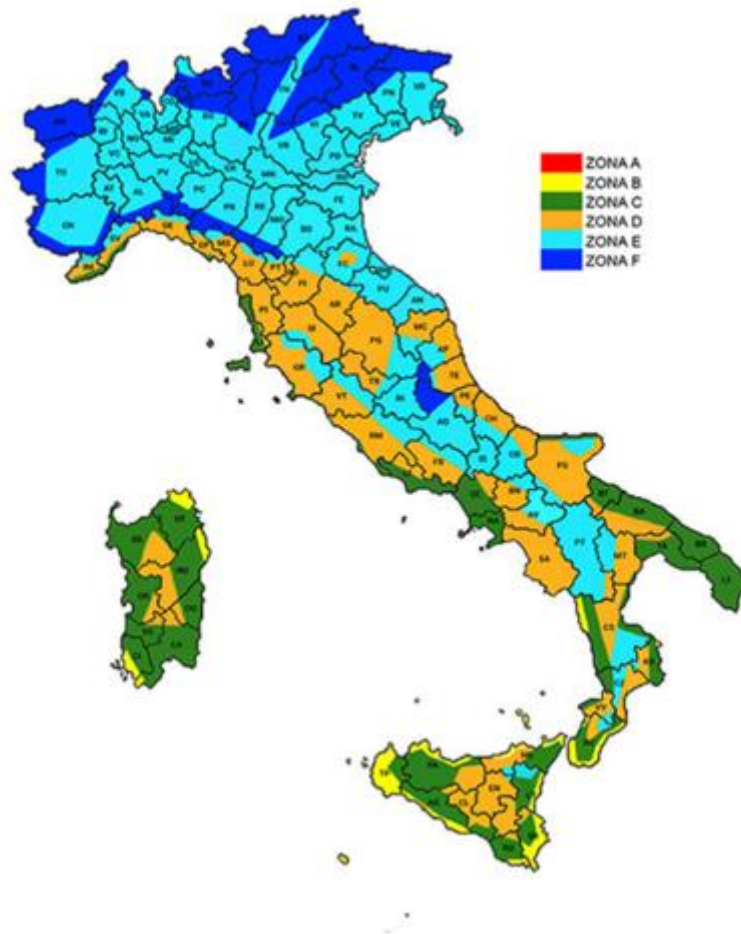


Figure 5. 8: climatic zones over the Italian territory (200)

| Climatic zone | Extension over the Italian territory [%] |
|---------------|--|
| A | 3 |
| B | 7 |
| C | 15 |
| D | 30 |
| E | 43 |
| F | 2 |

Table 5. 14: percentual extension of the climatic zones over Italy

6. Conclusions and future developments

The Solar Assisted Heat Pumps – SAHP are basically the result of the interface between a very efficient heat generator – the heat pump – and a renewable source – the solar panels. These two key elements take mutual advantage one from the other increasing their performance since the heat pump works at higher and more stable temperatures with respect to the air source. In addition, the low working temperature at the panels increases their efficiency, their operativity time during the day and it reduces the thermal losses, even in the case of poorly insulated panels/connection pipes.

Starting from this basic idea, many layouts of the SAHPs have been identified in the different studies, for instance considering hybrid panels instead of only thermal ones, or by installing a dual source heat pump (i.e., solar panels or external air or ground heat exchangers), with an automatic switch to the most convenient thermal source. Anyway, the actual state-of-art still presents many limits that affect the diffusion of the SAHPs:

- *Coupling of solar panels and heat pumps:* the SAHP works under transient regime, therefore the correct sizing of the HP and the solar panels is not trivial. Indeed, the HP operativity time must not be too long to reduce the electric consumption; in addition, the design of the solar panels should account for the variability of the solar radiation over the day with respect to the activation periods of the HP. These issues are complicated by the absence of a general and common design approach, leading to different plant configurations, based on both the calculations performed by the researchers and the available information.
- *Low ambient temperature:* in case of SAHPs installed at cold climates, the low ambient temperature is very likely to decrease the overall performance of the plant, starting from the higher thermal losses at the panels and the lower working temperature at the evaporator. This main issue comes with other operational problems, such as the risk of frosting, reduced efficiency at the HP compressor which can be worsened by the adoption of low cost, poorly insulated panels. Actually, this limit is more concerned with the HP instead of the solar panels, in fact most of recent, carried-out research is studying the improvement of this component (e.g., trans critical cycles, CO₂ cycles etc.).
- *Mismatch between heat requirement and heat supply:* the optimal situation for a SAHP is represented by the case in which the heat supply is required during the same period of maximum solar availability. Every time shift causes a relevant reduction of the SAHP performance, particularly emphasized during Summer when the peaks in solar radiation can remain even unexploited. So, also the sizing of elements with thermal inertia, such as water storage tanks, has to be carefully evaluated.
- *Low level of end users' acceptance of the SAHP:* independently from the cost effectiveness of the facility, many advanced technologies such as the SAHP are hardly chosen by the end users' because of their lack of confidence and skills to manage complex plants. This topic is of paramount importance since a plant needs to be used to reach the expected performances. The implementation of self-controlled SAHP, thanks to complete and extended data acquisition and management systems, is the main strategy, to avoid the end users' intervention. And increase their acceptance.
- *Coupling of the SAHP with existing heating systems:* one of the biggest obstacles in the large-scale adoption of SAHP based plants is represented by the coupling with existing, high-temperature emission systems (e.g., radiators). Indeed, the revamping of existing heating plants by means of the substitution of the generator is more likely than the realization of completely new buildings with specific reference to the Italian building stock. For this reason, the SAHPs have to cope with this problem, to make them more attractive if compared to traditional gas

burners. For instance, the interface between SAHP and gas burners could be introduced, keeping the burners only for integration or in case of extreme need, while the main part of the thermal load during the day is granted by means of the SAHP.

- *SAHP – scale effect?* The experimental facilities reported in all the available studies are concerned with small solar fields/HP size (e.g., about 10 -20 m² of capturing surface and about 5-10 kW_T of delivered thermal power by the HP). This aspect is mainly due to the initial cost of the plant and the reduced room available in laboratories to develop larger prototypes. As a consequence, there is still very little information about any operational problem linked to the increase in the size of the plant. The pilot plant under study in the present work is one of the few facilities of medium-large size (i.e., 120 m² of solar field and 48 kW_T of delivered thermal power by the HP) from which the difficulties caused by the increase in plant complexity and its different working conditions can be better understood. These issues were at the core of the optimization analyses run in TRNSYS environment to increase the plant efficiency resumed below.

The work has presented the topic and limits of the SAHPs, before introducing in detail the pilot plant under study.

Briefly, the plant is formed by a hybrid solar field (PVT) which is interfaced with the cold side of a Heat Pump (HP) to increase its efficiency during the heating season. Such plant covers the Domestic Hot Water (DHW) and Space Heating (SH) needs of a sport palace with the help of two integration gas burners (namely one for SH and one for DHW). During the remaining part of the year, the HP is off and the solar thermal field is directly interfaced with an integration burner to cover the DHW needs of the facility (solar bypass). This bypass is activated also each time the temperatures in the solar field are stable and high enough to be directly sent to the integration gas burners. In both cases the PV side of the solar field is expected to cover the electrical needs of the plant, with an increased efficiency thanks to the low working temperature determined by the thermal side.

Besides of the experimental approach, the numerical modelling results quite demanding also because of the extended recorded data set to perform the validation. The SAHP-PVT pilot plant under study represents a step forward the laboratory prototype since it is a real plant, covering the real DHW/SH needs of a sport palace, but it is equipped with an extended data acquisition and control system that allows detailed analyses about its working.

Then a numerical transient model of the plant has been implemented in TNSYS environment. Different stages of validations occurred, since the control on each component singularly may not be always feasible, because the boundaries must reproduce the same measured conditions to which the reference information is associated.

On the other hand, only the validation of the entire model of the plant as a single element may lead to unsatisfactory results, due to the relevant number of parameters to set for each component and the large number of checks under different working conditions.

In conclusion, the validation of the model was carried out according to the following criteria:

- Validation of single components, whenever information about the element working on its own is available.
- Validation of the smallest group of components when their working occurs simultaneously. This step involves also the elements singularly validated before shall be used again.

In any case, the validation of the plant has been concerned with both graphical comparison between simulated and measured trends of chosen parameters over time and the comparison with average, integral values.

Actually, such detailed approach would not have been possible without a complete and extended dataset of measurements of the different working parameters of the plant under different boundary conditions.

Then, the validation of the global working of the plant has been presented, to provide a last check on its reliability with reference to the expected design values contained in the original design calculation report. This comparison allows to highlight the differences between the design approach (almost steady state) and the transient simulation, showing how the steady state approach is likely to predict performances (e.g., COP) about 7% lower. The transient modelling also accounts for the actual distribution of the consumption profiles (e.g., DHW or SH) during the day, which affect the performance of the SAHP.

Concerning all the carried-out models, the simulation of transient systems with relevant mass flow rates poses a not negligible issue about the convergence analysis. In fact, the frequent switch on/off of the pumps (nominal flow rates between 5000 and 8000 kg/h) is very likely to cause a missed convergence of the non-linear equations involved, even accounting for hysteresis effects. Therefore, the optimal convergence values adopted in the simulations are concerned with a very small time-step (variable between 1 minute for the validation of the SAHP up to 10 minutes for the simulation over a reference year) and a tolerance convergence of 0.35. As shown in the previous chapters, these values allow reliable, converged results without requiring an excessive computation time.

Completed the validation and convergence stages, the model has been adopted to enquire the best interventions to increase the plant efficiency. Although the specific conclusions are drawn with reference to the pilot plant under study, the adopted approach and the main results can be applied to other similar SAHP plants. Part of the results of the simulations briefly resumed below have been already implemented inside the plant, while others are still under design.

- 1) *Influence of the thermal losses due to the pipes connection the solar field to the boiler room:* about 200 m long and not insulated pipes connect the solar field with the HP/boiler room. Usually, many SAHP are assembled adopting low cost and poorly insulated panels since the low working temperature with respect to the external one determines very small thermal losses independently from the level of insulation. Anyway, in the specific case study, the HP is switched off at the end of the heating season and the solar field is directly interfaced with the integration gas burners, bypassing the heat pump. This change in the plant working layout causes not negligible thermal losses as a consequence of the increased working temperature inside the panels. So, the numerical model has been used to evaluate the benefits deriving from the insulation of these pipes. Basing on the carried-out simulations, on the thermal side the insulation causes an reduction of the SAHP performance during winter since the pipes no longer act as an additional heat exchanger. On the other hand, the high thermal losses during summer are reduced (about 60% in the monthly values), when the HP is off and the solar field directly works with the integration gas burners. From the point of view of the annual balance, the insulation leads to a global improvement in the delivered thermal energy (about 8% - 600 €/year of saving), since the decrease in the thermal losses during summer is far higher than the slightly lower performance of the SAHP during the heating season. Anyway, the insulation generally increases the working temperature at the panels, with a lower generation

efficiency of the PV side of the solar field. According to the specific case study and the current unitary prices for electricity, the loss in the PV production is almost comparable to the increase in the provided thermal energy under the assumption of almost total self-consumption of the photovoltaic production. In conclusion, the cost-effectiveness of this intervention depends on the effective capability of the facility to consume the produced electricity on site. Actually, the plant layout and electrical consumption profile of the case study is not likely to truly benefit from the increased PV production and the insulation of the connection pipes has been therefore included in the intervention for the plant revamping under design.

2) *Changes in the regulation criteria to best exploit the SAHP-PVT:*

The simulated monthly results clearly show that there is a steep decrease in the produced thermal energy when the SAHP is switched off and the solar bypass is enabled. This aspect can be noticed in particular during Spring or Autumn (i.e., in October or April). So, the validated numerical model has been used to enquire the convenience of keeping the SAHP on even out of the heating season. According to the simulations, the SAHP is convenient both on the energy and economic point of view only in October and September. Indeed, the still low temperatures and solar radiation allow the HP to work without enabling the solar bypass with a saving preliminary estimated in about 500 €/year. On the other hand, during the other months (namely from May to September) the bypass activates frequently, with continuous stops of the HP. This in turn leads to almost the same delivered energy since it is mainly produced by means of the solar bypass. On the operational side, the HP is likely to be subjected to failures or blocks due to the frequent switch on and off. In conclusion, the data acquisition system has been implemented with the new regulation criterion, to increase the plant performance.

3) *Strategies to maximise the self-consumption of the photovoltaic field:*

The transient simulations show that the shift between the daily production and consumption profile requires that about 30% of the annual HP electric need is granted by the national grid, although the integral monthly/yearly PV production would cover it. In addition, almost 70% of the PV production is sent into the national grid without any specific refund or incentive (the net metering has been recently abolished). Assuming a unitary price of electricity of 0.5 €/kWh_E, this means that about 10.000 € could be saved each year. As a consequence, the main strategies to improve the management of the PVT field have been enquired: installation of batteries and increase of the direct, on-site consumption.

These specific simulations have been performed basing on the information available in the energy bills since the data and acquisition system is connected only with the SAHP-PVT, neglecting the other energy consuming services inside of the facility, such as the lighting plant which covers both the internal sports hall, offices, lockers and external courts.

The study preliminary assessed that the connection of the PV field to all the energy intensive services of the facility is very likely to self-consume almost all the produced energy even introducing wide margins of safety. In fact, only the consumptions occurring the periods with daylight have been accounted (about one third of the total need) and it was assumed a coverage of 35% of this need by means of the national grid, to account for the moments in which the solar radiation is either low or absent. Under these conditions only 15% of the annual PV production was sent to the grid and it entirely occurred during August and September, since the facility is either closed or partially open because of the holydays and the hot climate.

In addition, the installation of batteries proved not convenient for different reasons: firstly, the required capacity compared to their initial cost (approximated at 1000/kWh_E) determine a simple payback time of about twice their useful life (namely 20 years against the expected

useful life span of a battery of 10 years). Secondly the continuous discharge power is not comparable with the required one, unless large fields of batteries are installed (worsening their cost-effectiveness analysis). In the end, all the PV production is very likely to be consumed on site just connecting the PV field with both the HP and all the energy intensive services, so there is no preliminary real need for batteries.

Considering the specific pilot plant, only commercial batteries were taken into account. Indeed, the SAHP at Palacus sport palace represents a meeting point between a real plant associated to a real building and an experimental academic facility. All the plant was assembled using commercial components and not specifically tailored ones, trying to bring the technology closer to the step of industrial and serial production. For this reason, the plant is required to grant reliability, durability and economic convenience of the interventions, therefore excluding more effective but still not widely diffused prototypes (e.g., thermo-electric storages or more in general fuel cells).

4) *Performances of the SAHP-PVT at different climatic zones:*

The assembly and run of a numerical model for the SAHP is demanding in terms of both required time and computational capacity. In addition, a very complete set of measurements is needed to perform an exhaustive validation. So, the numerical model has been run at five different cities, representing the main Italian climatic zones, to provide a preliminary estimation of the SAHP potential, according to the Degree Days (DD) of the location.

The simulations were carried out assuming a negligible dependence of the SH/DHW needs on the different locations. This can be considered correct for the DHW since it mainly depends on the usage of the facility. On the other hand, the SH can be preliminary conceived as independent from the location, since the SAHP provides only a pre-heating of the SH circuit. In addition, no relevant obstructions or shadings were modelled on the PVT field.

The delivered thermal energy by means of the SAHP can even double from climatic zone E up to A or B, showing the convenience of the technology for the locations falling within the climatic zones A to D, which represent almost half of the Italian territory. The remaining places belonging to E or F require specific assessments referring to the installation site and the actual DHW/SH needs. From the point of view of the Seasonal COP (SCOP), the simulated values obtained for the five cities are very well approximated by a linear regression, only depending on the DD of the site. This equation represents a very useful tool to assess the preliminary performance of a SAHP at different locations, assuming negligible shading/obstructions on the solar field. In addition, the limit case of the Degree Days tending to zero identifies the theoretical limit of achievable performance for the SCOP (5.6) for the considered configuration and components of the SAHP.

More in general, the developed and validated transient model represents a powerful tool which can be adopted for different applications:

- Plant design/revamping: the transient model of the components reproducing the real working of the plant leads to more refined estimations comparing for each time step demand against production. Such model can be applied under a design stage using nominal performances in absence of operative, measured data. Then the same parameters of the different components (e.g., heat pump, burner etc) can be constantly, or at least regularly, updated basing on the collected information to follow the wearing of the components and their further performance degradation. In the specific case study, the transient simulations allowed to identify the possible interventions estimating their benefits also with a general validity. For instance, the insulation of the connection pipes between the solar field and the heat pump might result convenient or not, according to the

thermal and electric needs of the facility. In fact, the higher operating temperature achieved by means of insulation is a positive effect on the thermal side but it negatively affects the PV yield of the solar cells. In absence of efficient electricity storage systems or consistent energy withdrawals, the insulation of the pipes and adoption of insulated panels is generally advisable.

- Plant monitoring and maintenance: the role of the model interfaced with the data acquisition and control system is just not a mere flag of the failures, but it can help the schedule of maintenance interventions. Some instances are concerned with the cleaning of the heat exchangers once the efficiency is below a given threshold or activate a warning for pump substitution whenever the cumulate working period exceeds established ranges. As regards the specific pilot plant, these issues are currently under study and they belong to the future developments.

Clearly, the current model lacks perspective on the structure which is served by the heating plant and it should be extended to the facility, united with the data acquisition and control system, to assembly a global model (i.e., plant + heating plant). This extension would allow a further refinement of the regulation criteria which are currently concerned with just the production and storage of technical hot water used either for SH or DHW without effectively acting on the emission.

The original concept behind the plant design aims at a self-sufficient structure providing the DHW and SH demand with almost no fossil fuel consumption. In fact, the PV side of the solar field was designed to cover the electrical consumption of the heat pump, making this technology highly scalable, from a theoretical point of view. However, the feasibility of this concept depends on the policies which allowed the use of the national grid as a virtual storage for the produced/consumed energy over the year. Basing on the current state of policies and Italian laws, this strategy is no longer working, so proper storages must be included to allow the scalability of the plant as a whole, especially if hybrid panels are involved.

On the thermal side, the introduction of relevant storages on the DHW subsystem and the usage of the SAHP for pre-heating/normal operation on the SH service reduces the dependence of the plant on the energy demand of the building. More in general this layout is conceived to maximise the compatibility of the SAHP with existing buildings, eventually scaling the components according to the energy and power profiles of demand. Indeed, such hybrid systems are not meant to entirely substitute the traditional system, especially in existing buildings, but they are expected to cover most of the energy need, leaving the intervention of the traditional heating system to severe conditions.

Furthermore, these configurations of plants involving different energy sources (both fossil and renewable) provide an added degree of resilience to the plant. In fact, different regulation criteria could be set according to the unitary price of the energy sources, choosing the most convenient one time by time.

Anyway, the change in size of the plant has to be preliminary evaluated to identify the correct extension of the solar field to be coupled to the heat pump. This aspect belongs to the future developments, basing on the validated model described in the present work.

In fact, the installation of such plants might collide with different constraints. For instance, not enough available surface to install the solar field, municipal regulations that inhibit the installation of panels, incompatibility of the heat pump with the surrounding (e.g., exceeding of the noise limits).

As far as the future developments are concerned, on the short term, more locations should be added, to refine the assessment tool. In addition, the effect of shadings could be accounted, as well as varying the size/efficiency of the different components, to reach a predictive formulation of the SAHP

performance depending on these parameters (i.e., location, level of shading and characteristics of the main components). Furthermore, the numerical model of the plant could be implemented with the energetic simulation of the sport palace, for a better approximation of the SH/DHW needs.

Then, on the long term, such plant model should be implemented and interfaced with the data acquisition and control system, to enhance advanced machine learning and multi-objective evolutionary optimisation models, constantly updated using the real time measured parameters.

Publications

- L.A. Tagliafico, A. Cavalletti, C. Marafioti, A. Marchitto, “Optimisation strategies for solar assisted heat pumps coupled to traditional thermal fields”, 37th UIT Heat Transfer Conference
- L.A. Tagliafico, A. Cavalletti, C. Marafioti, A. Marchitto “The experience on a sport centre pilot plant with solar assisted heat pump and a look forward for new control strategies and technology upgrade”, 76th ATI National Congress
- L. A. Tagliafico, A. Cavalletti, C. Marafioti, A. Marchitto “End users’ acceptance of new technology renewable plants: the pilot case of a solar assisted heat pump” – under revision
- L.A. Tagliafico, A. Cavalletti, C. Marafioti, A. Marchitto “Solar assisted heat pump pilot plant management and troubleshooting by means of numerical modelling: a case study” UIT Heat Transfer Conference special issue of “Journal of Physics: conference series”
- L. A. Tagliafico, P. Cavalletti, A. Cavalletti, C. Marafioti, F. Poma, E. Sterpi “Numerical and experimental analysis of thermal penetration depth in bare reinforced concrete structures during fire accidents” 75o National Congress ATI Italian Association of Heat Engineering Proceedings.
- L.A. Tagliafico, A. Cavalletti, C. Marafioti, A. Marchitto “End Users’ Acceptance of New Technologies in Building Heating: An Experience on Solar Assisted Heat Pumps”, Italian Journal of Engineering Science vol.63, No. 2-4, pp. 198-204, June 2019
- L. A. Tagliafico, A. Arteconi A. Cavalletti, C. Marafioti, A. Marchitto “Performance Of A Solar Assisted Heat Pump For Building Heating: Control Problems And Improvements”, 37th UIT Heat Transfer Conference Proceedings
- L.A. Tagliafico, V. Bianco, A. Cavalletti, C. Marafioti, A. Marchitto, F. Scarpa “Monitoring and control of a pilot plant made of solar assisted heat pump with hybrid panels”, 74o National Congress ATI Italian Association of Heat Engineering Proceedings AIP Conference Proceedings, vol. 2191, 2019.
- A. Cavalletti, M. Marchesoni, A. Marchitto, L.A. Tagliafico, “Sistemi a pompa di calore elioassistiti: idee e spunti dall’impianto pilota presso l’Università di Genova”, La Termotecnica, n. 10 – Dicembre 2021
- L.A. Tagliafico, V. Bianco, A. Cavalletti, C. Marafioti, A. Marchitto, F. Scarpa, “Pompe di calore elioassistite: i problemi nel passaggio da impianti dimostrativi al mondo reale” – FIRE - Gestione Energia – strumenti e buone pratiche per l’energy management, 2021, n.1 pp. 24-29
- D. Borelli, A. Cavalletti, P. Cavalletti, L.A. Tagliafico – “Reliability analysis and economic evaluation of thermal reflective and nanotechnology-based insulators” Energies. 2022; 15(19):7238. <https://doi.org/10.3390/en15197238>

References

1. [Online] [Cited: 02 February 2022.] <https://www.macrotrends.net/1369/crude-oil-price-history-chart>.
2. [Online] February 2022. <https://www.euractiv.com/section/energy/news/germany-reactivates-coal-power-plants-amid-russian-gas-supply-threats/>.
3. [Online] February 2022. <https://www.thelocal.it/20220225/italy-may-reopen-coal-plants-amid-concerns-about-energy-supply-pm-says/>.
4. [Online] February 2022. <https://www.ren21.net/reports/global-status-report/>.
5. [Online] February 2022. <https://task44.iea-shc.org/>.
6. *A comparative study of solar assisted heat pump systems for canadian locations*. Chandrashekar, M., Sullivan, N.T. and Hollands , K.G.T. 3, 1982, Solar Energy, Vol. 28, pp. 217-226.
7. *Performance of combined solar-heat pump systems*. Freeman , T.L., Mitchell, J.W. and Audit, T.E. 2, 1979, Solar Energy, Vol. 22, pp. 125-135.
8. *Solar energy and the steam Rankine cycle for driving and assisting heat pumps in heating and cooling modes*. Lion, N. 3, 1977, Energy Conversion, Vol. 16, pp. 111-123.
9. *Solar assisted heat pump system: a parametric study for space heating of a characteristic house in Madison, Wisconsin*. Bosio, R.C. and Suryanarayana, N.V. 1975, American Society of Mechanical Engineers (Paper).
10. *Solar energy assisted heat pumps systems for commercial office buildings*. Gilman, S. F. and Sturz, D. H. 2, 1974, ASHRAE Transactions, Vol. 80, pp. 374-381.
11. *The heat pump and solar energy*. Sporn, P. and Ambrose, E.R. 1955, Proceedings of the world symposium on applied solar energy. Phoenix.
12. *Design and economics of solar energy heat pump system*. Jordan, R.C. and Threlkeld, J.L. 1954, Heat Pip Air Cond, Vol. 26.
13. *Hybrid solar-assisted heat pump system for residential applications*. Gordon, H.T. 1976, Sharing the Sun, Sol Technol in the Seventies, Jt Conf of the Int Sol Energy Soc, Am Sect and Sol Energy Soc of Can, Inc.
14. *Solartechnik und Wärmepumpe – sie finden zusammen*. Trojek, S. and Augsten, E. 6, 2009, Sonne Wind & Wärme, Vol. 33, pp. 62-71.
15. *Wärmepumpe und solar – solarenergie den vortritt lassen*. Berner, J. 8, 2011, Sonne Wind & Wärme, Vol. 35, pp. 182-186.
16. Hadorn, J.C. *Solar and heat pump systems for residential buildings*. s.l. : Ernst & Sohn Wile, 2015.
17. *Country Update for Sweden 2020*. Gehlin, S., Andersson, O. and Rosberg, J.E. 2020, Proceedings World Geothermal Congress .
18. *Research on the operation strategies of the solar assisted heat pump with triangular solar air collector*. Jiang, Y., et al. 2022, Energy, Vol. 246.

19. *Energy, exergy, economic and environmental assessment of the triangular solar collector assisted heat pump.* Jiang, Y., et al. 2022, *Solar Energy*, Vol. 236, pp. 280-293.
20. *Dynamic performance evaluation of LNG vaporization system integrated with solar-assisted heat pump.* Dai, R., et al. 2022, *Renewable Energy*, Vol. 188, pp. 561-572.
21. *An Experimental Approach for the Dynamic Investigation on Solar Assisted Direct Expansion Heat Pumps.* Scarpa, F., et al. 2015, *Chemical Engineering Transactions*, pp. 2485-2490.
22. *Performance analysis of integrated solar-assisted heat pumps for water heating.* Tagliafico, L.A., Scarpa, F. and Carrea, E. 2006, 61st ATI Congress proceedings, International session on solar heating and cooling, Perugia,.
23. *An approach to energy saving assessment of solar assisted heat pumps for swimming pool water heating.* Tagliafico, L.A., et al. 2012, *Energy and buildings* .
24. *On the economy of the heating or cooling of buildings by means of currents of air.* Thompson, W. 1852, *Glasgow Phil. Soc. Proc.*, pp. 269-272.
25. *Thermodynamic considerations in vapour compression heat pumps.* Holland, F.A. and Watson, F.A. 3, 1979, *Indian Chemistry Engineering Journal*, Vol. 21, pp. 41-50.
26. *Performance analyses of combined heating and photovoltaic power systems for residences.* Wolf, M. 1-2, 1976, *Energy Conversion*, Vol. 16, pp. 79-90.
27. *On heat rejection from terrestrial solar cell arrays with sunlight concentration.* Florschuetz, L.W. 1975, *Proceedings of the 11th IEEE PVSC conference*. New York, USA, pp. 318-326.
28. *Extension of the Hottel–Whiller model to the analysis of combined photovoltaic/thermal flat plate collectors.* Florschuetz, L.W. 1979, *Solar Energy*, Vol. 22, pp. 361-366.
29. *Combined photovoltaic and thermal hybrid collector systems.* Kern, E.C. and Russell, M.C. 1978, *Proceedings of the 13th IEEE photovoltaic specialists*.
30. *Evaluation of combined photovoltaic/thermal hybrid collectors.* Hendrie, S.D. 1979, *Proceeding of the ISES international congress*, Atlanta, USA.
31. *Simplified method for predicting photovoltaic array output.* Evans, D.L. 6, 1981, *Solar Energy*, Vol. 27, pp. 555-560.
32. *Study of a hybrid solar system—solar air heater combined with solar cells.* Bhargava, A.K., Garg, H.P. and Agarwal, R.K. 5, 1991, *Energy Conversion and Management*, Vol. 31, pp. 471-479.
33. *Some aspects of a PV/T collector/forced circulation flat plate solar water heater with solar cells.* Garg, H.P. and Agarwal, R.K. 2, 1995, *Energy Conversion and Management*, Vol. 36, pp. 87-99.
34. *Conventional hybrid photovoltaic/thermal (PV/T) air heating collectors: steady-state simulation.* Garg, H.P. and Adhikari, R.S. 3, 1997, *Renewable Energy*, Vol. 11, pp. 363-385.
35. De Vries, D.W. *Design of a photovoltaic/thermal combipanel.* Eindhoven Technical University Netherland : Ph.D. Thesis Eindhoven Technical University, 1998.
36. *Annual exergy evaluation on photovoltaic-thermal hybrid collector.* Fujisawa, T. and Tani, T. 1-4, 1997, *Solar Energy Materials and Solar Cells*, Vol. 47, pp. 135-148.

37. [Online] February 2022.
https://upload.wikimedia.org/wikipedia/commons/thumb/b/b1/Solar_panels%2C_Santorini2.jpg/640px-Solar_panels%2C_Santorini2.jpg.
38. *Conditioning of a Plus-energy House using Solar Systems for both Production of Heating and Nighttime Radiative Cooling*. Pèan, T. and Gennari, L. 2014.
39. *An Investigation into the Use of Hybrid Solar Power and Cloud Service Solutions for 24/7 Computing*. Ogunshile, E. 2017, pp. 743-754.
40. *Performance and cost of a roof-sized PV/thermal array combined with a ground coupled heat pump*. Bakker, M., et al. 2004, *Solar Energy*, Vol. 78, pp. 331-339.
41. *Electricity Demand Profile of Australian Low Energy Houses*. Lee, S., Whaley, D. and Saman, W. 62, 2014, *Energy Procedia*.
42. *Households' hourly electricity consumption and peak demand in Denmark*. Andersen, F.M., et al. 2017, *Applied Energy*, Vol. 208, pp. 607-619.
43. *Simulation of a ZEB Electrical Balance with a Hybrid Small Wind/PV*. Kasaeian, A., Sameti, M. and Razi Astaraei, F. 5, 2014, *Sustainable Energy*, Vol. 2.
44. *Hot weather and residential hourly electricity demand in Italy*. Alberini, A., et al. 2019, *Energy*, Vol. 177, pp. 44-56.
45. [Online] [Cited: April 1, 2022.] <https://www.eia.gov/todayinenergy/detail.php?id=42915>.
46. *Hourly consumption profiles of domestic hot water for different occupant groups in dwellings*. Ahmed, K., Pylsy, P. and Kurnitski, J. 2016, *Solar Energy*, Vol. 137, pp. 516-530.
47. *Efficiency, Economic and Environmental Assessment of Ground Source Heat Pumps in Central Pennsylvania*. Blumsack, S., Brownson, J. and Witmer, L. 2009.
48. *Control Strategy for Domestic Water Heaters during Peak Periods and its Impact on the Demand for Electricity*. Moreau, A. 2011, *Energy Procedia*, Vol. 12, pp. 1074-1082.
49. *Hourly optimization model for the sizing of district heating systems considering building refurbishment*. Pavičević, M., et al. 2017, *Energy*, Vol. 137, pp. 1264-1276.
50. *Hourly and daily domestic hot water consumption in social housing dwellings: An analysis in apartment buildings in Southern Brazil*. Sborz, J., et al. 2022, *Solar Energy*, Vol. 232, pp. 494-470.
51. *Detailed Modelling of the Deep Decarbonisation Scenarios with Demand Response Technologies in the Heating and Cooling Sector: A Case Study for Italy*. Calise, F., et al. 2017, *Energies*, Vol. 10, pp. 1535-1540.
52. [Online] <http://www.artistsdomain.com/dev/eere/web/1940.html>.
53. Law 133/1999. [Online] <https://www.normattiva.it/uri-res/N2Ls?urn:nir:stato:legge:1999;133>.
54. Net Metering - GSE. [Online]
https://www.gse.it/documenti_site/Documenti%20GSE/Servizi%20per%20te/SCAMBIO%20SUL%20POSTO/Regole%20e%20procedure/Regole%20Tecniche%20Scambio%20sul%20Posto_2019.pdf.

55. Law 77/2020. [Online] <https://www.normattiva.it/uri-res/N2Ls?urn:nir:stato:legge:2020-07-17;77>.
56. Law 234/2021. [Online] <https://www.normattiva.it/uri-res/N2Ls?urn:nir:stato:LEGGE:2021-12-30;234!vig=>.
57. *The effect of temperature on photovoltaic cell efficiency*. Fesharaki, V., et al. 2011, Proceedings of the 1st international conference on emerging trends in energy conservation, Tehran, Iran.
58. Reay, D.A. and Mac Michael, D.B.A. *Heat pumps design and applications*. Oxford : Pergamon Press, 1979. pp. 22-23.
59. *Systematic classification of combined solar thermal and heat pump systems*. Frank, E., et al. 2010, Proceedings of the EuroSun International Conference on Solar Heating, Cooling and Buildings.
60. *Solfångare och värmepump: Marknadsöversikt och preliminära simuleringsresultat*. Tepe, R. and Rönnelid, M. 2002, Solar Energy Research Center.
61. *Low exergy building systems implementation*. Meggers, F., et al. 2012, Energy, Vol. 41, pp. 48-55.
62. *The performance of a solar assisted heat pump heating system*. Hawlader, M.N.A., Chlou, S.K. and Ullah, M.Z. 10, 2001, Applied Thermal Engineering, Vol. 21.
63. *Longwave Sky Radiation Parameterizations*. Aubinet, M. 1994, Solar Energy, Vol. 53, pp. 147-154.
64. *Thermal performance of a variable capacity direct expansion solar-assisted heat pump*. Chaturvedi, S.K., Chen, D.T. and Kheireddine, A. 1998, Energy Conversion management, Vol. 39, pp. 181-191.
65. *Performance of a solar-air source heat pump system for water heating on different weather conditions*. Guoying, X., Xiaosong, Y. and Lei, Y. 2009, Asia-Pacific Power and Energy Engineering Conference.
66. *Experimental study on solar assisted heat pump system for heat supply*. Kuang, Y.H., Wang, R.Z. and Yu, L.Q. 2003, Energy Conversion and Management, Vol. 44, pp. 1089-1098.
67. *The theoretical and experimental investigation of the characteristic of solar assisted heat pump for clear days*. Yamankaradeniz, R. and Horuz, I. 1998, International Communications in Heat and Mass Transfer, pp. 885-898.
68. *Preliminary experimental evaluations of indirect solar assisted heat pump systems*. Bridgeman, A. and Harrison, S. 2008, 3rd Canadian Solar Building Conference, Fredericton.
69. *Experimental thermal performance of a solar source heat-pump system for residential heating in cold climate region*. Bakirci, K. and Yuksel, B. 8-9, 2011, Applied Thermal Engineering, Vol. 31, pp. 1508-1518.
70. *On the potential of using heat from solar thermal collectors for heat pump evaporators*. Haller, M.Y. and Frank, E. 2011, Proceedings of the ISES Solar World Congress 2011, August 28–September 2, Kassel, Germany.

71. *Experiments for combined solar and heat pump systems*. Pärtsch, P., et al. 2012, Proceedings of the EuroSun 2012 Conference, Rijeka and Opatija, Croatia.
72. *Performance of combined solar-heat pump systems*. Freeman, T.L., Mitchell, J.W. and Audit, T.E. 1979, Solar Energy, Vol. 22, pp. 125-135.
73. *Experimental and theoretical investigation of combined solar heat pump system for residential heating*. Kaygusuz, K. and Ayhan, T. 1999, Energy Conversion Management, Vol. 40, pp. 1377-1396.
74. *Impact of solar heat pump system concepts on € seasonal performance - simulation studies*. Bertram, E., Parish, P. and Tepe, R. 2012, EuroSun 2012 conference.
75. *Parallel vs series configurations in combined solar and heat pump systems: a control system analysis*. Vega, J. and Cuevas, C. 2020, Applied Thermal Engineering, Vol. 166, pp. 1146-1150.
76. *Experimental validation of a theoretical model for a direct-expansion solar-assisted heat pump applied to heating*. Moreno-Rodriguez, A., et al. 2013, Energy, Vol. 60, pp. 242-253.
77. *Experimental study on roll-bond collector/ evaporator with optimized-channel used in direct expansion solar assisted heat pump water heating system*. Sun, X., et al. 2014, Applied Thermal Engineering, Vol. 66, pp. 571-579.
78. *Experimental study of photovoltaic solar assisted heat pump system*. Ji, J., et al. 2008, Solar Energy, Vol. 82, pp. 43-52.
79. *Experimental study of a photovoltaic solar-assisted heat-pump/heat-pipe system*. Fu, H.D., et al. 2012, Applied Thermal Engineering, Vol. 40, pp. 343-350.
80. *Effects of refrigerant charge and structural parameters on the performance of a direct-expansion solar-assisted heat pump system*. Zhang, D., et al. 2014, Applied Thermal Engineering, Vol. 73, pp. 522-528.
81. *Control strategy and experimental analysis of a direct-expansion solar-assisted heat pump water heater with R134a*. Kong, X., et al. 2018, Energy, Vol. 145, pp. 17-24.
82. *Experimental studies of a variable capacity direct-expansion solar-assisted heat pump water heater in autumn and winter conditions*. Kong, X., et al. 2018, Solar Energy, Vol. 170, pp. 352-357.
83. *Performance analysis of a novel air source hybrid solar assisted heat pump*. Cai, J., et al. 2019, Renewable Energy, Vol. 139, pp. 1133-1145.
84. *Experimental study on a novel PV/T air dual-heat-source composite heat pump hot water system*. Wang, G., et al. 2015, Energy Buildings, Vol. 108, pp. 175-184.
85. *Numerical study of an external device for the improvement of the thermal stratification in hot water storage tanks*. Gomez, M.A., et al. 2018, Applied Thermal Engineering, Vol. 144, pp. 996-1009.
86. *Study on the PCM flat-plate solar collector system with antifreeze characteristics*. Zhou, F., et al. 2019, International Journal of Mass and Heat Transfer, Vol. 129, pp. 357-366.
87. *Design and thermal performance optimization of a forced collective solar hot water production system in Morocco for energy saving in residential buildings*. Fertahi, S., et al. 2018, Solar Energy, Vol. 160, pp. 260-274.

88. *Impact of load profile and collector technology on the fractional savings of solar domestic water heaters under various climatic conditions.* Bouhal, T., et al. 2017, International Journal of Hydrogen and Energy, Vol. 42, pp. 13245-13258.
89. *Review of solar water heaters incorporating solid-liquid organic phase change materials as thermal storage.* Yiing, S., Munusamy, Y. and Seng, K. 2018, Applied Thermal Engineering, Vol. 131, pp. 455-471.
90. *Effect of strain rate on compressive behavior of Ti45Zr16Ni9Cu10Be20 bulk metallic glass.* Zhang, J., et al. 2007, Journal of Materials and Scientific Engineering, Vol. 290, pp. 448-451.
91. *Application of an air source heat pump (ASHP) for heating in Harbin, the coldest provincial capital of China.* Zhang, Y., et al. 2017, Energy Buildings, Vol. 138, pp. 96-103.
92. *Characteristics of an air source heat pump with novel photoelectric sensors during periodic frost-defrost cycles.* Wang, W., et al. 2013, Applied Thermal Engineering, Vol. 50, pp. 177-186.
93. *Techno-economic evaluation of a solar assisted combined heat pump e organic Rankine Cycle system.* Schimpf, S. and Span, R. 2015, Energy Conversion and Management, Vol. 94, pp. 430-437.
94. *Field test investigation of a double-stage coupled heat pumps heating system for cold regions.* Wang, W., et al. 2005, International Journal fo Refrigeration, Vol. 28, pp. 672-679.
95. *Energy and exergy analyses of a solar-driven ejector-cascade heat pump cycle.* Li, F., et al. 2018, Energy, Vol. 165, pp. 419-431.
96. *Two-stage direct expansion solar-assisted heat pump for high temperature applications.* Chaturvedi, S.K., et al. 2009, Applied Thermal Engineering, Vol. 29, pp. 2093-2099.
97. *Performance optimization and analysis of solar combi-system with carbon dioxide heat pump.* Deng, S., Dai, Y.J. and Wang, R.Z. 2013, Solar Energy, Vol. 98, pp. 212-225.
98. *A thermodynamic analysis of an auto-cascade heat pump cycle for heating application in cold regions.* Zhao, L., Zheng, N. and Deng, S. 2014, Energy and Buildings, Vol. 82, pp. 621-631.
99. *Performance analysis of indirect-expansion solar assisted heat pump using CO₂ as refrigerant for space heating in cold climate.* Ma, J., et al. 2020, Solar Energy, Vol. 208, pp. 195-205.
100. *The field test and optimization of a solar assisted heat pump system for space heating in extremely cold area.* Liu, H., Jiang, Y. and Yao, Y. 2014, Sustainable Cities and Societies, Vol. 13, pp. 97-104.
101. *Thermodynamic analysis of two component, two-phase flow in solar collectors with application to a direct expansion solar-assisted heat pump.* Aziz, W., Chaturvedi, S.K. and Kheireddine, A. 1999, Energy, Vol. 24, pp. 247-259.
102. *Numerical simulation and experimental validation of indirect expansion solar-assisted multi-functional heat pump.* Cai, J., et al. 2016, Renewable Energy, Vol. 93, pp. 280-290.
103. *CFD modelling development and experimental validation of a phase change material (PCM) heat exchanger with spiral-wired tubes.* Youssef, W., Ge, Y.T. and Tassou, S.A. 2018, Energy Conversion and Management, Vol. 157, pp. 498-510.

104. *Research and developments on solar assisted compression heat pump systems-A comprehensive review (Part A: modeling and modifications)*. Mohanraj, M., et al. 2018, *Renewable Sustainable Energy*, Vol. 83, pp. 90-123.
105. *Improvement of thermal stratification in a hot water solar storage tank by using a sintered bronze conical equalizer*. Gonzalez Altozano, P., et al. 2012, *World renew. Energy Congr. XII color. Renew. Energy soc. Annu. Conf. May 13e may 17. Am. Sol. Energy Soc.*
106. *Polyethylene glycol based shape-stabilized phase change material for thermal energy storage with ultralow content of graphene oxide*. Qi, G., et al. 2014, *Solar Energy and Materials for Solar Cells*, Vol. 123, pp. 171-177.
107. *Review of solar assisted heat pump drying systems for agricultural and marine products*. Daghigh, R., et al. 2010, *Renewable and Sustainable Energy*, Vol. 14, pp. 2564-2579.
108. *Solar and ground source heat-pump system*. Bi, Y., et al. 2004, *Applied Energy*, Vol. 78, pp. 231-245.
109. *Advances in seasonal thermal energy storage for solar district heating applications: a critical review on large-scale hot-water tank and pit thermal energy storage systems*. Dahash, A., et al. 2019, *Applied Energy*, Vol. 239, pp. 296-315.
110. *The Stakeholder Perspective: How management of KPIs can support value generation to increase the success rate of complex projects*. Pirozzi, M. 16th International Conference on Project Management and Scheduling.
111. *Public Acceptance and Preferences Related to renewable Energy and Grid Expansion Policy: Empirical insights for Germany*. Bertsch, V., et al. 2016, *Energy*, Vol. 114, pp. 465-477.
112. *Public Acceptance*. Schumann, D., Kuckshinrichs, W. and Hake, F. 2015, *Carbon Capture, storage and use*, Springer, pp. 221-251.
113. *Social Acceptance of Renewable Energy Innovation: An Introduction to the Concepts*. Wüstenhagen, R., Wolsink, M. and Bürer, M.J. 2007, *Energy Policy*, Vol. 35, pp. 2683-2691.
114. *Social Acceptance of the Clean Energy Concept: Exploring the Clean Energy Understanding of Istanbul Residents*. Erbil, A.O. 2011, *Renewable and Sustainable Energy Reviews*, Vol. 15, pp. 4498-4506.
115. PMI's Pulse of the Profession, 10^o Global Project Management Survey. [Online] 2018. <https://www.pmi.org/-/media/pmi/documents/public/pdf/learning/thought-leadership/pulse/pulse-of-the-profession-2018.pdf>.
116. *Monitoring and control of a pilot plant made of solar assisted heat pump with hybrid panels*. Tagliafico, L.A., et al. 2019, *AIP Conference Proceedings*, Vol. 2191.
117. *Performance testing of a heat pump system with auxiliary hot water under different ambient temperatures*. Li, X., et al. 3, 2022, *Energy and Built Environment*, Vol. 3, pp. 316-326.
118. *Solar systems and their integration with heat pumps: A review*. Kamel, R.S., Fung, A.S. and Dash, P.R.H. 2015, *Energy and Buildings*, Vol. 87, pp. 395-412.

119. *Low-temperature solar-plate-assisted heat pump: A developed design for domestic applications in cold climate*. Elamin, M., Saffa, R. and Siddig, O. 2017, International Journal of Refrigeration, Vol. 81, pp. 134-150.
120. Istat - buildings. [Online] https://www.istat.it/it/files//2014/08/Nota-edifici-e-abitazioni_rev.pdf.
121. Istat - census of the population. [Online] http://dati-censimentopolazione.istat.it/Index.aspx?DataSetCode=DICA_EDIFICI1.
122. Italian Building stock over Italy. [Online] February 2022. <https://italiaindati.com/edilizia-e-costruzioni-in-italia/>.
123. *Performance of a multi-functional direct-expansion solar assisted heat pump system*. Kuang, Y.H. and Wang, R.Z. 7, 2006, Solar Energy, Vol. 80, pp. 795-803.
124. *Performance analysis of solar water heater combined with heat pump using refrigerant mixture*. Nuntaphan, A., Chansena, C. and Kiatsiriroat, T. 5, 2009, Applied Energy, Vol. 86, pp. 748-756.
125. *Theoretical model and experimental validation of a direct-expansion solar assisted heat pump for domestic hot water applications*. Moreno Rodriguez, A., et al. 1, 2012, Energy, Vol. 45, pp. 704-715.
126. *Experimental investigation of a solar driven direct-expansion heat pump system employing the novel PV/micro-channels-evaporator modules*. Zhou, J., et al. 2016, Applied Energy, Vol. 178, pp. 484-495.
127. *Experimental study on the operating characteristics of a novel photovoltaic/thermal integrated dual-source heat pump water heating system*. Qu, M., et al. 2016, Applied Thermal Engineering, Vol. 94, pp. 819-826.
128. *Air–water dual-source heat pump system with new composite evaporator*. Xu, J., et al. 2018, Applied Thermal Engineering, Vol. 141, pp. 483-493.
129. *Field study of a novel solar-assisted dual-source multifunctional heat pump*. Besagni, G., et al. 2019, Renewable Energy, Vol. 132, pp. 1185-1215.
130. *Heat transfer performance of an integrated solar-air source heat pump evaporator*. Long, J., et al. 2019, Energy Conversion and Management, Vol. 184, pp. 626-635.
131. *Heating performance of a novel solar–air complementary building energy system with an energy storage feature*. Wang, Y., et al. 2022, Solar Energy, Vol. 236, pp. 75-87.
132. *Design and performance monitoring of a novel photovoltaic-thermal solar-assisted heat pump system for residential applications*. Leonforte, F., et al. 2022, Applied Thermal Engineering, Vol. 210, pp. 1183-1204.
133. *A pilot plant with hybrid PV/T panels; system integration of a solar assisted heat pump with existing heating devices*. Tagliafico, L.A., et al. 2017, 35th UIT proceedings.
134. *Optimisation strategies for solar assisted heat pumps coupled to traditional thermal fields*. Tagliafico, L.A., et al. 2021, UIT 2021 conference proceedings, Vol. 2177.

135. *Solar assisted heat pump pilot plant management and troubleshooting by means of numerical modelling: a case study*. Tagliafico, L.A., et al. 2020, UIT 2020 Conference Proceedings Special issue, Journal of Physics: Conference series, Vol. 1868.
136. *Application of solar assisted heat pump technology to the Palacus Sport Palace: renewable sources integration for highly efficient and low energy consumption systems*. Marafioti, C. 2021, PhD Thesis.
137. *Study of the criteria and methodologies for existing buildings energetic and functional retrofit: architecture/energy systems integration towards nZEB (nearly Zero Energy Building)*. Saio, C. 2018, PhD Thesis.
138. UNI/TS 11300-2:2019 - Energy performance of buildings - Part 2: Evaluation of primary energy need and of system efficiencies for space heating, domestic hot water production, ventilation and lighting for non-residential buildings. [Online] http://store.uni.com/catalogo/uni-ts-11300-2-2019?__store=en&josso_back_to=http%3A%2F%2Fstore.uni.com%2Fjosso-security-check.php&josso_cmd=login_optional&josso_partnerapp_host=store.uni.com&__from_store=it.
139. Stabat, P. IEA ECBCS Annex 48 Subtask 1: Analysis of heating and cooling demands and equipment performances. *Annex 48 Project Report*. 2008.
140. Genoa Climate. [Online] <https://it.climate-data.org/europa/italia/liguria/genova-1133/>.
141. *An Analysis on the Loads of Hot Water Consumption in restaurants*. Murakawa, S.D.N., Takata, H. and Tanaka, A. 2005, 31rd International Symposium on Water Supply and Drainage for Buildings .
142. *A review of domestic hot water consumption profiles for application in systems and buildings energy performance analysis*. Fuentes, E., Arce, L. and Salom, J. 1, 2018, Renewable and Sustainable Energy Reviews, Vol. 81, pp. 1530-1547.
143. *Dynamic behaviour and control strategy optimization for conventional heating plants in buildings*. Tagliafico, L.A., et al. 2016, International Journal of Heating Technologies, Vol. 34, pp. 505-511.
144. *Hourly simulations of an hospital building for assessing the thermal demand and the best retrofit strategies for consumption reduction*. Silenzi, F., Priarone, A. and Fossa, M. 2018, Thermal Scientific Engineering Progress.
145. [Online] <https://www.investopedia.com/terms/e/efficiency.asp>.
146. *Inclusive Environmental Impact Assessment Indices with Consideration of Public Acceptance: Application to Power Generation Technologies in Japan*. Takashi, T. and Sato, T. 2015, Applied Engineering, Vol. 144, pp. 64-72.
147. *Strategies for the Deployment of Micro-Generation Implications for Social Acceptance*. Sauter, R. and Watson, J. 2007, Energy Policy, Vol. 35, pp. 2770-2779.
148. *Local acceptance of Renewable Energy – A Case study from Southeast Germany*. Musall, F.D. and Kuik, O. 2011, Energy Policy, Vol. 39, pp. 3252-3260.
149. *Understanding and Overcoming the Nimby Syndrome*. Dear, M. 1992, Journal of the American Planning Association, Vol. 58, pp. 288-300.

150. *Factors influencing the acceptance of wind energy in Switzerland*. Simon, A. and Wustenhagen, R. 2006, Workshop "Social acceptance of renewable energy innovation", Tramelan (Switzerland).
151. *Acceptability engineering: the study of user acceptance of innovative technologies*. Hee Cheol, K. 2015, Journal of Applied Research and Technology, Vol. 13, pp. 230-237.
152. *End users' acceptance of new technologies in building heating: An experience on solar assisted heat pumps*. Tagliafico, L.A., et al. 2-4, 2019, TECNICA ITALIANA-Italian Journal of Engineering Science, Vol. 63, pp. 198-204.
153. Cambridge Dictionary. [Online] <https://dictionary.cambridge.org/it/dizionario/inglese/acceptance>.
154. UNI EN 15459 – Energy performance of buildings – Economic evaluation procedure for energy systems in buildings. [Online] <https://store.uni.com/cen-tr-15459-2-2017>.
155. GSE. [Online] <https://www.gse.it/servizi-per-te/fotovoltaico/scambio-sul-posto>.
156. Law 199/2021. [Online] <https://www.normattiva.it/uri-res/N2Ls?urn:nir:stato:decreto.legislativo:2021;199>.
157. *The experience on a sport centre pilot plant with solar assisted heat pump and a look forward for new control strategies and technology upgrade*. Tagliafico, L.A., et al. 2021, 76° Italian National Congress ATI, E3S Web of Conferences.
158. *A study of predictive control of energy-saving of heating process*. Zhu, X., Zhu, S. and Guo, S. 2011, Advanced Materials Research, p. 18101813.
159. *Operational optimization in a district heating system*. Benonysson, A., Bøhm, B. and Ravn, H.F. 5, 1995, Energy Conversion and Management, Vol. 36, pp. 297-314.
160. *Transient numerical modelling and experimental validation of building heating plants*. Borelli, D., Repetto, S. and Schenone, C. 2018, Thermal Science and Engineering Progress, Vol. 6, pp. 436-446.
161. *Future distributed generation: An operational multi-objective optimization model for integrated small scale urban electrical, thermal and gas grids*. Lo Cascio, E., Borelli, D. and Schenone, C. 2017, Energy Conversion and Management, Vol. 143, pp. 348-359.
162. *Residential Building Retrofit through Numerical Simulation: A Case Study*. Lo Cascio, E., et al. 2017, Energy Procedia, Vol. 111, pp. 91-100.
163. *Development and integration of a user friendly validation module within whole building dynamic simulation*. Ben-Nakhi, A.E. and Aasem, E.O. 1, 2003, Energy Conversion and Management, Vol. 44, pp. 53-64.
164. *Straw bale constructions: Laboratory, in field and numerical assessment of energy and environmental performance*. D'Alessandro, F., et al. 2017, Journal of Building Engineering, Vol. 11, pp. 56-68.
165. *Thermal transients in buildings: Development and validation of a numerical model*. Nannei, E. and Schenone, C. 3, 1999, Energy and Buildings, Vol. 29, pp. 209-215.














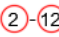

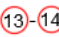




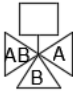
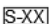
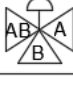

166. *Building thermal performance analysis by using matlab/simulink*. Mendes, N., Oliveira, G.H.C. and De Araujo, H.X. 2001, Seventh International IBPSA Conference, Rio de Janeiro, Brazil.
167. *A review study on the modeling of high-temperature solar thermal collector systems*. Hachicha, A.A., et al. 2019, Renewable and Sustainable Energy Reviews, Vol. 112, pp. 280-298.
168. *A simple building modelling procedure for MATLAB/SIMULINK*. Hudson, G. and Underwood, C.P. 2, 1999, Procedures of Building Simulation, Vol. 99.
169. *Development and validation of detailed building, plant and controller modelling to demonstrate interactive behaviour of system components*. Cockroft, J. 2009, 11th International IBPSA Conference.
170. *Matlab/Simulink for building and HVAC simulation-State of the art*. Riederer, P. 2005, Ninth International IBPSA Conference.
171. *Simplified thermal and hygric building models: A literature review*. Kramer, R., Van Schijndel, J. and Schellen, H. 4, 2012, Frontiers of Architectural Research, Vol. 1, pp. 318-325.
172. *Building energy simulation by an in-house full transient model for radiant systems coupled to a modulating heat pump*. Testi, D. 2015, Energy Procedia, Vol. 78, pp. 1135-1140.
173. *Energy and CO2 emissions performance assessment of residential micro-cogeneration systems with dynamic whole-building simulation programs*. Dorer, V. and Weber, A. 3, 2009, Energy Conversion and Management, Vol. 50, pp. 648-657.
174. Solar Energy Laboratory, University of Wisconsin-Madison, 2000. TRNSYS, A Transient Simulation Program, Reference Manual. [Online]
https://www.academia.edu/36897709/TRNSYS_STUDIO_MANUAL.
175. *Extension of the Hottel-Whillier model to the analysis of combined photovoltaic/thermal flat plate collectors*. Florschuetz, L.W. 4, 1979, Solar Energy, Vol. 22, pp. 361-366.
176. *The performance of flat-plate solar-heat collectors*. Hottel, W. 1942, Transactions of ASME, Vol. 64, pp. 91-104.
177. *The derivations of several "Plate-efficiency factors" useful in the design of flat-plate solar heat collectors*. Bliss, R.W. 4, 1959, Solar Energy, Vol. 3, pp. 55-64.
178. *A method of simulation of solar processes and its application*. Klein, S.A., et al. 1, 1975, Solar Energy, Vol. 17, pp. 29-37.
179. University, Arizona State. *Combined Photovoltaic/Thermal System Studies*. Tempe AZ : Report ERC-R-78017, 1978.
180. *Performance study of one-dimensional models for stratified thermal storage tanks*. Kleinbach, E. and Klein, S. 2, 1993, Solar Energy, Vol. 50, pp. 155-166.
181. *Validation of a single tank, multi-mode solar-assisted heat pump TRNSYS model*. Banister, C.J., Wagar, W. and Collins, M. 2014, Energy Procedia, pp. 499-504.
182. *Comparison of solar water tank storage modelling solutions*. Johannes, K. and Rusaouen, G. 2, 2005, Solar Energy, Vol. 79, pp. 216-218.

183. *A comprehensive overview on water-based energy storage systems for solar applications*. Shaghayegh, D. and Hossein, Y. 2022, Energy Reports, Vol. 8, pp. 8777-8797.
184. *Virtual prototyping of storage tanks by means of three-dimensional CFD and heat transfer numerical simulations*. Consul, R., et al. 2, 2004, Solar Energy, Vol. 77, pp. 179-191.
185. Klein, S.A. *A Design Procedure for Solar Heating Systems*. Wisconsin-Madison : Ph.D. Thesis Department of Chemical Engineering, University of Wisconsin-Madison, 1976.
186. TRNSYS manual – Volume 5 – Mathematical references. [Online] https://www.academia.edu/36897709/TRNSYS_STUDIO_MANUAL.
187. *Models of Sub-components and Validation for the IEA SHC Task 44/HPP Annex 38*. Dott, R. and Afjei, T. 2013, Report C2 Part C: Heat Pump Models. A Technical Report of Subtask C – Final Draft.
188. *A parameter estimation-based model of water-to-water heat pumps for use in energy calculation programs*. Jin, H. and Spitler, J.D. 1, 2002, ASHRAE Transactions, Vol. 108, pp. 3-17.
189. *A Yearly Utilization Model for Calculating the Seasonal Performance Factor of Electric Driven Heat Pump Heating Systems*. Afjei, T. 1989, Eidgenössische Technische Hochschule, Zürich.
190. *Simulation von Wärmepumpen-Systemen in Polysun*. Marti, J., et al. 2009, Auftrag des Bundesamt für Energie BFE, Bern.
191. Bühring, A. *Theoretische und experimentelle Untersuchungen zum Einsatz von Lüftungs-Kompaktgeräten mit integrierter Kompressionswärmepumpe*. Hamburg-Harburg : Ph.D. thesis, Technical University Hamburg-Harburg, 2001.
192. *Two-stage air-source heat pump for residential heating and cooling applications in northern US climates*. Bertsch, S.S. and Groll, E.A. 7, 2008, International Journal of Refrigeration, Vol. 31, pp. 1282-1292.
193. *Capacity control in ground source heat pump systems. Part I. Modeling and simulation*. Madani, H., Claesson, J. and Lundqvist, P. 6, 2011, International Journal of Refrigeration, Vol. 34, pp. 1338-1347.
194. Heinz, A. and Haller, M. *Appendix A3 – Description of TRNSYS Type 877 by IWT and SPF. Models of Sub-Components and Validation for the IEA SHC Task 44/HPP Annex 38 – Part C: Heat Pump Models – Draft*. s.l. : A Technical Report of Subtask C Deliverable C2.1 Part C, 2012.
195. *Performance ~ analysis and experimental validation of a solar-assisted heat pump fed by photovoltaic-thermal collectors*. Del Amo, A., et al. 2019, Energy, Vol. 169, pp. 1214-1223.
196. *Reversible heat pump model for seasonal performance optimization*. Kinab, E., et al. 2010, Energy and Buildings, Vol. 42, pp. 2269-2280.
197. *Energy consumption modelling of air source electric heat pump water heaters*. Bourke, G. and Bansal, P. 2010, Applied Thermal Engineering, Vol. 30, pp. 1769-1774.
198. *Modelling and simulation of a heat pump for simultaneous heating and cooling*. Byrne, P., Miriel, J. and Lenat, Y. 3, 2012, Building Simulation, Tsinghua University Press; Springer, Vol. 5, pp. 219-232.

199. Kays, W.M. and London, A.L. *Compact Heat Exchangers*. s.l. : Third edition Medtech, 2018.
200. Italian Climatic Zones. [Online] <https://www.studiomadera.it/news/387-zone-climatiche>.

Annex – complete plant layout

LEGEND

| | | | |
|--|--------------------------------|---|----------------------------|
|  | PUMP |  | HOT WATER |
|  | SHUT-OFF VALVE |  | COLD WATER |
|  | NON RETURN VALVE |  | WATER DUCT |
|  | CLOSED EXPANSION VESSEL |  | CONTROL SIGNAL |
|  | MOTORIZED TWO WAY ON/OFF VALVE |  | ACTUATION SIGNAL |
|  | SAFETY VALVE |  | POWER METER |
|  | PLATE HEAT EXCHANGER |  | TEMPERATURE SENSOR-PT100 |
|  | MOTORIZED THREE WAY VALVE |  | FLOW SENSOR |
|  | ANALOG THERMOMETER |  | ACTUATING SIGNAL |
|  | ANALOG MANOMETER |  | ACTUATING SIGNAL |
|  | THREE WAY VALVE |  | MEASUREMENT SIGNAL |
|  | THREE WAY MIXING VALVE |  | SIGNAL TO THE CONTROL UNIT |

